Title

Semiclassical Approximations in Chemical Dynamics

Author

Sun, Xiong

Publication Date

1998-12-01

LBNL-42760

ERNEST ORLANDO LAWRENCE
BERKELEY NATIONAL LABORATORY

Semiclassical Approximations in Chemical Dynamics

Xiong Sun

Chemical Sciences Division

December 1998

Ph.D. Thesis

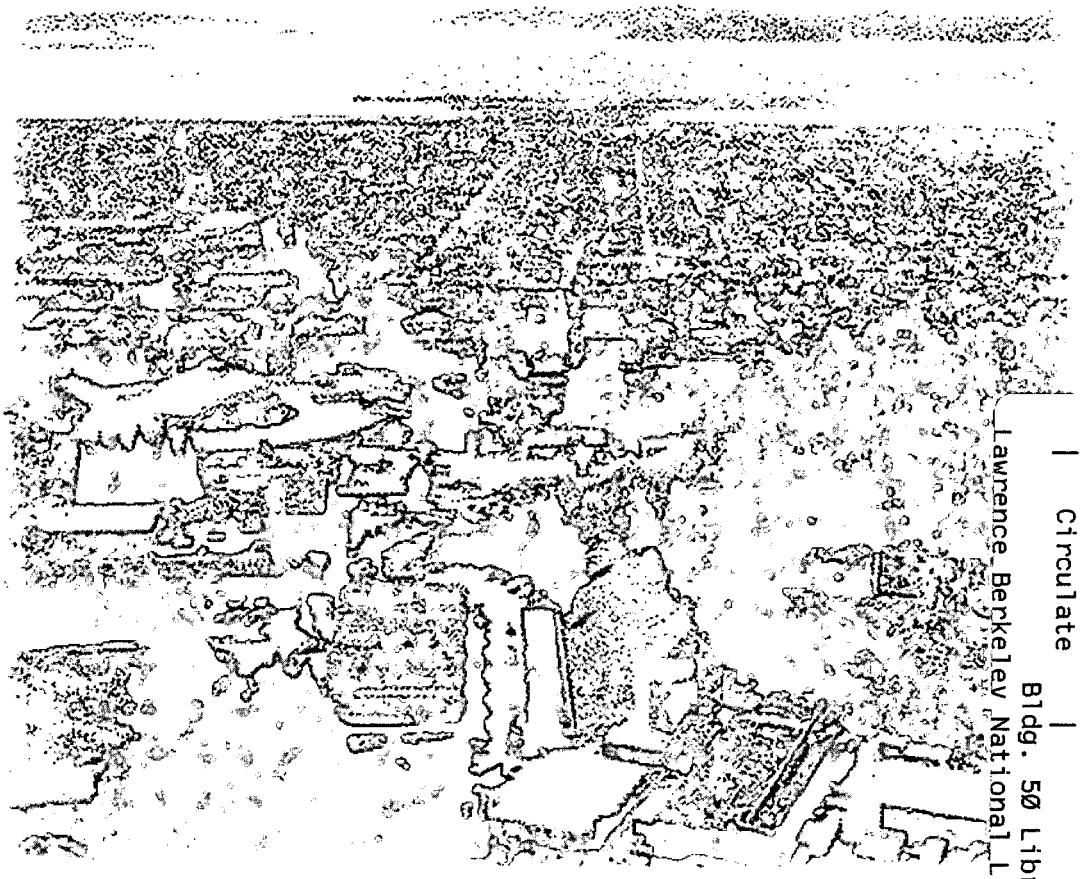

DISCLAIMER

LBNL-42760

Semiclassical Approximations in Chemical Dynamics

Xiong Sun
Ph.D. Thesis

Department of Chemistry
University of California, Berkeley

and

Chemical Sciences Division
Ernest Orlando Lawrence Berkeley National Laboratory
University of California
Berkeley, CA 94720

December 1998

This work was supported by the Director, Office of Energy Research, Office of Basic Energy Sciences, Chemical Sciences Division, of the U.S. Department of Energy under Contract No. DE-AC03-76SF00098.

Semiclassical Approximations in Chemical Dynamics

by

Xiong Sun

B. S. (Pennsylvania State University) 1994

A dissertation submitted in partial satisfaction of the

requirements for the degree of

Doctor of Philosophy

in

Chemistry

in the

GRADUATE DIVISION

of the

UNIVERSITY of CALIFORNIA at BERKELEY

Committee in charge:

Professor William H. Miller, Chair
Professor David Chandler
Professor Eugene Commins

1998

Semiclassical Approximations in Chemical Dynamics

by

Xiong Sun

Abstract

Semiclassical Approximations in Chemical Dynamics

by
Xiong Sun

Doctor of Philosophy in Chemistry
University of California at Berkeley
Professor William H. Miller, Chair

The semiclassical (SC) approximation is a fundamental topic in theoretical physics that connects quantum mechanics with classical mechanics. In the field of chemical dynamics, it has been envisioned as a valuable calculational tool that combines quantum effects with classical trajectories. However, in spite of these efforts, SC approximations have become practical only very recently. In this thesis, we further develop these semiclassical theories for applications in the dynamics of multidimensional systems. Specifically, we are interested in the semiclassical initial value representation (SC-IVR) and the possible approximations to it. Several applications are presented utilizing these methodologies.

On the topic of rigorous semiclassical theory, we explore a number of different SC-IVR's that are becoming useful as theoretical tools. In the process, we present a new derivation of the popular coherent state IVR that is conceptually simple in its approach. Numerical calculation of these IVR expressions are usually difficult, and for this purpose, the stationary phase Monte Carlo technique is seen to be an effective approach. Combining these ideas, the calculation of HCl dimer spectrum is offered as a nontrivial example that demonstrates the power of the SC-IVR.

It is also interesting to explore further approximations to the SC-IVR. To this end, we introduce the "linearized approximation" for correlation functions and apply it, in several ways, to complex systems with many degrees of freedom. We find that the result is a classical like expression which neglects interference effects completely. We also conjecture that the interference and coherence effects in complex systems may be negligible and therefore the linearized approximation can be useful. In order to retain these quantum

mechanical effects in correlation functions, we introduce the forward-backward IVR that reduces the oscillatory behavior to a minimum.

For the applications of these ideas to chemical problems, we focus on the topics of electronically nonadiabatic dynamics and the thermal rate constant. For electronically nonadiabatic dynamics, we present a new theoretical model that is exact if treated quantum mechanically, but has well defined semiclassical and classical limits. The SC-IVR and linearized approximation are applied to this model and excellent results are seen. For the thermal rate constant, we also apply the rigorous SC-IVR as well as the more approximate linearized version. We find that for a reaction in the condensed phase, the linearized approximation obtains excellent results for the rate and thus confirming our earlier conjecture about the disappearance of quantum interference in these systems. When quantum mechanical effects are important however, full SC-IVR must be used; and the forward-backward IVR is seen to capture these quantum effects efficiently.

To my parents

Contents

List of Figures

List of Tables

Acknowledgements

Last four years at Berkeley has been a wonderful experience, mainly due to the myriad of wonderful minds that are concentrated here. I have benefited greatly from many scientist and students met along this adventure. Here, I can only acknowledge some of the personalities that are directly responsible for the completion of this thesis.

The foremost person that I am grateful for is my thesis advisor, Prof. Bill Miller. Without his constant supply of ideas and insights, much of the work in this thesis would not have been possible. I have learned a great deal from him about science, about conducting research and about learning by getting one's "finger nails dirty." Working with him has been a thoroughly enjoyable experience.

In the physics department, I had the pleasure of attending the wonderful lectures of Prof. Robert Littlejohn and Prof. Eugene Commins. I still refer to their lecture notes on quantum mechanics and statistic mechanics in my research. Prof. Littlejohn also had the patience of discussing semiclassical mechanics with me on various occasions and I owe to him my understanding of the subject both through these discussions as well as through his articles. I also would like to thank Prof. Edgar Knobloch who introduced me to the subject of nonlinear dynamics.

The members of the Miller group were another source of many ideas. A large number of people need to be acknowledged, but among them, I have worked closely with Dr. Joshua Wilkie, Dr. Uri Peskin, Dr. Gunter Schmid, Dr. Srihari Keshavamurthy, Dr. Ward Thompson, Dr. Bill Poirier, Dr. Haobin Wang, David Skinner and Kathy Sorge. Dr. Haobin Wang is also a collaborator on some of the work presented in this thesis. My office mates, Bill Poirier, Kathy Sorge, Bruce Spath, David Skinner and Stephen Cotton, are admirable for putting up with me everyday and laughing at (resigning to?) my bad jokes.

During my undergraduate years, four people were very influential. Prof. Roger Herman's enthusiasm was extremely contagious. I learned all my fundamental physics from him. Prof. Bill Horrocks in chemistry introduced me to research that finally lead to my honors project. Prof. John Collins and Prof. Steve Heppelmann shared their own perspectives on physics with me on many occasions and helped me form ideas about what I wanted to do with my future. Before college, Mrs. Marguerite Ciolkosz was the exceptional teacher I had who started me on to the road of science.

My parents are most responsible for my views on life. They taught me to strive for a higher standard with their own example. For this I am eternally grateful. Finally, my life at Berkeley would not have been as cheerful without Tammy Pilisuk and her wonderful family, to them I must give my special thanks.

This work was supported by the Director, Office of Energy Research, Office of Basic Energy Sciences, Chemical Science Division of the U. S. Department of Energy under contract No. DE-AC03-76SF00098.

Chapter 1

Introduction

When applying the basic principles of quantum mechanics to physical processes, three approximations are usually made: *perturbation techniques* where successive approximations of a quantity is made by starting with a more solvable model; *variational principle* gives an estimate of a quantity with a trial (or guessed) solution; *semiclassical approximations* where wavefunctions, energy levels, transition and scattering amplitudes — essentially all quantities of interest — are expressed in terms of quantities occurring in the corresponding *classical* problem plus the parameter $\hbar$. The last of these approximate methods applied to chemical dynamics is the subject of this thesis.

Semiclassical (SC) approximation is an example of asymptotic approximation, referring to the fact that the method is valid when the ratio of classical actions in the problem to $\hbar$ is large. (Although, in general, quantum mechanical quantities cannot be trivially written as a power series in $\hbar$.) It needs to be emphasized that this is essentially every situation in chemical dynamics where the smallest particle one usually encounter is the hydrogen atom; given that the action is proportional to the square root of the mass, this ratio is on the order of 40. We therefore find that semiclassical approximation is undoubtly valid for most problems. In addition, because the semiclassical approximation is also exact for Hamiltonians that are at most quadratic (harmonic) in position and momentum, we find that short time dynamics of systems that are not harmonic is also modeled well. Clearly, the accuracy of semiclassical mechanics in chemistry makes it very attractive. For the pedagogical side of theorists, semiclassical mechanics also offers an enormous intellectual appeal. It answers, in part, the question from the earliest days of quantum mechanics: how does the quantum mechanical behavior of the microscopic world translate to the classical-like New-

tonian world of everyday life? This question which touches the most fundamental notions of physics is still one of the main motivations for studying semiclassical mechanics.

1.1 Historical Overview

1.1.1 Semiclassical Limit of Quantum Mechanics

The earliest example of semiclassical theory is the Wentzel-Kramers-Brillouin[1–4] (WKB) approximation for the quantum wavefunction in one dimension. The WKB wavefunction is expressed as

$$\psi(x) \propto \sum_{\pm} \frac{1}{\sqrt{\pm p(x)}} e^{\pm iR(x,E)/\hbar \pm i\pi/4}, \tag{1.1}$$

where the momentum, $p(x)$, is

$$p(x) = \sqrt{2m(E - V(x))}, \tag{1.2}$$

and $V(x)$ is the potential energy as a function of the coordinate. The classical action, $R(x, E)$, is

$$R(x, E) = \int^x p(x)dx, \tag{1.3}$$

where the lower limit of the integral is arbitrary. The $\pm$ in Eq. (1.1) refers to trajectories traveling to the left and right direction and the phase factor $\pi/4$ is the result of the famous WKB connection formula. The WKB wavefunction can be analytically continued into the classical forbidden region by replacing $p(x)$ with $i|p(x)|$. And, by imposing proper boundary conditions on the wavefunction, i.e., exponentially vanishing in the classically forbidden regions, one arrives at the Bohr-Sommerfeld[5] semiclassical quantization condition that the eigenenergies of the quantum Hamiltonian can be approximated by inverting the equation

$$\pi\hbar\left(n + \frac{1}{2}\right) = \int_{x_<}^{x_>} \sqrt{2m(E - V(x))}dx = \int_{x_<}^{x_>} p(x)dx \tag{1.4}$$

where $x_<$ and $x_>$ are the classical turning points of the bound motion in the potential $V(x)$. The curious fact of WKB is, though this procedure of finding the eigenvalues is approximate, it gives the correct result for virtually every exactly solvable case.

The multidimensional generalization of the WKB wavefunction has a similar form

$$\psi(\mathbf{q}) \propto \sum_j \left|\frac{\partial^2 R(\mathbf{q}, E)}{\partial \mathbf{q} \partial E}\right|^{\frac{1}{2}} e^{iR(\mathbf{q},E)/\hbar + i\phi_j}. \tag{1.5}$$

In classical phase space, $R(\mathbf{q}, E)$ is a multi-valued function of $\mathbf{q}$ and the summation over j is the sum over these multiple points. For an extensive discussion of the semiclassical wavefunction, the reader can refer to articles by Berry *et al.*[6] Multidimensional generalization of the Bohr-Sommerfeld quantization condition of Eq. (1.4) is also possible by analogy for classically integrable systems (i.e., an F dimensional system with F conserved actions), the result is referred to as the EBK quantization condition[7] after Einstein-Brillouin-Keller.

For the study of dynamical processes, however, one is invariably interested in the quantum mechanical propagator, $e^{-i\hat{H}t/\hbar}$. The knowledge of the propagator is equivalent to having solved the time-dependent Shrödinger equation, and the time evolution of a quantum system is thus determined. The semiclassical approximation to the propagator was conjectured very early on by Van Vleck.[8] By studying the form of the propagator for the free particle, he proposed that in general, the propagator might be written as

$$K(\mathbf{q}_2, \mathbf{q}_1, t) = \langle \mathbf{q}_2 | e^{-i\hat{H}t/\hbar} | \mathbf{q}_1 \rangle = \sum_j \left| \det \left(-\frac{\partial^2 S_j(\mathbf{q}_2, \mathbf{q}_1)}{\partial \mathbf{q}_2 \partial \mathbf{q}_1} \right) \right|^{\frac{1}{2}} (2\pi i\hbar)^{-\frac{F}{2}} e^{iS_j(\mathbf{q}_2, \mathbf{q}_1, t)/\hbar}, \tag{1.6}$$

where the summation is over all the classical trajectories that starts from $\mathbf{q}_1$ and end at $\mathbf{q}_2$ in time t. The function $S(\mathbf{q}_2, \mathbf{q}_1, t)$ is the Hamilton's principle function

$$S(\mathbf{q}_2, \mathbf{q}_1, t) = \int_{\mathbf{q}_1}^{\mathbf{q}_2} \mathbf{p}(\mathbf{q}) d\mathbf{q} - \int_0^t H[\mathbf{q}(\tau), \mathbf{p}(\tau)] d\tau. \tag{1.7}$$

Clearly, this quantity is related to the action defined in Eq. (1.3) by a Legendre transformation, but to confuse the terminology here, we will refer to this function as the action as well from here on. The guessed approximation for the propagator in Eq. (1.6) turns out to be almost correct. Gutzwiller[9] and others[10–12] were able to make the connection to this formula by starting with Feynman's path integral representation of the propagator, and by carrying out an asymptotic or stationary phase analysis (SPA) of the path integral, they discovered that there is an extra phase in the propagator,

$$K(\mathbf{q}_2, \mathbf{q}_1, t) = \sum_j \left| \det \left(-\frac{\partial^2 S_j(\mathbf{q}_2, \mathbf{q}_1)}{\partial \mathbf{q}_2 \partial \mathbf{q}_1} \right) \right|^{\frac{1}{2}} (2\pi i\hbar)^{-\frac{F}{2}} e^{iS_j(\mathbf{q}_2, \mathbf{q}_1, t)/\hbar - i\pi\nu_j/2}, \tag{1.8}$$

where ν_j is an integer that increments when the determinant prefactor changes sign. This phase index is frequently referred to as the Maslov index,[13–15] after Maslov who showed that the index arised when one encounters caustic points in phase space, very much like the WKB phase across a classical turning point.

Gutzwiller[16–23] was the first to examine quantization in a new way. He studied the level density of a Hamiltonian defined by

$$g(E) = \mathrm{tr}[\delta(E - \hat{H})]. \tag{1.9}$$

The level density operator is related to the propagator via the Greens function,

$$\delta(E - \hat{H}) = -\frac{1}{\pi}\mathrm{Im}\hat{G}(E), \tag{1.10}$$

$$\hat{G}(E) = \frac{1}{i\hbar}\int_0^\infty e^{iEt/\hbar}e^{-i\hat{H}t/\hbar}, \tag{1.11}$$

for which the semiclassical approximation in Eq. (1.8) can be utilized. The crucial steps are the stationary phase evaluation of the time integral and the trace integral. After some ingenious bookkeeping, Gutzwiller arrived at a trace formula that expresses the level density as a sum over the periodic orbits,

$$g(E) = \bar{g}(E) + \frac{1}{\pi\hbar}\sum_j \frac{\tau_j}{\sqrt{|\det(\mathbf{m}_j - \mathbf{I})|}}\cos\left(\frac{R_j(E)}{\hbar} - \frac{\mu_j\pi}{2}\right), \tag{1.12}$$

where $\bar{g}(E)$ is the classical (Thomas-Fermi) level density coming from contribution from periodic orbits of zero length, and the summation in the second part is over all traversals of every periodic orbit at energy E each having period τ_j. The matrix $\mathbf{m}_j$ is the non-trivial $2F-2\times 2F-2$ part of the monodromy matrix for the jth orbit. Equation (1.12) is referred to as Gutzwiller's trace formula. Due to the nature of the approximations (stationary phase integration) involved, it is really only valid for systems with "isolated" periodic orbits. This situation occurs when the system is completely chaotic. There is now an enormous literature on Gutzwiller's trace formula. Notably, Berry and Tabor[24] was able to derive an analogous trace formula for integrable systems, starting from the EBK quantization condition. Others have proposed uniformized trace formula that have better convergence properties,[25–27] higher $\hbar$ order corrects have been proposed[28] and large number of example systems have been studied.

The trace formula is certainly one of the most interesting achievements in field of semiclassical mechanics. For the first time, quantization of a Hamiltonian system is understood in terms of very mundane classical quantities. The marriage between the particle picture of classical mechanics and the wave picture of quantum mechanics is almost harmonious. However, the trace formula is not without its problems, mainly due to the fact that the number of periodic orbits that one need to enumerate can be extremely large; it is also

far from divergence free; for any realistic multidimensional system such as the most generic of chemical problems, finding all of these periodic orbits is next to impossible.

The development of the trace formula lead to further enrichment of the field. Similar arguments have been carried over to examine other semiclassical quantities. Berry[29] studied correlations in the energy level statistics of chaotic systems and established connections with random matrix theory. Berry[30] also showed that the semiclassical approximation to the Wigner transformation of the the density operator,

$$W(\mathbf{p},\mathbf{q};E) = \int d\Delta\mathbf{q} e^{i\mathbf{p}\cdot\Delta\mathbf{q}/\hbar}\langle \mathbf{q}+\frac{\Delta\mathbf{q}}{2}|\delta(E-\hat{H})|\mathbf{q}-\frac{\Delta\mathbf{q}}{2}\rangle, \tag{1.13}$$

which is a sum over Wigner transformations of the eigenstates

$$W(\mathbf{p},\mathbf{q};E) = \int d\Delta\mathbf{q} e^{i\mathbf{p}\cdot\Delta\mathbf{q}/\hbar}\sum_n \delta(E-E_n)\langle \mathbf{q}+\frac{\Delta\mathbf{q}}{2}|\phi_n\rangle\langle\phi_n|\mathbf{q}-\frac{\Delta\mathbf{q}}{2}\rangle, \tag{1.14}$$

can be expressed as

$$W(\mathbf{p},\mathbf{q};E) = \delta[E-H(\mathbf{p},\mathbf{q})] + \sum_j w_j(\mathbf{p},\mathbf{q};E) \tag{1.15a}$$

where the summation in the second part of the equation is again over all the periodic orbits at energy E and

$$\begin{aligned} w_j(\mathbf{p},\mathbf{q};E) &= \frac{2^F}{\det(\mathbf{m}_j+1)}\cos\left[\frac{R_j(E)}{\hbar} - \frac{1}{\hbar}\mathbf{X}^T\cdot\mathbf{J}\cdot(\mathbf{m}_j-\mathbf{I})\cdot(\mathbf{m}_j+\mathbf{I})^{-1}\cdot\mathbf{X}+\gamma_j\right] \\ &\times \frac{2}{(\hbar^2|\ddot{\mathbf{x}}^T\cdot\mathbf{J}\cdot\dot{\mathbf{x}}|)^{\frac{1}{3}}}\mathrm{Ai}\left\{\frac{2[H(\mathbf{x})-E]}{(-\hbar^2\ddot{\mathbf{x}}^T\cdot\mathbf{J}\cdot\dot{\mathbf{x}})^{\frac{1}{3}}}\right\}, \end{aligned} \tag{1.15b}$$

where the reader should refer to the original article for an explanation of the various terms. Eq. (1.15) is termed the scar expansion, confirming Heller's[31] earlier conjecture about the role of periodic orbits in quantum wavefunctions. If we integrate over the all the phase space variables, i.e., take a trace, we get the level density

$$(2\pi\hbar)^{-F}\int d\mathbf{p}d\mathbf{q}W(\mathbf{p},\mathbf{q};E) = g(E), \tag{1.16}$$

and it is exactly the Gutzwiller's trace formula of Eq. (1.12). Integrating over momenta (coordinate) $\mathbf{p}$ ($\mathbf{q}$) will also give the coordinate (momentum) wavefunctions of at energy E. Wilkie and Brumer[32,33] studied the semiclassical Wigner transform of off-diagnol elements of the density operator $\hat{\rho}$ where $\hat{\rho}_{nm} = |\phi_n\rangle\langle\phi_m|$ and thus generalizing Berry's results.

1.1.2 Semiclassical Methods in Chemical Dynamics

Chemists have been interested in semiclassical mechanics largely because its practical utility of describing chemical dynamics, include quantum mechanical effects, with classical quantities. Early applications include the use of WKB approximation for many one dimensional systems; spectroscopy of larger molecules at moderate energies was understood by finding the energy eigenvalues with the EBK quantization condition. In the early 60's, molecular beam measurements brought the experiments of molecular collision to a new level of detail, and scattering of molecules with each other became a central topic of study.

The scattering matrix, which describes the probability of transition from an incoming translation momentum plus internal states to an outgoing momentum with different internal states, is rigorously defined[34] as

$$S_{n,n'}(E) = \lim_{t\to\infty,t'\to-\infty} \langle \psi_{n'}, p' | e^{i\hat{H}_0 t/\hbar} e^{-i\hat{H}(t-t')/\hbar} e^{-i\hat{H}_0 t'/\hbar} | p, \psi_n \rangle \tag{1.17}$$

where $\hat{H}_0$ is the interaction free Hamiltonian that describes the asymptotic states of the collisional partners, $\hat{H}$ is the full Hamiltonian including the interaction and (p, ψ_n) $[(p', \psi_{n'})]$ is the translational plus internal eigenstate of the system before (after) the collision. Clearly, $|p, \psi_n\rangle$ is an eigenstate of $\hat{H}_0$, therefore the the task is to evaluate the matrix element

$$S_{n,n'}(E) \propto e^{iE(t-t')/\hbar} \langle \phi_{n'}, p' | e^{-i\hat{H}(t-t')/\hbar} | p, \phi_n \rangle, \tag{1.18}$$

which is again reduced to an evaluation of the propagator matrix element. Miller's proposal[35] for the S-matrix is to insert in action variables $\mathbf{n}_{1,2}$ of the interaction free Hamiltonian H_0,

$$S_{n,n'}(E) \propto e^{iE(t-t')/\hbar} \int d\mathbf{n}_1 \int d\mathbf{n}_2 \phi_{n'}(\mathbf{n}_2)^* \langle \mathbf{n}_2, p' | e^{-i\hat{H}(t-t')/\hbar} | p, \mathbf{n}_1 \rangle \phi_n(\mathbf{n}_1) \tag{1.19}$$

In the asymptotic region, the translational and internal part of the Hamiltonian $\hat{H}_0$ are uncoupled, therefore the action for the internal motion is conserved and quantized according to the EBK quantization condition and the action variable takes on integer (plus a fraction) values [i.e., $\phi_n(\mathbf{n}_1) = \delta(\mathbf{n}_1 - \mathbf{n})$]. Thus, the S-matrix can be approximated as a matrix element of two sets of classical variables

$$S_{n,n'}(E) \approx e^{iE(t-t')/\hbar} \langle \mathbf{n}', p' | e^{-i\hat{H}(t-t')/\hbar} | p, \mathbf{n} \rangle. \tag{1.20}$$

where $\mathbf{n}$ ($\mathbf{n}'$) is the EBK quantum number of the ϕ_n ($\phi_{n'}$) state. (Note that though $\mathbf{n}$ is uncoupled from the translation momentum p in the asymptotic region, it is not uncoupled,

however, during the collision.) With this identification, application of the semiclassical propagator expression of Eq. (1.8) is straightforward; and because $\mathbf{n}$ and $\mathbf{n}'$, and the incoming and outgoing momenta, p and p', are fixed, the S-matrix can eventually be reduced to the expression

$$S_{n,n'}(E) = i \sum_j \left| \det \left(-\frac{\partial^2 R_j(\mathbf{n}, \mathbf{n}'; E)}{\partial \mathbf{n} \partial \mathbf{n}'} \right) \right|^{\frac{1}{2}} e^{iR_j(\mathbf{n},\mathbf{n}';E)/\hbar + i\phi_j}, \tag{1.21}$$

where $R_j(\mathbf{n}, \mathbf{n}'; E)$ is the same action function appearing in Eq. (1.5) and the sum is over all the trajectories that satisfy the boundary conditions. [Since the values of $(\mathbf{n}, p)$ and $(\mathbf{n}', p')$ are fixed and the initial and final positions (r and r') must be in the asymptotic region, the only freedom is in choosing variables conjugate to $\mathbf{n}$ and $\mathbf{n}'$, i.e., θ and θ'.]

The semiclassical S-matrix, Eq. (1.21) is just one of the examples of applying the semiclassical propagator. Miller[36] also extended these semiclassical ideas to the thermal rate constants and arrived at the now called instanton (periodic orbits) model for reaction rates. Heller[37–41] and others[42–46] examined more approximate ways of combining quantum mechanics with classical dynamics such as propagating Wigner distribution functions and Gaussian wavepackets. All of approaches these have met with some success. All of these investigations have also added to the conceptual understanding of semiclassical mechanics: it is now understood (more or less) that all quantum mechanical effects such as interference, coherence, symmetry selection rules and tunneling can all be qualitatively (if not quantitatively) included in the semiclassical theories originated from the Van Vleck-Gutzwiller propagator.

These early application of the semiclassical propagator also exposed the difficulty of evaluating an expression such as Eq. (1.21): one has to find the trajectories that connects the double ended boundary condition, a task that is typically unpleasant, especially for chaotic systems. Applications in the past have been mostly restricted to small or model systems. However, much of the focus in recent years is in reformulating the semiclassical propagators in a computationally convenient way. The product of this effort is now call the semiclassical initial value representation (SC-IVR) that has fueled a rebirth of interest in applying the semiclassical approximation to a wide variety of topics. The theory and application of the semiclassical initial value representation, and its relationship with classical mechanics, are the central topics of this thesis.

1.2 Thesis Outline

The goal of this work has been to further understand the semiclassical theories as they are applied to the dynamics of chemical systems with increasing complexity. In particular, we are focused on the semiclassical initial value representation and are interested to see whether it is useful as a practical tool for approximating quantum mechanical effects. Because semiclassical theories are asymptotic approximations, there is no one uniquely correct version, therefore one finds a wide variety approaches each with its own interesting properties. I hope some of this richness reflected in the discussions henceforth.

This thesis is divided into two parts. Part one, which includes chapters two and three, discusses the methodology of various semiclassical methods. It starts by explaining the ideas behind the initial value representation and introduces the now ubiquitous coherent state (Herman-Kluk) propagator. Along the way, a new derivation of the coherent state propagator is presented. Numerical difficulty of implementing the SC-IVR is discussed along with the Filinov smoothing method which ameliorate some of these practical problems. At the end of chapter two, an example application to the HCl dimer is presented. Chapter three discusses the possible approximations to the SC-IVR and see how one arrives at a classical-like expression with the linearized approximation. This approximation can also be applied to the "system-bath" problems by carrying out the linearization procedure only in the bath degrees of freedom, arriving at the so call mixed semiclassical-classical model. Lastly, a new way of applying the SC-IVR to the calculation of correlation functions by evolving classical trajectories forward and backward in time is also presented.

Part two includes chapters four and five which examines the various applications of these semiclassical methods presented in part one. Specifically, chapter four presents a new dynamically consistent theory of electronically nonadiabatic dynamics, its semiclassical and classical limits are also discussed. Chapter five deals with applications involving the calculation of flux correlation functions and thermal rate constants. Chapter six concludes.

Chapter 2

Semiclassical Initial Value Representation

2.1 Introduction

The basic starting point of all semiclassical theories is the Van Vleck-Gutzwiller[8–12] propagator

$$\langle \mathbf{q}_2 | e^{-i\hat{H}t/\hbar} | \mathbf{q}_1 \rangle = \sum_j \left| \det \left(-\frac{\partial^2 S_j(\mathbf{q}_2, \mathbf{q}_1; t)}{\partial \mathbf{q}_2 \partial \mathbf{q}_1} \right) \right|^{\frac{1}{2}} (2\pi i\hbar)^{-\frac{F}{2}} e^{iS_j(\mathbf{q}_2,\mathbf{q}_1;t)/\hbar - i\pi\nu/2} \tag{2.1}$$

where the summation is over all the classical trajectories that connect $\mathbf{q}_2$ with $\mathbf{q}_1$ in time t and $S_j(\mathbf{q}_2, \mathbf{q}_1; t)$ is the action associated with the jth trajectory as defined in Eq. (1.7). ν_j — the Maslov index[13–15] — is an integer that increments whenever the determinant factor changes sign. It needs to be emphasized that the summation over these different classical trajectories is the essence of the various quantum mechanical effects: energy quantization, for example, is the result of an infinite sum over such trajectories; quantum mechanical interference and coherence effects are direct results from the interference between different trajectories; tunneling can also be understood as analytically continued interference,[35,47–52] etc. Therefore, in order to include these quantum mechanical effects properly, it is essential that one faithfully carry out this summation. These facts were understood from very early on and are the hall marks of this semiclassical theory.

Using the identity[53] that

$$\frac{\partial S(\mathbf{q}_2, \mathbf{q}_1)}{\partial \mathbf{q}_1} = -\mathbf{p}_1 \tag{2.2}$$

where $\mathbf{p}_1$ is the initial momentum of the trajectory, we can rewrite the SC propagator as

$$\langle \mathbf{q}_2 | e^{-i\hat{H}t/\hbar} | \mathbf{q}_1 \rangle = \sum_j \left| \det \left(\frac{\partial \mathbf{q}_2}{\partial \mathbf{p}_1} \right) \right|^{-\frac{1}{2}} (2\pi i\hbar)^{-\frac{F}{2}} e^{iS_j(\mathbf{q}_2,\mathbf{q}_1;t)/\hbar - i\pi\nu/2}. \tag{2.3}$$

To evaluate the matrix element of the propagator therefore involves finding these distinct trajectories that connects two coordinates, i.e., if $\mathbf{q}_t(\mathbf{p}_1, \mathbf{q}_1)$ is the trajectory at time t, one needs to find all the $\mathbf{p}_1$'s that satisfy the nonlinear equation

$$\mathbf{q}_t(\mathbf{p}_1, \mathbf{q}_1) = \mathbf{q}_2. \tag{2.4}$$

This is, in general, a highly cumbersome procedure where the only known method of finding these roots seems to be called the "shooting method". In addition, the semiclassical propagator becomes infinite when the determinant of $\partial \mathbf{q}_2 / \partial \mathbf{p}_1$ is zero. This in itself is not always wrong, for instance, the exact quantum mechanical propagator for the harmonic oscillator

$$\langle q_2 | e^{-i\hat{H}t/\hbar} | q_1 \rangle = \left[\frac{m\omega}{2\pi i\hbar \sin(\omega t)} \right]^{\frac{1}{2}} \exp \left\{ \frac{im\omega}{2\hbar \sin(\omega t)} [(q_1^2 + q_2^2)\cos(\omega t) - 2q_1 q_2] \right\}, \tag{2.5}$$

is in fact infinite at $t = n\pi/\omega$. However, numerically, this is usually a nuisance.

Miller, in 1970,[54] noticed that the situation is enormously simplified in the case of the state-to-state transition probability

$$\begin{aligned} \langle \psi_2 | e^{-i\hat{H}t/\hbar} | \psi_1 \rangle &= \int d\mathbf{q}_2 \int d\mathbf{q}_1 \psi_2(\mathbf{q}_2)^* \langle \mathbf{q}_2 | e^{-i\hat{H}t/\hbar} | \mathbf{q}_1 \rangle \psi_1(\mathbf{q}_1) \\ &= \int d\mathbf{q}_2 \int d\mathbf{q}_1 \psi_2(\mathbf{q}_2)^* \psi_1(\mathbf{q}_1) \sum_j \left| \det \left(\frac{\partial \mathbf{q}_2}{\partial \mathbf{p}_1} \right) \right|^{-\frac{1}{2}} \\ &\quad (2\pi i\hbar)^{-\frac{F}{2}} e^{iS_j(\mathbf{q}_2,\mathbf{q}_1;t)/\hbar - i\pi\nu/2}, \end{aligned} \tag{2.6}$$

where $\psi_{1,2}$ are the various wavefunctions of the system and the semiclassical propagator of Eq. (2.3) is substituted in for the quantum propagator. Standard semiclassical theories would perform the integral over $\mathbf{q}_1$ and $\mathbf{q}_2$ by SPA and obtain the semiclassical S-matrix like expression for the state-to-state transition probability. However, instead of proceeding this way and do all the root searching, one can do the integral over $\mathbf{q}_1$ and $\mathbf{q}_2$ exactly and *change the integration variable* from $\mathbf{q}_2$ to $\mathbf{p}_1$. Keeping all the Jacobian factor along the way, i.e.,

$$\int d\mathbf{q}_2 \sum_j \rightarrow \int d\mathbf{p}_1 \left| \det \left(\frac{\partial \mathbf{q}_2}{\partial \mathbf{p}_1} \right) \right|, \tag{2.7}$$

now the state-to-state transition probability is

$$\langle\psi_2|e^{-i\hat{H}t/\hbar}|\psi_1\rangle = \int d\mathbf{p}_1 \int d\mathbf{q}_1 \left| \det\left(\frac{\partial \mathbf{q}_t}{\partial \mathbf{p}_1}\right)\right|^{\frac{1}{2}} (2\pi i\hbar)^{-\frac{F}{2}} \psi_2(\mathbf{q}_t)^* \psi(\mathbf{q}_1) e^{iS_t(\mathbf{p}_1,\mathbf{q}_1)/\hbar - i\pi\nu/2} \tag{2.8}$$

where $\mathbf{q}_t = \mathbf{q}_t(\mathbf{p}_1, \mathbf{q}_1)$. By making this variable change, the summation over the various different classical trajectories in the Van Vleck-Gutzwiller formula is automatically included since the sum is simply over all the different initial momenta anyway. Indeed, the new expression, now called the initial value representation (IVR), is exactly the same as the Van Vleck-Gutzwiller propagator. [Another way of seeing this is that we have effectively made the following identification for the propagator

$$\langle\mathbf{q}_2|e^{-i\hat{H}t/\hbar}|\mathbf{q}_1\rangle = \int d\mathbf{p}_1 \delta(\mathbf{q}_t - \mathbf{q}_2) \left| \det\left(\frac{\partial \mathbf{q}_t}{\partial \mathbf{p}_1}\right)\right|^{\frac{1}{2}} (2\pi i\hbar)^{-\frac{F}{2}} e^{iS_t(\mathbf{p}_1,\mathbf{q}_1)/\hbar - i\pi\nu/2}, \tag{2.9}$$

and the integral over $\mathbf{p}_1$ can be carried out exactly to give Eq. (2.3).] Nevertheless, it is important to recognized that with this extremely simple transformation, we have circumevented the difficult root searching problem of Eq. (2.4) and now the expression takes on a simple phase space average that still retains all the interference/coherence quantum effects properly.

This very early example of IVR is the origin of much of today's activity. The current definition[55–61] of the IVR differs somewhat from the original one. Instead of working with the "primitive" IVR of Eq. (2.9), the idea is now to write the propagator as a phase space average over classical trajectories as

$$\langle\mathbf{q}_2|e^{-i\hat{H}t/\hbar}|\mathbf{q}_1\rangle = \int d\mathbf{p}_0 \int d\mathbf{q}_0 \; A_t(\mathbf{p}_0, \mathbf{q}_0) e^{i\phi_t(\mathbf{p}_0,\mathbf{q}_0)/\hbar}, \tag{2.10}$$

where $A_t(\mathbf{p}_0, \mathbf{q}_0)$ and $\phi_t(\mathbf{p}_0, \mathbf{q}_0)$ are some functions of the trajectory initial conditions $(\mathbf{p}_0, \mathbf{q}_0)$, and the restriction is if we carried out the integration over these initial conditions by the stationary phase approximation, we must recover the Van Vleck-Gutzwiller propagator of Eq. (2.3). The meaning of this statement is easily demonstrated with the following example: consider the identity

$$\langle\mathbf{q}_2|e^{-i\hat{H}t/\hbar}|\mathbf{q}_1\rangle = \int d\mathbf{p}_2 \langle\mathbf{q}_2|\mathbf{p}_2\rangle\langle\mathbf{p}_2|e^{-i\hat{H}t/\hbar}|\mathbf{q}_1\rangle, \tag{2.11}$$

where an analogous semiclassical approximation for the matrix element $\langle\mathbf{p}_2|e^{-i\hat{H}t/\hbar}|\mathbf{q}_1\rangle$ can be substituted in,

$$\langle\mathbf{p}_2|e^{-i\hat{H}t/\hbar}|\mathbf{q}_1\rangle = \sum_j \left| \det\left(-\frac{\partial^2 S_j(\mathbf{p}_2, \mathbf{q}_1)}{\partial \mathbf{p}_2 \partial \mathbf{q}_1}\right)\right|^{\frac{1}{2}} (2\pi i\hbar)^{-\frac{F}{2}} e^{iS_j(\mathbf{p}_2,\mathbf{q}_1;t)/\hbar}$$

$$= \sum_j \left| \det\left(\frac{\partial \mathbf{p}_2}{\partial \mathbf{p}_1}\right)\right|^{-\frac{1}{2}} (2\pi i\hbar)^{-\frac{F}{2}} e^{iS_j(\mathbf{q}_t,\mathbf{q}_1;t)/\hbar - i\mathbf{p}_2\cdot\mathbf{q}_t/\hbar}, \qquad (2.12)$$

and we have ignored the Maslov index for the moment. If one then proceeds to do the integration over $\mathbf{p}_2$ by the stationary phase approximation, one would recover the propagator of Eq. (2.3); therefore Eq. (2.11) is equivalent to Eq. (2.3) in the SPA. To get it into an IVR form is then very simple, again changing integration variable from $\mathbf{p}_2$ to $\mathbf{p}_1$, we get

$$\langle \mathbf{q}_2|e^{-i\hat{H}t/\hbar}|\mathbf{q}_1\rangle = \int d\mathbf{p}_1 \left| \det\left(\frac{\partial \mathbf{p}_t}{\partial \mathbf{p}_1}\right)\right|^{\frac{1}{2}} (2\pi\hbar)^{-F} e^{iS_j(\mathbf{p}_1,\mathbf{q}_1;t)/\hbar + i\mathbf{p}_t\cdot(\mathbf{q}_2-\mathbf{q}_t)/\hbar}. \qquad (2.13)$$

This is another IVR (commonly referred to as a momentum version) that one might use.

The initial value representation is therefore a term that refers to infinite number of possible expressions that are only asymptotically equivalent to the original semiclassical formulation of Eq. (2.1). They can differ widely in accuracy and ease of use. Kay, in a series of well written papers,[55–57] has summarized the basic concepts behind the IVR methodology and introduced a generalized IVR expression that reduces to the various commonly used ones. The reader can referred to his articles for further discussion on the subject.

A few words needs to be said about the Maslov index and its relevance to SC-IVR. Maslov, in his seminal book,[13] made a very detailed study of this now famous phase factor. At these so called caustic points, which are the points where $\det(\partial \mathbf{q}_2/\partial \mathbf{p}_1)$ is zero, the semiclassical expression of Eq. (2.1) is singular. However, these caustic points are not invariant properties of phase space; for instance, in the momentum representation of Eq. (2.12), these caustic points occur at times where $\det(\partial \mathbf{p}_2/\partial \mathbf{p}_1) = 0$. Maslov, taking advantage of this fact, was able to "connect through" these caustic points with propagators such as in Eq. (2.12) and found that the phase factor gained is the first guess one would make, namely continue the square root of the determinant onto the next branch. This procedure can be done for other representation of the propagator as well as the initial value representation.[60] In each case, one finds that by continuing the square root of the pre-exponential determinant onto the next branch, one should have the proper phase in the exponent. Therefore, from henceforth, we shall omit the phase factor and include it as a part of the square root of the determinant.

2.2 Coherent State Propagator

After examining the various different IVR's, one is left with the impression that any of these can be useful for approximating the propagator. And, in principle, this is indeed the case. However, computationally, IVR's are not equivalent in their convenience and accuracy. Kay found that the most accurate IVR is the one found by Herman and Kluk[62,63] based on the coherent state representation:

$$\langle \mathbf{q}_2|e^{-i\hat{H}t/\hbar}|\mathbf{q}_1\rangle = (2\pi\hbar)^{-F}\int d\mathbf{p}_0\int d\mathbf{q}_0\, C_t(\mathbf{p}_0,\mathbf{q}_0)\langle \mathbf{q}_2|\mathbf{p}_t\mathbf{q}_t\rangle\langle \mathbf{p}_0\mathbf{q}_0|\mathbf{q}_1\rangle e^{iS_t(\mathbf{p}_0,\mathbf{q}_0)/\hbar} \quad (2.14a)$$

where $\mathbf{p}_t = \mathbf{p}_t(\mathbf{p}_0,\mathbf{q}_0)$ and $\mathbf{q}_t = \mathbf{q}_t(\mathbf{p}_0,\mathbf{q}_0)$ are momenta and coordinates of classical trajectories at time t with initial conditions $(\mathbf{p}_0,\mathbf{q}_0)$ and the coherent state are defined as

$$\langle \mathbf{x}|\mathbf{pq}\rangle = \left[\frac{\det(\gamma)}{\pi^F}\right]^{\frac{1}{4}} e^{-(\mathbf{x}-\mathbf{q})^T\cdot\frac{\gamma}{2}\cdot(\mathbf{x}-\mathbf{q})+\frac{i}{\hbar}\mathbf{p}\cdot(\mathbf{x}-\mathbf{q})}, \quad (2.14b)$$

where γ is, in general, a diagnol matrix. The pre-exponential factor, $C_t(\mathbf{p}_0,\mathbf{q}_0)$, depends on the coherent state parameters, and if the coherent states at time t is not the same as the coherent states at time 0, i.e., $\gamma_t \neq \gamma_0$, $C_t(\mathbf{p}_0,\mathbf{q}_0)$ is

$$C_t(\mathbf{p}_0,\mathbf{q}_0) = \sqrt{\det\left[\frac{1}{2}\left(\gamma_t^{\frac{1}{2}}\mathbf{M}_{\mathbf{qq}}\gamma_0^{-\frac{1}{2}} + \gamma_t^{-\frac{1}{2}}\mathbf{M}_{\mathbf{pp}}\gamma_0^{\frac{1}{2}} - i\hbar\gamma_t^{\frac{1}{2}}\mathbf{M}_{\mathbf{qp}}\gamma_0^{\frac{1}{2}} + \frac{i}{\hbar}\gamma_t^{-\frac{1}{2}}\mathbf{M}_{\mathbf{pq}}\gamma_0^{-\frac{1}{2}}\right)\right]}, \quad (2.14c)$$

where the various $F\times F$ matrices $\mathbf{M}_{\mathbf{qq}},\mathbf{M}_{\mathbf{qq}}$, etc, are parts of the $2F\times 2F$ monodromy matrix

$$\mathbf{M}(t) = \begin{pmatrix} \mathbf{M}_{\mathbf{qq}} & \mathbf{M}_{\mathbf{qp}} \\ \mathbf{M}_{\mathbf{pq}} & \mathbf{M}_{\mathbf{pp}} \end{pmatrix} = \begin{pmatrix} \partial\mathbf{q}_t/\partial\mathbf{q}_0 & \partial\mathbf{q}_t/\partial\mathbf{p}_0 \\ \partial\mathbf{p}_t/\partial\mathbf{q}_0 & \partial\mathbf{p}_t/\partial\mathbf{p}_0 \end{pmatrix}. \quad (2.15)$$

If $\gamma_t = \gamma_0 = \gamma\cdot\ I$, $C_t(\mathbf{p}_0,\mathbf{q}_0)$ reduces to

$$C_t(\mathbf{p}_0,\mathbf{q}_0) = \sqrt{\det\left[\frac{1}{2}\left(\mathbf{M}_{\mathbf{qq}} + \mathbf{M}_{\mathbf{pp}} - i\hbar\gamma\mathbf{M}_{\mathbf{qp}} + \frac{i}{\hbar\gamma}\mathbf{M}_{\mathbf{pq}}\right)\right]}. \quad (2.16)$$

The monodromy matrix is a measure of the distortion of phase space as a function of time. For instance, at time 0, an infinitesimal phase space volume could simply be a small cube, but at time t, the shape of this phase space volume will no longer be a cube; although the total volume is still the same as demanded by the Louiville theorem. The expansion and contraction of this cube along various coordinates is described by the monodromy matrix. Because phase space volume is conserved, $\det[\mathbf{M}(t)] = 1$ for all times. $\mathbf{M}$ is also a *simpletic* matrix, i.e., it satisfies

$$\mathbf{MJM}^T = \mathbf{J}, \quad (2.17)$$

where

$$\mathbf{J} = \begin{pmatrix} \mathbf{0} & \mathbf{I} \\ -\mathbf{I} & \mathbf{0} \end{pmatrix}. \tag{2.18}$$

From these relations, $\mathbf{M}^{-1}$ is very easy to find, since $\mathbf{J}^{-1} = -\mathbf{J} = \mathbf{J}^T$, it is simply

$$\mathbf{M}^{-1} = -\mathbf{J}\mathbf{M}^T\mathbf{J}, \tag{2.19}$$

or

$$\mathbf{M}^{-1} = \begin{pmatrix} \mathbf{M}_{\mathbf{pp}}^T & -\mathbf{M}_{\mathbf{qp}}^T \\ -\mathbf{M}_{\mathbf{pq}}^T & \mathbf{M}_{\mathbf{qq}}^T \end{pmatrix} \tag{2.20}$$

In pratice, the numerical calculation of $\mathbf{M}$ is accomplished by differentiating the Hamilton's equations with respect to the initial conditions: if we define $(\mathbf{q}, \mathbf{p}) = \mathbf{z}$ ($\mathbf{M}$ would then be $\partial \mathbf{z}_t / \partial \mathbf{z}_0$), then the Hamilton's equations are

$$\dot{\mathbf{z}}_t = \mathbf{J} \cdot \frac{\partial H}{\partial \mathbf{z}_t} \tag{2.21}$$

and the equations of motion for the monodromy matrix is

$$\dot{\mathbf{M}}(t) = \mathbf{J} \cdot \frac{\partial H}{\partial \mathbf{z}_t \partial \mathbf{z}_t} \cdot \mathbf{M}. \tag{2.22}$$

The coherent state propagator of Eq. (2.14) has been applied to many different problems in chemical dynamics including calculations of bound state wavefunctions and spectrum,[64,65] reactive scattering[66–68] and tunneling,[51] etc. In situations where the integration over initial conditions of trajectories in Eq. (2.14) can be done properly and except for certain problem potential where deep tunneling occurs,[69] the accuracy of this approach is clearly superior. Essentially all quantum mechanical effects are captured in this model. Besides its great accuracy, the coherent state IVR has some very appealing properties that make the semiclassical applications of it very convenient. First, this propagator is manifestly invariant under a canonical transformation that exchange $\mathbf{q}_0$ with $\mathbf{p}_0$ (after one scales away the γ and $\hbar$ factors), therefore it is a fully phase space IVR. Second, the distribution of initial conditions of the trajectories, $\langle \mathbf{p}_0 \mathbf{q}_0 | \psi \rangle$, is generally localized in $\mathbf{p}_0$ and $\mathbf{q}_0$ and therefore convenient for random sampling of the inital conditions. Third, if $\gamma \to \infty$, Eq. (2.14) reverts to the coordinate IVR of Eq. (2.9); and if $\gamma \to 0$, it becomes the momentum IVR of Eq. (2.13). Therefore the coherent state IVR can be thought off as an interpolation between the coordinate and momentum representation.

In most cases however, dynamical aspect of the problems usually prohibit the expediant calculations of the integral. This is because the behavior of the integrand in Eq. (2.14) (and all IVR's for that matter) is problematic for Monte Carlo methods. The classical action, which generally increases with time, makes the integrand more and more oscillatory as time becomes large. The magnitude of the pre-exponential factor $C_t(\mathbf{p}_0, \mathbf{q}_0)$ also increase with time roughly algebraically if the trajectory is regular, exponentially if the trajectory is chaotic. Thus for large times, we have an integrand that is oscillating rapidly with a large amplitude, it is difficult for Monte Carlo to average out these oscillations. This type of behavior is common in any SC-IVR approach where the complex integrands always cause difficulties in converging the integral. Needless to say, this convergence problem is the bottleneck for the application of semiclassical methods to large systems. Attempts to remedy this situation is an active area of research. Below, we shall discuss one of such attempts with stationary phase Monte Carlo (Filinov) techniques.

2.3 A New Derivation of the Coherent State Propagator

In this section, we present a new derivation of the coherent state propagator using general semiclassical relations for coherent states. Some of these results can be found in an article by Weissman,[70] although the connection to the initial value representation is new. We begin by considering a linear canonical transformation from $(\mathbf{q}, \mathbf{p})$ variables to $(\mathbf{Q}, \mathbf{P})$ where the new variables are

$$\mathbf{Q} = \left(\frac{\hbar}{2i}\right)^{\frac{1}{2}} \left(\sqrt{\gamma}\mathbf{q} - \frac{i}{\hbar\sqrt{\gamma}}\mathbf{p}\right), \tag{2.23a}$$

$$\mathbf{P} = \left(\frac{\hbar}{2i}\right)^{\frac{1}{2}} \left(\sqrt{\gamma}\mathbf{q} + \frac{i}{\hbar\sqrt{\gamma}}\mathbf{p}\right). \tag{2.23b}$$

These expressions can be written in a matrix form where

$$\begin{pmatrix} \mathbf{Q} \\ \mathbf{P} \end{pmatrix} = \mathbf{A} \cdot \begin{pmatrix} \mathbf{q} \\ \mathbf{p} \end{pmatrix} = \left(\frac{\hbar}{2i}\right)^{\frac{1}{2}} \begin{pmatrix} \sqrt{\gamma}\cdot\mathbf{I} & -\frac{i}{\hbar\sqrt{\gamma}}\cdot\mathbf{I} \\ \sqrt{\gamma}\cdot\mathbf{I} & \frac{i}{\hbar\sqrt{\gamma}}\cdot\mathbf{I} \end{pmatrix} \cdot \begin{pmatrix} \mathbf{q} \\ \mathbf{p} \end{pmatrix}, \tag{2.24}$$

and one can verify that the determinant of $\mathbf{A}$ is indeed one. The four generator functions of the canonical transformation, $F_1(\mathbf{q}, \mathbf{Q})$, $F_2(\mathbf{q}, \mathbf{P})$, $F_3(\mathbf{p}, \mathbf{Q})$, $F_4(\mathbf{p}, \mathbf{P})$ can be computed with the aid of the relations such as

$$\frac{\partial F_1}{\partial \mathbf{q}} = \mathbf{p},$$

$$\frac{\partial F_1}{\partial \mathbf{Q}} = -\mathbf{P}, \tag{2.25a}$$

and they are

$$F_1(\mathbf{q},\mathbf{Q}) = -\frac{\hbar}{i}\left[-\frac{\gamma}{2}\mathbf{q}^2 + \left(\frac{2i}{\hbar}\right)^{\frac{1}{2}}\sqrt{\gamma}\mathbf{q}\cdot\mathbf{Q} - \frac{i}{2\hbar}\mathbf{Q}^2\right], \tag{2.26a}$$

$$F_2(\mathbf{q},\mathbf{P}) = \frac{\hbar}{i}\left[-\frac{\gamma}{2}\mathbf{q}^2 + \left(\frac{2i}{\hbar}\right)^{\frac{1}{2}}\sqrt{\gamma}\mathbf{q}\cdot\mathbf{P} - \frac{i}{2\hbar}\mathbf{P}^2\right], \tag{2.26b}$$

$$F_3(\mathbf{p},\mathbf{Q}) = -\frac{\hbar}{i}\left[-\frac{1}{2\gamma\hbar^2}\mathbf{p}^2 + \left(\frac{2i}{\hbar}\right)^{\frac{1}{2}}\frac{i}{\hbar\sqrt{\gamma}}\mathbf{p}\cdot\mathbf{Q} + \frac{i}{2\hbar}\mathbf{Q}^2\right], \tag{2.26c}$$

$$F_4(\mathbf{p},\mathbf{P}) = \frac{\hbar}{i}\left[-\frac{1}{2\gamma\hbar^2}\mathbf{p}^2 - \left(\frac{2i}{\hbar}\right)^{\frac{1}{2}}\frac{i}{\hbar\sqrt{\gamma}}\mathbf{p}\cdot\mathbf{P} + \frac{i}{2\hbar}\mathbf{P}^2\right]. \tag{2.26d}$$

In terms of the old canonical variables, one can resubsitute in the definitions for $(\mathbf{Q},\mathbf{P})$, i.e.,

$$\mathbf{Q} = \left(\frac{\hbar}{2i}\right)^{\frac{1}{2}}\left(\sqrt{\gamma}\mathbf{q}_0 - \frac{i}{\hbar\sqrt{\gamma}}\mathbf{p}_0\right), \tag{2.27}$$

$$\mathbf{P} = \left(\frac{\hbar}{2i}\right)^{\frac{1}{2}}\left(\sqrt{\gamma}\mathbf{q}_0 + \frac{i}{\hbar\sqrt{\gamma}}\mathbf{p}_0\right),$$

then these generating functions can be re-expressed as

$$F_1 = -\frac{\hbar}{i}\left[-\frac{\gamma}{2}(\mathbf{q}-\mathbf{q}_0)^2 - \frac{i}{\hbar}(\mathbf{q}\cdot\mathbf{p}_0 - \mathbf{q}_0\cdot\mathbf{p}_0/2) + \frac{1}{2\hbar}|\mathbf{Q}|^2\right], \tag{2.28a}$$

$$F_2 = \frac{\hbar}{i}\left[-\frac{\gamma}{2}(\mathbf{q}-\mathbf{q}_0)^2 + \frac{i}{\hbar}(\mathbf{q}\cdot\mathbf{p}_0 - \mathbf{q}_0\cdot\mathbf{p}_0/2) + \frac{1}{2\hbar}|\mathbf{P}|^2\right], \tag{2.28b}$$

$$F_3 = -\frac{\hbar}{i}\left[-\frac{1}{2\gamma\hbar^2}(\mathbf{p}-\mathbf{p}_0)^2 + \frac{i}{\hbar}(\mathbf{p}\cdot\mathbf{q}_0 - \mathbf{q}_0\cdot\mathbf{p}_0/2) + \frac{1}{2\hbar}|\mathbf{Q}|^2\right], \tag{2.28c}$$

$$F_4 = \frac{\hbar}{i}\left[-\frac{1}{2\gamma\hbar^2}(\mathbf{p}-\mathbf{p}_0)^2 - \frac{i}{\hbar}(\mathbf{p}\cdot\mathbf{q}_0 - \mathbf{q}_0\cdot\mathbf{p}_0/2) + \frac{1}{2\hbar}|\mathbf{P}|^2\right]. \tag{2.28d}$$

The generating functions, (F_1', F_2', F_3', F_4'), for the inverse transformation where $(\mathbf{Q},\mathbf{P})$ are the old variables and $(\mathbf{q},\mathbf{p})$ are the new ones have a simple relationship with (F_1, F_2, F_3, F_4), they are

$$F_1' = -F_1, \tag{2.29a}$$

$$F_2' = -F_3, \tag{2.29b}$$

$$F_3' = -F_2, \tag{2.29c}$$

$$F_4' = -F_4. \tag{2.29d}$$

The purpose of finding these generating functions is to obtain semiclassical expressions for complex ampitudes $\langle \mathbf{Q}|\mathbf{q}\rangle$, $\langle \mathbf{Q}|\mathbf{p}\rangle$, $\langle \mathbf{q}|\mathbf{P}\rangle$ and $\langle \mathbf{p}|\mathbf{P}\rangle$. These types of amplitudes where $(\mathbf{Q},\mathbf{P})$ and $(\mathbf{q},\mathbf{p})$ are connected by canonical transformations are extensively discussed by Miller.[35] However, the application of Miller's formuli here is not as straight forward because $(\mathbf{Q},\mathbf{P})$ are *complex* variables. In this case, however, we are helped by the fact that eigenfunctions of the operators $(\hat{\mathbf{Q}},\hat{\mathbf{P}})$ where

$$\hat{\mathbf{Q}} = \left(\frac{\hbar}{2i}\right)^{\frac{1}{2}}\left(\sqrt{\gamma}\hat{\mathbf{q}}_0 - \frac{i}{\hbar\sqrt{\gamma}}\hat{\mathbf{p}}_0\right),$$
$$\hat{\mathbf{P}} = \left(\frac{\hbar}{2i}\right)^{\frac{1}{2}}\left(\sqrt{\gamma}\hat{\mathbf{q}}_0 + \frac{i}{\hbar\sqrt{\gamma}}\hat{\mathbf{p}}_0\right), \tag{2.30}$$

can be obtained directly. The details of this calculation is in fact trivial, and we have

$$\begin{aligned}
\langle \mathbf{Q}|\mathbf{q}\rangle &= (2\pi\hbar/i)^{-\frac{1}{4}}\left(\frac{\partial^2 F_1'}{\partial\mathbf{Q}\partial\mathbf{q}}\right)^{\frac{1}{2}}\exp\left(\frac{i}{\hbar}F_1' - \frac{1}{2\hbar}|\mathbf{Q}|^2\right)\\
&= \left(\frac{\gamma}{\pi}\right)^{\frac{1}{4}}\exp\left[-\frac{\gamma}{2}(\mathbf{q}-\mathbf{q}_0)^2 - \frac{i}{\hbar}(\mathbf{q}\cdot\mathbf{p}_0 - \mathbf{q}_0\cdot\mathbf{p}_0/2)\right], \qquad (2.31a)\\
\langle \mathbf{Q}|\mathbf{p}\rangle &= (2\pi\hbar/i)^{-\frac{1}{4}}\left(\frac{\partial^2 F_2'}{\partial\mathbf{Q}\partial\mathbf{p}}\right)^{\frac{1}{2}}\exp\left(\frac{i}{\hbar}F_2' - \frac{1}{2\hbar}|\mathbf{Q}|^2\right)\\
&= \left(\frac{1}{\gamma\pi\hbar^2}\right)^{\frac{1}{4}}\exp\left[-\frac{1}{2\gamma\hbar^2}(\mathbf{p}-\mathbf{p}_0)^2 + \frac{i}{\hbar}(\mathbf{p}\cdot\mathbf{q}_0 - \mathbf{q}_0\cdot\mathbf{p}_0/2)\right], \qquad (2.31b)\\
\langle \mathbf{q}|\mathbf{P}\rangle &= (2\pi\hbar/i)^{-\frac{1}{4}}\left(\frac{\partial^2 F_2}{\partial\mathbf{P}\partial\mathbf{q}}\right)^{\frac{1}{2}}\exp\left(\frac{i}{\hbar}F_2 - \frac{1}{2\hbar}|\mathbf{P}|^2\right)\\
&= \left(\frac{\gamma}{\pi}\right)^{\frac{1}{4}}\exp\left[-\frac{\gamma}{2}(\mathbf{q}-\mathbf{q}_0)^2 + \frac{i}{\hbar}(\mathbf{q}\cdot\mathbf{p}_0 - \mathbf{q}_0\cdot\mathbf{p}_0/2)\right], \qquad (2.31c)\\
\langle \mathbf{p}|\mathbf{P}\rangle &= (2\pi\hbar/i)^{-\frac{1}{4}}\left(\frac{\partial^2 F_4}{\partial\mathbf{P}\partial\mathbf{p}}\right)^{\frac{1}{2}}\exp\left(\frac{i}{\hbar}F_4 - \frac{1}{2\hbar}|\mathbf{P}|^2\right)\\
&= \left(\frac{1}{\gamma\pi\hbar^2}\right)^{\frac{1}{4}}\exp\left[-\frac{1}{2\gamma\hbar^2}(\mathbf{p}-\mathbf{p}_0)^2 - \frac{i}{\hbar}(\mathbf{p}\cdot\mathbf{q}_0 - \mathbf{q}_0\cdot\mathbf{p}_0/2)\right]. \qquad (2.31d)
\end{aligned}$$

These ampitudes are commonly referred to as coherent states. One sees their explicit relationship with classical canonical transformations. The other four possible amplitudes, $\langle \mathbf{q}|\mathbf{Q}\rangle$, $\langle \mathbf{p}|\mathbf{Q}\rangle$, $\langle \mathbf{P}|\mathbf{q}\rangle$ and $\langle \mathbf{P}|\mathbf{p}\rangle$ can also be related to the generator functions but one sees that these amplitudes are in fact *not normalizable* (the real part of the exponents are positive) and therefore are unphysical. Thus the relevant bra and ket here are $|\mathbf{P}\rangle$ and $\langle \mathbf{Q}|$

and the identity operator in terms of them is

$$\hat{\mathbf{I}} = (2\pi\hbar)^{-F} \int d\mathbf{p}_0 \int d\mathbf{q}_0 \, |\mathbf{P}\rangle\langle\mathbf{Q}|. \tag{2.32}$$

With the help of Eq. (2.32), the coherent state representation for the matrix element of the propagator is

$$\langle \mathbf{q}_2 | e^{-i\hat{H}t/\hbar} | \mathbf{q}_1 \rangle = (2\pi\hbar)^{-2F} \int d\mathbf{p}_0' d\mathbf{q}_0' \int d\mathbf{p}_0 d\mathbf{q}_0 \langle \mathbf{q}_2 | \mathbf{P}_2 \rangle \langle \mathbf{Q}_2 | e^{-i\hat{H}t/\hbar} | \mathbf{P}_1 \rangle \langle \mathbf{Q}_1 | \mathbf{q}_1 \rangle, \tag{2.33}$$

where

$$\begin{aligned} \mathbf{Q}_1 &= \left(\frac{\hbar}{2i}\right)^{\frac{1}{2}} \left(\sqrt{\gamma}\mathbf{q}_0 - \frac{i}{\hbar\sqrt{\gamma}}\mathbf{p}_0\right), \qquad \mathbf{Q}_2 = \left(\frac{\hbar}{2i}\right)^{\frac{1}{2}} \left(\sqrt{\gamma}\mathbf{q}_0' - \frac{i}{\hbar\sqrt{\gamma}}\mathbf{p}_0'\right), \\ \mathbf{P}_1 &= \left(\frac{\hbar}{2i}\right)^{\frac{1}{2}} \left(\sqrt{\gamma}\mathbf{q}_0 + \frac{i}{\hbar\sqrt{\gamma}}\mathbf{p}_0\right), \qquad \mathbf{P}_2 = \left(\frac{\hbar}{2i}\right)^{\frac{1}{2}} \left(\sqrt{\gamma}\mathbf{q}_0' + \frac{i}{\hbar\sqrt{\gamma}}\mathbf{p}_0'\right). \end{aligned} \tag{2.34}$$

The quantity we need to evaluate is then the matrix element $\langle \mathbf{Q}_2 | e^{-i\hat{H}t/\hbar} | \mathbf{P}_1 \rangle$. Many authors[70,39,40,71,72] have studied this quantity semiclassically and the formula is in fact well known for a long time. Again, the standard semiclassical formula of the Van Vleck-Gutzwiller form in Eq. (2.3) does not apply because $(\mathbf{Q}_1, \mathbf{P}_1)$ are complex numbers. The correct formula[70] is the following

$$\langle \mathbf{Q}_2 | e^{-i\hat{H}t/\hbar} | \mathbf{P}_1 \rangle = \det \left(\frac{\partial^2 G}{\partial \mathbf{Q}_2 \partial \mathbf{P}_1} \right)^{\frac{1}{2}} \exp \left[\frac{i}{\hbar} G - \frac{1}{2\hbar} (|\mathbf{Q}_2|^2 + |\mathbf{P}_1|^2) \right], \tag{2.35}$$

where G is the standard classical generator that correspond to the canonical transformation of taking $\mathbf{P}_1$ at time 0 to $\mathbf{Q}_2$ at time t,

$$G = \int_0^t \mathbf{P}(\tau) \cdot \dot{\mathbf{Q}}(\tau) - H[\mathbf{P}(\tau), \mathbf{Q}(\tau)] d\tau + \mathbf{Q}_1 \cdot \mathbf{P}_1. \tag{2.36}$$

The meaning of Eq. (2.35) is somewhat similar to the Van Vleck-Gutzwiller propagator, namely one searches for all paths that connects $\mathbf{P}_1$ with $\mathbf{Q}_2$ in time t. Actually, "all paths" is not correct, there is always only *one* path because by specifying $\mathbf{P}_1$ we have specified a *distinct* initial condition $(\mathbf{p}_0, \mathbf{q}_0)$ and the subsequent classical trajectory is determined. Another feature that is different from the standard SC propagator is that if there is no classical trajectory that connects $\mathbf{P}_1$ with $\mathbf{Q}_2$, the amplitude $\langle \mathbf{Q}_2 | e^{-i\hat{H}t/\hbar} | \mathbf{P}_1 \rangle$ is not zero because the overlap $\langle \mathbf{Q}_2 | \mathbf{P}_t \rangle$ is not zero. [Here, $(\mathbf{Q}_t, \mathbf{P}_t)$ is the classical trajectory at time t with initial condition being $\mathbf{P}_1$.] This is the point where different authors have different views. Some[73] propose that one really should look for *non-classical* (complex) trajectories

that connects $\mathbf{P}_1$ with $\mathbf{Q}_2$, and one can indeed proceed from there. Here, however, we restrict ourselves with *classical* paths and simply write the propagator as

$$\begin{aligned}\langle \mathbf{Q}_2|e^{-i\hat{H}t/\hbar}|\mathbf{P}_1\rangle &\approx \langle \mathbf{Q}_2|\mathbf{P}_t\rangle\langle \mathbf{Q}_t|e^{-i\hat{H}t/\hbar}|\mathbf{P}_1\rangle \\ &= \det\left(\frac{\partial^2 G}{\partial \mathbf{Q}_t \partial \mathbf{P}_1}\right)^{\frac{1}{2}} \exp\left[\frac{i}{\hbar}G - \frac{1}{2\hbar}(|\mathbf{Q}_t|^2+|\mathbf{P}_1|^2)\right]\langle \mathbf{Q}_2|\mathbf{P}_t\rangle. \quad (2.37)\end{aligned}$$

The meaning of Eq. (2.37) is this: for every $\mathbf{P}_1$, we initiate a classical trajectory for which at time t, it becomes $(\mathbf{Q}_t, \mathbf{P}_t)$, we then simply multiply the overlap factor $\langle \mathbf{Q}_2|\mathbf{P}_t\rangle$ to obtain the semiclassical amplitude. With this approximation, the integral over $(\mathbf{p}_0', \mathbf{q}_0')$ in Eq. (2.33) can be done analytically to give

$$\begin{aligned}\langle \mathbf{q}_2|e^{-i\hat{H}t/\hbar}|\mathbf{q}_1\rangle &= (2\pi\hbar)^{-F}\int d\mathbf{p}_0 d\mathbf{q}_0 \langle \mathbf{q}_2|\mathbf{P}_t\rangle\langle \mathbf{Q}_1|\mathbf{q}_1\rangle \\ &\times \det\left(\frac{\partial^2 G}{\partial \mathbf{Q}_t \partial \mathbf{P}_1}\right)^{\frac{1}{2}} \exp\left[\frac{i}{\hbar}G - \frac{1}{2\hbar}(|\mathbf{Q}_t|^2+|\mathbf{P}_1|^2)\right]. \quad (2.38)\end{aligned}$$

The final step is to re-express Eq. (2.38) in terms of standard classical variables $(\mathbf{q}, \mathbf{p})$. For G in Eq. (2.36), $H[\mathbf{P}, \mathbf{Q}] = H[\mathbf{p}, \mathbf{q}]$ and is unchanged; the other part is

$$\begin{aligned}\int_0^t \mathbf{P}(\tau)\cdot\dot{\mathbf{Q}}(\tau)d\tau + \mathbf{Q}_1\cdot\mathbf{P}_1 &= \frac{\hbar}{2i}\int \gamma\mathbf{q}\cdot\dot{\mathbf{q}} + \frac{\mathbf{p}\cdot\dot{\mathbf{p}}}{\gamma\hbar^2} + \frac{i}{\hbar}(\mathbf{p}\cdot\dot{\mathbf{q}} - \mathbf{q}\cdot\dot{\mathbf{p}})d\tau \\ &\quad + \frac{\hbar}{2i}(\gamma\mathbf{q}_0^2 + \frac{1}{\gamma\hbar^2}\mathbf{p}_0^2) \\ &= \frac{\hbar}{4i}\left[\gamma(\mathbf{q}_t^2+\mathbf{q}_0^2) + \frac{1}{\gamma\hbar^2}(\mathbf{p}_t^2+\mathbf{p}_0^2)\right] \\ &\quad - \frac{1}{2}(\mathbf{p}_t\cdot\mathbf{q}_t - \mathbf{p}_0\cdot\mathbf{q}_0) + \int \mathbf{p}\cdot\dot{\mathbf{q}}\, d\tau. \quad (2.39)\end{aligned}$$

Combining everything, the exponent is

$$\frac{i}{\hbar}G - \frac{1}{2\hbar}(|\mathbf{Q}_t|^2+|\mathbf{P}_1|^2) = \frac{i}{\hbar}\int_0^t \mathbf{p}\cdot\dot{\mathbf{q}} - H[\mathbf{p}(\tau),\mathbf{q}(\tau)]\, d\tau - \frac{i}{2\hbar}(\mathbf{p}_t\cdot\mathbf{q}_t - \mathbf{p}_0\cdot\mathbf{q}_0). \quad (2.40)$$

The last quantity that needs to be explained is the pre-exponential factor which by using standard derivative relations is

$$\left(\frac{\partial^2 G}{\partial \mathbf{Q}_t \partial \mathbf{P}_1}\right)^{\frac{1}{2}} = \left(\frac{\partial \mathbf{P}_t}{\partial \mathbf{P}_1}\right)^{\frac{1}{2}}. \quad (2.41)$$

$\partial\mathbf{P}_t/\partial\mathbf{P}_1$ is a part of the monodromy matrix $\mathbf{m} \equiv \partial\mathbf{Z}_t/\partial\mathbf{Z}_1$ where $\mathbf{Z} = (\mathbf{Q}, \mathbf{P})$, an explicity formula for which can be obtained using the transformation equation

$$\mathbf{m} = \mathbf{A}\mathbf{M}\mathbf{A}^{-1}, \quad (2.42)$$

where $\mathbf{A}$ is the matrix appearing in Eq. (2.24) and $\mathbf{M}$ is the monodromy matrix in the $(\mathbf{p},\mathbf{q})$ coordinates. One can verify that $[\det(\partial\mathbf{P}_t/\partial\mathbf{P}_1)]^{\frac{1}{2}}$ is indeed $C_t(\mathbf{p}_0,\mathbf{q}_0)$ of Eq. (2.16). Pulling everything together, we arrive at the expression

$$\begin{aligned}\langle\mathbf{q}_2|e^{-i\hat{H}t/\hbar}|\mathbf{q}_1\rangle &= (2\pi\hbar)^{-F}\int d\mathbf{p}_0 d\mathbf{q}_0 \langle\mathbf{q}_2|\mathbf{P}_t\rangle\langle\mathbf{Q}_1|\mathbf{q}_1\rangle \\ &\times C_t(\mathbf{p}_0,\mathbf{q}_0)\exp\left[\frac{i}{\hbar}S_t(\mathbf{p}_0,\mathbf{q}_0)-\frac{i}{2\hbar}(\mathbf{p}_t\cdot\mathbf{q}_t-\mathbf{p}_0\cdot\mathbf{q}_0)\right], \quad (2.43)\end{aligned}$$

which is identical to the Herman-Kluk propagator of Eq. (2.14).

2.4 Stationary Phase Monte Carlo

With the coherent state propagator, applications to different chemical systems is in principle black box. But, as we have discussed earlier, the actual implementation is usually unfeasible due to the oscillatory nature of the integrand. This is especially acute when the dynamics of the system is chaotic. A method of remedying of this problem is usually term stationary phase Monte Carlo,[74,75] although the actual application has been around for a long time in different contexts. One example that I can think of is the Husumi distribution function of an operator $\hat{A}$ which is defined as

$$A_h(\mathbf{p},\mathbf{q}) = (2\pi\hbar)^{-F}\int d\mathbf{p}'\int d\mathbf{q}' e^{-\frac{\alpha}{2}(\mathbf{q}-\mathbf{q}')^2-(\mathbf{p}-\mathbf{p}')^2/(2\alpha\hbar^2)}A_w(\mathbf{p}',\mathbf{q}') = \langle\mathbf{pq}|\hat{A}|\mathbf{pq}\rangle, \quad (2.44)$$

where $A_w(\mathbf{p},\mathbf{q})$ is the corresponding Wigner distribution. By integrating the Wigner distribution (which can be oscillatory) with the Gaussian factors, the resulting Husumi function is less oscillatory. Filinov[76] was the first to suggest it for path integral calculations and we shall frequently term this method as the Filinov transformation also.

We first describe this simple procedure for "smoothing" and "filtering" an oscillatory integrand with an one dimensional example. Given an integral of the form

$$I = \int dx g(x) e^{f(x)}, \quad (2.45)$$

where f and g are complex, one can insert in an identity integral

$$I = \int dx dy \left(\frac{c}{2\pi}\right)^{\frac{1}{2}} g(x) e^{f(x)} e^{-\frac{c}{2}(x-y)^2}, \quad (2.46)$$

and expand $f(x)$ around y, usually to the second order,

$$f(x) \approx f(y) + f'(y)(y-x) + \frac{1}{2}f''(y)(y-x)^2. \quad (2.47)$$

The integration over x can now be performed to yield,

$$I \approx \int dy \left(\frac{c}{c - f''(y)}\right)^{\frac{1}{2}} g(y) \exp\left[\frac{f'(y)^2}{2(c - f''(y))} + f(y)\right]. \tag{2.48}$$

Here, we have set $g(x) = g(y)$ as what is customarily done. It is in principle more correct if we expanded $g(x)$ also, but for SC-IVR applications, this expansion is generally too cumbersome. In addition to this standard Filinov transformation, one perhaps can also benefit from a modified version. If one assumes that the second derivative of f is relatively smooth or constant, we can redefine the Filinov parameter as $c' = c - f''(y)$ and arrive at the expression

$$I \approx \int dy \left(\frac{c' + f''(y)}{c'}\right)^{\frac{1}{2}} g(y) \exp\left[\frac{f'(y)^2}{2c'} + f(y)\right]. \tag{2.49}$$

Notice that the dependence one f'' is kept in the pre-exponential factor. Alternatively, the f'' can be neglected completely, as Herman[77] has done, to obtain

$$I \approx \int dy g(y) \exp\left[\frac{f'(y)^2}{2c'} + f(y)\right]. \tag{2.50}$$

It is apparent from these equations that in the limit of $c = \infty$, we recover the original integral of Eq. 2.45. Thus, the Filinov parameter cannot be too large or we are confronted with the same oscillatory integral as before. However, it is important to have a sufficiently large c for several reasons. First, in the large c limit, the second order expansion is more accurate. Second, it is clear that the real part of the factor $f'(y)^2/(c - f''(y))$ must be negative or otherwise positive but small. A large c will prevent the integrand from becoming exponentially large. Thus, one expects the answer to be optimal for certain large values of c. We also desire that the integral becomes independent of c for a range of different values and within this range is the optimal value.

The Filinov transformation can now be applied to the semiclassical IVR methods with the hope that the transformed integrand will be better behaved numerically. There is however a great amount of flexibility and ambiguity in applying the Filinov transformation for the following reasons: 1) there are many versions of IVR's that one can begin with, 2) one can apply the Filinov transformation to the integration of initial momentum or initial position or both, 3) it is not trivial to identify the functions f and g. In principle, g should be a smooth function and f is the Log of the rapidly changing part. The choice for most of the applications so far seems to be $f = iS(\mathbf{p}, \mathbf{q})/\hbar$ or $f = iS(\mathbf{p}, \mathbf{q})/\hbar$ plus phase factors

from the wavefunction, the rest is set to g. However, this choice certainly does not leave g a smooth function of the initial conditions. In fact, for chaotic systems, this factor is a highly irregular function. Nevertheless, this choice of f and g is analytically tractable and thus is adopted.

If $f = iS(\mathbf{q},\mathbf{p})/\hbar$, we need to have the expansion to the second order for the classical action. Expanding around $(\mathbf{q}',\mathbf{p}')$, and defining $\delta\mathbf{q} = \mathbf{q} - \mathbf{q}'$, $\delta\mathbf{p} = \mathbf{p} - \mathbf{p}'$, we have

$$\begin{aligned} S(\mathbf{q},\mathbf{p}) &= S(\mathbf{q}',\mathbf{p}') + \frac{\partial S}{\partial \mathbf{q}'}\cdot\delta\mathbf{q} + \frac{\partial S}{\partial \mathbf{p}'}\cdot\delta\mathbf{p} + \frac{1}{2}\delta\mathbf{q}\cdot\frac{\partial^2 S}{\partial\mathbf{q}'\partial\mathbf{q}'}\cdot\delta\mathbf{q} \\ &\quad + \frac{1}{2}\delta\mathbf{q}\cdot\frac{\partial^2 S}{\partial\mathbf{q}'\partial\mathbf{p}'}\cdot\delta\mathbf{p} + \frac{1}{2}\delta\mathbf{p}\cdot\frac{\partial^2 S}{\partial\mathbf{p}'\partial\mathbf{q}'}\cdot\delta\mathbf{q} + \frac{1}{2}\delta\mathbf{p}\cdot\frac{\partial^2 S}{\partial\mathbf{p}'\partial\mathbf{p}'}\cdot\delta\mathbf{p}. \end{aligned} \tag{2.51}$$

The first derivatives of the action are

$$\frac{\partial S}{\partial \mathbf{q}'} = \mathbf{p}_t'^T\cdot\mathbf{M_{qq}} - \mathbf{p}', \tag{2.52a}$$

$$\frac{\partial S}{\partial \mathbf{p}'} = \mathbf{p}_t'^T\cdot\mathbf{M_{qp}}, \tag{2.52b}$$

and the second derivatives are approximately,

$$\frac{\partial^2 S}{\partial\mathbf{q}'\partial\mathbf{q}'} = \frac{\partial\mathbf{p}_t'}{\partial\mathbf{q}'}\cdot\mathbf{M_{qq}} = \mathbf{M_{pq}^T}\cdot\mathbf{M_{qq}}, \tag{2.53a}$$

$$\frac{\partial^2 S}{\partial\mathbf{p}'\partial\mathbf{q}'} = \frac{\partial\mathbf{p}_t'}{\partial\mathbf{p}'}\cdot\mathbf{M_{qq}} - \mathbf{I} = \mathbf{M_{pp}^T}\cdot\mathbf{M_{qq}} - \mathbf{I}, \tag{2.53b}$$

$$\frac{\partial^2 S}{\partial\mathbf{q}'\partial\mathbf{p}'} = \frac{\partial\mathbf{p}_t'}{\partial\mathbf{q}'}\cdot\mathbf{M_{qp}} = \mathbf{M_{pq}^T}\cdot\mathbf{M_{qp}}, \tag{2.53c}$$

$$\frac{\partial^2 S}{\partial\mathbf{p}'\partial\mathbf{p}'} = \frac{\partial\mathbf{p}_t'}{\partial\mathbf{p}'}\cdot\mathbf{M_{qp}} = \mathbf{M_{pp}^T}\cdot\mathbf{M_{qp}}, \tag{2.53d}$$

where we have followed the convention of neglecting terms such as

$$\mathbf{p}_t'^T\cdot\frac{\partial\mathbf{M_{qq}}}{\partial\mathbf{q}'}. \tag{2.54}$$

The reason for doing this is often attributed to the fact that in the harmonic case, these terms vanish, but it is also for convenience because if these terms are kept, they will require a calculational effort that scales as the cube of the number of degrees of freedom. However, since the second derivatives of the action are symmetric matrices, one needs to artificially impose the symmetric condition by taking an average of these matrices with their transpose, i.e.,

$$\frac{\partial^2 S}{\partial\mathbf{q}'\partial\mathbf{q}'} = \frac{1}{2}(\mathbf{M_{pq}^T}\cdot\mathbf{M_{qq}} + \mathbf{M_{qq}^T}\cdot\mathbf{M_{pq}}), \tag{2.55}$$

and so on.

Another choice for the function f is to include the phase factors from the wavefunctions. To illustrate this, the most convenient case is when the wavefunction is a coherent state, i.e.,

$$\phi(\mathbf{x}) = \left(\frac{\gamma}{\pi}\right)^{\frac{F}{4}} e^{-\frac{\gamma}{2}(\mathbf{x}-\mathbf{q})^2+\frac{i}{\hbar}\mathbf{p}\cdot(\mathbf{x}-\mathbf{q})}. \tag{2.56}$$

Since the phase factors coming from the coherent state are explicitly quadratic in $(\mathbf{q},\mathbf{p})$, we simply have to expand the trajectories to first order to obtain the second derivatives, namely

$$\mathbf{q}_t(\mathbf{q},\mathbf{p}) = \mathbf{q}_t(\mathbf{q}',\mathbf{p}') + \mathbf{M}_{\mathbf{qq}}\cdot\delta\mathbf{q} + \mathbf{M}_{\mathbf{qp}}\cdot\delta\mathbf{p}, \tag{2.57a}$$

$$\mathbf{p}_t(\mathbf{q},\mathbf{p}) = \mathbf{p}_t(\mathbf{q}',\mathbf{p}') + \mathbf{M}_{\mathbf{pq}}\cdot\delta\mathbf{q} + \mathbf{M}_{\mathbf{pp}}\cdot\delta\mathbf{p}. \tag{2.57b}$$

This is the so called linearized dynamics. For other forms of the wavefunction, the expansion in Eq. (2.57) is also possible, but general analytic formuli are not usually feasible.

2.4.1 Filinov Transformation on the Herman-Kluk IVR

Given these different ways of implementing the Filinov transformation, one is left with no choice but to try them all. And, we have performed an extensive study of the various possibilities by applying it to different IVR's [such as Eq. (2.9) and (2.13)] with different choices for f and g. The short of the story is that the most effective of these is when the Filinov transformation is performed on both $(\mathbf{q},\mathbf{p})$ for the coherent state IVR of Eq. (2.14). Walton and Manolopoulos[64] first suggested this approach.

Starting with the expression for the transition probability,

$$\begin{aligned}\langle\phi_2|e^{-i\hat{H}t/\hbar}|\phi_1\rangle &= (2\pi\hbar)^{-F}\int d\mathbf{p}_0 d\mathbf{q}_0\, C_t(\mathbf{p}_0,\mathbf{q}_0)e^{iS(\mathbf{q}_0,\mathbf{p}_0)/\hbar} \\ &\times\ e^{-\frac{\gamma}{4}(\mathbf{q}_0-\mathbf{q}_i)^2+\frac{i}{2\hbar}(\mathbf{q}_0-\mathbf{q}_i)\cdot(\mathbf{p}_0+\mathbf{p}_i)-\frac{(\mathbf{p}_0-\mathbf{p}_i)^2}{4\gamma\hbar^2}} \\ &\times\ e^{-\frac{\gamma}{4}(\mathbf{q}_t-\mathbf{q}_f)^2-\frac{i}{2\hbar}(\mathbf{q}_t-\mathbf{q}_f)\cdot(\mathbf{p}_t+\mathbf{p}_f)-\frac{(\mathbf{p}_t-\mathbf{p}_f)^2}{4\gamma\hbar^2}},\end{aligned} \tag{2.58}$$

where $(\mathbf{p}_{i,f},\mathbf{q}_{i,f})$ are the centers of the initial and final wavefunctions $\phi_{1,2}$ (they are coherent states also). Including everything that appears in the exponent for the function f and using the Filinov transformation in Eq. (2.48), Walton and Manolopolous obtained

$$\begin{aligned}\langle\phi_2|e^{-i\hat{H}t/\hbar}|\phi_1\rangle &= (2\pi\hbar)^{-F}\int d\mathbf{p}_0 d\mathbf{q}_0 \left(\frac{\alpha\beta}{4}\right)^{\frac{F}{2}}\frac{C_t(\mathbf{p}_0,\mathbf{q}_0)}{\det(\mathbf{U})} \\ &\times\ e^{iS(\mathbf{p}_0,\mathbf{q}_0)/\hbar}\exp\left[+\frac{1}{4}\mathbf{z}^T\cdot\mathbf{U}\cdot\mathbf{z}-y\right],\end{aligned} \tag{2.59}$$

where

$$\mathbf{U_{qq}} = \frac{\gamma}{4}\mathbf{M}_{\mathbf{qq}}^T \cdot \mathbf{M_{qq}} + \frac{\mathbf{M}_{\mathbf{pq}}^T \cdot \mathbf{M_{pq}}}{4\gamma\hbar^2} + (\frac{\gamma}{4} + \frac{\alpha}{2}) \cdot \mathbf{I}, \tag{2.60a}$$

$$\mathbf{U_{qp}} = \frac{\gamma}{4}\mathbf{M}_{\mathbf{qq}}^T \cdot \mathbf{M_{qp}} + \frac{\mathbf{M}_{\mathbf{pq}}^T \cdot \mathbf{M_{pp}}}{4\gamma\hbar^2}, \tag{2.60b}$$

$$\mathbf{U_{pq}} = \frac{\gamma}{4}\mathbf{M}_{\mathbf{qp}}^T \cdot \mathbf{M_{qq}} + \frac{\mathbf{M}_{\mathbf{pp}}^T \cdot \mathbf{M_{pq}}}{4\gamma\hbar^2}, \tag{2.60c}$$

$$\mathbf{U_{pp}} = \frac{\gamma}{4}\mathbf{M}_{\mathbf{qp}}^T \cdot \mathbf{M_{qp}} + \frac{\mathbf{M}_{\mathbf{pp}}^T \cdot \mathbf{M_{pp}}}{4\gamma\hbar^2} + (\frac{1}{4\gamma\hbar^2} + \frac{\beta}{2}) \cdot \mathbf{I}, \tag{2.60d}$$

$$\begin{aligned}\mathbf{z_q} &= \frac{\gamma}{2}\left[\mathbf{M}_{\mathbf{qq}}^T \cdot (\mathbf{q}_t - \mathbf{q}_f) + (\mathbf{q}_0 - \mathbf{q}_i)\right] + \frac{1}{2\gamma\hbar^2}\mathbf{M}_{\mathbf{pq}}^T \cdot (\mathbf{p}_t - \mathbf{p}_f) \\ &+ \frac{i}{2\hbar}\left[\mathbf{M}_{\mathbf{pq}}^T \cdot (\mathbf{q}_t - \mathbf{q}_f) - \mathbf{M}_{\mathbf{qq}}^T \cdot (\mathbf{p}_t - \mathbf{p}_f) + (\mathbf{p}_0 - \mathbf{p}_i)\right], \end{aligned} \tag{2.60e}$$

$$\begin{aligned}\mathbf{z_p} &= \frac{\gamma}{2}\left[\mathbf{M}_{\mathbf{qp}}^T \cdot (\mathbf{q}_t - \mathbf{q}_f)\right] + \frac{1}{2\gamma\hbar^2}\left[\mathbf{M}_{\mathbf{pp}}^T \cdot (\mathbf{p}_t - \mathbf{p}_f) + (\mathbf{p}_0 - \mathbf{p}_i)\right] \\ &+ \frac{i}{2\hbar}\left[\mathbf{M}_{\mathbf{pp}}^T \cdot (\mathbf{q}_t - \mathbf{q}_f) - \mathbf{M}_{\mathbf{qp}}^T \cdot (\mathbf{p}_t - \mathbf{p}_f) - (\mathbf{q}_0 - \mathbf{q}_i)\right], \end{aligned} \tag{2.60f}$$

and

$$\begin{aligned} y &= \frac{\gamma}{4}(\mathbf{q}_0 - \mathbf{q}_i)^2 - \frac{i}{2\hbar}(\mathbf{q}_0 - \mathbf{q}_i) \cdot (\mathbf{p}_0 + \mathbf{p}_i) + \frac{(\mathbf{p}_0 - \mathbf{p}_i)^2}{4\gamma\hbar^2} \\ &+ \frac{\gamma}{4}(\mathbf{q}_t - \mathbf{q}_f)^2 + \frac{i}{2\hbar}(\mathbf{q}_t - \mathbf{q}_f) \cdot (\mathbf{p}_t + \mathbf{p}_f) + \frac{(\mathbf{p}_t - \mathbf{p}_f)^2}{4\gamma\hbar^2}. \end{aligned} \tag{2.60g}$$

An important observation here is that the matrix $\mathbf{U}$ is already symmetric, there is no need to further symmetrize the second derivative of f.

We found that this IVR is very well behaved even for highly chaotic systems. The integrands are still oscillatory, however the amplitudes of the oscillations are much damped due to the det($\mathbf{U}$) factor in the denominator. The question that can be raised is: since the integrand is vastly different after the Filinov transformation, is the end result still accurate? The answer is, numerical tests (as we will see in the HCl dimer example below) seem to indicate that this is the case. Since the problem trajectories are the chaotic ones, and if the assumption that these trajectories will eventually contribute very little or be averaged out by other chaotic trajectories is true, then including them approximately as we have done in the integral presumably will not effect the final answer drastically. Others[57] have advocated removing these highly chaotic trajectories altogether. Personally, I do not believe this can be successful in every case because chaotic trajectories especially chaotic periodic orbits do contribute as we have seen in Gutzwiller's trace formula.

2.4.2 Other Filinov IVR's

For comparison purposes, we include here the some other Filinov IVR's that have been useful in the past. One of the earliest example[78] of the Filinov transformation applied to IVR expressions is actually based on the modified version of Eq. (2.49) applied to the momentum integral of Eq. (2.13). Taking $f = i[S(\mathbf{p}_0, \mathbf{q}_0) + \mathbf{p}_t \cdot (\mathbf{q}_1 - \mathbf{q}_t)]/\hbar$, the end result is,

$$\begin{aligned} \langle \mathbf{q}_1 | e^{-i\hat{H}t/\hbar} | \mathbf{q}_0 \rangle &= (2\pi\hbar)^{-F} \int d\mathbf{p}_0 \sqrt{\det\left(\mathbf{M}_{\mathbf{pp}} - i\mathbf{A} \cdot \mathbf{M}_{\mathbf{qp}}\right)} \\ & \quad e^{-(\mathbf{q}_1 - \mathbf{q}_t)^T \cdot \frac{\mathbf{A}}{2} \cdot (\mathbf{q}_1 - \mathbf{q}_t) + i[S(\mathbf{p}_0, \mathbf{q}_0) + \mathbf{p}_t \cdot (\mathbf{q}_1 - \mathbf{q}_t]/\hbar}. \end{aligned} \tag{2.61}$$

The modified Filinov parameter is,

$$\mathbf{A} = \frac{1}{2\hbar^2} \mathbf{M}_{\mathbf{pp}} \cdot (\mathbf{c} + i\mathbf{M}_{\mathbf{pp}}^T \cdot \mathbf{M}_{\mathbf{qp}}/\hbar)^{-1} \cdot \mathbf{M}_{\mathbf{pp}}^T, \tag{2.62}$$

and is treated as a constant diagonal matrix. The pre-exponential factor is found by solving for $\mathbf{c}$ in terms of $\mathbf{A}$ and substituting.

Herman[77] has suggested using Eq. (2.50) for the coherent state IVR of Eq. (2.14). Some authors[79] have found this to be useful. However, our experience is that it is not as effective as Eq. (2.59).

2.5 Application to the HCl Dimer

This section describes the application of current SC-IVR methodology to the low lying eigenvalues of a van der Waals complex, namely the HCl dimer, thus further widening the class of dynamical problems for which the approach has been demonstrated. This is a truly benchmark van der Waals system, having been thoroughly studied experimentally by far-infrared spectroscopic techniques and a highly accurate potential energy surface developed to fit this data.[80,81] This is quite a non-trivial test for semiclassical theory because the strong hydrogen bonding in the system leads to strong anharmonic coupling between the rotational and vibrational degrees of freedom. The dissociation energy is only about 690 cm^{-1}, and there are two equivalent minima separated by a barrier of about 70 cm^{-1}. The low lying eigenvalues are thus characterized by tunneling splittings ($\sim$ 16 cm^{-1} for the lowest doublet) and other non-classical effects. The goal of the present work is thus to see how well the SC-IVR approach is able to describe these phenomena.

To determine the eigenvalues of a bound molecular system, which is the application of interest in this section, we consider the spectral density with respect to some reference wavefunction $|\Psi\rangle$,

$$J(E) = \langle\Psi|\delta(E-\hat{H})|\Psi\rangle, \tag{2.63}$$

which of course has delta function peaks at the the eigenvalues $\{E_k\}$ of the Hamiltonian,

$$J(E) = \sum_k |\langle\Psi|\Psi_k\rangle|^2 \delta(E-E_k), \tag{2.64}$$

where $|\Psi_k\rangle$ are the corresponding eigenfunctions. The microcanonical density operator $\delta(E-\hat{H})$ can be expressed in terms of the propagator in the usual way,

$$\delta(E-\hat{H}) = -\frac{1}{\pi}\mathrm{Im}\hat{G}(E), \tag{2.65}$$

$$\hat{G}(E) = \frac{1}{i\hbar}\int_0^\infty e^{iEt/\hbar}e^{-i\hat{H}t/\hbar}, \tag{2.66}$$

so that the spectrum is given in terms of the propagator by

$$J(E) = \mathrm{Re}\frac{1}{\pi\hbar}\int_0^\infty e^{iEt/\hbar}\langle\psi|e^{-i\hat{H}t/\hbar}|\psi\rangle. \tag{2.67}$$

The semiclassical approximation corresponds to using an IVR of choice for the diagonal matrix element of the propagator in Eq. 2.67. In practice, one also typically includes a convergence factor to cutoff the time integral in Eq. 2.67, e.g., a Gaussian, to obtain

$$J(E) = \mathrm{Re}\frac{1}{\pi\hbar}\int_0^\infty e^{iEt/\hbar-\frac{1}{2}\Delta E^2t^2/\hbar^2}\langle\psi|e^{-i\hat{H}t/\hbar}|\psi\rangle, \tag{2.68}$$

for which the corresponding quantum expression that replaces Eq. 2.64 is

$$J(E) = \sum_k |\langle\Psi|\Psi_k\rangle|^2 \frac{e^{-\frac{1}{2}(E-E_k)^2/\Delta E^2}}{\sqrt{2\pi}\Delta E}. \tag{2.69}$$

In practice, one chooses ΔE as large as possible — so as to make the time integral in Eq. 2.67 converge in as short a time as possible — but not so large that the Gaussian peaks in Eq. 2.69 overlap too much for the individual eigenvalues to be resolved. Lastly, it is worth noting that in one-dimension, the semiclassical quantization condition derived from Eq. (2.67) (with a stationary phase evaluation of the time integral) is identical to the WKB quantization. Thus, this method of finding the eigenvalue can be viewed as a multi-dimensional generalization of the WKB analysis.

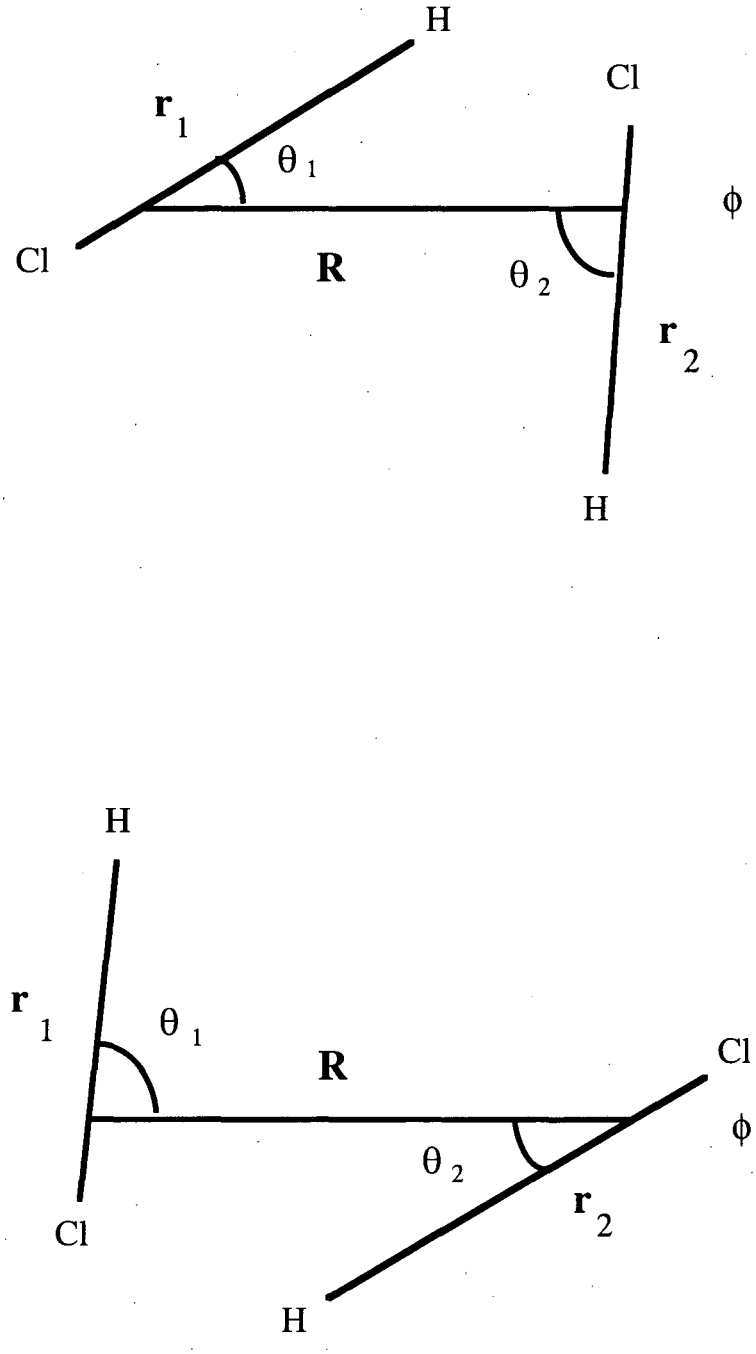

Figure 2.1: The two equilibrium configurations of the HCl dimer. The values of the coordinates are $R = 3.746$ Å, $\phi = 180°$, $\theta_1 = 9°$, $\theta_2 = 89.8°$. The HCl monomer bond lengths are fixed.

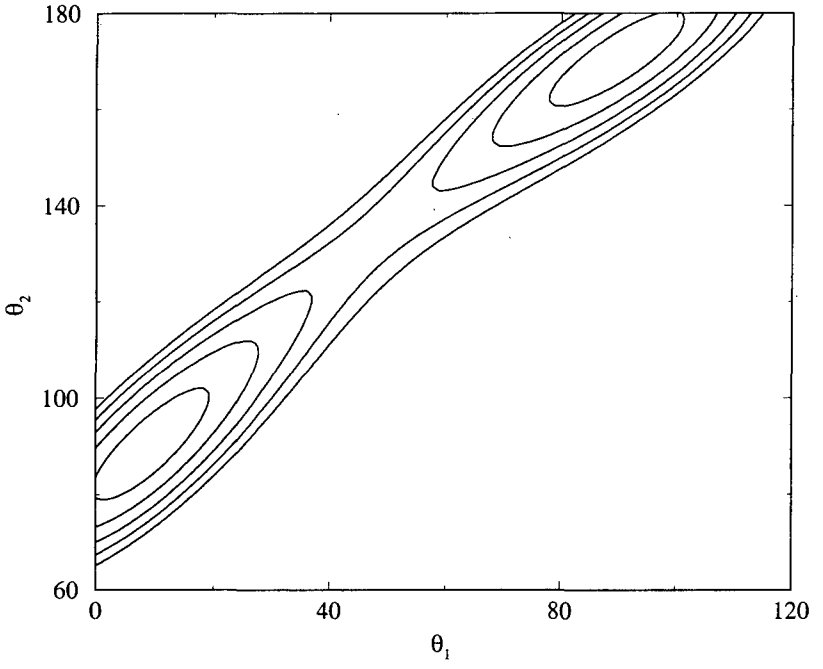

Figure 2.2: The two equilibrium configurations of the HCl dimer. The values of the coordinates are $R = 3.746$ Å, $\phi = 180°$, $\theta_1 = 9°$, $\theta_2 = 89.8°$. The HCl monomer bond lengths are fixed.

2.5.1 The HCl dimer Hamiltonian

In terms of the standard Jacobi coordinates shown in Figure 2.1 — $\mathbf{r}_1$ and $\mathbf{r}_2$ for the two diatomic monomers, and $\mathbf{R}$ the center of mass coordinate between the two — and their conjugate momenta, the classical Hamiltonian for the diatom-diatom system is

$$H = \frac{P_R^2}{2\mu} + \frac{l^2}{2\mu R^2} + \frac{p_{r_1}^2}{2m_1} + \frac{j_1^2}{2m_1 r_1^2} + \frac{p_{r_2}^2}{2m_2} + \frac{j_2^2}{2m_2 r_2^2} + V, \tag{2.70}$$

where $\mathbf{j}_n = \mathbf{r}_n \times \mathbf{p}_n$, for $n = 1$ and 2, and $\mathbf{l} = \mathbf{R} \times \mathbf{P}$. m_1, m_2 and μ are the appropriate reduced masses (and here, of course, $m_1 = m_2 = m$). Using the Van Vleck body-fixed axis procedure,[82] we choose $\mathbf{R}$ as the body-fixed axis, and the angular momentum of this axis, $\mathbf{l}$, is eliminated by the use of total angular momentum conservation,

$$\mathbf{l} = \mathbf{J} - (\mathbf{j}_1 + \mathbf{j}_2), \tag{2.71}$$

where $\mathbf{J}$ is the total angular momentum. In the present application, we consider only zero total angular momentum, $J = 0$, and also take the two monomer HCl's to be rigid rotors,

thus setting the two radial momenta $p_{r_1} = p_{r_2} = 0$. The Hamiltonian thus becomes

$$H = \frac{P_R}{2\mu} + \frac{|\mathbf{j}_1 + \mathbf{j}_2|^2}{2\mu R^2} + B(j_1^2 + j_2^2) + V, \tag{2.72}$$

where $B = (2mr^2)^{-1}$ is (with $\hbar = 1$) the monomer HCl rotation constant ($B = 10.44\ \mathrm{cm}^{-1}$). The rotational angular momenta of the two monomers, $\mathbf{j}_1$ and $\mathbf{j}_2$, are given by the standard expressions[83] in terms of the polar and azimuthal angles (θ_1, ϕ_1) and (θ_2, ϕ_2) that orient $\mathbf{r}_1$ and $\mathbf{r}_2$ with respect to the body-fixed axis $\mathbf{R}$, and their conjugate momenta, as

$$\mathbf{j}_n = \begin{pmatrix} -p_{\theta_n} \sin\phi_n - \cos\phi_n \cot\theta_n p_{\phi_n} \\ p_{\theta_n} \cos\phi_n - \sin\phi_n \cot\theta_n p_{\phi_n} \\ p_{\phi_n} \end{pmatrix}, \tag{2.73}$$

for $n = 1$ and 2. In Eq. 2.72, one thus has

$$j_n^2 = p_{\theta_n}^2 + \frac{p_{\phi_n}^2}{\sin^2\theta_n}, \tag{2.74}$$

$$\begin{aligned} \mathbf{j}_1 \cdot \mathbf{j}_2 &= p_{\theta_1} p_{\theta_2} \cos(\phi_1 - \phi_2) + p_{\phi_1} p_{\phi_2} \left[\cot\theta_1 \cot\theta_2 \cos(\phi_1 - \phi_2) + 1\right] \\ &+ p_{\theta_1} p_{\phi_2} \cot\theta_2 \sin(\phi_1 - \phi_2) + p_{\theta_2} p_{\phi_1} \cot\theta_1 \sin(\phi_2 - \phi_1). \end{aligned} \tag{2.75}$$

Finally, since the Hamiltonian (including the potential V) depends only on the difference of the two azimuthal angles $\phi_1 - \phi_2$, and not their sum, one makes a canonical transformation to the sum and difference variables,

$$\begin{aligned} \phi = \phi_1 - \phi_2 \quad &, \quad \Phi = \frac{1}{2}(\phi_1 + \phi_2), \\ p_\phi = \frac{1}{2}(p_{\phi_1} - p_{\phi_2}) \quad &, \quad p_\Phi = p_{\phi_1} + p_{\phi_2}. \end{aligned} \tag{2.76}$$

The Hamiltonian, as noted before, is independent of Φ, so that p_Φ is conserved (and equal to 0 for $J = 0$). Putting all this together, the final form for the $J = 0$ Hamiltonian involves four degrees of freedom, $(R, \theta_1, \theta_2, \phi)$ and their conjugate momenta, and is given explicitly by

$$\begin{aligned} H = (P_R, R, p_{\theta_1}, \theta_1, p_{\theta_2}, \theta_2, p_\phi, \phi) &= \frac{P_R^2}{2\mu} \\ &+ \left(B + \frac{1}{2\mu R^2}\right)\left(p_{\theta_1}^2 + \frac{p_\phi^2}{\sin^2\theta_1} + p_{\theta_2}^2 + \frac{p_\phi^2}{\sin^2\theta_2}\right) \\ &+ \frac{1}{\mu R^2}\left[p_{\theta_1} p_{\theta_2} \cos\phi - p_\phi^2(\cot\theta_1 \cot\theta_2 \cos\phi + 1) - p_\phi \sin\phi (p_{\theta_1} \cot\theta_2 + p_{\theta_2} \cot\theta_1)\right] \\ &+ V(R, \theta_1, \theta_2, \phi). \end{aligned} \tag{2.77}$$

The potential energy surface V has been determined by Elrod *et al.*[80,81] in the form of the follow expansion

$$V(R,\theta_1,\theta_2,\phi) = \sum_{l_1 l_2 l} A_{l_1 l_2 l}(R) g_{l_1 l_2 l}(\theta_1,\theta_2,\phi), \tag{2.78}$$

the parameters for which are determined by fitting quantum mechanical calculation to the experimental spectra. Figure 2.2 shows a contour plot of the potential surface as a function of (θ_1,θ_2) for planar geometry ($\phi = 180°$) and a fixed value of R. This clearly displays the $\theta_1 \leftrightarrow \theta_2$ exchange symmetry and the two equivalent minima indicated in Figure 2.1. As noted earlier, the barrier separating the two minima ($\sim$ 70 cm^{-1}) is sufficiently low that tunneling between them gives rise to a splitting of about 16 cm^{-1} between the lowest two energy levels. Even and odd states with respect to this $\theta_1 \leftrightarrow \theta_2$ exchange are designated by A and B, respectively. The potential is also symmetric in the out of plane coordinate ϕ, so that the states are also even or odd with respect $\phi \rightarrow 2\pi - \phi$. This symmetry is designated $+$ or $-$. The states thus have four possible symmetries in this system, A^+, A^-, B^+, B^-.

2.5.2 Results and Discussion

The reference wavefunction in Eq. 2.67 is, to some extent, arbitrary, the primary requirement being that it has significant overlap with the states whose energy levels one is wishing to extract from the calculation. One may in fact wish to use several different reference wavefunctions. Because the Herman-Kluk IVR expression (Eq. 2.14) involves coherent states, it is natural to choose Ψ also of this form. Thus, we have used a direct product of such functions,

$$\Psi(R,\theta_1,\theta_2,\phi) = \psi_1(R)\psi_2(\theta_1)\psi_3(\theta_2)\psi_4(\phi), \tag{2.79}$$

where each factor is related to a coherent state,

$$\psi_1(R) = \left(\frac{\gamma_1}{\pi}\right)^{\frac{1}{4}} R^{-2} e^{-\frac{\gamma_1}{2}(R-R_0)^2 + iP_{R0}(R-R_0)/\hbar}, \tag{2.80}$$

$$\psi_2(\theta_1) = \left(\frac{\gamma_2}{\pi}\right)^{\frac{1}{4}} (\sin\theta_1)^{-1} e^{-\frac{\gamma_2}{2}(\theta_1-\theta_{10})^2 + iP_{\theta_1 0}(\theta_1-\theta_{10})/\hbar}, \tag{2.81}$$

$$\psi_3(\theta_2) = \left(\frac{\gamma_3}{\pi}\right)^{\frac{1}{4}} (\sin\theta_2)^{-1} e^{-\frac{\gamma_3}{2}(\theta_2-\theta_{20})^2 + iP_{\theta_2 0}(\theta_2-\theta_{20})/\hbar}, \tag{2.82}$$

$$\psi_4(\phi) = \left(\frac{\gamma_4}{\pi}\right)^{\frac{1}{4}} e^{-\frac{\gamma_4}{2}(\phi-\phi_0)^2 + iP_{\phi 0}(\phi-\phi_0)/\hbar}, \tag{2.83}$$

where R^{-2} and $(\sin\theta_n)^{-1}$ will cancel with the Jacobian factors when calculating the overlap $\langle \mathbf{q},\mathbf{p}|\Psi\rangle$, and the coherent state widths $\{\gamma_i\}$ are choosen large enough so that the following approximation

$$\begin{aligned}\langle \mathbf{q},\mathbf{p}|\Psi\rangle &= \int_0^\infty dR \int_0^\pi d\theta_1 \int_0^\pi d\theta_2 \int_0^{2\pi} d\phi R^2 \sin\theta_1 \sin\theta_2 \\ &\times \Psi(R,\theta_1,\theta_2,\phi)\langle \mathbf{q},\mathbf{p}|R,\theta_1,\theta_2,\phi\rangle \\ &\approx \int_{-\infty}^\infty dR \int_{-\infty}^\infty d\theta_1 \int_{-\infty}^\infty d\theta_2 \int_{-\infty}^\infty d\phi R^2 \sin\theta_1 \sin\theta_2 \\ &\times \Psi(R,\theta_1,\theta_2,\phi)\langle \mathbf{q},\mathbf{p}|R,\theta_1,\theta_2,\phi\rangle, \end{aligned} \tag{2.84}$$

is valid. Actually, we use a linear combination of functions of the type in Eq. 2.79 in order to take advantage of symmetry: to determine the energy levels for a given symmetry, one chooses the reference wavefunction to be of this symmetry so that only states with this symmetry will appear in the spectral density (as most easily seen in the quantum expression, Eq. 2.64). In the present case, for example, the reference wavefunction of Eq. 2.79 is modified as follows,

$$\begin{aligned}\Psi_{\sigma,\sigma'}(R,\theta_1,\theta_2,\phi) &= \psi_1(R)\left[\psi_2(\theta_1)\psi_3(\theta_2) + \sigma\psi_2(\theta_2)\psi_3(\theta_1)\right] \\ &\cdot \left[\psi_4(\phi) + \sigma'\psi_4(2\pi-\phi)\right], \end{aligned} \tag{2.85}$$

where $\sigma\sigma' = ++, +-, -+$, and $--$ correspond to the A^+, A^-, B^+, and B^- states, respectively. The semiclassical calculation can thus be carried out separately for each symmetry. The actual IVR we use for this calculation is the version in Eq. (2.59).

Figure 2.3 shows a typical semiclassical correlation function $\langle\Psi|e^{-i\hat{H}t/\hbar}|\Psi\rangle$ for A^+ symmetry. It is obtained with ~ 3000 bounded classical trajectories whose initial conditions are chosen by Monte Carlo from the coherent state overlap with the reference wavefunction, $|\langle \mathbf{q},\mathbf{p}|\Psi\rangle|$. (Trajectories which dissociated are discarded since their Fourier transform cannot contribute to delta function peaks in the energy spectrum.) Figure 2.4 shows the energy spectrum obtained from this correlation function, indicating the peaks corresponding to the energy levels. No attempt was made at using more sophisticated "signal processing" algorithms[84,85] to extract the energy levels from the time correlation function, though this would perhaps make the overall procedure more efficient.

The lowest few SC-IVR energy levels of each symmetry are listed in Table 2.1, along with the corresponding quantum mechanical (QM) values calculated by Elrod *et al.*[80,81] The SC-IVR and QM energy levels are listed relative to the ground state of each, and one sees

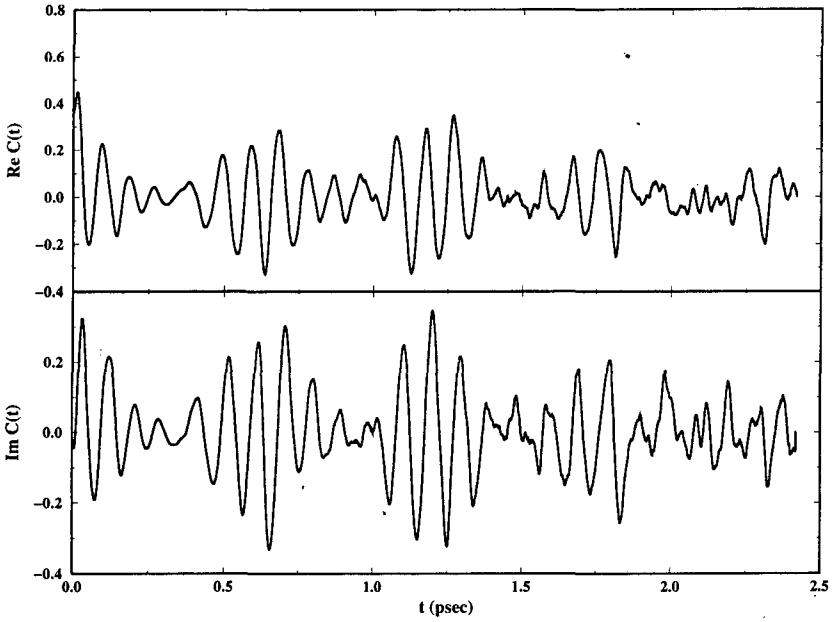

Figure 2.3: The real and imaginary parts of the semiclassical correlation function, $\langle\Psi|e^{-i\hat{H}t/\hbar}|\Psi\rangle$, where Ψ is of A^+ symmetry. This is obtained with about 3000 bound trajectories.

quite good agreement overall. The average error in the semiclassical energy levels for these states is 1.65 cm^{-1}, with the maximum being about 4 cm^{-1}. It is particularly interesting to see that the tunneling splitting of the ground state — the difference of the lowest A^+ and B^+ energy levels — is described reasonably well, 18 cm^{-1} compared to the correct value of 15.7 cm^{-1}. We consider this level of success for the SC-IVR model to be excellent and further evidence that it is capable of describing a wide range of dynamical phenomena to a useful accuracy, even at the most detailed level where quantum effects are very significant.

The result obtained for the SC-IVR ground state (-395.5 cm^{-1}), however, is 16.3 cm^{-1} above the quantum ground state (-411.8 cm^{-1}). Therefore, on an absolute energy scale, all SC-IVR energy levels are about this much larger than the corresponding QM values. From the discussion at the end of the Appendix, it is not surprising that the SC energies are shifted by an approximately constant value relative to the QM ones, but it is not easy to reconcile the value of the shift (16.3 cm^{-1}) we observe. If the two HCl rigid diatomics were free rotors, then the discussion in the Appendix shows that the SC energy levels would be $\frac{1}{2}B$ above the QM values ($\frac{1}{4}B$ for each rotor), and since the rotation constant of HCl is $B = 10.44$ cm^{-1}, this suggests a shift about 5.2 cm^{-1}. (We in fact carried out the

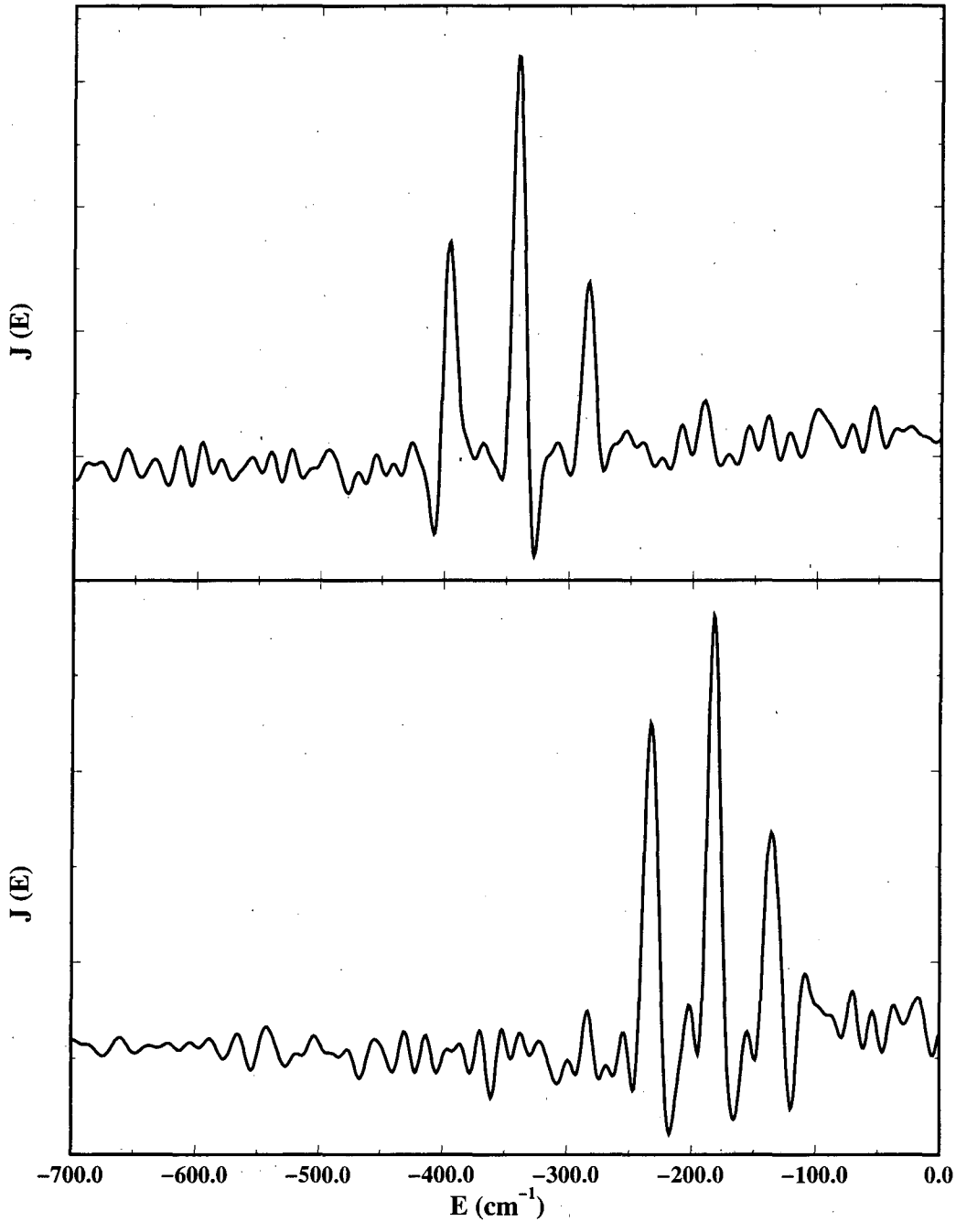

Figure 2.4: Representative spectra for A^+ (upper panel) and A^- (lower panel) symmetries.

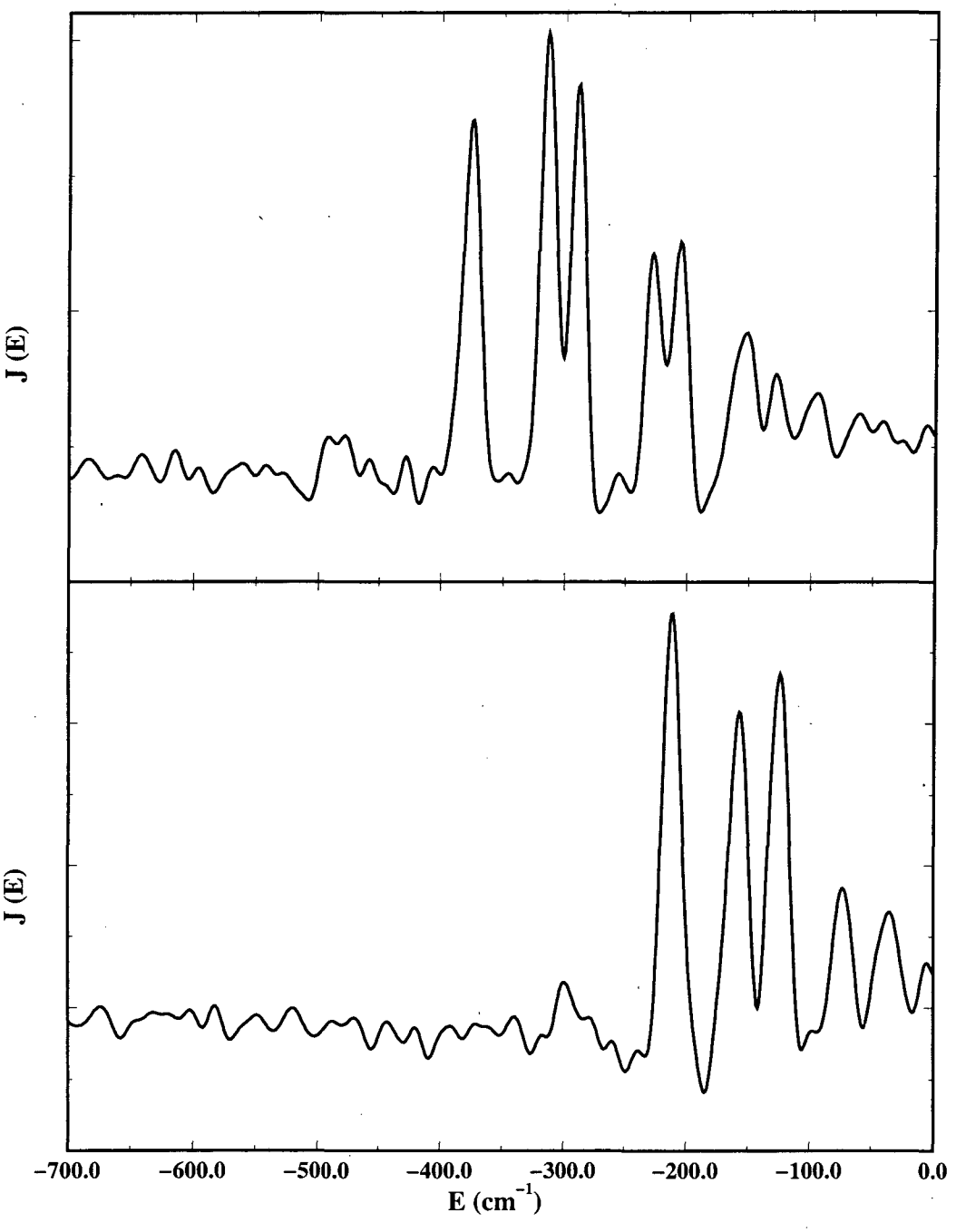

Figure 2.5: Representative spectra for B^+ (upper panel) and B^- (lower panel) symmetries.

	QM	SC-IVR
A^+	0.0*	0.0*
	53.3	55.5
	72.1	76.6
	111.2	111.4
	147.8	147.8
A^-	160.6	162.6
	212.0	212.7
B^+	15.7	18.0
	79.6	80.9
	104.0	106.7
	167.5	166.4
	188.0	190.8
B^-	185.1	186.7
	240.3	240.0

Table 2.1: The semiclassical energy eigenvalues of the HCl dimer in cm^{-1}. Quantum mechanics and SC-IVR energy levels are shown relative to the ground state of each. The SC-IVR ground state is 16.3 cm^{-1} above the QM ground state.

SC-IVR calculation for the uncoupled case and did indeed obtain energy levels shifted by this amount.) Why one obtains a significantly larger shift than this for the fully coupled case is not clear to us, but it is nevertheless reassuring that the SC-IVR energy levels are good approximations to the QM values for *some* constant (and modest) shift.

2.6 Concluding Remarks

The semiclassical initial value representation is indeed becoming a practical way of incorporating quantum mechanical effects with simple classical quantities. The examples studied by us and others have shown that the accuracy of SC-IVR is good for most types of chemical problems, including tunneling. And because one is basically running classical trajectories, in the best case scenario, it can be more efficient than exact quantum mechanical calculations.

Another idea we explored for calculating the SC-IVR integral is to use the ergodic (chaotic) properties of the system and instead of a phase space average, one performs a

time average, i.e.,

$$\int d\mathbf{p}_0 \int d\mathbf{q}_0 \rightarrow \frac{1}{T}\int_0^T dt, \tag{2.86}$$

where T is some large number. The essential assumption is that a single trajectory will explore the entire phase space and therefore averaging over the past of the trajectory exploration is equivalent to the integrating over the phase space. This, of course, assumes the ergodic hypothesis and is only applicable for really large systems. For intermediate sized systems, this assumption is generally not valid.

For most problems however, SC-IVR calculation is considerably more complex than just running classical trajectories. The remaining question is how can one implement the SC-IVR with a reasonable amount of effort, to systems with more degrees of freedom. One method we reviewed here which reduces the oscillatory nature of the integrand is the stationary phase Monte Carlo filtering technique, and we have seen improved convergence properties with this approach. Thus, it seems that one is ready to take advantage of these developments to study more complex systems. There maybe other methods which are also improvements on the concepts of SC-IVR, this is also an ongoing area of research.

2.7 Appendix: SC-IVR for Angular Coordinates

Here we note some specific features of the SC-IVR when treating angular variables for rotational degrees of freedom. Consider first a one dimensional rotor whose orientation in a plane is characterized by angle ϕ, with the Hamiltonian

$$\hat{H} = -\frac{\hbar^2}{2I}\frac{d^2}{d\phi^2} + V(\phi), \tag{2.87}$$

where I is the moment of inertia. A typical matrix element of the propagator thus has the form

$$S_{2,1} \equiv \langle \Psi_2 | e^{-i\hat{H}t/\hbar} | \Psi_1 \rangle = \int_0^{2\pi} d\phi_1 \int_0^{2\pi} d\phi_2 \Psi_2(\phi_2)^* \langle \phi_2 | e^{-i\hat{H}t/\hbar} | \phi_1 \rangle \Psi_1(\phi_1), \tag{2.88}$$

with the wavefunctions normalized on the interval $(0, 2\pi)$ in the usual way,

$$\int_0^{2\pi} d\phi \, |\Psi(\phi)|^2 = 1. \tag{2.89}$$

If $K_t(\phi_2, \phi_1)$ is the standard semiclassical amplitude for the $\phi_1 \rightarrow \phi_2$ transition in time t, i.e.,

$$K_t(\phi_2, \phi_1) = \sum \left[2\pi i\hbar \left| \frac{\partial \phi_t}{\partial p_{\phi_1}} \right| \right]^{-\frac{1}{2}} e^{iS_t(\phi_2, \phi_1)/\hbar}, \tag{2.90}$$

then the new feature than arises here is that the net amplitude for the transition must take account of the fact that all final angles $\phi_2 + 2\pi n$ (n = any integer) correspond to the same physical orientation as angle ϕ_2, so that the amplitude in the integrand of Eq. 2.88 must be a sum over all these symmetrically equivalent final angles,

$$\langle \phi_2 | e^{-i\hat{H}t/\hbar} | \phi_1 \rangle = \sum_{n=-\infty}^{\infty} K_t(\phi_2 + 2\pi n, \phi_1). \tag{2.91}$$

Eq. 2.88 thus reads

$$S_{2,1} = \sum_{n=-\infty}^{\infty} \int_0^{2\pi} d\phi_1 \int_0^{2\pi} d\phi_2 \Psi_2(\phi_2)^* K_t(\phi_2 + 2\pi n, \phi_1) \Psi_1(\phi_1), \tag{2.92}$$

and if one changes the integration variable from ϕ_2 to $\phi_2' = \phi_2 + 2\pi n$, it becomes

$$S_{2,1} = \sum_{n=-\infty}^{\infty} \int_0^{2\pi} d\phi_1 \int_{2\pi n}^{2\pi(n+1)} d\phi_2' \Psi_2(\phi_2')^* K_t(\phi_2', \phi_1) \Psi_1(\phi_1), \tag{2.93}$$

where it has been assumed that the wavefunction Ψ_2 is periodic, i.e., $\Psi_2(\phi_2' - 2\pi n) = \Psi_2(\phi_2')$. But,

$$\sum_{n=-\infty}^{\infty} \int_{2\pi n}^{2\pi(n+1)} d\phi_2' = \int_{-\infty}^{\infty} d\phi_2', \tag{2.94}$$

so that Eq. 2.93 becomes

$$S_{2,1} = \int_0^{2\pi} d\phi_1 \int_{-\infty}^{\infty} d\phi_2 \Psi_2(\phi_2)^* K_t(\phi_2, \phi_1) \Psi_1(\phi_1), \tag{2.95}$$

where the prime has now been dropped from the integration variable ϕ_2'. The integral over the entire interval $(-\infty, \infty)$ of the final angle ϕ_2, together with the periodicity of the final wavefunction $\Psi_2(\phi_2)$, thus properly takes account of the sum over all symmetrically equivalent final angles in Eq. 2.91. One now applies the standard IVR transformation to Eq. 2.95, i.e.,

$$\int_{-\infty}^{\infty} d\phi_2 = \int_{-\infty}^{\infty} dp_{\phi_1} \left| \frac{\partial \phi_t}{\partial p_{\phi_1}} \right|, \tag{2.96}$$

to give the final result

$$\langle \Psi_2 | e^{-i\hat{H}t/\hbar} | \Psi_1 \rangle = \int_0^{2\pi} d\phi_1 \int_{-\infty}^{\infty} dp_{\phi_1} \Psi_2(\phi_t)^* \left[\left| \frac{\partial \phi_t}{\partial p_{\phi_1}} \right| / 2\pi i\hbar \right]^{\frac{1}{2}} e^{iS_t(\phi_1, p_{\phi_1})/\hbar} \Psi_1(\phi_1), \tag{2.97}$$

which is of the standard IVR form. With the wavefunction normalized in the standard way, the integral over the initial angle is thus over the primary interval $(0, 2\pi)$ and that of the conjugate initial momentum is over all values $(-\infty, \infty)$.

To illustrate the importance of including all symmetrically equivalent final angles, consider the *free* plane rotor, i.e., $V(\phi) = 0$ in Eq. 2.87. The SC propagator of Eq. 2.90 is then of the standard free particle form

$$K_t(\phi_2, \phi_1) = \sqrt{\frac{I}{2\pi i\hbar t}} e^{iI(\phi_2-\phi_1)^2/2\hbar t}, \tag{2.98}$$

which give the following micro-canonical density matrix

$$\langle\phi_2|\delta(E-\hat{H})|\phi_1\rangle \equiv \frac{\mathrm{Re}}{\pi\hbar}\int_0^\infty dt e^{iEt/\hbar} K_t(\phi_2,\phi_1) = \frac{I}{\pi\hbar^2 k}\cos[k(\phi_2-\phi_1)], \tag{2.99}$$

where $k = \sqrt{2IE}/\hbar$. Including the sum over all equivalent final angles, however, changes this to

$$\begin{aligned}\langle\phi_2|\delta(E-\hat{H})|\phi_1\rangle &= \frac{I}{\pi\hbar^2 k}\sum_{n=-\infty}^{\infty}\cos[k(\phi_2-\phi_1)+2\pi nk], \\ &= \frac{I}{\pi\hbar^2 k}\cos[k(\phi_2-\phi_1)]\sum_{n=-\infty}^{\infty}\cos(2\pi nk),\end{aligned} \tag{2.100}$$

and the Poisson sum formula,[86]

$$\sum_{n=-\infty}^{\infty}\cos(2\pi nk) = \sum_{l=-\infty}^{\infty}\delta(l-k), \tag{2.101}$$

requires k to be an *integer*. This is therefore what quantizes the energy $E = \hbar^2k^2/2I$ and gives delta function peaks at the these values in the matrix element of $\delta(E-\hat{H})$.

Finally, there is another feature in the semiclassical description of rotational motion that should be noted. Consider a free linear rotor in 3-d space, for which the classical Hamiltonian is

$$H = \frac{1}{2I}(p_\theta^2 + \frac{p_\phi^2}{\sin^2\theta}). \tag{2.102}$$

Quantization of the ϕ motion, as discussed above, requires $p_\phi = m\hbar$, m an integer. The θ motion thus takes place in the centrifugal potential well $V(\theta)$,

$$V(\theta) = B\frac{m^2}{\sin^2\theta}, \tag{2.103}$$

where $B = \hbar^2/2I$ is the rotational constant. The standard WKB (Bohr-Sommerfeld) quantization of this bound motion

$$(n+\frac{1}{2})\pi = \int d\theta\sqrt{2I(E-V(\theta))}/\hbar, \tag{2.104}$$

gives the following energy levels,

$$\begin{aligned} E_{n,m} &= B(n+\frac{1}{2}+|m|)^2, \\ n &= 0,1,2,\ldots\ldots, \end{aligned} \tag{2.105}$$

or in terms of the usual quantum number $l = n + |m|$,

$$E_l = B(l+\frac{1}{2})^2 = Bl(l+1) + \frac{1}{4}B. \tag{2.106}$$

The semiclassical energy levels are thus too large by a constant value. In any applications to rotational problems, therefore, one may expect that energy level *spacings* given by the semiclassical theory will be more accurate than their absolute value.

Chapter 3

Further Approximations of the SC-IVR

3.1 Introduction

The successful application of the semiclassical initial value representation to the multidimensional system of the HCl dimer demonstrates its potential as an useful dynamical theory for many problems in chemistry. But before we use it to study cell biology, it is perhaps interesting to examine some approximate theories based on the SC-IVR. Clearly, an approximate theory that reduces the complexity in the implementation is desirable, but also conceptual understanding of the origin of quantum effects and their role in complex systems can perhaps be gained.

In this chapter we concentrate on the calculation of *probabilities* with the semiclassical theory and discuss three possible approaches for further approximating the SC-IVR. Section 3.2 proceeds with the strategy of dividing a problem into a "system" and a "bath" and retain, as much as possible, the interference and coherence effects in the system but discard them for the bath. The end product is a mixed semiclassical-classical treatment where systematic improvements of the system-bath interaction is possible. In section 3.3, we explore the same type of approach but being even more crude and treat everything approximately. This allows us to establish a connection to a classical-like theory that has been used before. Nevertheless, we find it useful to see that the possibility of systematically improving upon this theory also exists. In section 3.4, another approach of implementing

the SC-IVR where the time-dependent expectation value of an operator is written as a single phase space integral over initial conditions is presented. The end result is similar to the SC-IVR expression for amplitudes in Eq. (2.8) but now utilizing classical trajectories that travel forward and backward in time.

3.2 Mixed Semiclassical-Classical Dynamics

Many dynamical phenomena in chemical/molecular systems involve only a few degrees of freedom (the "system") that characterize the process of interest (e.g., the reaction coordinate(s) in a chemical reaction) but which are coupled to many other "environmental" degrees of freedom (the "bath") that can nevertheless influence the dynamics. A common strategy for treating this ubiquitous "system-bath" situation is to describe the low dimensional system as accurately as possible, namely with full quantum mechanics, while the many degrees of freedom of the bath are handled more approximately, such as by classical mechanics or approximations thereto.

There are thus many variations of "mixed quantum-classical" theoretical approaches that have been used in this regard[87–96]. The most common of these might be called the Ehrenfest model[97,98], where one simultaneously integrates the time-dependent Schrödinger equation for the system and the classical equations of motion for the bath. If x and $\mathbf{Q}$ denote the system and bath coordinates, respectively, and $V(x,\mathbf{Q})$ is the total potential energy function for the system plus bath, then the (time-dependent) potential for the Schrödinger equation of the system is

$$V_{QM}(x,t) = V(x,\mathbf{Q}(t)), \tag{3.1}$$

and the (time-dependent) classical potential for the bath trajectory $\mathbf{Q}(t)$ is the Ehrenfest average of V,

$$V_{CL}(\mathbf{Q},t) = \langle\Psi(t)|V|\Psi(t)\rangle \equiv \int dx \Psi(x,t)^* V(x,\mathbf{Q})\Psi(x,t), \tag{3.2}$$

where $\Psi(x,t)$ is the system wavefunction. If $\phi_{n_1}(x)$ is the wavefunction for the initial quantum state of the system, then one chooses it as the initial wavefunction for the Schrödinger equation, $\Psi(x,t=0) = \phi_{n_1}(x)$. Also, if $\rho_b(\mathbf{Q}_1,\mathbf{P}_1)$ is the probability distribution of initial conditions for the bath trajectories (for example, a Boltzmann distribution), then the average probability for a transition to the final quantum state ϕ_{n_2} of the system is given by

$$P_{n_2\leftarrow n_1}(t) = \int d\mathbf{Q}_1 d\mathbf{P}_1 \rho_b(\mathbf{Q}_1,\mathbf{P}_1) P_{n_2\leftarrow n_1}(t;\mathbf{Q}_1,\mathbf{P}_1), \tag{3.3}$$

where

$$P_{n_2 \leftarrow n_1}(t; \mathbf{Q}_1, \mathbf{P}_1) \equiv |\langle \phi_{n_2} | \Psi(t) \rangle|^2 \tag{3.4}$$

is the transition probability for a single bath trajectory (the one with the indicated initial conditions). This model may also be thought of as an approximate version of the time-dependent self consistent field (TDSCF) method[99,100], the approximation being that the bath wavefunction is taken to be an infinitely narrow Gaussian wavepacket about its classical trajectory. The TDSCF approximation seems to work best when the system is coupled *weakly* to *many* bath modes, but can fail dramatically in other cases[101,102]. It can be systematically improved, however, by introducing a multi-configuration generalization (MC-TDSCF)[103–105], but there is then no obvious way to go to the classical limit for the bath dynamics.

Other mixed quantum-classical approaches are a variety of "surface-hoping" models[106–110], whereby the quantum motion of the system is assumed to be adiabatic except for localized transitions from one adiabatic quantum state to another. Though such approaches have a number of *ad hoc* features, they have been useful, particularly when the "system" consists of the electronic degrees of freedom of a molecular system. There are other approaches based explicitly on density matrix formulations that incorporate approximations for the bath that lead to macroscopic relaxation descriptions (Redfield equations)[111–113]. The most accurate treatment of system-bath dynamics is possible when the bath is a set of harmonic modes that are linearly coupled to the system; here the bath can be integrated out (in a Feynman path integral sense) analytically and recent progress has shown how then essentially exact (numerical) treatments of the system are possible in some cases[114,115].

In this section, we offer another type of mixed quantum-classical approach, where the "quantum" description of the system is approximated semiclassically via an initial value representation (IVR). It is thus a mixed "semiclassical-classical" approximation. The potential advantage of this approach over a mixed *quantum*-classical approach is that in it the dynamics of both system and bath are treated by classical mechanics; i.e., a full classical trajectory simulation of all degrees of freedom is involved. The semiclassical aspect of the description of the system degrees of freedom simply means that the phase interference structure is retained for these degrees of freedom, giving rise to interference/coherence structure and/or classically forbidden dynamics/tunneling behavior in the system degrees of freedom, while such phase information is discarded in the bath, so that only classical

dynamics is obtained for these degrees of freedom. Since the system, bath, and their interaction are all treated via classical mechanics, one thinks (or at least hopes) that a more dynamically consistent treatment will result than using the Schrödinger equation for some degrees of freedoms and Newton's equations for the others. Whether this potential advantage is realized or not will of course require computational applications, and some elementary examples of these are presented herein.

3.2.1 The Semiclassical-Classical Model

There are a variety of quantities that one might consider for this development, e.g., thermally averaged or state-specific rate constants or transition probabilities. For definiteness we consider the time-dependent transition probability from one state of the system to another, summed and averaged over initial and final states of the bath,

$$P_{n_2\leftarrow n_1}(t) \equiv \sum_{m_1,m_2} \wp_{m_1} \left| \langle \chi_{m_2}\phi_{n_2}|e^{-i\hat{H}t/\hbar}|\chi_{m_1}\phi_{n_1}\rangle \right|^2, \tag{3.5}$$

where $\phi(x)$ and $\chi(\mathbf{Q})$ are the basis states for the system and bath, respectively, and $\wp_m$ is the initial probability distribution for the bath states (typically a Boltzmann distribution). Eq. (3.5) can also be written as a trace,

$$P_{n_2\leftarrow n_1}(t) = \mathrm{tr}\left[e^{-\beta\hat{H}_b}|\phi_{n_1}\rangle\langle\phi_{n_1}|e^{i\hat{H}t/\hbar}|\phi_{n_2}\rangle\langle\phi_{n_2}|e^{-i\hat{H}t/\hbar}\right], \tag{3.6}$$

where $\hat{H}_b$ is the Hamiltonian for the bath at $t = 0$. For simplicity of presentation the system and bath coordinates x and $\mathbf{Q}$ are indicated as one-dimensional and many-dimensional, respectively, though in practice the "system" might involve a few degrees of freedom, with obvious changes in notation below.

IVR for the System-Bath

Applying the semiclassical IVR of Eq. (2.9) to the system-bath transition probability defined in Eq. (3.5) thus gives (since $\mathbf{q} \equiv (x, \mathbf{Q}), \mathbf{p} \equiv (p, \mathbf{P})$, with $(\mathbf{Q}, \mathbf{P})$ F-dimensional)

$$P_{n_2\leftarrow n_1}(t) = \sum_{m_2,m_1} \wp_{m_1} \left| \int dx_1 \int dp_1 \int d\mathbf{Q}_1 \int d\mathbf{P}_1 \phi_{n_2}(x_t)^* \chi_{m_2}(\mathbf{Q}_t)^* \right.$$
$$\left. \phi_{n_1}(x_1)\chi_{m_1}(\mathbf{Q}_1) e^{iS(x_1,p_1,\mathbf{Q}_1,\mathbf{P}_1)/\hbar} \sqrt{\det\left[\frac{\partial(x_t,\mathbf{Q}_t)}{\partial(p_1,\mathbf{P}_1)}\right]/(2\pi i\hbar)^{F+1}} \right|^2, \tag{3.7}$$

and upon squaring the integral explicitly this becomes

$$P_{n_2\leftarrow n_1}(t) = (2\pi\hbar)^{-(F+1)} \int dx_1 dp_1 \int dx_1' dp_1' \int d\mathbf{Q}_1 d\mathbf{P}_1 \int d\mathbf{Q}_1' d\mathbf{P}_1' \\ \phi_{n_1}(x_1)\phi_{n_1}(x_1')^* \phi_{n_2}(x_t)^* \phi_{n_2}(x_t') e^{i[S_t(x_1,p_1,\mathbf{Q}_1,\mathbf{P}_1) - S_t(x_1',p_1',\mathbf{Q}_1',\mathbf{P}_1')]/\hbar} \\ \sqrt{\det\left[\frac{\partial(x_t,\mathbf{Q}_t)}{\partial(p_1,\mathbf{P}_1)}\right]} \sqrt{\det\left[\frac{\partial(x_t',\mathbf{Q}_t')}{\partial(p_1',\mathbf{P}_1')}\right]} \langle \mathbf{Q}_1'|\rho_b|\mathbf{Q}_1\rangle \delta(\mathbf{Q}_t - \mathbf{Q}_t') \tag{3.8}$$

where x_t and x_t' denote $x_t(x_1, p_q, \mathbf{Q}_1, \mathbf{P}_1)$ and $x_t(x_1', p_1', \mathbf{Q}_1', \mathbf{P}_1')$, respectively, and similarly for $\mathbf{Q}_t$ and $\mathbf{Q}_t'$, and where

$$\langle \mathbf{Q}_1|\rho_b|\mathbf{Q}_1'\rangle \equiv \sum_{m_1} \wp_{m_1} \chi_{m_1}(\mathbf{Q}_1')^* \chi_{m_1}(\mathbf{Q}_1) \tag{3.9}$$

is the initial density matrix of the bath. The F-dimensional delta function results from

$$\sum_{m_2} \chi_{m_2}(\mathbf{Q}_t)^* \chi_{m_2}(\mathbf{Q}_t') = \delta_F(\mathbf{Q}_t - \mathbf{Q}_t'). \tag{3.10}$$

It is also useful to express the bath density matrix in terms of its Wigner distribution,

$$\langle \mathbf{Q}_1|\rho_b|\mathbf{Q}_1'\rangle = \int d\mathbf{P} e^{i\mathbf{P}\cdot(\mathbf{Q}_1 - \mathbf{Q}_1')/\hbar} \rho_w\left(\frac{\mathbf{Q}_1 + \mathbf{Q}_1'}{2}, \mathbf{P}\right), \tag{3.11}$$

the inverse relation of which is

$$\rho_w(\mathbf{Q},\mathbf{P}) = (2\pi\hbar)^{-F} \int d\Delta\mathbf{Q} e^{-i\Delta\mathbf{Q}\cdot\mathbf{P}/\hbar} \left\langle \mathbf{Q} + \frac{\Delta\mathbf{Q}}{2}\middle| \rho_b \middle| \mathbf{Q} - \frac{\Delta\mathbf{Q}}{2}\right\rangle. \tag{3.12}$$

The "double phase space integral" that results in Eq. (3.8) upon squaring the amplitude in Eq. (3.7) is the semiclassical counterpart to Liouville space in a corresponding quantum mechanical development. The principle idea of the present mixed semiclassical-classical model is to retain the full double phase space integral for the system degrees of freedom - so as to retain the full semiclassical description of interference and tunneling effects in the system dynamics - but to approximate the treatment of the bath in such a way as to reduce it to a *single* phase space average over its initial conditions (as in a classical mechanical description). All of the classical trajectory functions throughout, however, are those from the full system-bath Hamiltonian. It is this feature of the model, namely that the mechanics of all degrees of freedom is treated classically, only with the interference structure fully retained for the system and approximated for the bath, that makes us believe that the *semiclassical*-classical approach may have something more to offer than a *quantum*-classical approach, i.e., because the dynamics of the system and the bath are treated in a dynamically consistent way in the present approach.

To implement this approximation for the bath one changes the integration variables over bath initial conditions to the sum and difference variables

$$\begin{aligned} \mathbf{Q}_1 &= \bar{\mathbf{Q}} + \tfrac{\Delta\mathbf{Q}}{2} \quad \mathbf{Q}_1' = \bar{\mathbf{Q}} - \tfrac{\Delta\mathbf{Q}}{2}, \\ \mathbf{P}_1 &= \bar{\mathbf{P}} + \tfrac{\Delta\mathbf{P}}{2} \quad \mathbf{P}_1' = \bar{\mathbf{P}} - \tfrac{\Delta\mathbf{P}}{2}, \end{aligned} \tag{3.13}$$

so that in Eq. (3.8)

$$\int d\mathbf{Q}_1 d\mathbf{Q}_1' \int d\mathbf{P}_1 d\mathbf{P}_1' = \int d\bar{\mathbf{Q}}_1 d\bar{\mathbf{P}}_1 \int d\Delta\mathbf{Q} d\Delta\mathbf{P}. \tag{3.14}$$

One then expands the $\Delta\mathbf{Q}$ and $\Delta\mathbf{P}$ dependence of the various quantities in the integrand in powers of $\Delta\mathbf{Q}$ and $\Delta\mathbf{P}$; e.g., in the argument of the delta function in Eq. (3.8)

$$\begin{aligned} &\mathbf{Q}_t\left(x_1, p_1, \bar{\mathbf{Q}}_1 + \frac{\Delta\mathbf{Q}}{2}, \bar{\mathbf{P}}_1 + \frac{\Delta\mathbf{P}}{2}\right) - \mathbf{Q}_t\left(x_1', p_1', \bar{\mathbf{Q}}_1 - \frac{\Delta\mathbf{Q}}{2}, \bar{\mathbf{P}}_1 - \frac{\Delta\mathbf{P}}{2}\right) \\ &\quad = \mathbf{Q}_t - \mathbf{Q}_t' + \frac{1}{2}\left(\frac{\partial\mathbf{Q}_t}{\partial\bar{\mathbf{Q}}_1} + \frac{\partial\mathbf{Q}_t'}{\partial\bar{\mathbf{Q}}_1}\right)\cdot\Delta\mathbf{Q} + \frac{1}{2}\left(\frac{\partial\mathbf{Q}_t}{\partial\bar{\mathbf{P}}_1} + \frac{\partial\mathbf{Q}_t'}{\partial\bar{\mathbf{P}}_1}\right)\cdot\Delta\mathbf{P}, \end{aligned} \tag{3.15}$$

where on the right hand side of Eq. (3.15),

$$\begin{aligned} \mathbf{Q}_t &\equiv \mathbf{Q}_t(x_1, p_1, \bar{\mathbf{Q}}_1, \bar{\mathbf{P}}_1), \\ \mathbf{Q}_t' &\equiv \mathbf{Q}_t(x_1', p_1', \bar{\mathbf{Q}}_1, \bar{\mathbf{P}}_1). \end{aligned} \tag{3.16}$$

Thus, $\mathbf{Q}_t$ and $\mathbf{Q}_t'$ have different *system* initial conditions but the same *bath* initial conditions. Similarly, the phase of the integrand of Eq. (3.8), the difference of actions, is expanded (through quadratic order) in $\Delta\mathbf{Q}$ and $\Delta\mathbf{P}$:

$$\begin{aligned} &S_t\left(x_1, p_1, \bar{\mathbf{Q}}_1 + \frac{\Delta\mathbf{Q}}{2}, \bar{\mathbf{P}}_1 + \frac{\Delta\mathbf{P}}{2}\right) - S_t\left(x_1', p_1', \bar{\mathbf{Q}}_1 - \frac{\Delta\mathbf{Q}}{2}, \bar{\mathbf{P}}_1 - \frac{\Delta\mathbf{P}}{2}\right) \\ &\quad = S_t - S_t' + \frac{1}{2}\left(\frac{\partial S_t}{\partial\bar{\mathbf{Q}}_1} + \frac{\partial S_t'}{\partial\bar{\mathbf{Q}}_1}\right)\cdot\Delta\mathbf{Q} + \frac{1}{2}\left(\frac{\partial S_t}{\partial\bar{\mathbf{P}}_1} + \frac{\partial S_t'}{\partial\bar{\mathbf{P}}_1}\right)\cdot\Delta\mathbf{P} \\ &\quad + \frac{1}{8}\Delta\mathbf{Q}^T\cdot\left(\frac{\partial^2 S_t}{\partial\bar{\mathbf{Q}}_1\partial\bar{\mathbf{Q}}_1} - \frac{\partial^2 S_t'}{\partial\bar{\mathbf{Q}}_1\partial\bar{\mathbf{Q}}_1}\right)\cdot\Delta\mathbf{Q} + \frac{1}{8}\Delta\mathbf{P}^T\cdot\left(\frac{\partial^2 S_t}{\partial\bar{\mathbf{P}}_1\partial\bar{\mathbf{P}}_1} - \frac{\partial^2 S_t'}{\partial\bar{\mathbf{P}}_1\partial\bar{\mathbf{P}}_1}\right)\cdot\Delta\mathbf{P} \\ &\quad + \frac{1}{4}\Delta\mathbf{P}^T\cdot\left(\frac{\partial^2 S_t}{\partial\bar{\mathbf{P}}_1\partial\bar{\mathbf{Q}}_1} - \frac{\partial^2 S_t'}{\partial\bar{\mathbf{P}}_1\partial\bar{\mathbf{Q}}_1}\right)\cdot\Delta\mathbf{Q}, \end{aligned} \tag{3.17}$$

where on the right hand side here, we again have

$$\begin{aligned} S_t &\equiv S_t(x_1, p_1, \bar{\mathbf{Q}}_1, \bar{\mathbf{P}}_1), \\ S_t' &\equiv S_t(x_1', p_1', \bar{\mathbf{Q}}_1, \bar{\mathbf{P}}_1). \end{aligned} \tag{3.18}$$

One can furthermore use the various derivative relations for the classical action to express the derivatives in Eq. (3.17) in terms of derivatives of final coordinates and momenta with respect to initial conditions (monodromy matrices):

$$\frac{\partial S_t}{\partial \bar{\mathbf{Q}}_1} + \frac{\partial S'_t}{\partial \bar{\mathbf{Q}}_1} = \mathbf{P}_t^T \cdot \mathbf{M}_{QQ} + \mathbf{P}_t'^T \cdot \mathbf{M}'_{QQ} - 2\bar{\mathbf{P}}_1^T, \tag{3.19}$$

$$\frac{\partial S_t}{\partial \bar{\mathbf{P}}_1} + \frac{\partial S'_t}{\partial \bar{\mathbf{P}}_1} = \mathbf{P}_t^T \cdot \mathbf{M}_{QP} + \mathbf{P}_t'^T \cdot \mathbf{M}'_{QP}, \tag{3.20}$$

$$\frac{\partial^2 S_t}{\partial \bar{\mathbf{Q}}_1 \partial \bar{\mathbf{Q}}_1} - \frac{\partial^2 S'_t}{\partial \bar{\mathbf{Q}}_1 \partial \bar{\mathbf{Q}}_1} = \mathbf{M}_{PQ}^T \cdot \mathbf{M}_{QQ} - \mathbf{M}_{PQ}'^T \cdot \mathbf{M}'_{QQ}, \tag{3.21}$$

$$\frac{\partial^2 S_t}{\partial \bar{\mathbf{P}}_1 \partial \bar{\mathbf{P}}_1} - \frac{\partial^2 S'_t}{\partial \bar{\mathbf{P}}_1 \partial \bar{\mathbf{P}}_1} = \mathbf{M}_{PP}^T \cdot \mathbf{M}_{QP} - \mathbf{M}_{PP}'^T \cdot \mathbf{M}'_{QP}, \tag{3.22}$$

$$\frac{\partial^2 S_t}{\partial \bar{\mathbf{P}}_1 \partial \bar{\mathbf{Q}}_1} - \frac{\partial^2 S'_t}{\partial \bar{\mathbf{P}}_1 \partial \bar{\mathbf{Q}}_1} = \mathbf{M}_{PP}^T \cdot \mathbf{M}_{QQ} - \mathbf{M}_{PP}'^T \cdot \mathbf{M}'_{QQ}, \tag{3.23}$$

where [analogous to Eq. (3.16)] $\mathbf{P}_t = \mathbf{P}_t(x_1, p_1, \bar{\mathbf{Q}}_1, \bar{\mathbf{P}}_1)$ and $\mathbf{P}'_t = \mathbf{P}_t(x'_1, p'_1, \bar{\mathbf{Q}}_1, \bar{\mathbf{P}}_1)$, and where the monodromy matrices are defined as

$$\mathbf{M}_{QQ} \equiv \mathbf{M}_{QQ}(x_1, p_1, \bar{\mathbf{Q}}_1, \bar{\mathbf{P}}_1) = \frac{\partial \mathbf{Q}_t}{\partial \bar{\mathbf{Q}}_1}, \tag{3.24}$$

$$\mathbf{M}_{PP} = \frac{\partial \mathbf{P}_t}{\partial \bar{\mathbf{P}}_1}, \tag{3.25}$$

$$\mathbf{M}_{QP} = \frac{\partial \mathbf{Q}_t}{\partial \bar{\mathbf{P}}_1}, \tag{3.26}$$

$$\mathbf{M}_{PQ} = \frac{\partial \mathbf{P}_t}{\partial \bar{\mathbf{Q}}_1}, \tag{3.27}$$

and similarly for $\mathbf{M}'_{ij}$ such as $\mathbf{M}'_{QQ} = \mathbf{M}'_{QQ}(x'_1, p'_1, \bar{\mathbf{Q}}_1, \bar{\mathbf{P}}_1)$. (Note: In Eqs. (3.19)-(3.23), terms involving the *second* derivatives of final coordinate and momenta with respect to initial conditions have been omitted.) The $\Delta\mathbf{Q}$ and $\Delta\mathbf{P}$ dependence of x_t and x'_t is also linearized,

$$\begin{aligned} x_t\left(x_1, p_1, \bar{\mathbf{Q}}_1 + \frac{\Delta\mathbf{Q}}{2}, \bar{\mathbf{P}}_1 + \frac{\Delta\mathbf{P}}{2}\right) &= x_t + \frac{1}{2}\mathbf{M}_{xQ} \cdot \Delta\mathbf{Q} + \frac{1}{2}\mathbf{M}_{xP} \cdot \Delta\mathbf{P}, \\ x_t\left(x'_1, p'_1, \bar{\mathbf{Q}}_1 - \frac{\Delta\mathbf{Q}}{2}, \bar{\mathbf{P}}_1 - \frac{\Delta\mathbf{P}}{2}\right) &= x'_t - \frac{1}{2}\mathbf{M}'_{xQ} \cdot \Delta\mathbf{Q} - \frac{1}{2}\mathbf{M}'_{xP} \cdot \Delta\mathbf{P}, \end{aligned} \tag{3.28}$$

where on the right hand side of Eq. (3.28)

$$\begin{aligned} x_t &= x_t(x_1, p_1, \bar{\mathbf{Q}}_1, \bar{\mathbf{P}}_1), \\ x'_t &= x_t(x'_1, p'_1, \bar{\mathbf{Q}}_1, \bar{\mathbf{P}}_1), \end{aligned} \tag{3.29}$$

and

$$\begin{aligned} \mathbf{M}_{xQ} &= \frac{\partial x_t}{\partial \bar{\mathbf{Q}}_1}, \\ \mathbf{M}_{xP} &= \frac{\partial x_t}{\partial \bar{\mathbf{P}}_1}, \end{aligned} \tag{3.30}$$

and similarly for $\mathbf{M}'_{xQ}$, etc. Finally, consistent with these linearizations, the $\Delta\mathbf{Q}$ and $\Delta\mathbf{P}$ dependence of the Jacobian in Eq. (3.8) is neglected.

With this set of expansions and approximations, Eq. (3.8) becomes

$$\begin{aligned} P_{n_2\leftarrow n_1}(t) = (2\pi\hbar)^{-(F+1)} &\int d\mathbf{Q}_1 d\mathbf{P}_1 \int dx_1 dp_1 \int dx'_1 dp'_1 \phi_{n_1}(x_1)\phi_{n_1}(x'_1) \\ & e^{i(S_t - S'_t)/\hbar} \sqrt{\det\left[\frac{\partial(x_t,\mathbf{Q}_t)}{\partial(p_1,\mathbf{P}_1)}\right]} \sqrt{\det\left[\frac{\partial(x'_t,\mathbf{Q}'_t)}{\partial(p'_1,\mathbf{P}'_1)}\right]} \int d\Delta\mathbf{Q} d\Delta\mathbf{P} \\ & \phi_{n_2}\left(x_t + \frac{1}{2}\mathbf{M}_{xQ}\cdot\Delta\mathbf{Q} + \frac{1}{2}\mathbf{M}_{xP}\cdot\Delta\mathbf{P}\right)^* \phi_{n_2}\left(x'_t - \frac{1}{2}\mathbf{M}'_{xQ}\cdot\Delta\mathbf{Q} - \frac{1}{2}\mathbf{M}'_{xP}\cdot\Delta\mathbf{P}\right) \\ & \delta_F(\mathbf{Q}_t - \mathbf{Q}'_t + \frac{1}{2}(\mathbf{M}_{QQ} + \mathbf{M}'_{QQ})\cdot\Delta\mathbf{Q} + \frac{1}{2}(\mathbf{M}_{QP} + \mathbf{M}'_{QP})\cdot\Delta\mathbf{P}) \\ & \left\langle \mathbf{Q}_1 + \frac{\Delta\mathbf{Q}}{2}\middle|\, \rho_b \,\middle| \mathbf{Q}_1 - \frac{\Delta\mathbf{Q}}{2}\right\rangle \exp\frac{i}{\hbar}\Bigg[\frac{1}{2}\left(\mathbf{P}_t^T\cdot\mathbf{M}_{QQ} + \mathbf{P}_t'^T\cdot\mathbf{M}'_{QQ} - 2\mathbf{P}_1^T\right)\cdot\Delta\mathbf{Q} \\ & + \frac{1}{2}\left(\mathbf{P}_t^T\cdot\mathbf{M}_{QP} + \mathbf{P}_t'^T\cdot\mathbf{M}'_{QP}\right)\cdot\Delta\mathbf{P} + \frac{1}{8}\Delta\mathbf{Q}^T\cdot(\mathbf{M}_{PQ}^T\cdot\mathbf{M}_{QQ} - \mathbf{M}_{PQ}'^T\cdot\mathbf{M}_{QQ'})\cdot\Delta\mathbf{Q} \\ & + \frac{1}{8}\Delta\mathbf{P}^T\cdot(\mathbf{M}_{PP}^T\cdot\mathbf{M}_{QP} - \mathbf{M}_{PP}'^T\cdot\mathbf{M}_{QP'})\cdot\Delta\mathbf{P} \\ & + \frac{1}{4}\Delta\mathbf{P}^T\cdot(\mathbf{M}_{PP}^T\cdot\mathbf{M}_{QQ} - \mathbf{M}_{PP}'^T\cdot\mathbf{M}'_{QQ})\cdot\Delta\mathbf{Q}\Bigg], \end{aligned} \tag{3.31}$$

where the "bars" over the integration variables $\bar{\mathbf{Q}}_1$ and $\bar{\mathbf{P}}_1$ have been dropped. All the primed and unprimed functions at time t differ only in whether they are functions of (x_1, p_1) or (x'_1, p'_1). To emphasize again, the purpose of the above set of approximations has been to obtain the best possible result that still allows one to integrate analytically over $\Delta\mathbf{Q}$ and $\Delta\mathbf{P}$, so as to reduce the average over the bath variables to that of a *classical* description, namely an average over a single set of phase space initial conditions for the bath. (Many of the above approximations are actually exact for a *harmonic* bath, because the action for a harmonic bath is quadratic in $\mathbf{Q}_1$ and $\mathbf{P}_1$, and thus in $\Delta\mathbf{Q}$ and $\Delta\mathbf{P}$, so that the expansion of the actions to quadratic order in $\Delta\mathbf{Q}$ and $\Delta\mathbf{P}$ is exact.)

Because of the F-dimensional delta function in the integrand of Eq. (3.31), the integral over $\Delta\mathbf{P}$ in Eq. (3.31) can be immediately performed. This sets $\Delta\mathbf{P}$ to the value

$$\Delta\mathbf{P} = -2(\mathbf{M}_{QP} + \mathbf{M}'_{QP})^{-1}\cdot[\mathbf{Q}_t - \mathbf{Q}'_t + \frac{1}{2}(\mathbf{M}_{QQ} + \mathbf{M}'_{QQ})\cdot\Delta\mathbf{Q}]. \tag{3.32}$$

The remaining integral over $\Delta\mathbf{Q}$ in Eq. (3.31) will then have a phase factor that is quadratic in $\Delta\mathbf{Q}$ but which cannot be evaluated in general because of the $\Delta\mathbf{Q}$ dependence of the pre-exponential factors (in the wavefunction $\phi_{n_2}()$ and in the bath density matrix element $\langle\ldots|\rho_b|\ldots\rangle$). One can either neglect this dependence, in which case the integral of the complex Gaussian is immediately doable, or somewhat more generally, one can assume that the $\Delta\mathbf{Q}$ dependence of the pre-exponential factors is small and the integral can be evaluated via stationary phase approximation (which will be exact if the pre-exponential factor is independent of $\Delta\mathbf{Q}$).

Zeroth Order Model

It is useful first to consider the simplest version of the approach. Thus if in the integration over $\Delta\mathbf{Q}$ and $\Delta\mathbf{P}$ in Eq. (3.31), one neglects all monodromy matrix elements in the phase of the integral, then this part of the integral in Eq. (3.31) reduces to

$$\begin{aligned}
&\phi_{n_2}(x_t)^*\phi_{n_2}(x_t')\int d\Delta\mathbf{Q}d\Delta\mathbf{P}\left\langle \mathbf{Q}_1+\frac{\Delta\mathbf{Q}}{2}\middle|\rho_b\middle|\mathbf{Q}_1-\frac{\Delta\mathbf{Q}}{2}\right\rangle \\
&\qquad \delta_F(\mathbf{Q}_t-\mathbf{Q}_t'+\frac{1}{2}(\mathbf{M}_{QQ}+\mathbf{M}'_{QQ})\cdot\Delta\mathbf{Q}+\frac{1}{2}(\mathbf{M}_{QP}+\mathbf{M}'_{QP})\cdot\Delta\mathbf{P})e^{-i\mathbf{P}_1^T\cdot\Delta\mathbf{Q}/\hbar} \\
&= \phi_{n_2}(x_t)^*\phi_{n_2}(x_t')(2\pi\hbar)^F\frac{\rho_w(\mathbf{Q}_1,\mathbf{P}_1)}{\det\left[\frac{1}{2}(\mathbf{M}_{QP}+\mathbf{M}'_{QP})\right]},
\end{aligned} \tag{3.33}$$

where the definition of ρ_w in Eq. (3.12) has been used. If one further neglects the system-bath coupling in the Jacobian, namely,

$$\det\left[\frac{\partial(x_t,\mathbf{Q}_t)}{\partial(p_1,\mathbf{P}_1)}\right]\approx\frac{\partial x_t}{\partial p_1}\det\left(\frac{\partial\mathbf{Q}_t}{\partial\mathbf{P}_1}\right)\equiv\frac{\partial x_t}{\partial p_1}\det(\mathbf{M}_{QP}), \tag{3.34}$$

and

$$\det\left[\frac{\partial(x_t',\mathbf{Q}_t')}{\partial(p_1',\mathbf{P}_1')}\right]\approx\frac{\partial x_t'}{\partial p_1'}\det(\mathbf{M}'_{QP}), \tag{3.35}$$

then Eq. (3.31) reduces to

$$\begin{aligned}
P_{n_2\leftarrow n_1}(t)=\frac{1}{2\pi\hbar}\int d\mathbf{Q}_1d\mathbf{P}_1\rho_w(\mathbf{Q}_1,\mathbf{P}_1)\int dx_1dp_1\int dx_1'dp_1' \\
\phi_{n_1}(x_1)\phi_{n_1}(x_1')^*\phi_{n_2}(x_t)^*\phi_{n_2}(x_t')e^{i(S_t-S_t')/\hbar} \\
\sqrt{\frac{\partial x_t}{\partial p_1}}\sqrt{\frac{\partial x_t'}{\partial p_1'}}\frac{\sqrt{\det(\mathbf{M}_{QP}\cdot\mathbf{M}'_{QP})}}{\det\left[\frac{1}{2}(\mathbf{M}_{QP}+\mathbf{M}'_{QP})\right]}.
\end{aligned} \tag{3.36}$$

Finally, if one then assumes that the geometric and arithmetic averages of the monodromy matrices $\mathbf{M}_{QP}$ and $\mathbf{M}'_{QP}$ are approximately equal, then the last factor in the integral of Eq.

(3.36) is unity, whereby the double phase integral over the system initial conditions factors, giving

$$P_{n_2\leftarrow n_1}(t) = \int d\mathbf{Q}_1 d\mathbf{P}_1 \rho_w(\mathbf{Q}_1,\mathbf{P}_1)\left|\int dx_1 dp_1 \phi_{n_1}(x_1)\phi_{n_2}(x_t)^* e^{iS_t/\hbar} \sqrt{\frac{\partial x_t}{\partial p_1}/(2\pi i\hbar)}\right|^2 . \tag{3.37}$$

Eq. (3.37) above is the zeroth order limit of the present semiclassical-classical approach. It is also recognized to be the precise *semiclassical analog of the Ehrenfest quantum-classical model* described earlier. The square modulus quantity in the integrand of Eq. (3.37) is the semiclassical IVR expression for the quantum transition probability for the one-dimensional system, with the bath following the trajectory determined by initial conditions $(\mathbf{Q}_1,\mathbf{P}_1)$:

$$P^{IVR}_{n_2\leftarrow n_1}(t;\mathbf{Q}_1,\mathbf{P}_1) = \left|\int dx_1 dp_1 \phi_{n_1}(x_1)\phi_{n_2}(x_t)^* e^{iS_t/\hbar}\sqrt{\frac{\partial x_t}{\partial p_1}/(2\pi i\hbar)}\right|^2 . \tag{3.38}$$

Here the trajectory functions $x_t \equiv x_t(x_1,p_1,\mathbf{Q}_1,\mathbf{P}_1)$ and $S_t \equiv S_t(x_1,p_1,\mathbf{Q}_1,\mathbf{P}_1)$ which go into the one-dimensional-like transition probability involve the (exact) classical mechanics of the fully coupled system and bath, analogous to the coupled Schrödinger equation-classical equations which appear in the quantum-classical Ehrenfest model. The phase ν is the number of zeros of the one-dimensional Jacobian of the system degree of freedom. Eq. (3.37) is also identical to what was called "partial averaging" in some applications many years ago.[116]

An attractive feature of the present semiclassical-classical approach, however, is that we now have the possibility of going beyond this primitive zeroth version of the treatment. The major price to be paid is that it will not be possible to factor the double phase space integral over the system initial conditions as was done in going from Eq. (3.36) to Eq. (3.37).

First Order Model

Returning to Eq. (3.31), we now retain the terms in the phase of integrand that are linear in $\Delta\mathbf{Q}$ and $\Delta\mathbf{P}$. If the wavefunction ϕ_{n_2} were a coherent state (complex Gaussian), then it would be easy to include the $\Delta\mathbf{Q}$ and $\Delta\mathbf{P}$ dependence of its arguments, but here we

do not assume this and simply ignore this dependence. The $(\Delta\mathbf{Q}, \Delta\mathbf{P})$ part of the integral thus becomes

$$\begin{aligned}
&\phi_{n_2}(x_t)^*\phi_{n_2}(x_t') \int \Delta\mathbf{Q} \int \Delta\mathbf{P} \left\langle \mathbf{Q}_1 + \frac{\Delta\mathbf{Q}}{2} \middle| \rho_b \middle| \mathbf{Q}_1 - \frac{\Delta\mathbf{Q}}{2} \right\rangle \\
&\quad \delta_F(\mathbf{Q}_t - \mathbf{Q}_t' + \frac{1}{2}(\mathbf{M}_{QQ} + \mathbf{M}_{QQ}') \cdot \Delta\mathbf{Q} + \frac{1}{2}(\mathbf{M}_{QP} + \mathbf{M}_{QP}') \cdot \Delta\mathbf{P}) \\
&\quad \exp \frac{i}{\hbar} \left[\frac{1}{2}(\mathbf{P}_t^T \cdot \mathbf{M}_{QQ} + \mathbf{P}_t'^T \cdot \mathbf{M}_{QQ}' - 2\mathbf{P}_1^T) \cdot \Delta\mathbf{Q} + \frac{1}{2} \left(\mathbf{P}_t^T \cdot \mathbf{M}_{QP} + \mathbf{P}_t'^T \cdot \mathbf{M}_{QP}' \right) \cdot \Delta\mathbf{P} \right],
\end{aligned} \tag{3.39}$$

which gives the following generalization of the zeroth result in Eq. (3.33):

$$\begin{aligned}
&= \phi_{n_2}(x_t)^*\phi_{n_2}(x_t')(2\pi\hbar)^F \rho_w(\mathbf{Q}_1, \mathbf{P}_1 - \mathbf{P}_{cor}) \frac{2^F}{\det(\mathbf{M}_{QP} + \mathbf{M}_{QP}')} \\
&\quad \exp \left[-\frac{i}{\hbar}(\mathbf{P}_t^T \cdot \mathbf{M}_{QP} + \mathbf{P}_t'^T \cdot \mathbf{M}_{QP}') \cdot (\mathbf{M}_{QP} + \mathbf{M}_{QP}')^{-1} \cdot (\mathbf{Q}_t - \mathbf{Q}_t') \right],
\end{aligned} \tag{3.40}$$

where the momentum correction $\mathbf{P}_{cor}$ is

$$\begin{aligned}
\mathbf{P}_{cor} &= \frac{1}{2} \left(\mathbf{P}_t^T \cdot \mathbf{M}_{QQ} + \mathbf{P}_t'^T \cdot \mathbf{M}_{QQ}' \right) \\
&\quad -\frac{1}{2} \left(\mathbf{P}_t^T \cdot \mathbf{M}_{QP} + \mathbf{P}_t'^T \cdot \mathbf{M}_{QP}' \right) \cdot \left(\mathbf{M}_{QP} + \mathbf{M}_{QP}' \right)^{-1} \cdot \left(\mathbf{M}_{QQ} + \mathbf{M}_{QQ}' \right).
\end{aligned} \tag{3.41}$$

The first order expression for the average transition probability is then

$$\begin{aligned}
P_{n_2 \leftarrow n_1}(t) &= \frac{1}{2\pi\hbar} \int d\mathbf{Q}_1 d\mathbf{P}_1 \int dx_1 dp_1 \int dx_1' dp_1' \rho_w(\mathbf{Q}_1, \mathbf{P}_1 - \mathbf{P}_{cor}) \\
&\quad \phi_{n_1}(x_1)\phi_{n_1}(x_1')^*\phi_{n_2}(x_t)^*\phi_{n_2}(x_t')e^{i(S_t - S_t')/\hbar} \\
&\quad \sqrt{\det \left[\frac{\partial(x_t, \mathbf{Q}_t)}{\partial(p_1, \mathbf{P}_1)} \right]} \sqrt{\det \left[\frac{\partial(x_t', \mathbf{Q}_t')}{\partial(p_1', \mathbf{P}_1')} \right]} \frac{2^F}{\det(\mathbf{M}_{QP} + \mathbf{M}_{QP}')} \\
&\quad \exp \left[-\frac{i}{\hbar}(\mathbf{P}_t^T \cdot \mathbf{M}_{QP} + \mathbf{P}_t'^T \cdot \mathbf{M}_{QP}') \cdot (\mathbf{M}_{QP} + \mathbf{M}_{QP}')^{-1} \cdot (\mathbf{Q}_t - \mathbf{Q}_t') \right].
\end{aligned} \tag{3.42}$$

Again, we can make the same approximations on the Jacobian factors as for the zeroth order model, yielding a numerically better behaved result (since the determinant of the monodromy matrices in the denominator can go through zero),

$$\begin{aligned}
P_{n_2 \leftarrow n_1}(t) &= \frac{1}{2\pi\hbar} \int d\mathbf{Q}_1 d\mathbf{P}_1 \int dx_1 dp_1 \int dx_1' dp_1' \rho_w(\mathbf{Q}_1, \mathbf{P}_1 - \mathbf{P}_{cor}) \\
&\quad \phi_{n_1}(x_1)\phi_{n_1}(x_1')^*\phi_{n_2}(x_t)^*\phi_{n_2}(x_t')e^{i(S_t - S_t')/\hbar} \sqrt{\frac{\partial x_t}{\partial p_1}} \sqrt{\frac{\partial x_t'}{\partial p_1'}} \\
&\quad \exp \left[-\frac{i}{\hbar}(\mathbf{P}_t^T \cdot \mathbf{M}_{QP} + \mathbf{P}_t'^T \cdot \mathbf{M}_{QP}') \cdot (\mathbf{M}_{QP} + \mathbf{M}_{QP}')^{-1} \cdot (\mathbf{Q}_t - \mathbf{Q}_t') \right].
\end{aligned} \tag{3.43}$$

Equations (3.42), (3.43) involve a classical (single phase space) average over the initial conditions of the bath degrees of freedom, but a double phase space average over the system degrees of freedom. The extra phase factor in the integrand and the momentum correction in the Wigner distribution prevent the factorization and serve as corrections to the zeroth order result of Eq. (3.36). Actually, as will be seen in Section 3.2.2, the momentum correction in the Wigner distribution will not be so important as the phase correction in the exponent. In practical calculations, it is often neglected.

A second order version of the model would be obtained by retaining all the terms in the phase of the integrand in Eq. (3.31) and also the second order $\Delta\mathbf{Q}$ and $\Delta\mathbf{P}$ dependence of the bath density matrix element $\langle\mathbf{Q}_1+\Delta\mathbf{Q}/2|\rho_b|\mathbf{Q}_1-\Delta\mathbf{Q}/2\rangle$. If the bath is harmonic, then the density matrix element is a simple Gaussian function of $\Delta\mathbf{Q}$ and $\Delta\mathbf{P}$. Furthermore, if the initial and final system wavefunctions are coherent states, then they too would contribute Gaussian factors in $\Delta\mathbf{Q}$ and $\Delta\mathbf{P}$. Integration over $\Delta\mathbf{Q}$ or $\Delta\mathbf{P}$ would then be a standard Gaussian integral that is readily doable.

3.2.2 Numerical Applications to Simple Systems

To help elucidate the nature of the mixed semiclassical-classical approaches described above, numerical tests have to be made. We have chosen a simple system that can be treated fully quantum mechanically, fully semiclassically, as well as via the above semiclassical-classical models, namely an anharmonic (Morse) oscillator linearly coupled to a single harmonic mode. The Hamiltonian for this system is

$$\mathbf{H} = \frac{p^2}{2m} + \frac{P^2}{2m} + a_0(1-e^{-c_0 x})^2 + \frac{1}{2}m\omega^2 Q^2 + fxQ. \tag{3.44}$$

where the parameters are $m = 1772.3302, a_0 = 0.1697, c_0 = 0.9885, \omega = 0.0156$, all in atomic units. The coupling constant f is varied to see the effect of the strength of the system-bath coupling.

To implement the semiclassical IVR calculations, we utilize the Herman-Kluk procedure of Eq. (2.14). The Herman-Kluk IVR thus modifies the integrand for the zeroth order semiclassical-classical expression, Eq. (3.38), to the following

$$P^{IVR}_{n_2\leftarrow n_1}(t;Q_1,P_1) = \left|\frac{1}{2\pi\hbar}\int dx_1 dp_1 \mathbf{C}_{xpt}\phi^g_{n_1}(x_1,p_1)\phi^g_{n_2}(x_t,p_t)^* e^{iS_t/\hbar}\right|^2, \tag{3.45}$$

where

$$\phi^g_{n_{1,2}}(x,p) = \langle xp|\phi_{n_{1,2}}\rangle = \int dx' \phi_{n_{1,2}}(x') \left(\frac{\gamma}{\pi}\right)^{\frac{1}{4}} e^{-\frac{\gamma}{2}(x'-x)^2 - ip(x'-x)/\hbar}, \tag{3.46}$$

and similarly the first order expression of Eq (3.43), becomes

$$\begin{aligned} P_{n_2 \leftarrow n_1}(t) = \frac{1}{(2\pi\hbar)^2} \int dQ_1 dP_1 \int dx_1 dp_1 \int dx_1' dp_1' \rho_w(Q_1, P_1 - P_{cor}) \\ \phi^g_{n_1}(x_1,p_1)\phi^g_{n_1}(x_1',p_1')^* \phi^g_{n_2}(x_t,p_t)^* \phi^g_{n_2}(x_t',p_t') e^{i(S_t - S_t')/\hbar} \mathbf{C}_{xpt}\mathbf{C}'_{xpt} \\ \exp\left[-\frac{i}{\hbar}(P_t \cdot M_{QP} + P_t' \cdot M'_{QP}) \cdot (M_{QP} + M'_{QP})^{-1} \cdot (Q_t - Q_t')\right]. \end{aligned} \tag{3.47}$$

Since the bath in this example consists of only one mode, the monodromy matrices in these equations are all simple scalars. Furthermore, the bath is harmonic, so that the Wigner distribution ρ_w is given by

$$\rho_w(Q,P) = \frac{\tanh(u)}{\pi\hbar} \exp\left[-\frac{2\tanh(u)}{\hbar\omega}\left(\frac{P^2}{2m} + \frac{1}{2}m\omega^2 Q^2\right)\right], \tag{3.48}$$

where $u = \beta\hbar\omega/2$ and β is the usual $1/k_B T$.

Lastly, for efficient integration, weighted Monte Carlo sampling of the initial condition is used. For the quantum mechanical calculations, we utilized the split operator method of propagation.

Survival Probability of a Gaussian

We first consider the diagonal transition probability (i.e., the survival probability) of a displaced Gaussian,

$$P_{1,1}(t) \equiv \sum_{m_1,m_2} \wp_{m_1} \left|\langle \chi_{m_2}\phi_1 | e^{-i\hat{H}t/\hbar} | \chi_{m_1}\phi_1\rangle\right|^2, \tag{3.49}$$

where

$$\phi_1(x) \equiv \left(\frac{\alpha}{\pi}\right)^{\frac{1}{4}} e^{-\frac{\alpha}{2}(x-x_0)^2}, \tag{3.50}$$

and the $\chi_m(Q)$'s are the harmonic oscillator eigenstates of the bath. The center of the initial state Gaussian wavefunction is chosen to be $x_0 = 1.5a_0$, corresponding to the classical turning point of the $n = 6$ eigenstate of the Morse oscillator. We have considered three values for the coupling constant f, from the relatively small coupling of $f = -0.02$, to $f = -0.05$, to the largest value, $f = -0.1$, all in atomic units. We also used two different values of temperature, $T = 300K$, where the probabilities are dominated by transitions

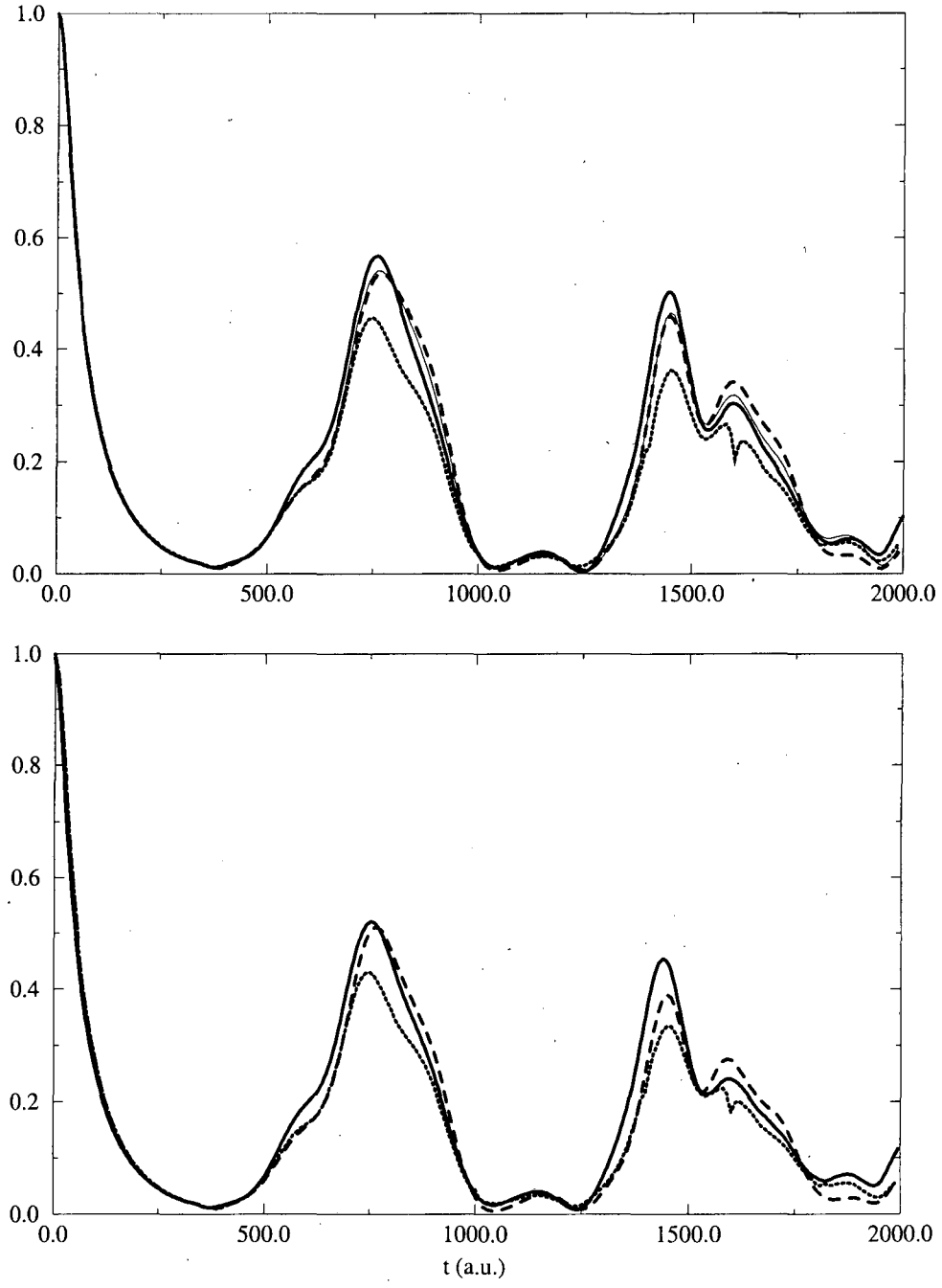

Figure 3.1: Survival probability, $P_{1,1}(t)$ of Eq. (3.49), for coupling constant $f = -0.02$. $T = 300K$ in the upper graph, $T = 5000K$ in the lower graph. Solid line: exact quantum. Dashed line: zeroth order mixed semiclassical-classical method. Dotted line: first order method. Thin line: full semiclassical.

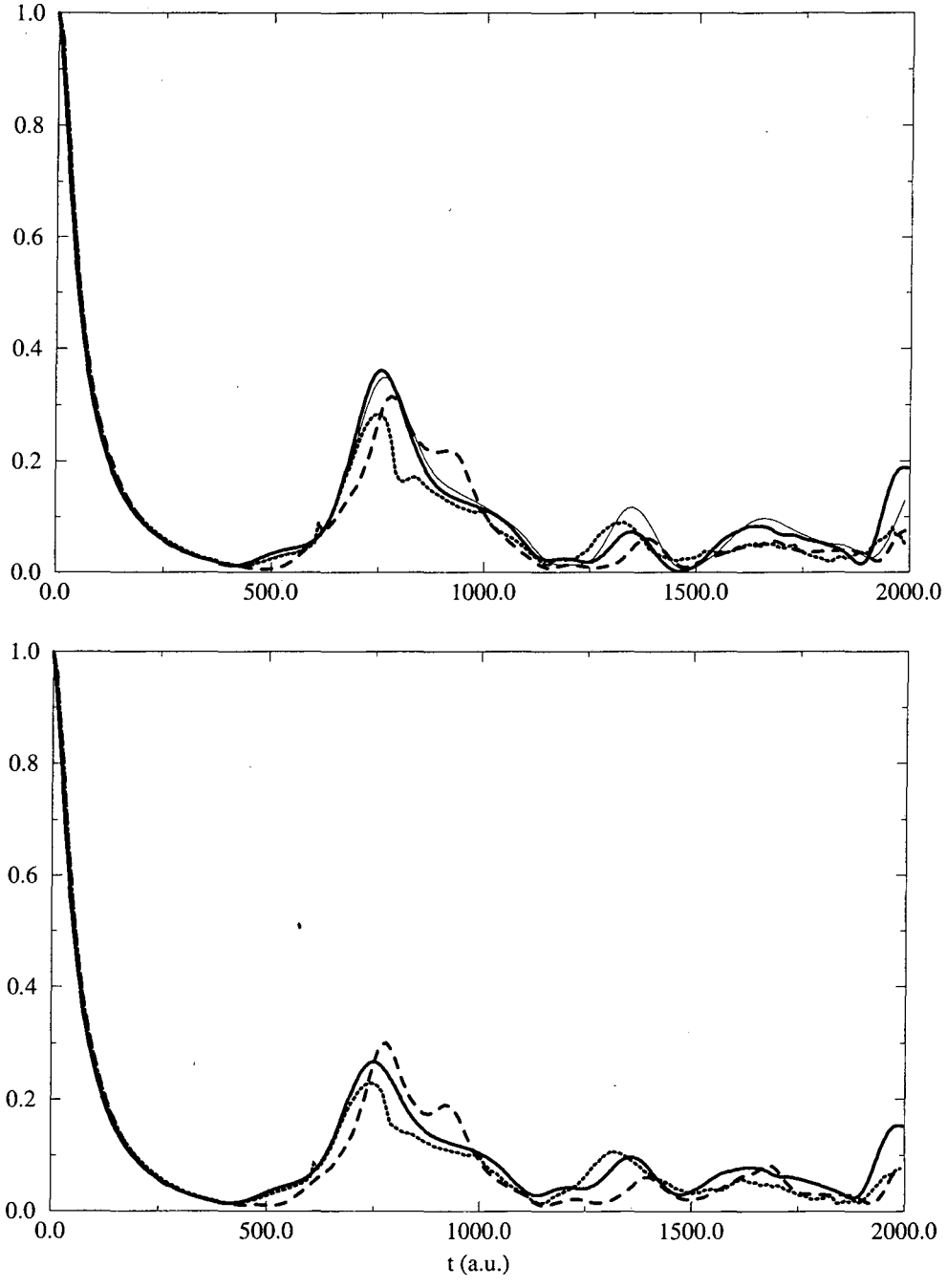

Figure 3.2: Same as Figure 3.1, with $f = -0.05$

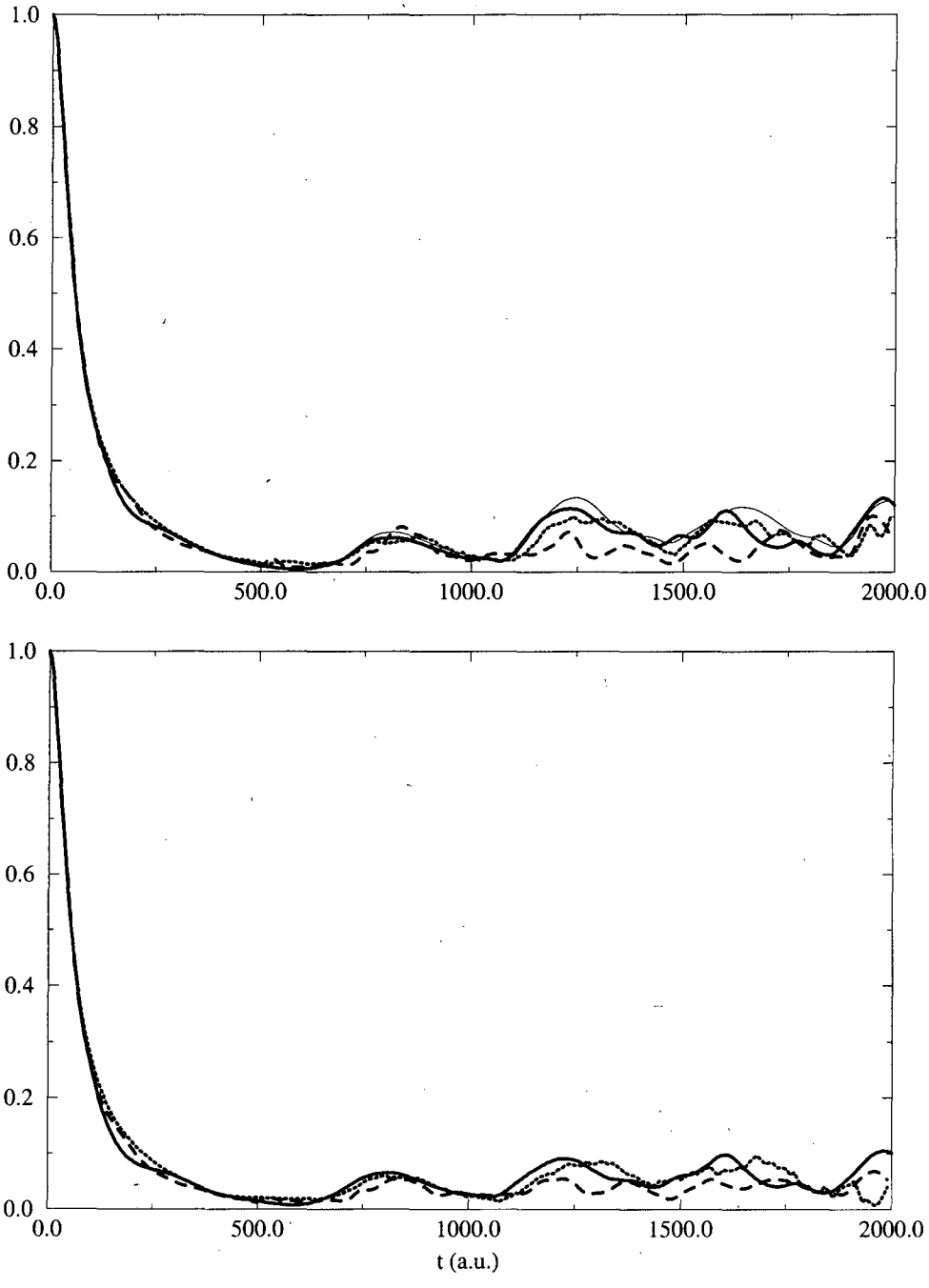

Figure 3.3: Same as Figure 3.1, with $f = -0.1$

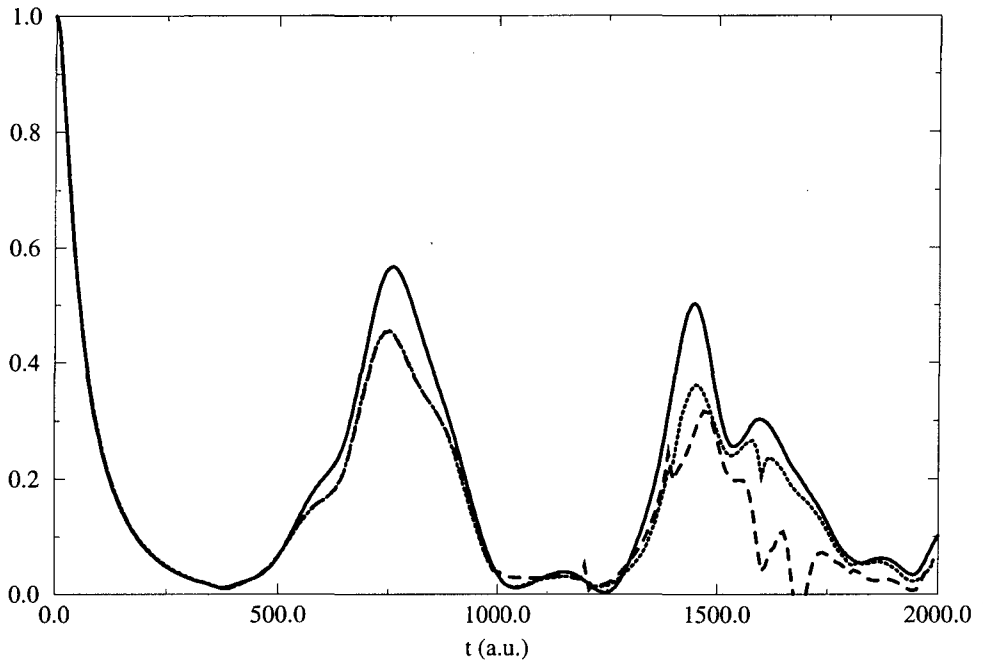

Figure 3.4: Survival probability $P_{1,1}(t)$ of Eq. (3.49), comparison between the first order expression without momentum correction in the Wigner distribution (dotted line), and with momentum correction (dashed line). Solid line is the full quantum mechanical result. $f = -0.02$.

from the ground state of the bath, and $T = 5000K$, where there are several bath states involved. The calculated survival probabilities are shown in Figures 3.1, 3.2 and 3.3, where the results of the semiclassical-classical methods and the full semiclassical method similar to Eq. (3.7) but with the Herman-Kluk IVR (calculations are performed only for the lower temperature due to the large numerical effort needed for the high temperature case) are compared with the results of the exact quantum mechanical calculation. In Figure 3.4, the results of the first order model with and without the momentum correction in the Wigner distribution are compared.

From these results one can make several observations. First, the full semiclassical IVR result is in excellent agreement with the correct quantum mechanical result for all coupling strengths considered. Second, the zeroth order ("partial averaging") version of the semiclassical-classical model is in quantitative agreement with the quantum results for weak coupling, but only in qualitative agreement for strong coupling. Third, the first order version of the model is not a systematic improvement over the zeroth order version. Fourth,

the qualitative effect of the temperature, i.e. higher temperatures reduces the magnitude of the recurrences, is also well reproduced by these mixed semiclassical-classical methods.

State-to-State Transition Probabilities

Non-diagonal transition probabilities of the system are a more challenging quantity to describe correctly. Specifically, we consider here the vibrational relaxation of the Morse oscillator from $n = 1$ to 0. Thus, Morse eigenfunctions are used for $\phi(x)$. Again, we vary the coupling from -0.02 to -0.1 and the temperature from $300K$ to $5000K$. To facilitate the semiclassical calculations, we fit the $n = 1$ eigenfunction by the difference two Gaussians and approximated the $n = 0$ eigenfunction with one. This way, $\phi^g(x,p)$ in Eq. (3.45) and Eq. (3.47) can be obtained analytically. Figures 3.5, 3.6 and 3.7 show the results for these calculations. Here, the first order calculation is with $P_{cor} = 0$.

The comparisons are now quite different from the diagonal transition probabilities of the previous section. First, the immediate conclusion is that the zeroth order (partial averaging) formula is *no longer adequate.* In fact, if the mixed *quantum*-classical TDSCF method were applied here, it would give similar results. The first order model, though not spectacularly accurate, does agree qualitatively with the correct quantum results; in comparison with the zeroth order model, which is off by a factor of four or five, it is a significant improvement. Again, the full semiclassical IVR results are practically indistinguishable from the correct quantum results in all cases.

One then naturally asks, why the zeroth order (partial averaging) approximation works well for the survival (diagonal transition) probability of a single Gaussian as in the previous section, but fails for the present non-diagonal state-to-state transition probability? The answer goes back to the Ehrenfest (TDSCF) model discussed in the Introduction, where it was noted that the zeroth order (partial averaging) version of the semiclassical-classical model is the semiclassical equivalent of the Ehrenfest model. In this approximation the classical potential for the bath is the Ehrenfest average of the potential, cf. Eq. (3.2). When the system wavefunction is well localized, one has

$$V_{CL}(Q,t) = \int dx \Psi(x,t)^* V(x,Q) \Psi(x,t) \approx V(x_{CL}(t),Q), \tag{3.51}$$

where

$$x_{CL}(t) = \int dx \Psi(x,t)^* x \Psi(x,t); \tag{3.52}$$

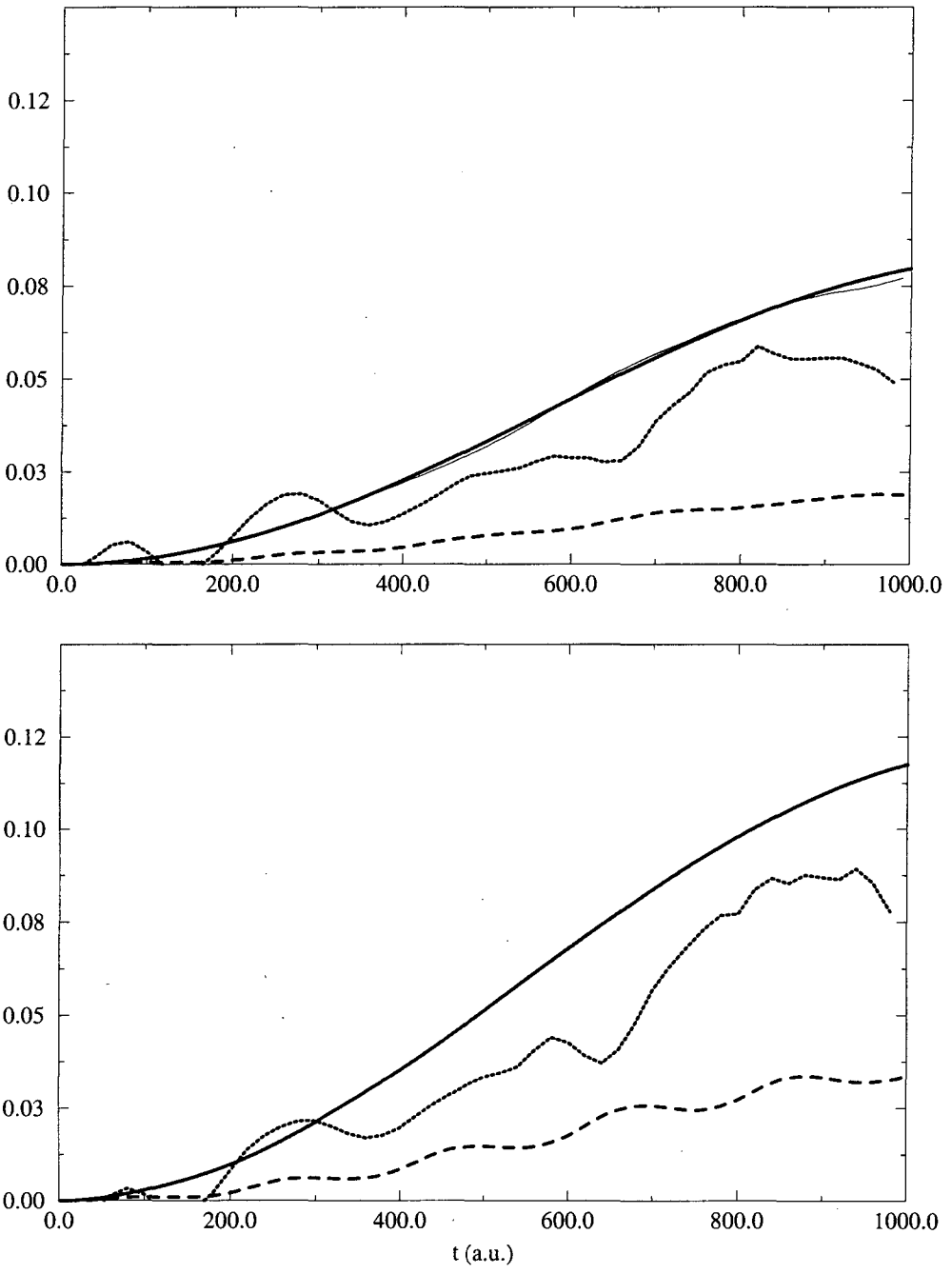

Figure 3.5: Relaxation probability from $n = 1$ to $n = 0$ of the Morse oscillator. $f = -0{,}02$. $T = 300K$ in the upper graph, $T = 5000K$ in the lower graph. Solid line: exact quantum. Dashed line: zeroth order mixed semiclassical-classical method. Dotted line: first order method. Thin line: full semiclassical.

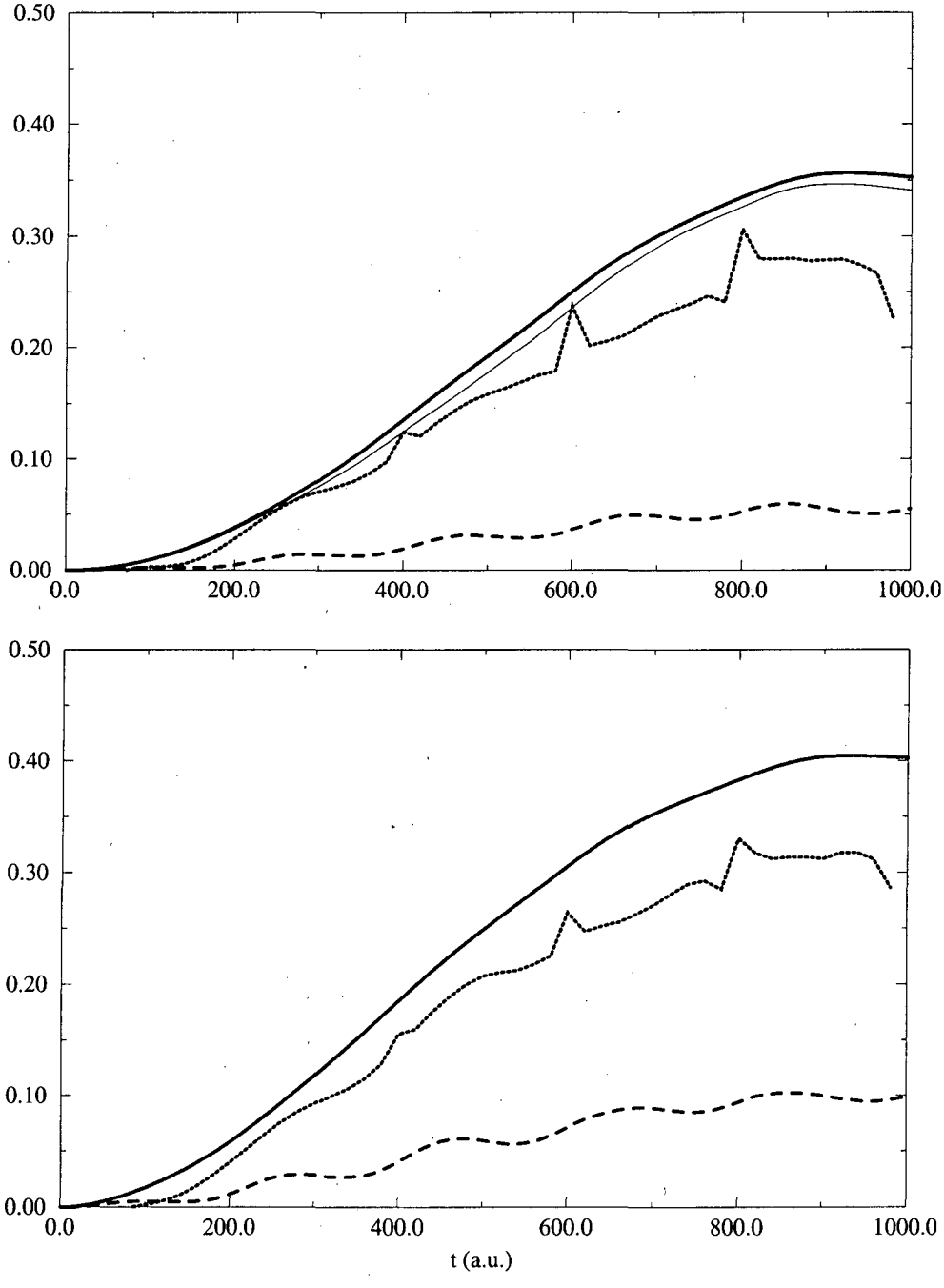

Figure 3.6: Same as Figure 3.5, with $f = -0.05$

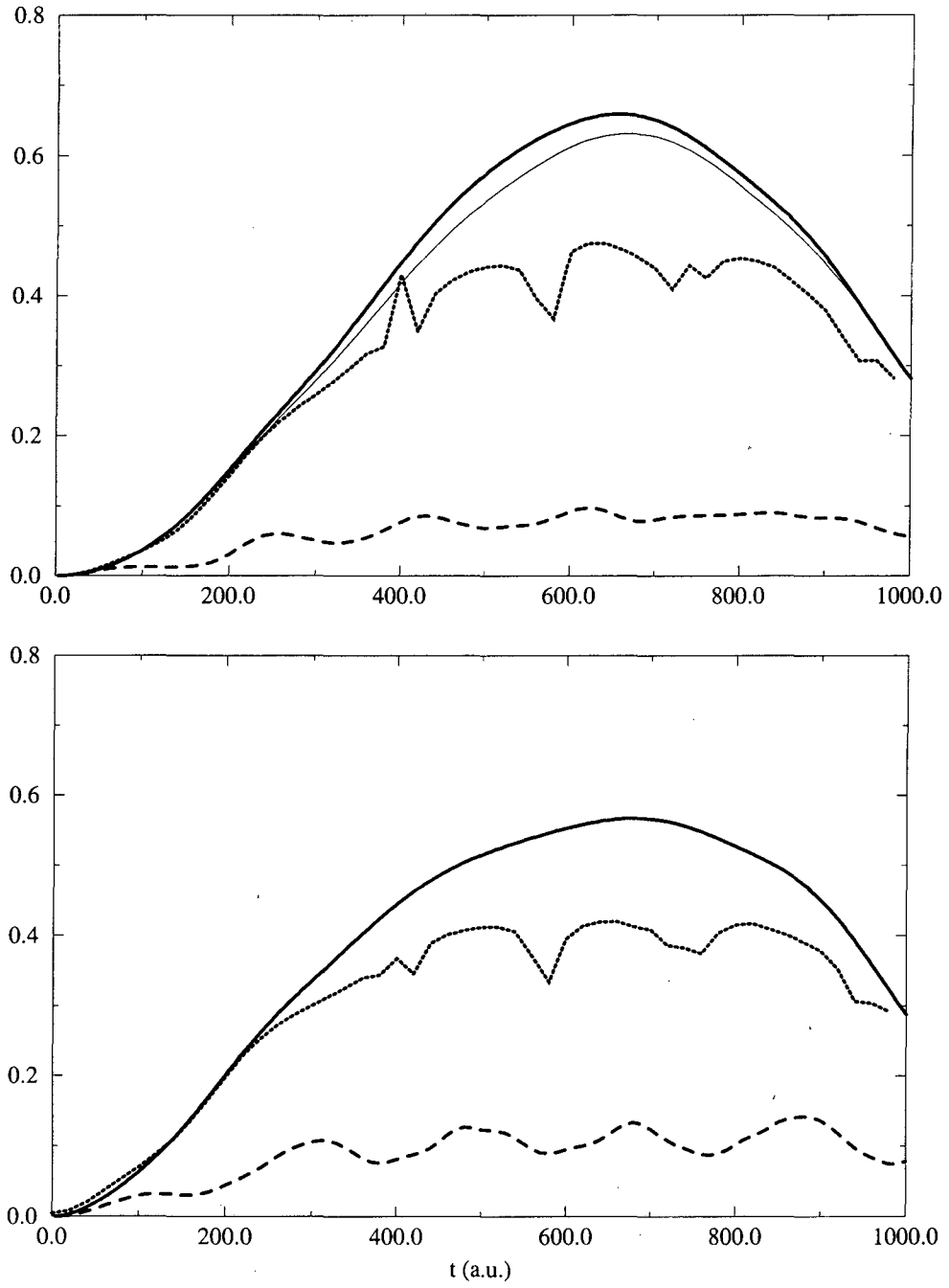

Figure 3.7: Same as Figure 3.5, with $f = -0.1$

this is the correct classical description of the system-bath dynamics. But when the system wavefunction is extended, as it must be in describing transitions between the various eigenstates $\{\phi_n\}$, Eqs. (3.51) and (3.52) cease to be valid. This is simply an example of the failure of the single configuration TDSCF approximation, because the classical bath in reality sees a different potential for different states of the system, not one average potential.

3.2.3 Concluding Remarks

Given the semiclassical IVR description of the complete molecular system, it was then shown how one can make systematic approximations that retain the full semiclassical description of the "system" degrees of freedom — thereby describing quantum interference and tunneling effects in them — while neglecting such effects in the "bath" degrees of freedom, resulting in a classical description of them. The zeroth order version of this mixed semiclassical-classical model was seen to be a semiclassical version of the Ehrenfest model (closely related to the TDSCF approximation). For the examples considered in Section 3.2.2, it was seen to work well for the survival (diagonal transition) probability of a single Gaussian if the coupling is sufficiently weak, but to fail for strong coupling and for non-diagonal transition probabilities. A first order version of the mixed semiclassical-classical model was a significant improvement over the zeroth version (at least for the non-diagonal transition probabilities), though still significantly less accurate than the full semiclassical IVR treatment.

There are two ways to improve the accuracy of the treatment within the present formulation: (1) to use a higher (i.e. second) order version of the mixed semiclassical-classical model, or (2) to include more of the "bath" modes — the most strongly coupled ones — in an enlarged "system", i.e., to retain the full semiclassical IVR description for a large number of degrees of freedom. Our present feeling is that route (2) may be more profitable, but applications to more complex system of physical interest will be necessary to decide whether or not this is feasible.

3.3 Full Linearization Approximation

In the previous section, we considered the case where approximations are made to some degrees of freedom in the problem, but not to others and arrived at a "mixed semiclassical-classical" treatment for the dynamics. We saw that there is the possibility of

systematically improving the model by going to higher order terms. However, as with any mixed treatment, the choice of system-bath separation is not unique and impacts greatly upon the results.[117] And for different quantities of interest, different choices of system and bath are usually required. It is therefore desirable to treatment every variable in the problem at the same level of approximation.

Toward this end, we shall carry out the same expansion in the Δ variables but now for all degrees of freedom in the problem and try to see if this is a fruitful route to proceed. Consider a generic quantum mechanical transition probability from state $|\Psi_1\rangle$ to $|\Psi_2\rangle$ in time t; the quantum expression for this is

$$P_{2\leftarrow 1}(t) = |S_{2,1}(t)|^2 \tag{3.53a}$$

with

$$\begin{aligned} S_{2,1}(t) &= \langle \Psi_2 | e^{-i\hat{H}t/\hbar} | \Psi_1 \rangle & (3.53b) \\ &= \int d\mathbf{q}_1 d\mathbf{q}_0 \Psi_2(\mathbf{q}_1)^* \langle \mathbf{q}_1 | e^{-i\hat{H}t/\hbar} | \mathbf{q}_0 \rangle \Psi_1(\mathbf{q}_0), & (3.53c) \end{aligned}$$

where $\hat{H}$ is the (time-independent) Hamiltonian of the system. With the standard semiclassical approximation of [Eq. (2.1)] for the matrix element of the propagator, $e^{-i\hat{H}t/\hbar}$, and the IVR transformation of Eq. (2.9), the SC-IVR expression for the amplitude becomes

$$S_{2,1}(t) = \int d\mathbf{q}_0 d\mathbf{p}_0 \left[\det \left(\frac{\partial \mathbf{q}_t}{\partial \mathbf{p}_0} \right) / (2\pi i\hbar)^F \right]^{\frac{1}{2}} e^{iS_t(\mathbf{q}_0,\mathbf{p}_0)/\hbar} \Psi_2(\mathbf{q}_t)^* \Psi_1(\mathbf{q}_0) \tag{3.54}$$

where $\mathbf{q}_t(\mathbf{q}_0, \mathbf{p}_0)$ is the coordinate at time t for the classical trajectory with initial condition $(\mathbf{q}_0, \mathbf{p}_0)$, and $S_t(\mathbf{q}_0, \mathbf{p}_0)$ is the action integral along it. (The phase factor $e^{-i\pi\nu_t/2}$, where ν_t is the Maslov index[13–15] — the number of zeros experienced by the determinant of $\partial \mathbf{q}_t / \partial \mathbf{p}_0$ in the time interval $(0, t)$ — is included in Eq. (3.54) as part of the pre-exponential square root.) It is the oscillatory nature of the integrand in Eq. 3.54 that complicates the integration over the phase space of initial conditions.

If one explicitly squares the amplitude in Eq. (3.54) to obtain the transition probability via Eq. (3.53c), and this leads to a double phase space average,

$$\begin{aligned} P_{2\leftarrow 1}(t) &= \frac{1}{(2\pi\hbar)^F} \int d\mathbf{q}_0 d\mathbf{p}_0 \int d\mathbf{q}_0' d\mathbf{p}_0' \left[\det \left(\frac{\partial \mathbf{q}_t}{\partial \mathbf{p}_0} \cdot \frac{\partial \mathbf{q}_t'}{\partial \mathbf{p}_0'} \right) \right]^{\frac{1}{2}} e^{i[S_t(\mathbf{q}_0,\mathbf{p}_0) - S_t(\mathbf{q}_0',\mathbf{p}_0')]/\hbar} \\ & \Psi_2(\mathbf{q}_t)^* \Psi_2(\mathbf{q}_t') \Psi_1(\mathbf{q}_0) \Psi_1(\mathbf{q}_0')^*. \end{aligned} \tag{3.55}$$

where $\mathbf{q}_t = \mathbf{q}_t(\mathbf{q}_0, \mathbf{p}_0)$ and $\mathbf{q}'_t = \mathbf{q}_t(\mathbf{q}'_0, \mathbf{p}'_0)$. One then makes a sum and difference transformation of the integration variables,

$$\mathbf{q}_0 = \bar{\mathbf{q}}_0 + \frac{\Delta\mathbf{q}}{2} \qquad \mathbf{q}'_0 = \bar{\mathbf{q}}_0 - \frac{\Delta\mathbf{q}}{2}, \tag{3.56a}$$

$$\mathbf{p}_0 = \bar{\mathbf{p}}_0 + \frac{\Delta\mathbf{p}}{2} \qquad \mathbf{p}'_0 = \bar{\mathbf{p}}_0 - \frac{\Delta\mathbf{p}}{2}, \tag{3.56b}$$

so that in Eq. (3.55)

$$\int d\mathbf{p}_0 d\mathbf{q}_0 \int d\mathbf{p}'_0 d\mathbf{q}'_0 \to \int d\bar{\mathbf{p}}_0 d\bar{\mathbf{q}}_0 \int \Delta d\mathbf{p} \Delta d\mathbf{q}. \tag{3.56c}$$

In order to make tractable approximations, one expands the phase of the integrand in Eq. (3.55) through second order in $\Delta\mathbf{q}$ and $\Delta\mathbf{p}$,

$$\begin{aligned} S_t(\mathbf{q}_0, \mathbf{p}_0) - S_t(\mathbf{q}'_0, \mathbf{p}'_0) &= \frac{\partial S_t(\bar{\mathbf{q}}_0, \bar{\mathbf{p}}_0)}{\partial \bar{\mathbf{q}}_0} \cdot \Delta\mathbf{q} + \frac{\partial S_t(\bar{\mathbf{q}}_0, \bar{\mathbf{p}}_0)}{\partial \bar{\mathbf{p}}_0} \cdot \Delta\mathbf{p} \\ &= (\bar{\mathbf{p}}_t^T \cdot \mathbf{M}_{\mathbf{qq}} - \bar{\mathbf{p}}_0^T) \cdot \Delta\mathbf{q} + \bar{\mathbf{p}}_t^T \cdot \mathbf{M}_{\mathbf{qp}} \cdot \Delta\mathbf{p}; \end{aligned} \tag{3.57}$$

the quadratic terms vanish because the phase difference is an odd function of the difference variables. Consistent with this approximation to the phase, the trajectories $\mathbf{q}_t$ and $\mathbf{q}'_t$ are expanded to first order in $\Delta\mathbf{q}$ and $\Delta\mathbf{p}$

$$\mathbf{q}_t = \bar{\mathbf{q}}_t(\bar{\mathbf{p}}_0, \bar{\mathbf{q}}_0) + \mathbf{M}_{\mathbf{qq}} \cdot \frac{\Delta\mathbf{q}}{2} + \mathbf{M}_{\mathbf{qp}} \cdot \frac{\Delta\mathbf{p}}{2}, \tag{3.58a}$$

$$\mathbf{p}_t = \bar{\mathbf{p}}_t(\bar{\mathbf{p}}_0, \bar{\mathbf{q}}_0) + \mathbf{M}_{\mathbf{pq}} \cdot \frac{\Delta\mathbf{q}}{2} + \mathbf{M}_{\mathbf{pp}} \cdot \frac{\Delta\mathbf{p}}{2}, \tag{3.58b}$$

and within this approximation the Jacobian factors are thus independent of $\Delta\mathbf{q}$ and $\Delta\mathbf{p}$, i.e.,

$$\frac{\partial \mathbf{q}_t}{\partial \mathbf{p}_0} \approx \frac{\partial \mathbf{q}'_t}{\partial \mathbf{p}'_0} \approx \frac{\partial \bar{\mathbf{q}}_t}{\partial \bar{\mathbf{p}}_0} = \mathbf{M}_{\mathbf{qp}}, \tag{3.59a}$$

and similarly

$$\frac{\partial \bar{\mathbf{q}}_t}{\partial \bar{\mathbf{q}}_0} = \mathbf{M}_{\mathbf{qq}}. \tag{3.59b}$$

[As a matter of interest, note that all of the above approximations following Eq. (3.55) are exact if the system is a set of harmonic oscillators.] Equation (3.55) now becomes

$$\begin{aligned} P_{2\leftarrow 1}(t) = \frac{1}{(2\pi\hbar)^F} \int d\bar{\mathbf{p}}_0 d\bar{\mathbf{q}}_0 \int \Delta d\mathbf{p} \Delta d\mathbf{q} \, \det(\mathbf{M}_{\mathbf{qp}}) \, e^{-i\bar{\mathbf{p}}_0^T \cdot \Delta\mathbf{q}/\hbar} \\ \Psi_2(\bar{\mathbf{q}}_t + \mathbf{M}_{\mathbf{qq}} \cdot \frac{\Delta\mathbf{q}}{2} + \mathbf{M}_{\mathbf{qp}} \cdot \frac{\Delta\mathbf{p}}{2})^* \Psi_2(\bar{\mathbf{q}}_t - \mathbf{M}_{\mathbf{qq}} \cdot \frac{\Delta\mathbf{q}}{2} - \mathbf{M}_{\mathbf{qp}} \cdot \frac{\Delta\mathbf{p}}{2}) \\ \Psi_1(\bar{\mathbf{q}}_0 + \frac{\Delta\mathbf{q}}{2}) \Psi_1(\bar{\mathbf{q}}_0 - \frac{\Delta\mathbf{q}}{2})^* e^{i\bar{\mathbf{p}}_t^T \cdot (\mathbf{M}_{\mathbf{qq}} \cdot \Delta\mathbf{q} + \mathbf{M}_{\mathbf{qp}} \cdot \Delta\mathbf{p})/\hbar}. \end{aligned} \tag{3.60}$$

The integration over the difference variables $\Delta\mathbf{q}$ and $\Delta\mathbf{p}$ can now be carried out exactly by changing variables again to $\Delta\mathbf{q}$ and $\Delta\mathbf{q}'$

$$\begin{pmatrix} \Delta\mathbf{q} \\ \Delta\mathbf{q}' \end{pmatrix} = \begin{pmatrix} \mathbf{I} & \mathbf{0} \\ \mathbf{M_{qq}} & \mathbf{M_{qp}} \end{pmatrix} \cdot \begin{pmatrix} \Delta\mathbf{q} \\ \Delta\mathbf{p} \end{pmatrix}, \tag{3.61}$$

and the final result is a linearized approximation to the SC-IVR, or LSC-IVR,

$$P_{2\leftarrow 1}(t) = \frac{1}{(2\pi\hbar)^F} \int d\mathbf{q}_0 d\mathbf{p}_0 \; \rho_2(\mathbf{q}_t, \mathbf{p}_t)^* \rho_1(\mathbf{q}_0, \mathbf{p}_0), \tag{3.62}$$

where the "bars" have been dropped from $\mathbf{q}_0$ and $\mathbf{p}_0$, and $\rho_n(\mathbf{q}, \mathbf{p})$ is the Wigner distribution function[118] of state n, defined as

$$\rho_n(\mathbf{q}, \mathbf{p}) = \int d\Delta\mathbf{q} \; e^{-i\mathbf{p}^T \cdot \Delta\mathbf{q}/\hbar} \langle \mathbf{q} + \frac{\Delta\mathbf{q}}{2} | \Psi_n \rangle \langle \Psi_n | \mathbf{q} - \frac{\Delta\mathbf{q}}{2} \rangle. \tag{3.63}$$

It should be clear that it is much easier to evaluate the LSC-IVR expression than in Eq. (3.62) than the full SC-IVR expression of Eq. 3.54 because the integrand in Eq. (3.62) is essentially free of high frequency oscillations. [The oscillatory character has been subsumed in the Fourier transforms that define the Wigner distribution functions, Eq. (3.63).]

The same manipulations and approximations can also be carried out for a more general time correlation function of the form

$$C_{AB}(t) = \mathrm{tr}[\hat{A} e^{i\hat{H}t/\hbar} \hat{B} e^{-i\hat{H}t/\hbar}]. \tag{3.64}$$

($P_{2\leftarrow 1}(t)$ above corresponds to Eq. (3.64) with

$$\hat{A} = |\Psi_1\rangle\langle\Psi_1| \tag{3.65}$$

$$\hat{B} = |\Psi_2\rangle\langle\Psi_2|.) \tag{3.66}$$

Writing out the full SC-IVR expression for Eq. (3.64) and making the linearization approximation as above gives

$$C_{AB}(t) = \frac{1}{(2\pi\hbar)^F} \int d\mathbf{q}_0 d\mathbf{p}_0 A_w(\mathbf{q}_0, \mathbf{p}_0) B_w(\mathbf{q}_t, \mathbf{p}_t), \tag{3.67}$$

where $A_w(\mathbf{q}, \mathbf{p})$ and $B_w(\mathbf{q}, \mathbf{p})$ are the Wigner-Weyl transforms of operators $\hat{A}$ and $\hat{B}$, e.g.,

$$A_w(\mathbf{q}, \mathbf{p}) = \int d\Delta\mathbf{q} \; e^{-i\mathbf{p}^T \cdot \Delta\mathbf{q}/\hbar} \langle \mathbf{q} + \frac{\Delta\mathbf{q}}{2} | \hat{A} | \mathbf{q} - \frac{\Delta\mathbf{q}}{2} \rangle. \tag{3.68}$$

For instance, for our later discussion of thermal rate constants, it corresponds to the case of $\hat{A}$ being the Boltzmannized flux operator,

$$\hat{A} = e^{-\beta\hat{H}/2}\hat{F}e^{-\beta\hat{H}/2}, \tag{3.69}$$

and $\hat{B}$ being the projection operator onto products

$$\hat{B} = \hat{h}(\mathbf{q}), \tag{3.70}$$

where $h(\mathbf{q})$ is 1(0) for coordinates $\mathbf{q}$ on the product (reactant) side of the dividing surface which separates reactants and products.

It is clear from both Eq. (3.62) and Eq. (3.67) that this LSC-IVR includes quantum effects only via the Wigner functions of the initial and final states; all the real time dynamics is purely classical. This is seen from the analogous classical expression for the correlation function of Eq. (3.64)

$$C(t) = (2\pi\hbar)^{-F}\int d\mathbf{p}_0 \int d\mathbf{q}_0 A_{\mathrm{CL}}(\mathbf{p}_0,\mathbf{q}_0)B_{\mathrm{CL}}(\mathbf{p}_t,\mathbf{q}_t), \tag{3.71}$$

where A_{CL} and B_{CL} are *classical* distribution functions of operators $\hat{A}$ and $\hat{B}$. The LSC-IVR expression of Eq. (3.67) therefore imposes the exact quantum initial and final conditions on classical trajectories. In our later discussion on the thermal rate constants, we shall see that quantum effects are well described for *short time*, but the longer time dynamics is that given by classical rather than quantum mechanics. Whether or not this is adequate will depend on the application at hand.

Finally, we note that what we have called the LSC-IVR, i.e., Eq. (3.62) or (3.67), has appeared in many approximate dynamical theories.[119–123,38,124,125] With regard to thermal rate constants, for example, it is very similar to a SC approximation put forth many years ago by one of us.[126] Heller[38,124] has given a particularly illuminating discussion of this type of "Wigner overlap" approximation (and its limitations) and used it for photodissociation. Lee and Scully[125] have used it to treat inelastic scattering. More recently, Filinov[127,128] has presented an approach for evaluating time correlation functions that starts with the Wigner transform of the quantum trace expression, the lowest order approximation to which is Eq. (3.67). Pollack *et al.*[119,120] have presented a "quantum transition state theory" that utilizes this expression also. The reason we have emphasized that the result is obtained by linearizing the SC-IVR expression [Eq. (3.54)] is that it suggests immediately how one can improve the LSC-IVR: e.g., by keeping higher order terms in the expansion in $\Delta\mathbf{q}$ and $\Delta\mathbf{p}$, or simply by evaluating the full SC-IVR expression numerically.

3.3.1 Linearized Approximation for Scattering Probability

A similar (but slightly more involved) analysis can be carried out for the energy-dependent transition probability of an isolated bimolecular collision. For a generic inelastic (or reactive) collision the F-dimensional coordinate space $(\mathbf{r}, R)$ consists of the translational coordinate R and the (F-1) coordinates $\mathbf{r}$ for the internal degrees of freedom, with corresponding momenta $(\mathbf{p}, P)$. The S-matrix element for the $1 \rightarrow 2$ transition in the internal degrees of freedom at total energy E can be expressed as[35]

$$\begin{aligned} S_{2,1} &= -\frac{\hbar}{\mu}\sqrt{k_1 k_2}e^{-i[k_1 R_{\max}+k_2 R'_{\max}]}\int_0^\infty dt \int d\mathbf{r}\int d\mathbf{r}' e^{iEt/\hbar}\phi_2(\mathbf{r}') \\ &\quad \langle \mathbf{r}' R'_{\max}|e^{-i\hat{H}t/\hbar}|\mathbf{r}R_{\max}\rangle \phi_1(\mathbf{r}) \end{aligned} \tag{3.72}$$

where $\{\phi_n\}$ are the wavefunctions for the asymptotic eigenstates of the internal degrees of freedom, $R_{\max}$ and $R'_{\max}$ are large values of the translational coordinate, and $\{k_n\}$ are the magnitudes of the translational momenta (in units of $\hbar$) determined by energy conservation

$$k_n = \sqrt{2\mu(E - E_n)/\hbar^2}, \tag{3.73}$$

$\{E_n\}$ being the internal energies corresponding to states $\{\phi_n\}$. (Note that for a *reactive* collision $(\mathbf{r}, R)$ and $(\mathbf{r}', R')$ are actually different coordinates, but that makes no essential difference in the present development.) It is convenient to turn Eq. (3.72) into a full coordinate space integral by inserting the factor $\delta(R-R_{\max})\delta(R'-R'_{\max})$ into the integrand and integrating over R and R',

$$S_{2,1}(E) = -\frac{\hbar}{\mu}\sqrt{k_1 k_2}e^{-i[k_1 R_{\max}+k_2 R'_{\max}]}\int dt \int d\mathbf{q}\int d\mathbf{q}' e^{iEt/\hbar}\psi_2(\mathbf{q}')^* \langle \mathbf{q}'|e^{-i\mathbf{H}t/\hbar}|\mathbf{q}\rangle \psi_1(\mathbf{q}), \tag{3.74a}$$

where here $\mathbf{q}$ and $\mathbf{q}'$ denote the full coordinate space, e.g., $(\mathbf{r}, R)$, and

$$\psi_n(\mathbf{q}) = \phi_n(\mathbf{r})\delta(R - R_{\max}). \tag{3.74b}$$

The SC-IVR, Eq. (2.9), is now used for the matrix element of the propagator in Eq. (3.74a) and the square modulus of the S-matrix element formed to obtain the $1 \rightarrow 2$ transition probability

$$\begin{aligned} P_{2\leftarrow 1}(E) &= \frac{\hbar^2 k_1 k_2}{\mu^2 (2\pi\hbar)^F}\int dt dt' \int d\mathbf{p}_0 d\mathbf{q}_0 \int d\mathbf{p}'_0 d\mathbf{q}'_0\, e^{iE(t-t')/\hbar}\psi_2(\mathbf{q}_t)^*\psi_2(\mathbf{q}'_t) \\ &\quad \psi_2(\mathbf{q}_0)\psi_1(\mathbf{q}')^* \left[\det\left(\frac{\partial \mathbf{q}_t}{\partial \mathbf{p}_0}\cdot\frac{\partial \mathbf{q}'_t}{\partial \mathbf{p}'_0}\right)\right]^{\frac{1}{2}} e^{\frac{i}{\hbar}[S_t(\mathbf{q}_0,\mathbf{p}_0)-S_t(\mathbf{q}'_0,\mathbf{p}'_0)]}, \end{aligned} \tag{3.75}$$

where $\mathbf{q}'_t = \mathbf{q}(\mathbf{q}'_0, \mathbf{p}'_0; t)$. Changing to sum and difference integration variables as in Eq. (3.56c) above — and here also for $\bar{t} = \frac{1}{2}(t + t')$ and $\Delta t = t - t'$ — expanding the difference of the action to first order in $\Delta\mathbf{q}$, $\Delta\mathbf{p}$ and Δt, and performing the integral over them as done in going from Eq. (3.57) to (3.62), gives

$$\begin{aligned} P_{2\leftarrow 1}(E) &= \frac{\hbar^2 k_1 k_2}{\mu^2 (2\pi\hbar)^F} \int_0^\infty dt \int d\mathbf{p}_0 \int d\mathbf{q}_0 \, 2\hbar \, \frac{\sin\left([E - H(\mathbf{q}_0, \mathbf{p}_0)]t/2\right)}{[E - H(\mathbf{q}_0, \mathbf{p}_0)]} \\ &\quad \rho_2(\mathbf{q}_t, \mathbf{p}_t)^* \rho_1(\mathbf{q}_0, \mathbf{p}_0), \end{aligned} \tag{3.76}$$

where the "bars" have been dropped from $\mathbf{p}_0, \mathbf{q}_0, t$, and we have used the fact that

$$\frac{\partial}{\partial t} S_t(\mathbf{q}, \mathbf{p}) = -H(\mathbf{q}, \mathbf{p}), \tag{3.77}$$

and

$$\int_{-\bar{t}/2}^{\bar{t}/2} d\Delta t \, e^{i\Delta t[E - H(\mathbf{q}_0, \mathbf{p}_0)]/\hbar} = 2\hbar \, \frac{\sin\left([E - H(\mathbf{q}_0, \mathbf{p}_0)]\bar{t}/2\right)}{[E - H(\mathbf{q}_0, \mathbf{p}_0)]}, \tag{3.78}$$

which if $\bar{t} \to \infty$, it becomes $2\pi\hbar\delta[E - H(\mathbf{q}_0, \mathbf{p}_0)]$. In our calculations, we found that it makes little difference whether we take the exact result of Eq. (3.78) or the delta function limit of it, thus for simplicity we shall use the delta function approximation for here on. It is also easy to show that

$$\rho_n(\mathbf{q}, \mathbf{p}) = \rho_n(\mathbf{r}, \mathbf{p}_\mathbf{r}) \delta(R - R_{\max}), \tag{3.79}$$

where $\rho_n(\mathbf{r}, \mathbf{p}_\mathbf{r})$ is the Wigner function corresponding to nth state of the internal degrees of freedom as defined in Eq. (3.63). Combining all of these results together and writing the phase space integral in Eq. (3.76) in terms of the internal and translational variables thus gives

$$\begin{aligned} P_{2\leftarrow 1}(E) &= \frac{\hbar^2 k_1 k_2}{\mu^2 (2\pi\hbar)^{F-1}} \int d\mathbf{r}_0 \int d\mathbf{p}_{\mathbf{r}0} \int dR_0 \int dP_0 \int dt \, \delta[E - h(\mathbf{r}_0, \mathbf{p}_{\mathbf{r}0}) - \frac{P_0^2}{2\mu}] \\ &\quad \delta(R_0 - R_{\max}) \delta(R_t - R'_{\max}) \rho_2(\mathbf{r}_t, \mathbf{p}_{\mathbf{r}t})^* \rho_1(\mathbf{r}_0, \mathbf{p}_{\mathbf{r}0}), \end{aligned} \tag{3.80}$$

where $h(\mathbf{r}_0, \mathbf{p}_{\mathbf{r}0})$ is the asymptotic Hamiltonian of the internal degrees of freedom. The three delta functions in the integrand of Eq. (3.80) allow the integrals over R_0, P_0, and t to be performed, giving the final result

$$P_{2\leftarrow 1}(E) = \frac{1}{(2\pi\hbar)^{F-1}} \int d\mathbf{r}_0 d\mathbf{p}_{\mathbf{r}0} \, \frac{\hbar^2 k_1 k_2}{|P_0 P_t|} \rho_2(\mathbf{r}_t, \mathbf{p}_{\mathbf{r}t})^* \rho_1(\mathbf{r}_0, \mathbf{p}_{\mathbf{r}0}). \tag{3.81}$$

Comparing this energy dependent result, Eq. (3.81), to the time-dependent one, Eq. (3.62), one sees that it involves an integral over the initial phase space variables only

of the internal degrees of freedom, the initial values of translational variables being given by $R_0 = R_{\max}$, $P_0 = -\sqrt{2\mu(E - h(\mathbf{r}_0, \mathbf{p}_{r0}))}$. The classical trajectories which give $(\mathbf{r}_t, \mathbf{p}_{rt})$ in Eq. (3.81) are of course computed in the full space of all degrees of freedom.

Eq. (3.81) was proposed (with some minor differences) some years ago by Lee and Scully[125] and tested for collinear inelastic scattering of $He+H_2(v) \rightarrow He+H_2(v')$, for which they observed reasonably good agreement with quantum coupled channel calculations.

3.3.2 Connections with Classical Mechanics

Here we explicitly consider a one dimensional integral of the form

$$I = \int dx e^{iS(x)/\hbar}, \tag{3.82}$$

but have in mind multidimensional integrals of this type that represent quantum transition amplitudes. In the applications in this paper, the integration is over the phase space $(\mathbf{q}_0, \mathbf{p}_0)$ of initial conditions for classical trajectories, but a fully quantum path integral representation of the time evolution operator is also a multidimensional integral of this form.

Standard semiclassical approximations result when one evaluates the integral via the stationary phase approximation (SPA),

$$I_{\text{SPA}} = \sum_k \left[\frac{2\pi i\hbar}{S''(x_k)}\right]^{\frac{1}{2}} e^{iS(x_k)/\hbar}, \tag{3.83a}$$

where $\{x_k\}$ are the points of stationary phase, i.e., the roots of the equation

$$S'(x_k) = 0. \tag{3.83b}$$

Eq. (3.83a) is often suggestively written as

$$I_{\text{SPA}} = \sum_k P_k^{1/2} e^{i\phi_k}, \tag{3.84a}$$

where

$$P_k = \frac{2\pi\hbar}{|S''(x_k)|} \tag{3.84b}$$

$$\phi_k = S(x_k)/\hbar + \frac{\pi}{4}\text{Sign}\left[S''(x_k)\right], \tag{3.84c}$$

so that the *probability*, or the observable, $|I|^2$ has the form

$$\begin{aligned} |I_{\rm SPA}|^2 &= \sum_k P_k + \sum_{k<k'} 2\sqrt{P_k P_{k'}}\cos(\phi_k - \phi_{k'}) \\ &= |I_{\rm CL}|^2 + \text{interference.} \end{aligned} \tag{3.84d}$$

This is the typical semiclassical result for a transition probability,[35] say, the classical result plus interference, i.e., quantum coherence. If there are no real roots to Eq. (3.83b), one may analytically continue the phase function $S(x)$ and look for complex roots; the approximation for $|I|^2$ then is[35]

$$|I|^2 \approx \frac{2\pi\hbar}{|S''(x_k)|} e^{-2{\rm Im}S(x_k)/\hbar} \tag{3.85}$$

where x_k is the complex root for which $S(x_k)$ has the smallest positive imaginary part. In this case the transition is said to be "classically forbidden", or to proceed by tunneling (or "dynamical tunneling" in the multidimensional case).

One would like to go beyond the stationary phase approximation, e.g., to evaluate integrals of this type numerically, but the oscillatory character of the integrand prevents the straight-forward use of Monte Carlo methods. There are ways of converting Eq. (3.82) into an integral amenable to Monte Carlo evaluation, such as various filtering methods,[76,75,74] but the strategy we are employing in this section is to deal directly with the probability,

$$|I|^2 = \int_{-\infty}^{\infty} dx \int_{-\infty}^{\infty} dx' e^{i(S(x)-S(x'))/\hbar}. \tag{3.86}$$

(This also arises most naturally when using a density matrix formulation.) Changing to sum and difference integration variables $\bar{x} = (x + x')/2$, $\Delta x = x - x'$, gives

$$|I|^2 = \int_{-\infty}^{\infty} d\bar{x} \int_{-\infty}^{\infty} d\Delta x e^{i(S(\bar{x}+\frac{\Delta x}{2})-S(\bar{x}-\frac{\Delta x}{2}))/\hbar}, \tag{3.87}$$

and the linearization approximation corresponds to expanding the phase difference to first order in Δx,

$$S(\bar{x} + \frac{\Delta x}{2}) - S(\bar{x} - \frac{\Delta x}{2}) \approx S'(\bar{x})\Delta x. \tag{3.88}$$

The integral over Δx is then immediately doable,

$$\int_{-\infty}^{\infty} d\Delta x e^{iS'(\bar{x})\Delta x/\hbar} = 2\pi\hbar\delta[S'(\bar{x})], \tag{3.89}$$

so that Eq. (3.87) becomes

$$|I|^2 = \int_{-\infty}^{\infty} d\bar{x} 2\pi\hbar\delta[S'(\bar{x})]. \tag{3.90}$$

Having approximated the phase difference this way has indeed eliminated the oscillatory problem: the integral over $\bar{x}$ in Eq. (3.90) now involves a positive definite integral, and one can readily proceed by Monte Carlo methods in the multidimensional case. One immediately sees, however, that Eq. (3.90) gives only the classical probability: there are contributions to the integral only at values $\bar{x}$ for which $S'(\bar{x}) = 0$, i.e., the stationary phase points, and the evaluation of the delta function integration gives

$$|I|^2 = \sum_k \frac{2\pi\hbar}{|S''(x_k)|}, \tag{3.91}$$

the classical part of Eq. (3.84d).* One may thus say that taking interference [i.e., the phase difference in Eq. (3.87)] into account only infinitesimally (i.e., to first order in Δx) leads only to the classical result; one cannot describe the quantum interference/coherence effects in Eq. (3.84d) because these arise from the difference of discrete points of stationary phase, $\Delta x = x_k - x_{k'}$.

Comparing the classical result of Eq. (3.91) (which is always positive definite) to the semiclassical result of Eq. (3.84d), one sees that the oscillatory part is a sum over cosines of the action difference between various different stationary phase points. There are reasons to suspect that this oscillatory term is a small contribution to the overall probability for a complex system. First, generally speaking, the number of stationary phase points (or classical trajectories) is usually quite large, therefore the summation in Eq. (3.84d) is over a large number of oscillatory terms. Second, in a complex system, the classical action is generally bigger than that of a smaller system simply because the number of degrees of freedom is larger. And if the system exhibit chaotic behavior, the different trajectories will have very different actions. Therefore, the summation is over many of these rapidly oscillating terms that can lead to destructive interference, diminishing the magnitude of the coherence term in Eq. (3.84d). If these two conditions are fulfilled, then quantum mechanical effects should contribute very little. This argument is somewhat related to that put forth by Zurek and Paz,[129] however, their discussion initiated from different starting points. In chapter 5, we shall test this hypothesis for an example of hundreds of degrees of freedom and see if quantum effects are still important.

One systematic approach for improving the linearization approximation is simply to carry the expansion in Eq. (3.88) to the next order in Δx, which is $S'''(x_k)\Delta x^3/24$. The

*We note that this linearization approximation was actually used to *derive* the classical pre-exponential factor of the semiclassical S-matrix, *J. Chem. Phys.*, **53**, 1949 (1970).

integral over Δx is then an Airy integral, and in this case Eq. (3.87) becomes

$$|I|^2 = \int d\bar{x}\, \frac{2\pi\hbar}{\epsilon(\bar{x})} \mathrm{Ai}[S'(\bar{x}/\epsilon(\bar{x}))] \tag{3.92}$$

where

$$\epsilon(\bar{x}) = \hbar^{2/3} S'''(\bar{x})^{1/3}/2. \tag{3.93}$$

The integrand here is also peaked at values of $\bar{x}$ for which $S'(\bar{x}) = 0$ — these are the turning points, or Franck-Condon peaks of the Airy function [†]— but there is some residual interference structure in the integrand. Eq. (3.92) should indeed be a useful approximation because it is accurate when the two interfering stationary points were not too far apart, which probably is the most important practical situation. (If they are very far apart, the interference is presumably of very high frequency and thus most easily quenched by any averaging that one carries out.) The only problem is that the generalized cubic expansion of the phase difference in the multidimensional case does not yield a separable integrand, so the Δx integration is not easily doable. If one attempts a direct numerical attack on Eq. (3.87), this sum and difference analysis suggests that the integration over the sum variable $\bar{x}$ could be treated by classical (Monte Carlo) methods, while only integration over the difference variable Δx must deal with the interference nature of the problem.

3.3.3 Concluding Remarks

We have presented an linearized approximation to the SC-IVR. and discussed the connection between semiclassical dynamics with classical mechanics that arised from this approximation. We saw that classical dynamics does not emerge from $\hbar \to 0$, rather it comes from the disappearance, or cancellation, of the interference terms in the probability. We conjectured that this perhaps is true in complex systems where chaos and large numbers of degrees of freedom can have this effect.

The linearized approximation, however, is not a completely classical theory. The initial and final conditions of the classical trajectories are determined by Wigner functions which are exact quantum mechanical entities. Therefore, non-dynamical (equilibrium)

[†]Comparing Eqs. 3.89 and 3.92 identifies the following representation of a delta function,

$$\delta(z) = \lim_{\epsilon \to 0} \frac{1}{\epsilon} \mathrm{Ai}(z/\epsilon),$$

and one can indeed show that the RHS of this equation does satisfy the defining properties of the delta function.

quantities such as the partition function are treated exactly. The usefulness of this will be seen in chapter 5 where we apply the LSC-IVR to reaction rate constants. We will also see in that chapter that when quantum mechanical interference effects are important, the LSC-IVR is not an adequate approach.

The linearized approximation also points out the possible ways of including quantum mechanical effects, namely by keeping higher order terms in the expansion that contain interference, albeit approximately. So far, this direction have proved difficult for practical implementation, but this is an on going subject of research.

3.4 Forward-Backward Propagation for Correlation Functions

In a complex molecular system, i.e., one with many degrees of freedom, one will almost always be interested in calculating some kind of time correlation function of the form

$$C_{AB}(t) = \mathrm{tr}\left[\hat{A}e^{i\hat{H}t/\hbar}\hat{B}e^{-i\hat{H}t/\hbar}\right], \tag{3.94}$$

where $\hat{A}$ and $\hat{B}$ are various operators and $\hat{H}$ is the Hamiltonian of the system. (Typically, $\hat{A}$ will involve the Boltzmann operator, $\exp(-\beta\hat{H})$, and thus all the degrees of freedom of the complete molecular system, while $\hat{B}$ will involve only the few degrees of freedom of a "probe" molecule or reaction coordinate.) Use of Eq. (2.14) for each of the time evolution operators in Eq. (3.94) thus leads to the following double phase space average for the correlation function,

$$\begin{aligned} C_{AB}(t) &= (2\pi\hbar)^{-2F}\int d\mathbf{p}_0\int d\mathbf{q}_0\int d\mathbf{p}_0'\int d\mathbf{q}_0' C_t(\mathbf{p}_0,\mathbf{q}_0)C_t(\mathbf{p}_0',\mathbf{q}_0')^* \\ &\quad e^{i[S_t(\mathbf{p}_0,\mathbf{q}_0)-S_t(\mathbf{p}_0',\mathbf{q}_0')]/\hbar}\langle\mathbf{p}_0\mathbf{q}_0|\hat{A}|\mathbf{p}_0'\mathbf{q}_0'\rangle\langle\mathbf{p}_t'\mathbf{q}_t'|\hat{B}|\mathbf{p}_t\mathbf{q}_t\rangle \end{aligned} \tag{3.95}$$

where $\mathbf{p}_t' = \mathbf{p}_t(\mathbf{p}_0',\mathbf{q}_0'), \mathbf{q}_t' = \mathbf{q}_t(\mathbf{p}_0',\mathbf{q}_0')$. For comparison, classical mechanics gives the correlation function as a single phase space average over initial conditions

$$C_{AB}^{\mathrm{CL}}(t) = (2\pi\hbar)^{-F}\int d\mathbf{p}_0\int d\mathbf{q}_0 A(\mathbf{p}_0,\mathbf{q}_0)B(\mathbf{p}_t,\mathbf{q}_t), \tag{3.96}$$

where here A and B are the classical functions of coordinates and momenta corresponding to the operators $\hat{A}$ and $\hat{B}$. The integral in the SC-IVR expression for the correlation function, Eq. (3.95), is thus twice the dimension of the classical expression, Eq. (3.96), but more serious than this is the fact that the integrand of the SC expression is oscillatory due to the phase differences between the trajectories with different initial conditions.

It is clear however, that the phase difference in Eq. (3.95) is what is responsible for the quantum interference/coherence structure in the correlation function. We have seen in the previous section where the linearization approximation assumed that the phase difference is infinitesimal and therefore the result is a classical like expression for the correlation function without any quantum interference. In many systems, this assumption is inadequate.

In this section we describe a way of evaluating the full SC-IVR expression without invoking the linearization approximation for any of the degrees of freedom but still retains most of the interference effects. It is based on a generalization of the *forward-backward* (FB) procedure introduced by Makri and Thompson[130,131] to evaluate anharmonic influence functionals in their Feynman path integral approaches. The basic idea is to combine the two time evolution operators in Eq. (3.64) into one overall SC-IVR time propagation, so that the double phase space average in Eq. (3.95) becomes a single phase space average (plus a bit more because of the operator $\hat{B}$ which sits between the forward and backward time evolution operators). More important than the reduction of the dimensionality of the integral is that the forward-backward nature of the classical trajectories leads to a partial self-cancellation that makes the integrand less oscillatory. Section 3.4.1 develops this FB-IVR approach in general and it is also shown how an approximate form of the FB-IVR reverts to the LSC-IVR approximation of Eq. (3.62), so that one may think of it as a systematic way of going beyond this linearized approximation. The FB-IVR, unlike the LSC-IVR, is thus able to describe true quantum coherence effects arising from the interference of distinct classical trajectories. Section 3.4.2 discusses some other applications of the forward-backward idea for quantities other than standard time correlation functions.

3.4.1 Forward-Backward Initial Value Representation

It is useful to work up to the general result in several stages. First, consider the case that operator $\hat{B}$ is a local (in coordinate space) phase factor,

$$\hat{B} = e^{i\phi(\hat{\mathbf{q}})/\hbar}. \tag{3.97}$$

The operator $\hat{U}$

$$\hat{U} \equiv e^{i\hat{H}t/\hbar} e^{i\phi(\hat{\mathbf{q}})/\hbar} e^{-i\hat{H}t/\hbar}, \tag{3.98}$$

is thus a unitary operator (since it is the product of three unitary operators) and can in fact be thought of as the time-evolution operator forward from $0 \rightarrow t$ and backward from

$t \to 0$ via the time-dependent Hamiltonian

$$\hat{H}(t') = \begin{cases} \hat{H} - \delta(t-t')\phi(\hat{\mathbf{q}}), & 0 \to t \\ \hat{H}, & t \to 0 \end{cases} \tag{3.99}$$

where $\hat{H}$ is the original (time independent) molecular Hamiltonian. Since the semiclassical approximation has the same form also for a time-dependent Hamiltonian, the Herman-Kluk IVR for operator $\hat{U}$ has the same form as Eq. (2.14),

$$\hat{U} = (2\pi\hbar)^{-F} \int d\mathbf{p}_0 \int d\mathbf{q}_0 C_0(\mathbf{p}_0, \mathbf{q}_0) e^{iS_0(\mathbf{p}_0,\mathbf{q}_0)/\hbar} |\mathbf{p}_0' \mathbf{q}_0'\rangle\langle \mathbf{p}_0 \mathbf{q}_0| \tag{3.100}$$

where the forward-backward classical trajectory that results from the Hamiltonian Eq. (3.99) is as follows: one begins with initial conditions $(\mathbf{p}_0, \mathbf{q}_0)$ at time 0 and integrates the classical equations of motion — with the molecular Hamiltonian $\hat{H}$ — to time t, where the momenta and coordinates are $(\mathbf{p}_t, \mathbf{q}_t)$; here the momenta are changed according to

$$\mathbf{p}_t \to \mathbf{p}_t + \left[\frac{\partial \phi(\mathbf{q})}{\partial \mathbf{q}}\right]_{\mathbf{q}=\mathbf{q}_t}, \tag{3.101}$$

and one then integrates back to time 0, yielding the final values $\mathbf{p}_0' = \mathbf{p}_0'(\mathbf{p}_0, \mathbf{q}_0)$, $\mathbf{q}_0' = \mathbf{q}_0'(\mathbf{p}_0, \mathbf{q}_0)$. The action integral in Eq. (3.100) is

$$S_0(\mathbf{p}_0, \mathbf{q}_0) = \int_0^t dt' [\mathbf{p} \cdot \dot{\mathbf{q}} - H(\mathbf{p}, \mathbf{q})] + \phi(\mathbf{q}_t) + \int_t^0 dt' [\mathbf{p} \cdot \dot{\mathbf{q}} - H(\mathbf{p}, \mathbf{q})], \tag{3.102}$$

and the pre-exponential factor C_0 is the same as Eq. (2.14c) with monodromy matrix elements $\partial \mathbf{q}_0'(\mathbf{p}_0, \mathbf{q}_0)/\partial \mathbf{q}_0$, etc. Appendix A also shows how Eqs. (3.101) and (3.102) arise from the "primitive" or stationary phase approximation for matrix elements of the operator $\hat{U}$.

With the operator $\hat{U} \equiv e^{i\hat{H}t/\hbar}\hat{B}e^{-i\hat{H}t/\hbar}$ given by the FB-IVR of Eq. (3.100) [for $\hat{B}$ of the form of Eq. (3.97)], the correlation function $C_{AB}(t)$ becomes

$$C_{AB}(t) = (2\pi\hbar)^{-F} \int d\mathbf{p}_0 \int d\mathbf{q}_0 C_0(\mathbf{p}_0, \mathbf{q}_0) e^{iS_0(\mathbf{p}_0,\mathbf{q}_0)/\hbar} \langle \mathbf{p}_0 \mathbf{q}_0 | \hat{A} | \mathbf{p}_0' \mathbf{q}_0' \rangle, \tag{3.103}$$

and this exemplifies the basic simplification and efficiency of FB-IVR. By making an SC-IVR for the total operator $\hat{U}$ one has only a single, rather than a double phase space average over initial conditions as in Eq. (3.95). Probably more important than this, however, is the fact that the net phase — i.e., the forward-backward action of Eq. (3.102) — has partial cancellation from the forward and backward nature of the trajectory. If, for example, the

phase $\phi(\mathbf{q})$ were zero, then the forward and backward parts of the trajectory would cancel exactly, and the net phase of Eq. (3.102) would be zero. The operator $\hat{U}$ would in this case, of course, be the trivial identity operator, but Eq. (3.100) would in fact be an efficient way to represent the identity operator, whereas using two separate IVR's for $e^{-i\hat{H}t/\hbar}$ and $e^{i\hat{H}t/\hbar}$, and the resulting double phase space average, would require a great deal of effort to represent the identity operator accurately.

The above procedure can be generalized to an arbitrary local operator $\hat{B} = B(\hat{\mathbf{q}})$ by writing it as a Fourier integral

$$B(\hat{\mathbf{q}}) = \int d\mathbf{p}\tilde{B}(\mathbf{p})e^{i\mathbf{p}\cdot\hat{\mathbf{q}}/\hbar}, \tag{3.104a}$$

where

$$\tilde{B}(\mathbf{p}) = (2\pi\hbar)^{-f}\int d\mathbf{q}B(\mathbf{q})e^{-i\mathbf{p}\cdot\mathbf{q}/\hbar}, \tag{3.104b}$$

and f is the number of coordinates on which $B(\mathbf{q})$ depends. The operator $e^{i\mathbf{p}\cdot\hat{\mathbf{q}}/\hbar}$ is thus of the form of Eq. (3.97), so the FB-IVR, Eq. (3.100), can be applied to it and the result integrated over the Fourier transform variable $\mathbf{p}$. The result for the correlation function $C_{AB}(t)$ is therefore

$$C_{AB}(t) = (2\pi\hbar)^{-F}\int d\mathbf{p}\tilde{B}(\mathbf{p})\int d\mathbf{p}_0\int d\mathbf{q}_0 C_0(\mathbf{p}_0,\mathbf{q}_0)e^{iS_0(\mathbf{p}_0,\mathbf{q}_0;\mathbf{p})/\hbar}\langle\mathbf{p}_0\mathbf{q}_0|\hat{A}|\mathbf{p}_0'\mathbf{q}_0'\rangle, \tag{3.104c}$$

where the "momentum jump" condition at time t [cf. Eq. (3.101)] is

$$\mathbf{p}_t \to \mathbf{p}_t + \mathbf{p}, \tag{3.104d}$$

and the FB action is

$$S_0(\mathbf{p}_0,\mathbf{q}_0;\mathbf{p}) = \int_0^t dt'[\mathbf{p}\cdot\dot{\mathbf{q}} - H(\mathbf{p},\mathbf{q})] + \mathbf{p}\cdot\mathbf{q}_t + \int_t^0 dt'[\mathbf{p}\cdot\dot{\mathbf{q}} - H(\mathbf{p},\mathbf{q})]; \tag{3.104e}$$

the final values $(\mathbf{p}_0',\mathbf{q}_0')$ are functions of the Fourier transform variable $\mathbf{p}$ as well as initial conditions $(\mathbf{p}_0,\mathbf{q}_0)$. In addition to the phase space average over initial conditions, Eq. (3.104c) also involves an integral over the Fourier transform variable $\mathbf{p}$. It should be emphasized, though, that the operator $\hat{B}$ — the "probe" operator — will typically involve only a few degrees of freedom, those of a sub-system, even though the complete molecular system involves many degrees of freedom. For the flux-side correlation function, for example, the Fourier transform variable involves only *one* variable. Thus in general the Fourier transform variable $\mathbf{p}$ in Eq. (3.104c) will involve only a few degrees of freedom, while the initial conditions $(\mathbf{p}_0,\mathbf{q}_0)$ involve all the degrees of freedom of the complete molecular system.

An even simpler way of expressing the operator $\hat{B}$ as a unitary operator is to notice that

$$B(\hat{\mathbf{q}}) = -i\hbar \left[\frac{d}{d\lambda} e^{i\lambda \hat{B}/\hbar}\right]_{\lambda=0}, \tag{3.105a}$$

where λ is an arbitrary parameter. The correlation function of Eq. (3.94) then becomes

$$C_{AB}(t) = -i\hbar(2\pi\hbar)^{-F} \frac{d}{d\lambda} \left[\int d\mathbf{p}_0 d\mathbf{q}_0 C_0(\mathbf{p}_0, \mathbf{q}_0) e^{iS_0(\mathbf{p}_0,\mathbf{q}_0;\lambda)/\hbar} \langle \mathbf{p}_0\mathbf{q}_0|\hat{A}|\mathbf{p}_0'\mathbf{q}_0'\rangle\right]_{\lambda=0}, \tag{3.105b}$$

where

$$S_0(\mathbf{p}_0, \mathbf{q}_0; \lambda) = \int_0^t dt'[\mathbf{p}\cdot\dot{\mathbf{q}} - H(\mathbf{p},\mathbf{q})] + \lambda B(\mathbf{q}_t) + \int_t^0 dt'[\mathbf{p}\cdot\dot{\mathbf{q}} - H(\mathbf{p},\mathbf{q})], \tag{3.105c}$$

and the momentum jump at t is

$$\mathbf{p}_t \to \mathbf{p}_t + \lambda \left[\frac{\partial B(\mathbf{q})}{\partial \mathbf{q}}\right]_{\mathbf{q}=\mathbf{q}_t}. \tag{3.105d}$$

Because taking a derivative with respect to λ does not require as many points as an integral as in Eq. (3.104c), this may be a more efficient approach.

Finally, to treat a general operator $\hat{B}$ we express it in terms of its Weyl ordered product[132,133]

$$\hat{B} = \int d\mathbf{p} \int d\mathbf{q} \tilde{B}(\mathbf{p},\mathbf{q}) e^{i\mathbf{p}\cdot\hat{\mathbf{q}}/\hbar} e^{-i\mathbf{q}\cdot\hat{\mathbf{p}}/\hbar}, \tag{3.106a}$$

where

$$\tilde{B}(\mathbf{p},\mathbf{q}) = (2\pi\hbar)^{-f} \int d\bar{\mathbf{q}} e^{-i\mathbf{p}\cdot\bar{\mathbf{q}}/\hbar} \langle \bar{\mathbf{q}}|\hat{B}|\bar{\mathbf{q}} - \mathbf{q}\rangle. \tag{3.106b}$$

One can verify Eq. (3.106a) directly by using the fact that matrix elements of the exponential operators are given by

$$\langle \mathbf{q}''|e^{i\mathbf{p}\cdot\hat{\mathbf{q}}/\hbar} e^{-i\mathbf{q}\cdot\hat{\mathbf{p}}/\hbar}|\mathbf{q}'\rangle = e^{i\mathbf{p}\cdot\mathbf{q}''/\hbar} \delta_f(\mathbf{q} + \mathbf{q}' - \mathbf{q}''). \tag{3.106c}$$

One thus utilizes an SC-IVR for the unitary operator

$$\hat{U}(\mathbf{p},\mathbf{q}) = e^{i\hat{H}t/\hbar} e^{i\mathbf{p}\cdot\hat{\mathbf{q}}/\hbar} e^{-i\mathbf{q}\cdot\hat{\mathbf{p}}/\hbar} e^{-i\hat{H}t/\hbar}. \tag{3.107}$$

The FB-IVR for $\hat{U}(\mathbf{p},\mathbf{q})$ has the same generic form as Eq. (3.100), but as Appendix B shows, there is a "phase space jump" at time t

$$\mathbf{p}_t \to \mathbf{p}_t + \mathbf{p} \tag{3.108a}$$

$$\mathbf{q}_t \to \mathbf{q}_t + \mathbf{q}, \tag{3.108b}$$

and the FB action integral is

$$S_0(\mathbf{p}_0,\mathbf{q}_0;\mathbf{p},\mathbf{q}) = \int_0^t dt'[\mathbf{p}\cdot\dot{\mathbf{q}} - H(\mathbf{p},\mathbf{q})] + \mathbf{p}\cdot(\mathbf{q}_t+\mathbf{q}) + \int_t^0 dt'[\mathbf{p}\cdot\dot{\mathbf{q}} - H(\mathbf{p},\mathbf{q})]. \quad (3.109)$$

The general FB-IVR result for the correlation function is therefore

$$\begin{aligned} C_{AB}(t) &= (2\pi\hbar)^{-F}\int d\mathbf{p}\int d\mathbf{q}\tilde{B}(\mathbf{p},\mathbf{q})\int d\mathbf{p}_0\int d\mathbf{q}_0 C_0(\mathbf{p}_0,\mathbf{q}_0;\mathbf{p},\mathbf{q}) \\ &\quad e^{iS_0(\mathbf{p}_0,\mathbf{q}_0;\mathbf{p},\mathbf{q})/\hbar}\langle\mathbf{p}_0\mathbf{q}_0|\hat{A}|\mathbf{p}_0'\mathbf{q}_0'\rangle, \end{aligned} \quad (3.110)$$

with $\tilde{B}(\mathbf{p},\mathbf{q})$ given by Eq. (3.63). Again it should be emphasized that though the phase space average over initial conditions $(\mathbf{p}_0,\mathbf{q}_0)$ in Eq. (3.110) involve all the degrees of freedom of the complete molecular system, the dimension of the integrals over the transform variables $(\mathbf{p},\mathbf{q})$ will typically involve only a few degrees of freedom, those in terms of which operator $\hat{B}$ is expressed.

Several observations about the general FB-IVR result, Eq. (3.110), are in order. First, it is useful to see how Eq. (3.110) reverts to the LSC-IVR expression, Eq. (3.62), with appropriate approximations. One notes that the net FB action integral $S_0(\mathbf{p}_0,\mathbf{q}_0;\mathbf{p},\mathbf{q})$ of Eq. (3.109) is zero if $\mathbf{p}=\mathbf{q}=0$; this is because, in this case, the trajectory is continuous at time t [cf. Eq. (3.108)], so that the forward and backward trajectories are identical and the forward and backward action integrals exactly cancel. Furthermore, from the derivative relations in Appendix B, it is not hard to show that to first order in $\mathbf{p}$ and $\mathbf{q}$, the FB action is given by

$$S_0(\mathbf{p}_0,\mathbf{q}_0;\mathbf{p},\mathbf{q}) \approx \mathbf{q}_t(\mathbf{p}_0,\mathbf{q}_0)\cdot\mathbf{p} - \mathbf{p}_t(\mathbf{p}_0,\mathbf{q}_0)\cdot\mathbf{q}. \quad (3.111)$$

Since $\mathbf{p}_0'(\mathbf{p}_0,\mathbf{q}_0)\approx\mathbf{p}_0$ and $\mathbf{q}_0'(\mathbf{p}_0,\mathbf{q}_0)\approx\mathbf{q}_0$ to lowest order in $\mathbf{p}$ and $\mathbf{q}$, and thus $C_0\approx 1$, and since one can also show that

$$\langle\mathbf{p}_0\mathbf{q}_0|\hat{A}|\mathbf{p}_0\mathbf{q}_0\rangle \approx A_w(\mathbf{p}_0,\mathbf{q}_0), \quad (3.112)$$

the general FB-IVR result, Eq. (3.110), becomes

$$C_{AB}(t) \approx \int d\mathbf{p}_0\int d\mathbf{q}_0 A_w(\mathbf{p}_0,\mathbf{q}_0)(2\pi\hbar)^{-F}\int d\mathbf{p}\int d\mathbf{q}\tilde{B}(\mathbf{p},\mathbf{q})e^{i(\mathbf{q}_t\cdot\mathbf{p}-\mathbf{p}_t\cdot\mathbf{q})/\hbar}. \quad (3.113)$$

The exact relationship between $\tilde{B}(\mathbf{p},\mathbf{q})$ and the Wigner function $B_w(\mathbf{p}_t,\mathbf{q}_t)$ is

$$B_w(\mathbf{p}_t,\mathbf{q}_t) = \int d\mathbf{p}\int d\mathbf{q}\tilde{B}(\mathbf{p},\mathbf{q})e^{\frac{i}{\hbar}\mathbf{p}\cdot\mathbf{q}/2}e^{i(\mathbf{q}_t\cdot\mathbf{p}-\mathbf{p}_t\cdot\mathbf{q})/\hbar}, \quad (3.114)$$

but to first order in $\mathbf{p}$ and $\mathbf{q}$ one can drop the phase $e^{\frac{i}{\hbar}\mathbf{p}\cdot\mathbf{q}/2}$ in Eq. (3.114), whereby Eq. (3.113) becomes

$$C_{AB}(t) = (2\pi\hbar)^{-F} \int d\mathbf{p}_0 \int d\mathbf{q}_0 A_w(\mathbf{p}_0, \mathbf{q}_0) B_w(\mathbf{p}_t, \mathbf{q}_t), \tag{3.115}$$

precisely the linearized SC-IVR (LSC-IVR) result of Eq. (3.62). Thus, a linearization of the FB-IVR action in the Fourier transform parameters $(\mathbf{p}, \mathbf{q})$, as in Eq. (3.111), leads back to the earlier LSC-IVR result.

Second, the general FB-IVR result, Eq. (3.110), bears a interesting relation to our earlier "mixed semiclassical-classical" model.[134] To see this, we divide the complete molecular system into an f-dimensional "system" and a remaining "bath", with $\mathbf{q} \equiv (\mathbf{r}, \mathbf{R})$; $(\mathbf{r}, \mathbf{p})$ are the coordinates and momenta of the "system" and $(\mathbf{R}, \mathbf{P})$ those of the "bath." If operator $\hat{B}$ depends only on the system degrees of freedom — in fact this would typically be the definition of the system — then Eq. (3.110) reads

$$\begin{aligned} C_{AB}(t) \;=\; & (2\pi\hbar)^{-F} \int d\mathbf{p} \int d\mathbf{r} \tilde{B}(\mathbf{p}, \mathbf{r}) \int d\mathbf{p}_0 \int d\mathbf{r}_0 \int d\mathbf{P}_0 \int d\mathbf{R}_0 C_0 e^{iS_0} \\ & \langle \mathbf{p}_0 \mathbf{r}_0 \mathbf{P}_0 \mathbf{R}_0 | \hat{A} | \mathbf{p}_0' \mathbf{r}_0' \mathbf{P}_0' \mathbf{R}_0' \rangle, \end{aligned} \tag{3.116}$$

where C_0 and S_0 are functions of all the integration variables. There is thus a double phase space average over the system degrees of freedom, $(\mathbf{p}, \mathbf{r})$ and $(\mathbf{p}_0, \mathbf{r}_0)$, but only a single phase space average over bath degrees of freedom, $(\mathbf{P}_0, \mathbf{R}_0)$, precisely the same structure as the "mixed semiclassical-classical" approximation. Unlike this previous work,[134] however, the FB methodology has achieved this form without introducing any linearization approximations to the SC-IVR approach.

Third, it is useful to note that degrees of freedom which are not coupled to the operator $\hat{B}$ do not contribute to quantum interference structure in the correlation function. To see this, suppose that the "bath" degrees of freedom $(\mathbf{R}, \mathbf{P})$ in Eq. (3.116) above were not coupled to the "system" variables $(\mathbf{r}, \mathbf{p})$: since the phase jump at time t, Eq. (3.108), involves only system variables (on which $\hat{B}$ depends), the trajectory of the bath variables would be continuous at t, so that their contribution to the FB action S_0 would cancel out and thus makes no contribution to the quantum interference in the correlation function. It also follows, of course, that modes that are coupled only weakly to $(\mathbf{r}, \mathbf{p})$ make a small contribution to S_0.

Finally, we note that the only awkward feature of the general FB-IVR result, Eq. (3.110), is the forward-backward aspect of the calculation itself; i.e., one averages over initial

conditions for trajectories that go forward, $0 \to t$, and then backward, $t \to 0$, for a given value of t, so that there is a separate set of such trajectories for each value of t. In a classical (or LSC-IVR) calculation, on the other hand, in Eq. (3.96) [or Eq. (3.62)], one integrates only forward in time and obtains $C_{AB}(t)$ for all times t with one set of trajectories. The FB-IVR can actually be cast in this more deterministic form (though not without introducing other inconveniences). This is accomplished by invoking Liouville's theorem, namely,

$$\int d\mathbf{p}_0 \int d\mathbf{q}_0 = \int d\mathbf{p}_t \int d\mathbf{q}_t \tag{3.117a}$$

so that $(\mathbf{p}_t, \mathbf{q}_t)$ are now the "initial conditions" by which the trajectories are specified. Eq. (3.110) thus becomes

$$\begin{aligned} C_{AB}(t) &= (2\pi\hbar)^{-F} \int d\mathbf{p} \int d\mathbf{q} \tilde{B}(\mathbf{p},\mathbf{q}) \int d\mathbf{p}_t \int d\mathbf{q}_t C_0(\mathbf{p}_0,\mathbf{q}_0;\mathbf{p},\mathbf{q}) \\ &\quad e^{iS_0(\mathbf{p}_0,\mathbf{q}_0;\mathbf{p},\mathbf{q})/\hbar} \langle \mathbf{p}_0\mathbf{q}_0|\hat{A}|\mathbf{p}_0'\mathbf{q}_0'\rangle, \end{aligned} \tag{3.117b}$$

where here $\mathbf{p}_0 = \mathbf{p}_0(\mathbf{p}_t, \mathbf{q}_t)$, $\mathbf{q}_0 = \mathbf{q}_0(\mathbf{p}_t, \mathbf{q}_t)$ are the momenta and coordinates that result at time 0 by integrating the equations of motion from $t \to 0$ with initial conditions $(\mathbf{p}_t, \mathbf{q}_t)$. Similarly [and in light of the jump conditions in Eq. (3.108)], $(\mathbf{p}_0', \mathbf{q}_0')$ are the variables that result from integrating the equations motion from $t \to 0$ with initial conditions $(\mathbf{p}_t + \mathbf{p}, \mathbf{q}_t + \mathbf{q})$. (One can make this look more conventional by now switching time t and time 0.) The FB trajectory now has the more convenient form of two forward trajectories, but with a less convenient weighting function with which to sample initial conditions for the trajectories. This latter inconvenience can perhaps be overcome by using clever importance sampling techniques, so that it may emerge that Eq. (3.117b) is actually the prefered form of the FB approach.

3.4.2 Other Applications of Forward-Backward Idea

The forward-backward idea can be readily applied to simplify other kinds of semi-classical calculations. For example, the spectral density with respect to some reference state $|\chi\rangle$ is defined by

$$I(E) = \langle \chi|\delta(E - \hat{H})|\chi\rangle, \tag{3.118a}$$

and with the Fourier representation of the delta function, this becomes

$$I(E) = (\pi\hbar)^{-1} \mathrm{Re} \int_0^\infty dt e^{iEt/\hbar} \langle \chi|e^{-i\hat{H}t/\hbar}|\chi\rangle. \tag{3.118b}$$

The SC-IVR expression for the t-dependent survival amplitude is readily obtainable from Eq. (2.14),

$$\langle\chi|e^{-i\hat{H}t/\hbar}|\chi\rangle = (2\pi\hbar)^{-F}\int d\mathbf{p}_0\int d\mathbf{q}_0 C_t(\mathbf{p}_0,\mathbf{q}_0)e^{iS_t(\mathbf{p}_0,\mathbf{q}_0)/\hbar}\langle\chi|\mathbf{p}_t\mathbf{q}_t\rangle\langle\mathbf{p}_0\mathbf{q}_0|\chi\rangle. \quad (3.118c)$$

Eqs. (3.118a)–(3.118c) are often used to calculation photon excitation cross section, for which $|\chi\rangle$ is the initial state multiplied by the dipole momentum operator, and also to obtain the discrete energy levels of a bound-state system since in this case Eq. (3.118a) can be written as

$$I(E) = \sum_i |\langle\chi|\psi_i\rangle|^2\,\delta(E-E_i), \quad (3.118d)$$

where $\{E_i\}$ and $\{|\psi_i\rangle\}$ are the eigenvalues and eigenstates of $\hat{H}$; in this latter case $|\chi\rangle$ can be any convenient reference state.

The forward-backward idea can be implemented if $|\chi\rangle$ is chosen to be the eigenstate of some zeroth order Hamiltonian $\hat{H}_0$, i.e.,

$$\hat{H}_0|\chi\rangle = E_0|\chi\rangle. \quad (3.119)$$

One then has the following elementary identity for the survival amplitude

$$\begin{aligned}\langle\chi|e^{-i\hat{H}t/\hbar}|\chi\rangle &= \langle\chi|e^{-i\hat{H}_0t/\hbar}e^{i\hat{H}_0t/\hbar}e^{-i\hat{H}t/\hbar}|\chi\rangle \\ &= e^{-iE_0t/\hbar}\langle\chi|e^{i\hat{H}_0t/\hbar}e^{-i\hat{H}t/\hbar}|\chi\rangle, \end{aligned} \quad (3.120)$$

so that Eq. (3.118b) becomes

$$I(E) = (\pi\hbar)^{-1}\mathrm{Re}\int_0^\infty dt e^{i(E-E_0)t/\hbar}\langle\chi|e^{i\hat{H}_0t/\hbar}e^{-i\hat{H}t/\hbar}|\chi\rangle, \quad (3.121)$$

and the FB-IVR is applied to the operator

$$\hat{U} = e^{i\hat{H}_0t/\hbar}e^{-i\hat{H}t/\hbar}, \quad (3.122)$$

which clearly corresponds to propagation forward $0\to t$ with the Hamiltonian $\hat{H}$ and then backward $t\to 0$ with Hamiltonian $\hat{H}_0$. The FB-IVR for the matrix element in Eq. (3.121) is thus given by

$$\langle\chi|e^{i\hat{H}_0t/\hbar}e^{-i\hat{H}t/\hbar}|\chi\rangle = (2\pi\hbar)^{-F}\int d\mathbf{p}_0\int d\mathbf{q}_0 C_0(\mathbf{p}_0,\mathbf{q}_0)e^{iS_0(\mathbf{p}_0,\mathbf{q}_0)/\hbar}\langle\chi|\mathbf{p}_0'\mathbf{q}_0'\rangle\langle\mathbf{p}_0\mathbf{q}_0|\chi\rangle, \quad (3.123)$$

where the final values $(\mathbf{p}_0', \mathbf{q}_0')$ are obtained from the trajectory that begins with initial conditions $(\mathbf{p}_0, \mathbf{q}_0)$ at $t = 0$ and evolves via the full Hamiltonian H to time t, and then back to $t = 0$ via Hamiltonian H_0, with both the coordinate and momenta being continuous at time t; i.e., there are no coordinate or momentum "jumps" because there is no operator between the two propagators in Eq. (3.122).

The advantage of using Eqs. (3.121) and (3.123), rather than Eqs. (3.118b) and (3.118c) are obvious: the integrand of Eq. (3.123) will be much less oscillatory than that of Eq. (3.118c) because of the partial cancellation of the forward and backward action integrals, i.e., $S_0(\mathbf{p}_0, \mathbf{q}_0)$ of Eq. (3.123) is given by

$$S_0(\mathbf{p}_0, \mathbf{q}_0) = \int_0^t dt'(\mathbf{p} \cdot \dot{\mathbf{q}} - H) + \int_t^0 dt'(\mathbf{p} \cdot \dot{\mathbf{q}} - H_0). \tag{3.124}$$

This will be increasingly true the better H_0 approximates H.

3.4.3 Concluding Remarks

In section 3.4.1, it was shown how an SC-IVR of the two time evolution operators that appear in a typical quantum time correlation function can be combined into one overall IVR, involving trajectories that propagate forward from 0 to t and the backward from t to 0. Section 3.4.2 demonstrated other examples of how multiple time evolution operators in quantum expressions can also be so combined.

We have seen that the origin of quantum mechanical effects such as interference and coherent are due to interference between different classical trajectories. The linearized approximation does not take these interference terms into account. With the present forward-backward approach, however, the interference is not discarded because the forward and backward parts of the trajectory are different due to the jump conditions at time t, therefore this method should be much more accurate than the LSC-IVR. On the other hand, the inclusion of interference means that the convergence of the integral will again have the same oscillatory problems encountered with the standard SC-IVR, But, the oscillatory nature in the FB-IVR should be much less because the forward-backward parts of the trajectory may cancel more effectively than in the SC-IVR. And, degrees of freedom not strongly coupled to the "probe" operator are especially canceled out in the forward-backward trajectory. Therefore, the FB-IVR is a promising approach for extending the semiclassical theories to complex systems.

In chapter 5, the FB-IVR methodology will be applied to the calculation of flux-side correlation functions for thermal rate constants. It will be seen that the quantum effects are indeed well captured in this theory even for very long times.

3.4.4 Appendix A

The "primitive" semiclassical approximation for the matrix elements of the operator $\hat{U}$ of Eq. (3.98) is given by

$$\langle \mathbf{q}_0' | \hat{U} | \mathbf{q}_0 \rangle = \int d\mathbf{q} \langle \mathbf{q}_0' | e^{i\hat{H}t/\hbar} | \mathbf{q} \rangle e^{i\phi(\mathbf{q})/\hbar} \langle \mathbf{q} | e^{-i\hat{H}t/\hbar} | \mathbf{q}_0 \rangle, \tag{3.125}$$

where the integral over $\mathbf{q}$ is to be evaluated by the stationary phase approximation (SPA). The "primitive" (or Van Vleck) approximation for the individual propagator matrix elements in Eq. (3.125) have the standard form

$$\langle \mathbf{q} | e^{-i\hat{H}t/\hbar} | \mathbf{q}_0 \rangle \sim e^{iS(\mathbf{q},\mathbf{q}_0;0\to t)/\hbar} \tag{3.126a}$$

$$\langle \mathbf{q}_0' | e^{i\hat{H}t/\hbar} | \mathbf{q} \rangle \sim e^{iS(\mathbf{q}_0',\mathbf{q};t\to 0)/\hbar} \tag{3.126b}$$

where for this qualitative discussion we do not keep track of pre-exponential factors. The stationary phase condition for the integral in Eq. (3.125) is

$$0 = \frac{\partial S(\mathbf{q}, \mathbf{q}_0; 0 \to t)}{\partial \mathbf{q}} + \frac{\partial \phi(\mathbf{q})}{\partial \mathbf{q}} + \frac{\partial S(\mathbf{q}_0', \mathbf{q}; t \to 0)}{\partial \mathbf{q}}, \tag{3.127}$$

and the usual derivative relations identify $\partial S(\mathbf{q}, \mathbf{q}_0; 0 \to t)/\partial \mathbf{q} \equiv \mathbf{p}_t(\mathbf{q}, \mathbf{q}_0)$ as the momentum at time t from the $0 \to t$ trajectory, and $\partial S(\mathbf{q}_0', \mathbf{q}; t \to 0)/\partial \mathbf{q} \equiv -\mathbf{p}_t(\mathbf{q}_0', \mathbf{q})$, where $\mathbf{p}_t(\mathbf{q}_0', \mathbf{q})$ is the momentum at time t for the $t \to 0$ trajectory. Eq. (3.127) thus gives the "momentum jump" at time t in Eq. (3.101). Furthermore, the SPA gives the net phase of the matrix element,

$$\langle \mathbf{q}_0' | \hat{U} | \mathbf{q}_0 \rangle \sim e^{iS(\mathbf{q}_0', \mathbf{q}_0)/\hbar}, \tag{3.128}$$

as

$$S(\mathbf{q}_0', \mathbf{q}_0) = S(\mathbf{q}, \mathbf{q}_0; 0 \to t) + \phi(\mathbf{q}) + S(\mathbf{q}_0', \mathbf{q}; t \to 0) \tag{3.129}$$

with $\mathbf{q} \equiv \mathbf{q}_t$ evaluated at the stationary phase value determined by Eq. (3.127); this is the net forward-backward action given by Eq. (3.102).

3.4.5 Appendix B

Here we consider the "primitive" semiclassical approximation for the unitary operator in Eq. (3.107),

$$\langle \mathbf{q}_0'|\hat{U}(\mathbf{p},\mathbf{q})|\mathbf{q}_0\rangle = \int d\mathbf{q}'' \int d\mathbf{q}' \langle \mathbf{q}_0'|e^{i\hat{H}t/\hbar}|\mathbf{q}''\rangle\langle \mathbf{q}''|e^{i\mathbf{p}\cdot\hat{\mathbf{q}}/\hbar}e^{-i\mathbf{q}\cdot\hat{\mathbf{p}}/\hbar}|\mathbf{q}'\rangle\langle \mathbf{q}'|e^{-i\hat{H}t/\hbar}|\mathbf{q}_0\rangle. \quad (3.130)$$

Utilizing the matrix elements in Eq. (3.106c) gives

$$\langle \mathbf{q}_0'|\hat{U}(\mathbf{p},\mathbf{q})|\mathbf{q}_0\rangle = \int d\mathbf{q}' \langle \mathbf{q}_0'|e^{i\hat{H}t/\hbar}|\mathbf{q}'+\mathbf{q}\rangle e^{i\mathbf{p}\cdot(\mathbf{q}+\mathbf{q}')/\hbar}\langle \mathbf{q}'|e^{-i\hat{H}t/\hbar}|\mathbf{q}_0\rangle, \quad (3.131)$$

and with the primitive semiclassical approximation to the two propagator matrix elements, (again neglecting the pre-exponential factors),

$$\langle \mathbf{q}'|e^{-i\hat{H}t/\hbar}|\mathbf{q}_0\rangle \sim e^{iS(\mathbf{q}',\mathbf{q}_0;0\to t)/\hbar} \quad (3.132a)$$

$$\langle \mathbf{q}_0'|e^{i\hat{H}t/\hbar}|\mathbf{q}'+\mathbf{q}\rangle \sim e^{iS(\mathbf{q}_0',\mathbf{q}'+\mathbf{q};t\to 0)/\hbar}, \quad (3.132b)$$

the stationary phase condition for the integral in Eq. (3.131) is

$$0 = \frac{\partial}{\partial \mathbf{q}'}S(\mathbf{q}_0',\mathbf{q}'+\mathbf{q};t\to 0) + \mathbf{p} + \frac{\partial}{\partial \mathbf{q}'}S(\mathbf{q}',\mathbf{q}_0;0\to t). \quad (3.133)$$

Again using the derivative relations of the action integrals, $\mathbf{p}_t(\mathbf{q}',\mathbf{q}_0) \equiv \partial S(\mathbf{q}',\mathbf{q}_0;0\to t)/\partial \mathbf{q}'$ is identified as the momentum at time t for the forward $0\to t$ trajectory, and $\mathbf{p}_t(\mathbf{q}_0',\mathbf{q}+\mathbf{q}') \equiv -\partial S(\mathbf{q}_0',\mathbf{q}+\mathbf{q}';t\to 0)/\partial \mathbf{q}'$ is the momentum at time t for the $t\to 0$ backward trajectory, so that Eq. (3.133) implies the following "momentum jump" at time t,

$$\mathbf{p}_t \to \mathbf{p}_t + \mathbf{p}. \quad (3.134a)$$

Also, the coordinate at time t for the forward $0\to t$ trajectory is $\mathbf{q}'$, and for the backward $t\to 0$ trajectory it is $\mathbf{q}'+\mathbf{q}$, which is equivalent to the "coordinate jump" at time t

$$\mathbf{q}_t \to \mathbf{q}_t + \mathbf{q}. \quad (3.134b)$$

Finally, the net phase of the matrix element is

$$S_0(\mathbf{q}_0',\mathbf{q}_0) = S(\mathbf{q}_0,\mathbf{q}+\mathbf{q}';t\to 0) + \mathbf{p}\cdot(\mathbf{q}+\mathbf{q}') + S(\mathbf{q}',\mathbf{q}_0;0\to t) \quad (3.135)$$

with $\mathbf{q}' \equiv \mathbf{q}_t$ determined by the stationary phase condition Eq. (3.133).

The coherent state IVR for $\hat{U}(\mathbf{p},\mathbf{q})$ therefore has the standard form, Eq. (3.100), where the net trajectory begins at time 0 with initial conditions $(\mathbf{p}_0,\mathbf{q}_0)$ and evolves for

time t to phase point $(\mathbf{p}_t, \mathbf{q}_t)$; here the momenta and coordinates are changed according to Eq. (3.134) and one integrates the classical equations of motion back to $t = 0$, where the final values are $\mathbf{p}'_0 \equiv \mathbf{p}'_0(\mathbf{p}_0, \mathbf{q}_0; \mathbf{p}, \mathbf{q})$ and $\mathbf{q}'_0 \equiv \mathbf{q}'_0(\mathbf{p}_0, \mathbf{q}_0; \mathbf{p}, \mathbf{q})$. The action S_0 for this forward backward trajectory is given by Eq. (3.135), i.e.,

$$S_0(\mathbf{p}_0, \mathbf{q}_0; \mathbf{p}, \mathbf{q}) = \int_0^t dt'[\mathbf{p} \cdot \mathbf{q} - H(\mathbf{p}, \mathbf{q})] + \mathbf{p} \cdot (\mathbf{q}_t + \mathbf{q}) + \int_t^0 dt'[\mathbf{p} \cdot \mathbf{q} - H(\mathbf{p}, \mathbf{q})]. \quad (3.136)$$

Chapter 4

Electronically Nonadiabatic Dynamics

4.1 Introduction

Although the Born-Oppenheimer approximation, i.e., the motion of atomic nuclei on one potential energy surface, is the theoretical basis of much of chemical/molecular dynamics, there are many situations that involve coupling and transitions between different potential energy surfaces (adiabatic electronic states). The purpose of this paper is to present and test a new theoretical model for carrying out calculations for such non-adiabatic processes.

For the collisions of two atoms, or equivalently, nuclear motion in a diatomic molecule, it is usually possible to treat the coupled electronic-nuclear Schrödinger equations without significant approximation. Semiclassical approximations for the atom-atom motion, such as the Landau-Zener-Stuckelberg[135–137] approximation and its refinements[138], are well known and useful for the insight they provide, but they are actually not necessary as a computation/simulation tool.

The situation is quite different for molecular dynamics involving more than two atoms, where the number of nuclear degrees of freedom, and the many vibrational/rotational states associated with them, typically precludes an exact quantum mechanical treatment of the combined electronic-nuclear dynamics. Indeed, the rigorous quantum treatment of the nuclear dynamics for more than three atoms on only *one* potential surface is itself a

challenging task[139,140], so that even in this simpler one surface case, classical mechanics (i.e., classical trajectory simulations) is often used to describe the nuclear dynamics[141,142]. It is thus natural to try to treat electronically non-adiabatic processes by using classical mechanics to describe the nuclear dynamics while still retaining a quantum description of the electronic degrees of freedom (i.e., the several adiabatic electronic states involved in the process).

There are several ways this mixed "classical nuclear-quantum electronic" idea has been implemented. The surface hopping model introduced by Tully and Preston[106] may be thought of as a polyatomic generalization of the Landau-Zener approximation (though Tully's latest version of the model is able to treat more than simple curve crossing problems[107]). In this model the nuclei move on one adiabatic potential surface at a time with localized (instantaneous) transitions from one potential surface to another. The probability of such "hops" is determined by an electronic transition probability obtained by integrating the time-dependent electronic Schrödinger equation simultaneously with the nuclear trajectory. (Miller and George[47–49] upgraded this model by using a classical S-matrix description of the nuclear degrees of freedom, but this has not seen much application because of practical difficulties in applying it.)

Another popular mixed quantum-classical approach is the Ehrenfest model[97,98], in which the classical equations of motion for the nuclear coordinates are also integrated simultaneously with the time-dependent Schrödinger equation, but the nuclear potential energy function which determines the trajectory in this case is the expectation value of the electronic-nuclear potential energy with respect to the electronic wavefunction,

$$V(\mathbf{R},t) = \int d\mathbf{x}\Psi^*_{el}(\mathbf{x},t)V(\mathbf{x},\mathbf{R})\Psi_{el}(\mathbf{x},t), \tag{4.1}$$

where $\mathbf{x}$ and $\mathbf{R}$ denote electronic and nuclear coordinates, respectively, and Ψ_{el} the electronic wavefunction. (The Ehrenfest model maybe thought of as a semiclassical version of the time-dependent self consistent field (TDSCF) approximation[99,100].) Since Ψ_{el} is a linear combination of the various adiabatic electronic wavefunctions involved in the dynamics, the nuclear potential energy surface in Eq. (4.1) is a combination of all the adiabatic potential surfaces, so that this approach is quite a different situation from the surface hopping model described above.

A more rigorous mixed quantum-classical model is that put forth by Pechukas[143], whereby the nuclear trajectory is determined by a semiclassical evaluation of the electronic-

nuclear path integral representation of the time evolution operator. The effective nuclear potential energy surface in this case turns out to be non-local in time, and because of the practical difficulties associated with this it has not seen much application (but see Webster *et al.*[144]). The Pechukas model is discussed in more detail at the end of section 4.3 in its relation to the present model developed below.

A very different approach to the problem of non-adiabatic dynamics was taken by Miller and co-workers[145–148]. Here the several electronic states (and the coupling between them) are replaced by classical degrees of freedom, yielding a classical Hamiltonian in terms of the nuclear coordinates and momenta, and coordinates and momenta for the (collective) electronic degrees of freedom. Classical trajectories for the combined electronic and nuclear degrees of freedom are then computed with the standard "quasiclassical" treatment of initial and final conditions. In the "classical electron analog" model of Meyer and Miller, the equations of motion for the electronic-nuclear system are the same as in the Ehrenfest/TDSCF model, but the way the boundary condition are interpreted and applied makes the models quite different.

These various models all have their advantages as well as their shortcomings, a detailed analysis of which would be lengthy. In brief, the Ehrenfest/TDSCF approach is best when there is weak (and diffuse) coupling between many electronic states for which the nuclear forces are similar, and the surface hopping model is better when the coupling between the different adiabatic states is localized (though possibly strong). The "classical electron" model was constructed to provide a more even-handed description of the nuclear and electronic degrees of freedom, but it achieves this by reducing the rigor in the description of both sets of degrees of freedom to that of the quasiclassical model. There are also a variety of semiclassical treatments[149,150] based on a perturbative (i.e., "golden rule") approximation for the non-adiabatic coupling that are often very useful, but we are concerned in this paper with approaches that are, in principle at least, not restricted to the perturbative regime.

The new model we present here for treating non-adiabatic dynamics is based on the quantized version of the Meyer and Miller approach. It will be seen that this model is exact if it is treated quantum mechanically. Furthermore, it has well defined semiclassical and classical limits, one does not have the ad-hoc and ambiguous features of mixed quantum classical models reviewed above. Thus, it is a fully a rigorous but dynamically consistent theory of electronic nonadiabatic dynamics.

4.2 Theoretical Development

There are several ways of presenting the model discussed below: one is based on the Classical Electron Analog model of Meyer and Miller where one starts with a classical model Hamiltonian for electronic and nuclear dynamics and then "quantize" it with semiclassical mechanics. Another way is to proceed with the direct second quantized Hamiltonian for the nonadiabatic problem. These two procedures, in their essence, are really the same. However, conceptual interpretations may be different. Therefore, we will present both of them in this section.

4.2.1 The Classical Electron Analog Model

Meyer and Miller (MM) began by considering a $N \times N$ time-dependent electronic Hamiltonian matrix $\{H_{k,k'}(t)\}$, $k, k' = 1, \ldots, N$, with the time-dependent electronic wavefunction expanded in the (diabatic) electronic basis,

$$|\Psi_{el}(t)\rangle = \sum_{k=1}^{N} c_k(t)|k\rangle. \tag{4.2}$$

They noted that if the complex amplitudes $c_k(t)$ are written in terms of the real variables $\{n_k(t), q_k(t)\}$,

$$c_k(t) = \sqrt{n_k(t)}e^{-iq_k(t)}, \tag{4.3}$$

and the classical electron analog Hamiltonian defined as ($\hbar$ being 1 throughout this paper),

$$\begin{aligned} H_{el}(\mathbf{n}, \mathbf{q}; t) &= \langle \Psi_{el}|\hat{H}_{el}|\Psi_{el}\rangle \qquad (4.4)\\ &= \sum_{k,k'=1}^{N} c_k^* H_{k,k'}(t) c_{k'} \\ &= \sum_{k,k'=1}^{N} \sqrt{n_k n_{k'}}\cos(q_k - q_{k'})H_{k,k'}(t), \end{aligned}$$

then the classical equations of motion generated by this Hamiltonian,

$$\dot{q}_k(t) = \frac{\partial H_{el}(\mathbf{n}, \mathbf{q}; t)}{\partial n_k}, \tag{4.5a}$$

$$\dot{n}_k(t) = -\frac{\partial H_{el}(\mathbf{n}, \mathbf{q}; t)}{\partial q_k}, \tag{4.5b}$$

are equivalent of the time-dependent Schrödinger equation for the complex amplitudes,

$$i\dot{c}_k(t) = \sum_{k'=1}^{N} H_{k,k'}c_{k'}(t). \tag{4.6}$$

This correspondence has been noted before.[151]

In molecular systems, however, the electronic matrix is actually a function of nuclear coordinate $\mathbf{Q}$, $\{H_{k,k'}(\mathbf{Q})\}$. [It becomes a time-dependent electronic matrix if $\mathbf{Q}$ is assumed to follow a given trajectory $\mathbf{Q}(t)$.] With this realization, Eq. (4.4) defines the classical electronic Hamiltonian as a function of nuclear coordinates,

$$H_{el}(\mathbf{n},\mathbf{q};\mathbf{Q}) = \sum_{k,k'=1}^{N} \sqrt{n_k n_{k'}} \cos(q_k - q_{k'}) H_{k,k'}(\mathbf{Q}), \tag{4.7}$$

and the classical Hamiltonian for the complete electronic plus nuclear system is obtained by simply adding the nuclear kinetic energy to it,

$$H(\mathbf{n},\mathbf{q},\mathbf{Q},\mathbf{P}) = \frac{\mathbf{P}^2}{2m} + H_{el}(\mathbf{n},\mathbf{q};\mathbf{Q}). \tag{4.8}$$

Here, we have assumed for simplicity that the nuclear coordinates $\mathbf{Q}$ are Cartesian-like, scaled to have a common mass.

It is useful to make a canonical transformation from the electronic action-angle variables (n_k, q_k) to the corresponding Cartesian-like electronic variables (x_k, p_k) which are defined in the standard way[53],

$$x_k = \sqrt{2n_k}\cos q_k, \tag{4.9a}$$

$$p_k = -\sqrt{2n_k}\sin q_k. \tag{4.9b}$$

In terms of these variables, the classical electronic Hamiltonian of Eq. (4.7) becomes,

$$\begin{aligned} H_{el}(\mathbf{x},\mathbf{p};\mathbf{Q}) &= \sum_{k,k'=1}^{N} \frac{1}{2}(p_k p_{k'} + x_k x_{k'}) H_{k.k'}(\mathbf{Q}) \\ &= \sum_{k=1}^{N} \frac{1}{2}(p_k^2 + x_k^2) H_{k,k}(\mathbf{Q}) + \sum_{k<k'=1}^{N} (p_k p_{k'} + x_k x_{k'}) H_{k,k'}(\mathbf{Q}), \end{aligned} \tag{4.10}$$

where it has been assumed in the last line that the diabatic electronic Hamiltonian matrix is real and symmetric. The reason the Cartesian electronic representation is useful is readily apparent: for fixed nuclear coordinates $\mathbf{Q}$, the Hamiltonian of Eq. (4.10) is that of N harmonic oscillators for which the semiclassical IVR is exact! The SC-IVR treatment is also exact for the time-dependent harmonic Hamiltonian that results if $\mathbf{Q}$ is a given nuclear trajectory $\mathbf{Q}(t)$. The full electronic-nuclear Hamiltonian is of course not harmonic in the full coordinate space $(\mathbf{x},\mathbf{Q})$, but the fact that part of the problem is harmonic is expected to help the accuracy of the SC-IVR approach of the next section.

Still following MM's arguments, there is one final modification to the classical electron Hamiltonian of Eq. (4.10), namely to subtract from it the term,

$$\frac{1}{2}\sum_{k=1}^{N} H_{k,k} = \frac{1}{2}\mathrm{tr}(H_{el}). \tag{4.11}$$

The classical electron Hamiltonian then becomes,

$$H_{el}(\mathbf{x},\mathbf{p},\mathbf{Q}) = \sum_{k=1}^{N}\frac{1}{2}(p_k^2+x_k^2-1)H_{k,k}(\mathbf{Q}) + \sum_{k<k'=1}^{N}(p_kp_{k'}+x_kx_{k'})H_{k,k'}(\mathbf{Q}). \tag{4.12}$$

MM argued for this modification based on a "Langer modification": since the N electronic states correspond to the N oscillator states that each have one quantum of excitation in one mode and zero quanta in all the other modes — i.e., the wavefunctions of the N oscillator states are,

$$\Phi_k(\mathbf{x}) = \phi_1(x_k)\prod_{k'=1,k'\neq k}^{N}\phi_0(x_{k'}), \tag{4.13}$$

where $\{\phi_n(x)\}$ are the standard 1-d harmonic oscillator wavefunctions — it is easy to show using standard harmonic oscillator matrix elements that,

$$\langle\Phi_k|\hat{H}_{el}|\Phi_{k'}\rangle = H_{k,k'}. \tag{4.14}$$

Thus, it is necessary to subtract the term in Eq. (4.11) (which is the zero point energy of the N oscillators). This point will be seen more clearly in the next section.

The final form of the electronic-nuclear Hamiltonian is then obtained by adding the nuclear kinetic energy to the electronic Hamiltonian of Eq. (4.12),

$$H(\mathbf{x},\mathbf{p},\mathbf{Q},\mathbf{P}) = \frac{\mathbf{P}^2}{2m} + \sum_{k=1}^{N}\frac{1}{2}(p_k^2+x_k^2-1)H_{k,k'}(\mathbf{Q}) + \sum_{k<k'=1}^{N}(p_kp_{k'}+x_kx_{k'})H_{k,k'}(\mathbf{Q}). \tag{4.15}$$

We also note that one can express the classical electronic-nuclear Hamiltonian of Eq. (4.15) in the *adiabatic* representation. Following MM, if $(\bar{\mathbf{x}},\bar{\mathbf{p}})$ are the adiabatic (Cartesian-like) electronic variables, then in terms of them the classical electronic-nuclear Hamiltonian is,

$$H(\bar{\mathbf{x}},\bar{\mathbf{p}},\mathbf{Q},\mathbf{P}) = \frac{|\mathbf{P}+\mathbf{F}(\bar{\mathbf{x}},\bar{\mathbf{p}},\mathbf{Q})|^2}{2m} + \sum_{k=1}^{N}\frac{1}{2}(\bar{p}_k^2+\bar{x}_k^2-1)E_k(\mathbf{Q}), \tag{4.16}$$

where $E_k(\mathbf{Q})$ are the adiabatic potential energy surfaces (i.e., the eigenvalues of the matrix $H_{k,k'}(\mathbf{Q})$), and $\mathbf{F}$ is a vector potential,

$$\mathbf{F}(\bar{\mathbf{x}},\bar{\mathbf{p}},\mathbf{Q}) = \sum_{k<k'=1}^{N}(\bar{x}_k\bar{p}_{k'}-\bar{x}_{k'}\bar{p}_k)\mathbf{T}_{k,k'}(\mathbf{Q}), \tag{4.17}$$

where $\mathbf{T}_{k,k'}(\mathbf{Q})$ is the skew-symmetric non-adiabatic coupling matrix,

$$\mathbf{T}_{k,k'}(\mathbf{Q}) = \langle \bar{\Phi}_k | \frac{\partial \bar{\Phi}_{k'}}{\partial \mathbf{Q}} \rangle, \tag{4.18}$$

$|\bar{\Phi}_k\rangle$ being the adiabatic electronic eigenfunctions.

4.2.2 Second Quantized Hamiltonian for Nonadiabatic Dynamics

Imagine that the N electronic states represent N Boson particles created from the vaccum state $|0,\ldots,0\rangle$, i.e,

$$|k\rangle = |0,\ldots,1,\ldots,0\rangle = a_k^\dagger |0,\ldots,0\rangle. \tag{4.19}$$

If the energy of the first excited state for the kth particle is given by $H_{k,k}(\mathbf{Q})$, and these are independent bosons (for the moment), the total Hamiltonian is then

$$\hat{H}_{\text{el}} = \sum_{i=k}^{N} H_{k,k}(\mathbf{Q}) a_k^\dagger a_k. \tag{4.20}$$

Notice that higher excitations from the vacuum such as $|0,\ldots,2,\ldots,0\rangle$ are also eigenstates of this Hamiltonian.

To introduce the correct coupling between these N-bosons, we remember that electronic transition from the kth state to the k'th state corresponds to the destruction of the kth particle and simultaneously the creation of the k'th particle. This is accomplished by the operator $a_{k'}^\dagger a_k$. Similarly, the reverse process of going from the k'th state to kth state is accomplished by the operator $a_k^\dagger a_{k'}$. These two processes are happening simultaneously and therefore the coupling between these N-bosons is simply

$$\sum_{k<k'=1}^{N} H_{k,k'}(\mathbf{Q})(a_{k'}^\dagger a_k + a_k^\dagger a_{k'}). \tag{4.21}$$

The total Hamiltonian is therefore

$$\hat{H}_{\text{el}} = \sum_{k=1}^{N} H_{k,k}(\mathbf{Q}) a_k^\dagger a_k + \sum_{k<k'=1}^{N} H_{k,k'}(\mathbf{Q})(a_{k'}^\dagger a_k + a_k^\dagger a_{k'}), \tag{4.22}$$

and now one sees that if the initial state of the N-particle system has one quanta, then the higher excitations such as $|0,\ldots,2,\ldots,0\rangle$ are not coupled to it. In other words, the total electronic population, $\langle \sum_{k=1}^{N} a_k^\dagger a_k \rangle$, is conserved.

To make the connection with the MM Hamiltonian of Eq. (4.15), one has to put in the coordinate and momentum representation for the creation and annihilation operators, the end result is an exact quantum Hamiltonian for the N-state problem,

$$\hat{H}_{\rm el} = \sum_{k=1}^{N} \frac{1}{2} H_{k,k}(\mathbf{Q})(\hat{x}_k^2 + \hat{p}_k^2 - 1) + \sum_{k<k'=1}^{N} H_{k,k'}(\mathbf{Q})(\hat{x}_k \hat{x}_{k'} + \hat{p}_k \hat{p}_{k'}). \tag{4.23}$$

The wavefunction for the kth electronic state is

$$\langle \mathbf{x}|k\rangle = \langle \mathbf{x}|0,\ldots,1,\ldots,0\rangle \tag{4.24}$$

and this is the same wavefunction in Eq. (4.13).

Thus, we have shown that the MM Hamiltonian of Eq. (4.15) is the classical counterpart of the second quantized Hamiltonian of Eq. (4.23) and it is an exact analog Hamiltonian. One can now carry out dynamically consistent calculations, either quantum mechanically or semiclassical, or even classically, with this approach.

Finally, we note that this is not the only way of deriving the Hamiltonian of Eq. (4.23). Stock and Thoss[152] have utilized the Schwinger oscillator model of angular momentum[153] and arrived at the same Hamiltonian as above. We see now that these formulation are really equivalent and can afford different interpretations, but practical implementation of this model is the same. It is also important to point out that the real utility of this model is in its semiclassical and classical limit since we have mapped a discrete system on to a continuous system. As in the original MM spirit, this Hamiltonian allows us to treat all degrees of freedom, electronic and nuclear, on an equal footing so that these limits are well defined. In the following sections, the semiclassical and classical limits of this Hamiltonian are discussed.

4.3 Semiclassical Treatment of Nonadiabatic Dynamics

Various dynamical quantities of interest are transition amplitudes from one electronic/nuclear state to another which matrix elements of the time evolution operator,

$$\begin{aligned} S_{2,1}(t) \equiv\ & \langle \chi_2 \Phi_{k_2}|e^{-i\hat{H}t}|\Phi_{k_1}\chi_1\rangle = \int d\mathbf{x}_1 d\mathbf{Q}_1 \int d\mathbf{x}_2 d\mathbf{Q}_2 \\ & \chi_2^*(\mathbf{Q}_2)\Phi_{k_2}^*(\mathbf{x}_2)\langle \mathbf{x}_2, \mathbf{Q}_2|e^{-i\hat{H}t}|\mathbf{x}_1, \mathbf{R}_1\rangle \Phi_{k_1}(\mathbf{x}_1)\chi_1(\mathbf{R}_1), \end{aligned} \tag{4.25}$$

where $\chi_1(\chi_2)$ is the initial (final) nuclear wavefunction, $\Phi_k(\mathbf{x})$ are the "electronic' oscillator wavefunctions of Eq. (4.13), and H is the electronic-nuclear Hamiltonian of Eq. (4.15). As

was described in detail in chapter 2, the SC-IVR expression for the amplitude in Eq.(4.25) is

$$S_{2,1}(t) = \int d\mathbf{x}_1 d\mathbf{Q}_1 \int d\mathbf{p}_1 d\mathbf{P}_1 \sqrt{\frac{\partial(\mathbf{x}_t, \mathbf{Q}_t)}{\partial(\mathbf{p}_1, \mathbf{P}_1)}} / (2\pi i\hbar)^{F+N} \tag{4.26}$$

$$\chi_2^*(\mathbf{Q}_t)\Phi_{k_2}^*(\mathbf{x}_t)\Phi_{k_1}(\mathbf{x}_1)\chi_1(\mathbf{Q}_1)e^{iS_t(\mathbf{x}_1,\mathbf{p}_1,\mathbf{Q}_1,\mathbf{P}_1)}, \tag{4.27}$$

where $\mathbf{x}_t(\mathbf{x}_1, \mathbf{p}_1, \mathbf{Q}_1, \mathbf{P}_1)$ and $\mathbf{Q}_t(\mathbf{x}_1, \mathbf{p}_1, \mathbf{Q}_1, \mathbf{P}_1)$ are the coordinates at time t that evolve along classical trajectory with the indicated initial conditions, S_t is the corresponding action integral, and ν_t is the number of zeros experienced by the Jacobian determinant in the interval $(0, t)$. The classical trajectories here are for the full set of N electronic and F nuclear degrees of freedom obtain from the classical Hamiltonian of Eq. (4.15). It is also possible to calculate explicitly the nuclear wavefunctions on the various electronic surfaces by projecting out the electronic wavefunctions,

$$\begin{aligned}
\chi_{k_2 \leftarrow k_1}(\mathbf{Q}, t) &= \langle \mathbf{Q}, \Phi_{k_2} | e^{-i\hat{H}t} | \Phi_{k_1}\chi_1 \rangle \\
&= \int d\mathbf{x}_1 d\mathbf{Q}_1 \int d\mathbf{p}_1 d\mathbf{P}_1 \sqrt{\frac{\partial(\mathbf{x}_t, \mathbf{Q}_t)}{\partial(\mathbf{p}_1, \mathbf{P}_1)}} / (2\pi i\hbar)^{F+N} \\
&\quad \delta(\mathbf{Q} - \mathbf{Q}_t)\Phi_{k_2}^*(\mathbf{x}_t)\Phi_{k_1}(\mathbf{x}_1)\chi_1(\mathbf{Q}_1)e^{iS_t(\mathbf{x}_1,\mathbf{p}_1,\mathbf{Q}_1,\mathbf{P}_1)}.
\end{aligned} \tag{4.28}$$

It is of course not possible to obtain this quantity via the usual mixed quantum-classical surface hopping methods.

It is interesting to note the relation of the present SC-IVR model, Eq. (4.26), to that of the Pechukas approach. In the latter one writes a Feynman path integral expression for the time evolution operator in Eq. (4.25),

$$\langle \mathbf{x}_2, \mathbf{Q}_2 | e^{-i\hat{H}t} | \mathbf{x}_1, \mathbf{Q}_1 \rangle = \int_{\mathbf{Q}_1}^{\mathbf{Q}_2} \mathcal{D}[\mathbf{Q}] \int_{\mathbf{x}_1}^{\mathbf{x}_2} \mathcal{D}[\mathbf{x}] e^{iS[\mathbf{x}(t),\mathbf{Q}(t)]}, \tag{4.29}$$

and imagines first evaluating (exactly) the path integral over the electronic degrees of freedom, whereby Eq. (4.25) becomes

$$S_{2,1}(t) = \int d\mathbf{Q}_2 \int d\mathbf{Q}_1 \chi_2^*(\mathbf{Q}_2)\chi_1(\mathbf{Q}_1) \int_{\mathbf{Q}_1}^{\mathbf{Q}_2} \mathcal{D}[\mathbf{Q}] e^{i\int_0^t \frac{1}{2}m\dot{\mathbf{Q}}^2(\tau)d\tau} K_{2,1}[\mathbf{Q}(t)], \tag{4.30}$$

where $K_{2,1}[\mathbf{Q}(t)]$ is the electronic transition amplitude as a functional of the nuclear path $\mathbf{Q}(t)$. Up to this point the formulation is exact, but one now evaluates the nuclear path integral semiclassically via the functional version of the stationary phase approximation. This determines the nuclear classical trajectory. (The Miller-George[47–49] approach corresponds to the further approximation that the electronic transition amplitude functional

$K_{2,1}[\mathbf{Q}(t)]$ is also obtained semiclassically via the generalized Stuckelberg (complex crossing time) procedure.) As noted in section 4.2.1, however, the SC-IVR treatment of the time-dependent electronic problem is *exact* for a given nuclear path. The SC-IVR model thus gives $K_{2,1}[\mathbf{Q}(t)]$ of the Pechukas approach exactly. It also effectively makes a semiclassical approximation to the nuclear path integral but evaluates the integral over $\mathbf{Q}_1$ and $\mathbf{Q}_2$ exactly rather than via stationary phase. The present SC-IVR treatment of the MM classical electronic-nuclear Hamiltonian may thus be viewed as a practical way to implement the Pechukas model, with the further advantage that it treats the nuclear degrees of freedom within the SC-IVR framework.

The present approach is also seen to be of the same spirit as the original MM model in that it treats the electronic and nuclear degrees of freedom on the same dynamical footing, except here the treatment is via the SC-IVR description rather than the more primitive quasiclassical procedure. (We note that MM and others[154] did carry out semiclassical treatments of the classical electron model within the classical S-matrix formulation, and that the results were in fact excellent. Applications to more general situations, however, were difficult.)

4.3.1 Applications to Test Systems

To gain some indication of how well the present SC-IVR quantization of the classical electronic-nuclear model works in practice we have carried out applications to the "Tully canon", i.e., the three model problems suggested by Tully[107] for testing a variety of situations in non-adiabatic dynamics. These scattering problems involve one nuclear degree of freedom (e.g. an atom-atom collision system) and two electronic states, so the Hamiltonian of Eq. (4.15) takes the specific form,

$$\begin{aligned} H(x_1,p_1,x_2,p_2,Q,P) &= \frac{P^2}{2m} + \frac{1}{2}(p_1^2+x_1^2-1)H_{11}(Q) + \frac{1}{2}(p_2^2+x_2^2-1)H_{22}(Q) \\ &+ (p_1p_2+x_1x_2)H_{12}(Q), \end{aligned} \tag{4.31}$$

for various forms of the 2×2 diabatic electronic matrix $\{H_{k,k'}(Q)\}$. The two electronic wavefunctions are,

$$\Phi_1(x_1,x_2) = \sqrt{\frac{2}{\pi}}x_1 e^{-\frac{1}{2}(x_1^2+x_2^2)}, \tag{4.32a}$$

$$\Phi_2(x_1,x_2) = \sqrt{\frac{2}{\pi}}x_2 e^{-\frac{1}{2}(x_1^2+x_2^2)}. \tag{4.32b}$$

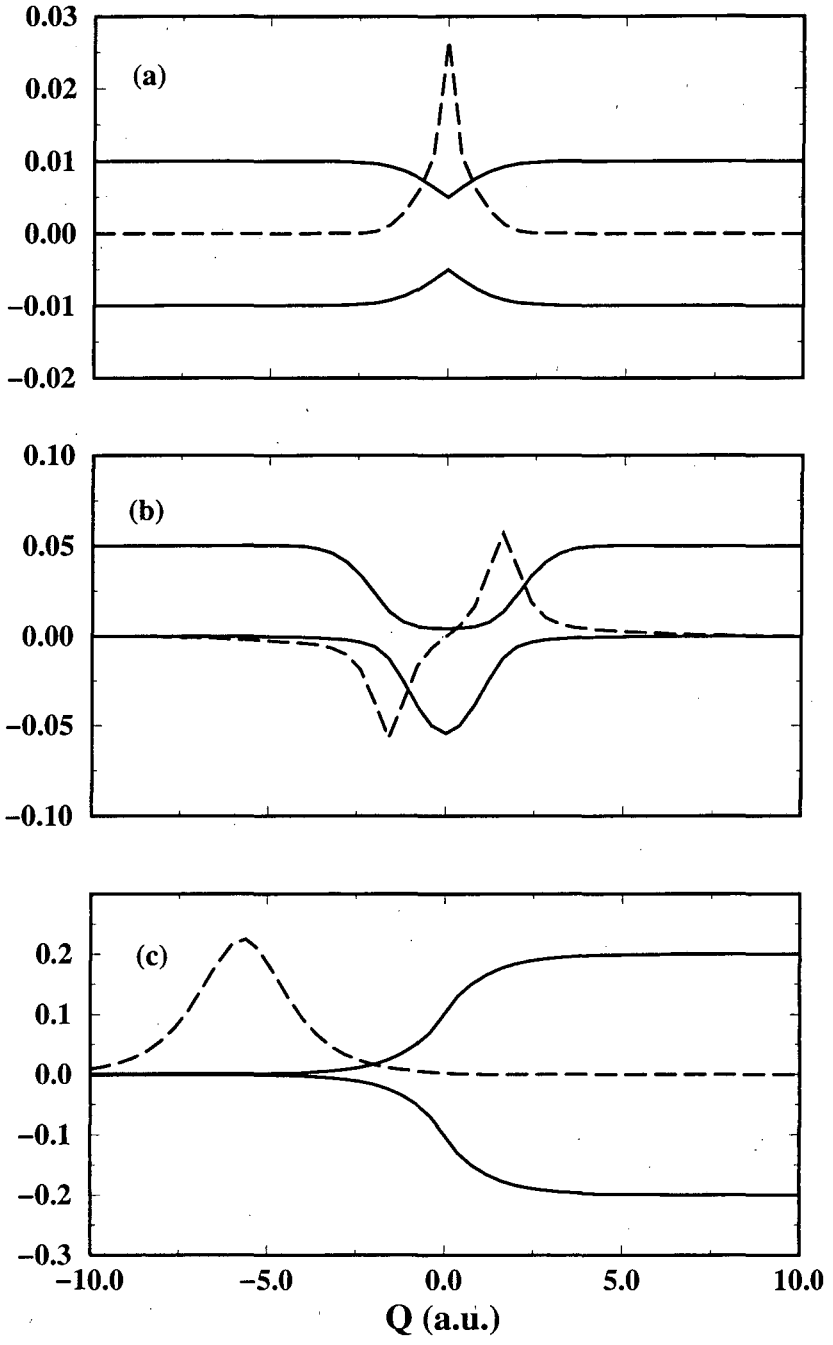

Figure 4.1: The adiabatic potential curves (solid) and the non-adiabatic coupling (dash) for the three systems considered. (1) Single avoided crossing. (2) Dual crossing. (3) Extended coupling.

The specific forms of the 2×2 diabatic electronic matrix $\{H_{k,k'}(Q)\}$ correspond to a single avoided crossing, a double avoided crossing, and an extended coupling problem. The adiabatic potentials for the three cases are shown in Figure 4.1. The nuclear mass is $m = 2000 a.u.$, about the mass of an H atom. As with Tully's calculations, the initial nuclear wavefunction is a Gaussian wavepacket (coherent state) located in the reactant asymptotic region (to the far left in Figure 4.1),

$$\chi_1(Q) = \left(\frac{f}{\pi}\right)^{\frac{1}{4}} e^{-\frac{f}{2}(Q-Q_0)^2 + iP_0Q}, \tag{4.33}$$

where Q_0 is far from the interaction region, and P_0 is the initial momentum. f is taken to be 1. The total wavefunction at $t = 0$ is therefore,

$$\Psi_1(Q, x_1, x_2, 0) = \chi_1(Q)\Phi_1(x_1, x_2). \tag{4.34}$$

This wavefunction is then propagated in time to the product asymptotic region ($Q \to \infty$) using the SC-IVR formalism described in the previous section. The nuclear wavefunctions on each surface are found by projecting out the electronic part as described before. The quantities Tully calculated are the various transmission and reflection probabilities on either surface. We obtain these by integrating the final nuclear probability density in the asymptotic regions,

$$P_k^{trans} = \lim_{t\to\infty} \int_0^\infty dQ |\chi_k(Q,t)|^2, \tag{4.35a}$$

$$P_k^{refl} = \lim_{t\to\infty} \int_{-\infty}^0 dQ |\chi_k(Q,t)|^2. \tag{4.35b}$$

Because the initial wavefunction is narrow in momentum, the final transmission and reflection probabilities are approximately the scattering probabilities as a function of initial translational energy $P_0^2/2m$.

The specific IVR we used for the calculation is the coherent state IVR of Eq. (2.14). The integration over the initial conditions is done with weighted Monte-Carlo sampling. A typical number of trajectories required for convergence is 2×10^4. From the wavefunctions, transmission probabilities and reflection probabilities are calculated for both electronic states. Quantum mechanical calculations are also performed for comparison purposes with the standard split operator technique.

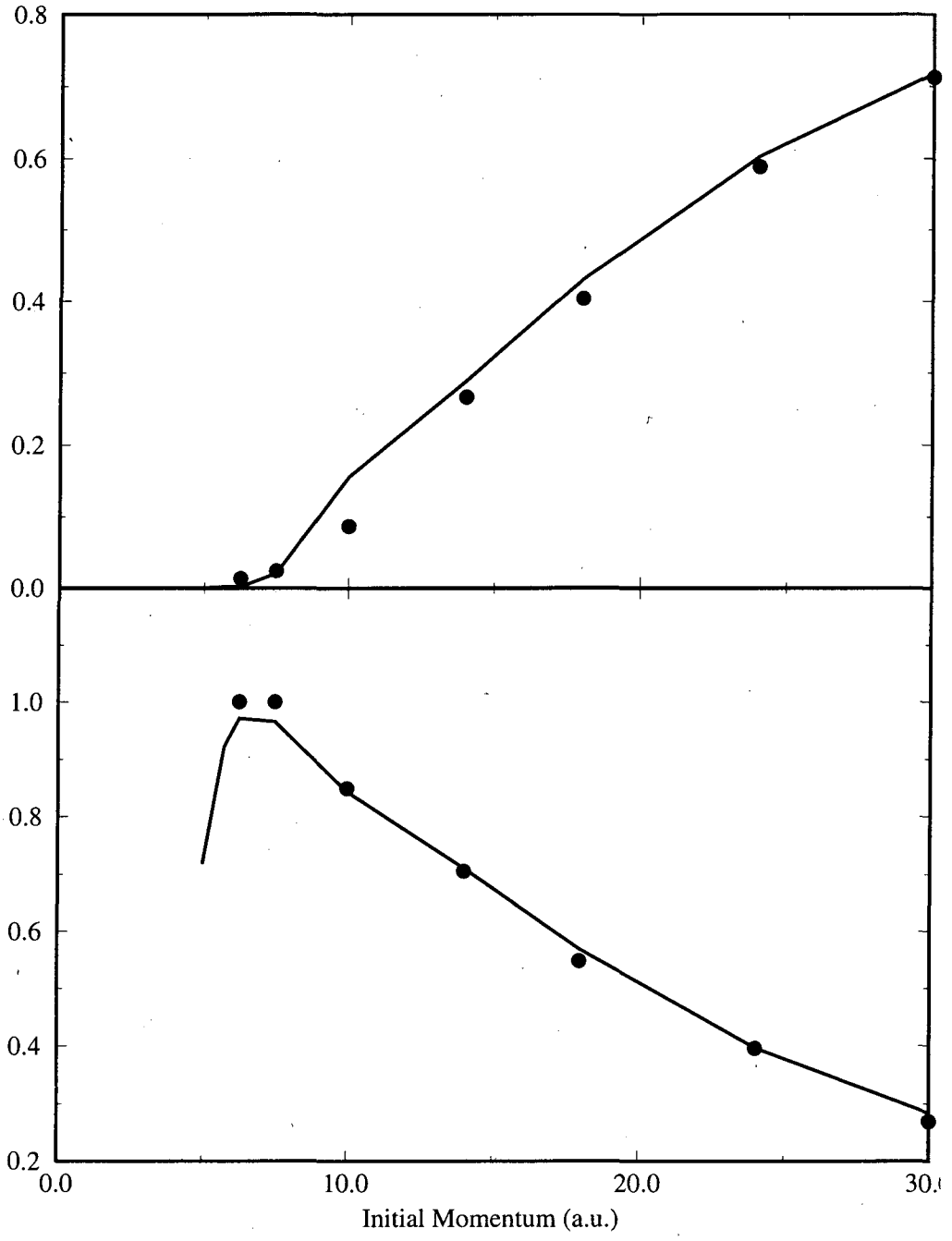

Figure 4.2: Case 1, single avoided crossing. Upper panel, transmission probabilities on the first diabatic state (upper adiabatic state). Lower panel: transmission probabilities on the second diabatic state (lower adiabatic state). Solid lines are the quantum mechanical results. Filled circles are the SC-IVR model.

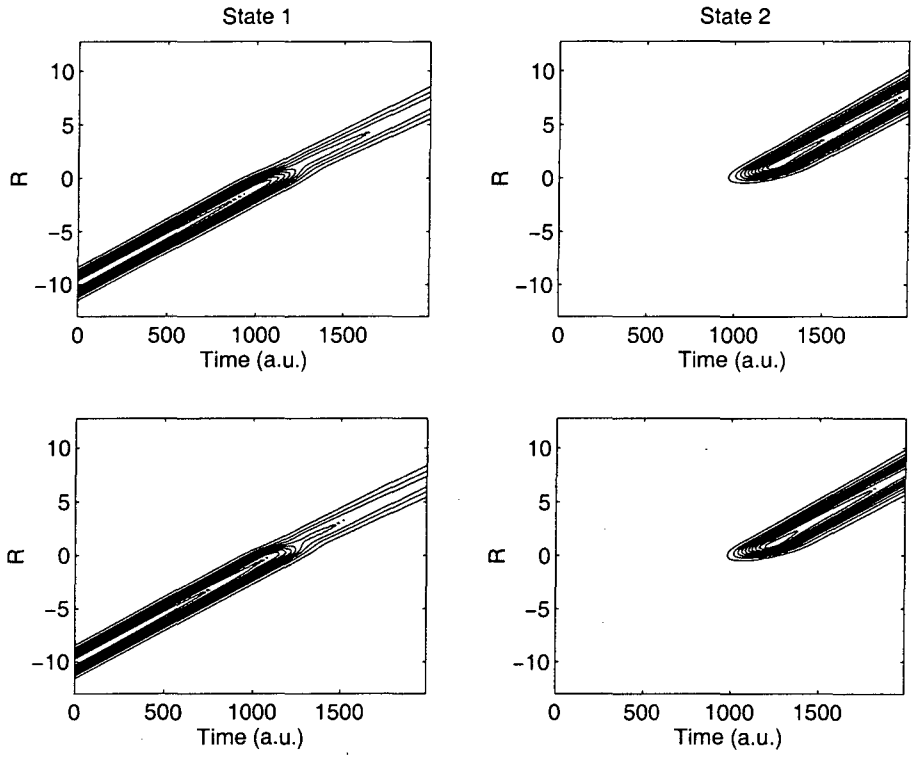

Figure 4.3: Case 1, avoided crossing. Contours of the absolute value of the nuclear wavefunctions squared on each of the diabatic states, quantum (upper two panels) versus SC-IVR (lower two panels). The initial momentum is $P_0 = 18.0$

Case 1, Avoided Crossing

This example of an isolated avoided crossing of adiabatic potential surfaces is the most elementary and most common situation. The diabatic potentials in the case are,

$$H_{11}(Q) = \begin{cases} V_0(1 - e^{-\alpha Q}) & Q > 0, \\ -V_0(1 - e^{\alpha Q}) & Q < 0, \end{cases} \tag{4.36a}$$

$$H_{22}(Q) = -H_{11}(Q), \tag{4.36b}$$

$$H_{12}(Q) = V_1 e^{-\beta Q^2}. \tag{4.36c}$$

The parameter used here are the same as used by Tully, $V_0 = 0.01$, $V_1 = 0.005$, $\alpha = 1.6$, and $\beta = 1.0$, all in atomic units. The transmission probabilities in state 1 and 2 versus the initial momentum are shown in Figure 4.2. The quantum results are plotted also. The semiclassical results are essentially quantitative for higher initial energies. For lower energies, can be further improved with more trajectories.

In addition to the probabilities, with this method, we are able to obtain also the wavefunctions on each surface. These wavefunctions and their time evolution are shown as contours in Figure 4.3. Compared with the quantum mechanical results, they are in excellent agreement.

Case 2, Double Crossing

This example is more challenging in that there is quantum mechanical interference between the two crossings, giving Stuckelberg oscillations[155]. The diabatic potentials in this case are,

$$H_{11}(Q) = 0, \tag{4.37a}$$

$$H_{22}(Q) = -V_0 e^{-\alpha Q^2} + E_0, \tag{4.37b}$$

$$H_{12}(Q) = V_1 e^{-\beta Q^2}, \tag{4.37c}$$

with $V_0 = 0.1$, $E_0 = 0.05$, $V_1 = 0.015$, $\alpha = 0.28$, and $\beta = 0.06$. Again, comparisons between quantum and semiclassical results are shown in Figure 4.4. The present SC-IVR model reproduces the oscillatory transmission probabilities at higher energies very well.

Case 3, Extended Coupling

This case is a still more difficult test for the semiclassical method. Here, the coupling between the diabatic states do not go to zero in the asymptotic region. The diabatic potentials are,

$$H_{11}(Q) = -V_0, \tag{4.38a}$$

$$H_{22}(Q) = V_0, \tag{4.38b}$$

$$H_{12}(Q) = \begin{cases} V_1 e^{\beta Q} & Q < 0, \\ V_1(2 - e^{-\beta Q}) & Q > 0, \end{cases} \tag{4.38c}$$

with $V_0 = 6 \times 10^{-4}$, $V_1 = 0.1$, and $\beta = 0.9$. Since the diabatic states are very close in energy, the transmission and reflection probabilities are essentially identical for both states. The adiabatic states show a barrier for the upper state, thus one would expect some reflection for energies below this barrier. These effects are all observed in the quantum and the semiclassical calculations. Their comparison is again very good. Tully in his calculations observed unphysical oscillatory effects with the surface-hopping model. We do not observe

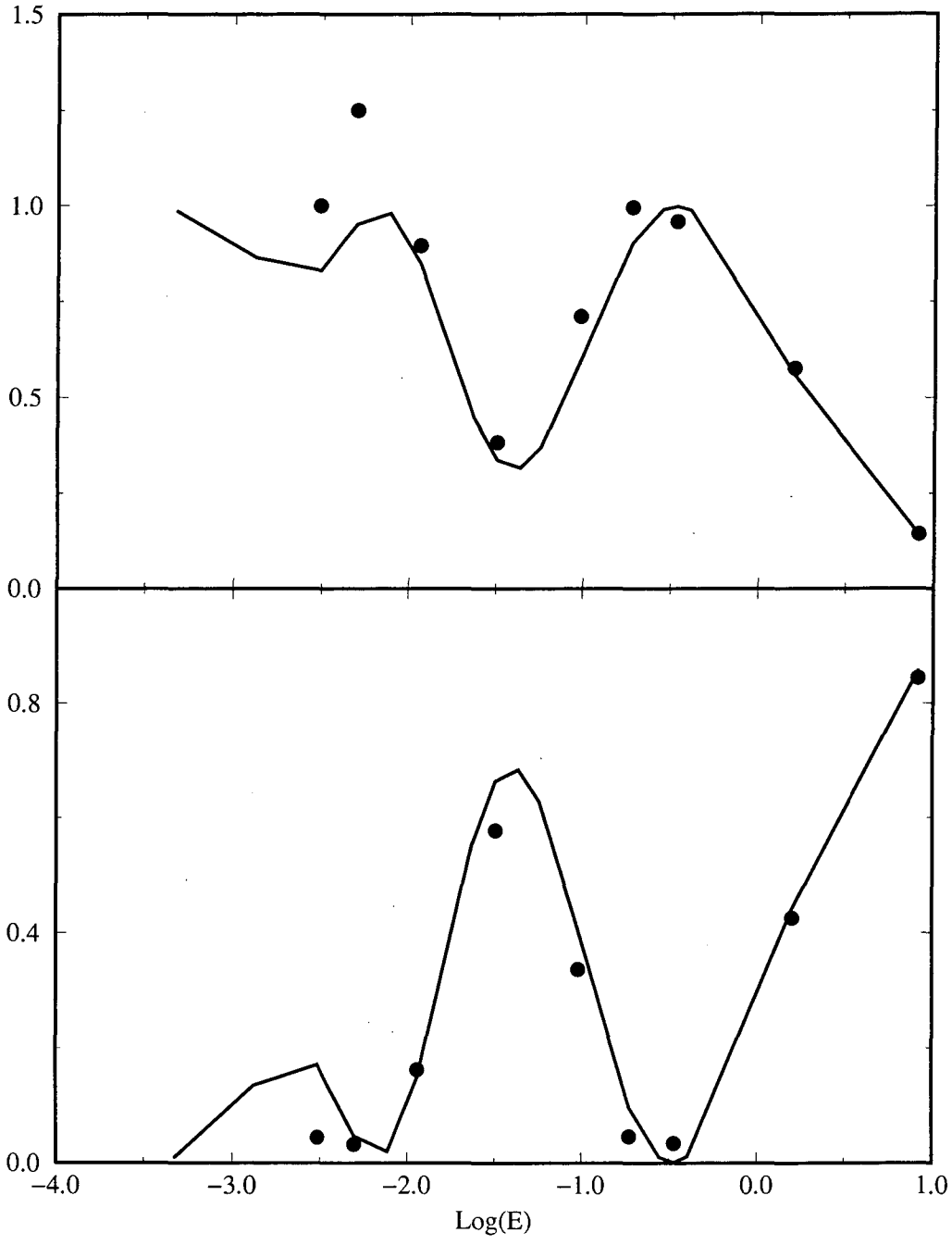

Figure 4.4: Case 2, dual avoided crossing. Upper panel, transmission probabilities on the first diabatic state. Lower panel, transmission probabilities on the second diabatic state. Symbols are the same as Figure 4.2.

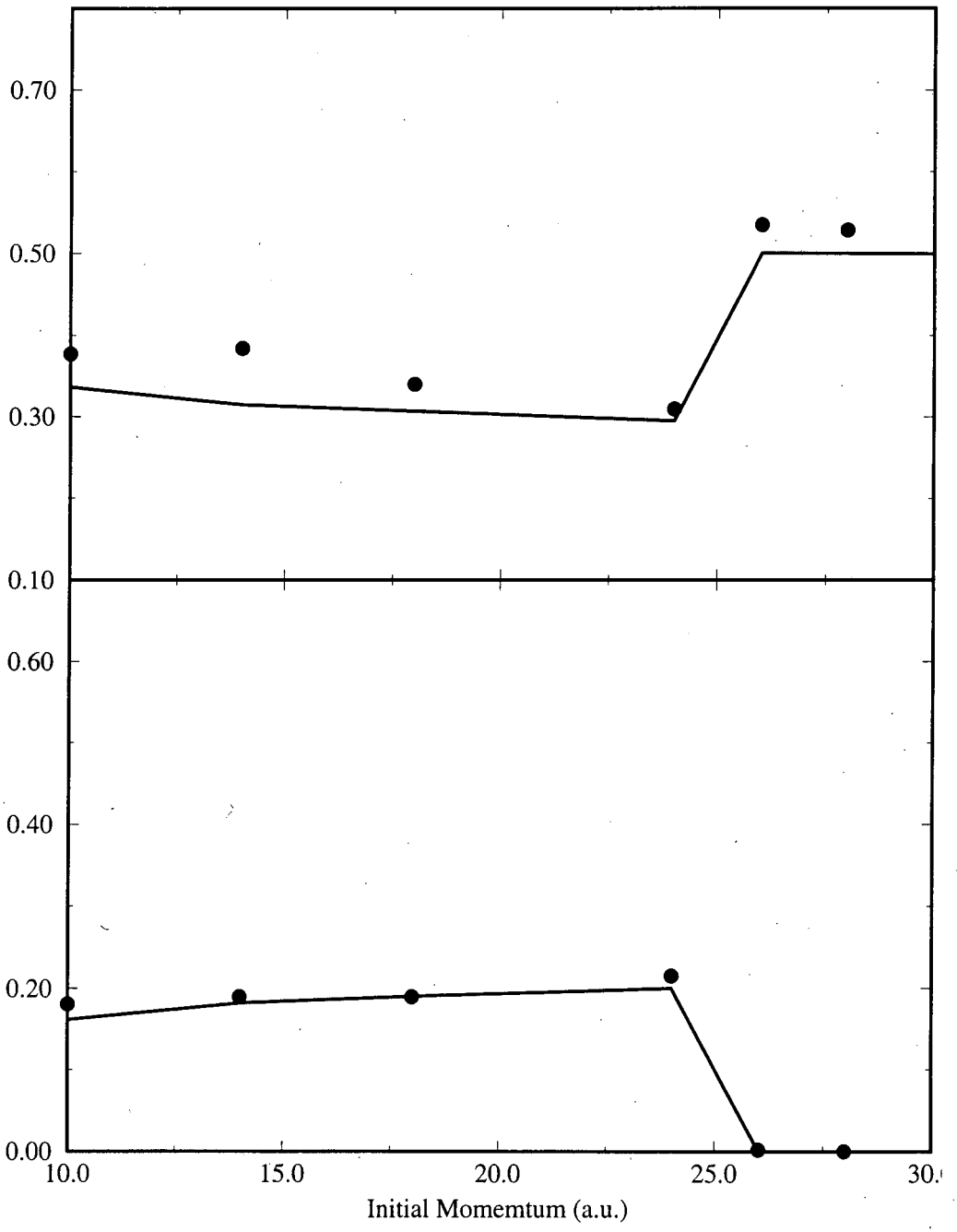

Figure 4.5: Case 3, extended coupling. Upper panel, transmission probabilities for both of the diabatic states. Lower panel, reflection probabilities for both of the diabatic states. Symbols are the same as Figure 4.2.

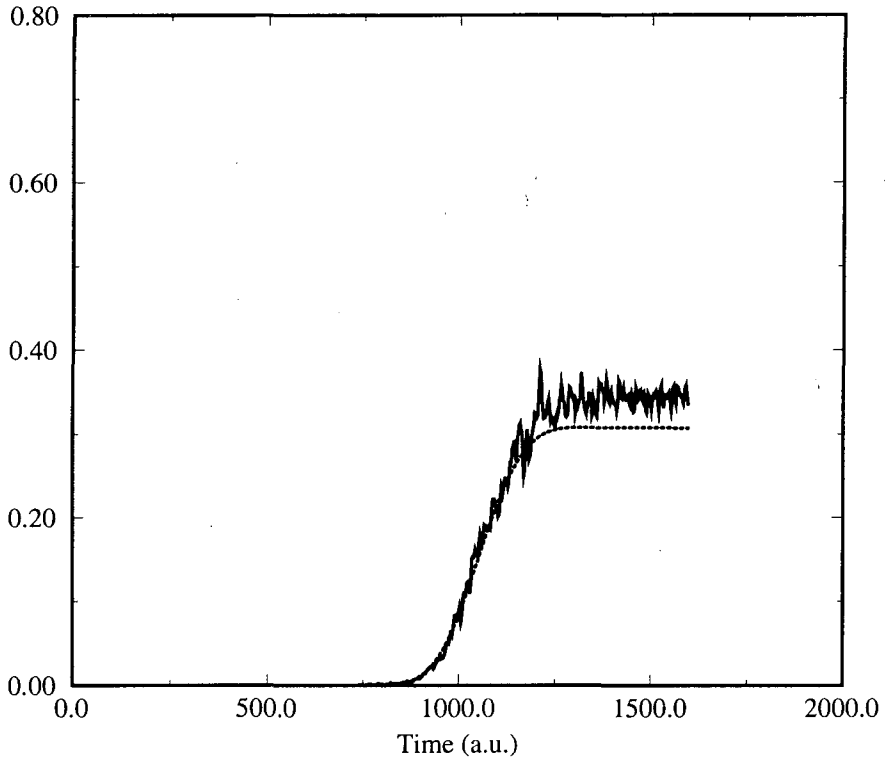

Figure 4.6: Transmission probability as function of time for the extended coupling. The initial momentum is P_0=18.0. This plot is the same for either diabatic state. Solid line, SC-IVR. Dashed line, quantum mechanical.

this in the transmission and reflection probabilities as shown in Figure 4.5. However, the probabilities as a function of time do show some small oscillations around the correct value in Figure 4.6. These oscillations are of course due to the extended coupling in the asymptotic region. The extend to which they effect the final answer however is small.

4.4 Linearized Approximation

The aim of this section is to apply the simplified but approximate version of the SC-IVR, i.e., the LSC-IVR result given by Eq. (3.62) and (3.67), to the present model of electronically nonadiabatic processes, to see if it is capable of describing them to a useful degree of accuracy. In chapter 3, we have shown that the linearized approximation is a well defined classical limit of the semiclassical theory without any of the interference and coherence effects. Therefore, the model we present in this section can be thought of as a

classical limit of electronically nonadiabatic dynamics, even though (as we shall discuss) it has some relations to the mixed quantum-classical theories mentioned earlier.

One thus needs the Wigner functions corresponding to initial and final wavefunctions of the form in Eq. (4.34) and (4.13), and it is easy to see that they are given by

$$\rho_{i,\mathrm{n}}(\mathbf{x},\mathbf{p},\mathbf{Q},\mathbf{P}) = \rho_i^{\mathrm{el}}(\mathbf{x},\mathbf{p})\rho_{\mathrm{n}}(\mathbf{Q},\mathbf{P}), \tag{4.39}$$

where the electronic factor is especially simple,

$$\rho_i^{\mathrm{el}}(\mathbf{x},\mathbf{p}) = 2^{(N+1)}(x_i^2 + p_i^2 - \frac{1}{2}) \exp\left[-\sum_{k=1}^{N}(x_k^2 + p_k^2)\right]. \tag{4.40}$$

It is useful to remind the reader of the connection of the present approach to the "mixed quantum-classical" (or semiclassical time-dependent self consistent field, SC-TDSCF) model that is popular for treating nonadiabatic molecular dynamics. As has been noted before,[147] the classical equations of motion generated by the MM Hamiltonian (Eq. (4.15)) are equivalent to the time-dependent Schrödinger equation for the electronic degrees of freedom, the time-dependence coming from the classical motion of the nuclear degrees of freedom (whose trajectory is determined by the Ehrenfest average force); these are the same equations of motion as in the mixed quantum-classical/SC-TDSCF model. However, the way the boundary conditions are imposed makes the models different. In the usual implementation of the mixed quantum-classical/SC-TDSCF approach, for example, a given classical trajectory begins in one electronic state but ends up in a mixture of states. The quasiclassical implementation by MM assigns each trajectory to a particular final electronic (and nuclear) state by histogramming the final electronic (and nuclear) action variables; this makes the approach more akin to the surface-hopping model in that a given trajectory is assigned to only one final electronic state. The SC-IVR imposes the initial and final state boundary conditions on the equations of motion through the initial and final wavefunctions of the electronic and nuclear degrees of freedom. The LSC-IVR imposes the boundary conditions via the initial and final Wigner distributions of the quantum electronic wavefunction which are really the exact classical boundary conditions. As noted above, if the Hamiltonian of Eq. (4.15) were implemented fully quantum mechanically, one would have an exact quantum description of the process. The point of view of all of our work, starting with that of McCurdy *et al*,[145–148] is that the Hamiltonian of Eq. (4.15) allows one to treat the electronic and nuclear degrees of freedom on an equivalent dynamical footing, be it done classically, semiclassically, or fully quantum mechanically.

4.4.1 One Dimensional 2-State Scattering Problems

We again go back to the set of three one (nuclear) dimensional 2 (electronic)-state scattering problems of section 4.3.1. The initial nuclear wavefunction is again a minimum uncertainty wavepacket,

$$\chi(Q) = \left(\frac{\gamma}{\pi}\right)^{\frac{1}{4}} e^{-\frac{\gamma}{2}(Q-Q_0)^2+iP_0Q/\hbar}, \tag{4.41}$$

with the initial position Q_0 far to the left of the interaction region and initial momentum $P_0 > 0$. The quantity of interest is the transmission probability to the right asymptotic region for each final electronic state j as a function of the initial momentum, which is given by Eq. (4.35a). This can be written equivalently as

$$P_{j\leftarrow i}(P_0) = \lim_{t\to\infty} \mathrm{tr}\left[|\chi\phi_i\rangle\langle\chi\phi_i|e^{i\hat{H}t/\hbar}|\phi_j\rangle\hat{h}(Q)\langle\phi_j|e^{-i\hat{H}t/\hbar}\right], \tag{4.42}$$

so as to be in the form of Eq. (3.67) with

$$\hat{A} = |\chi\phi_i\rangle\langle\chi\phi_i|, \tag{4.43}$$

$$\hat{B} = |\phi_j\rangle\langle\phi_j|\hat{h}(Q). \tag{4.44}$$

The Wigner functions corresponding to these operators are easily found to be,

$$A_w(Q,P,\mathbf{x},\mathbf{p}) = \rho(Q,P)\rho_i^{\mathrm{el}}(\mathbf{x},\mathbf{p}), \tag{4.45}$$

$$B_w(Q,P,\mathbf{x},\mathbf{p}) = h(Q)\rho_j^{\mathrm{el}}(\mathbf{x},\mathbf{p}), \tag{4.46}$$

where $\rho(Q,P)$ is the Wigner function for the initial nuclear wavefunction of Eq. (4.41),

$$\rho(Q,P) = 2e^{-\gamma(Q-Q_0)^2-(P-P_0)^2/\gamma\hbar^2}, \tag{4.47}$$

and $\{\rho_i^{\mathrm{el}}(\mathbf{x},\mathbf{p})\}, i = 1,2$ is given by Eq. (4.40) for $N = 2$. In actual calculations, these Wigner distributions allow naturally for Monte Carlo importance sampling which we have used for the results presented below.

Figure 4.7 shows the transmission probability from initial electronic state 1 to each of the two final electronic states for the first test case, which corresponds to a single avoided crossing (cf. figure 4.1a). The agreement between the LSC-IVR results of Eq. (3.67) and the exact quantum mechanical values is quite good for all energies except those close to the threshold region. Here, quantum mechanical effects such as tunneling through the crossing

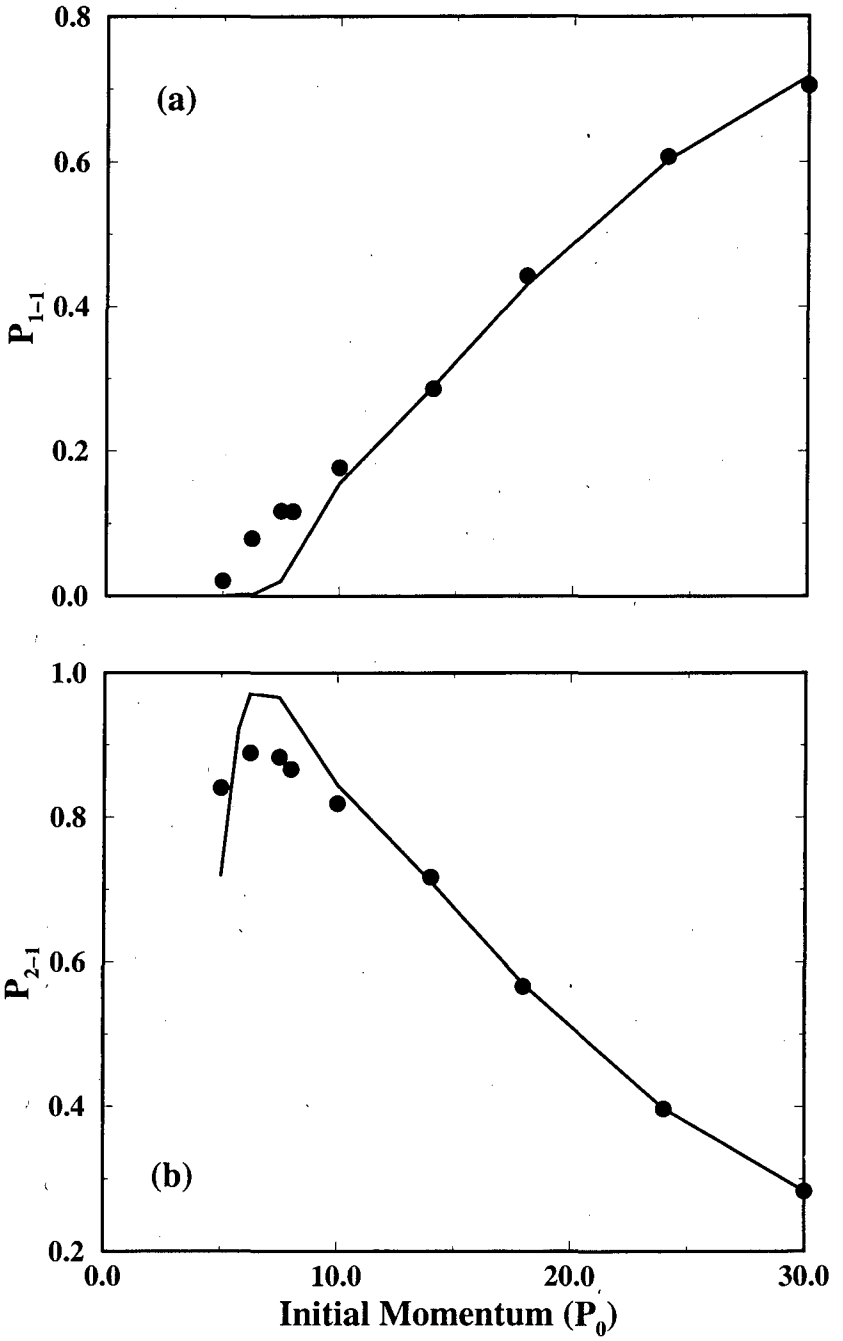

Figure 4.7: The transmission probability $P_{j\leftarrow1}$ as a function of the initial momentum P_0 for the single avoided crossing case. The solid lines are the exact quantum results and the points are the LSC-IVR results. (a) $j = 1$, (b) $j = 2$.

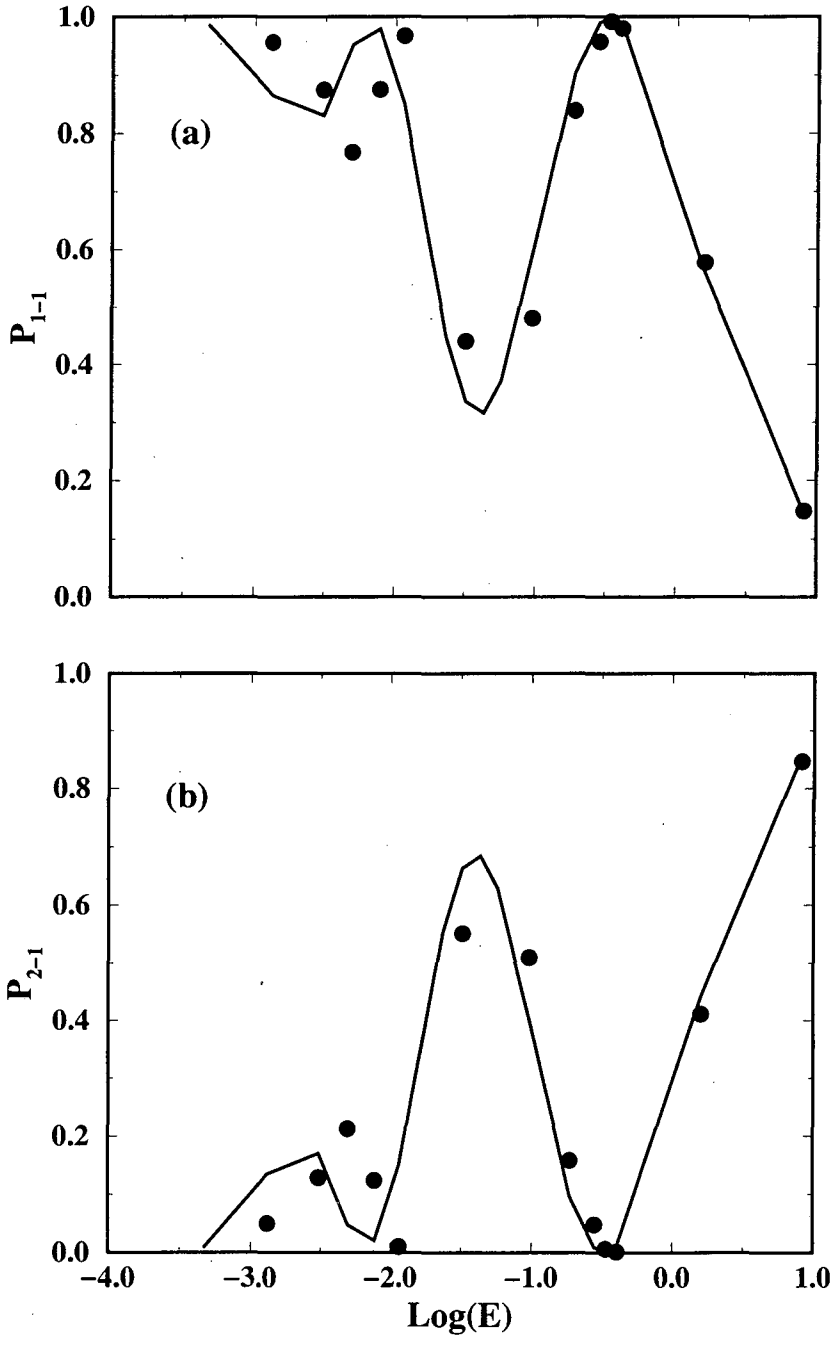

Figure 4.8: The transmission probability $P_{j\leftarrow 1}$ as a function of the log of initial energy $E = P_0^2/2m$ for the double crossing case. The solid lines are the exact quantum results and the points are the LSC-IVR results. (a) $j = 1$, (b) $j = 2$.

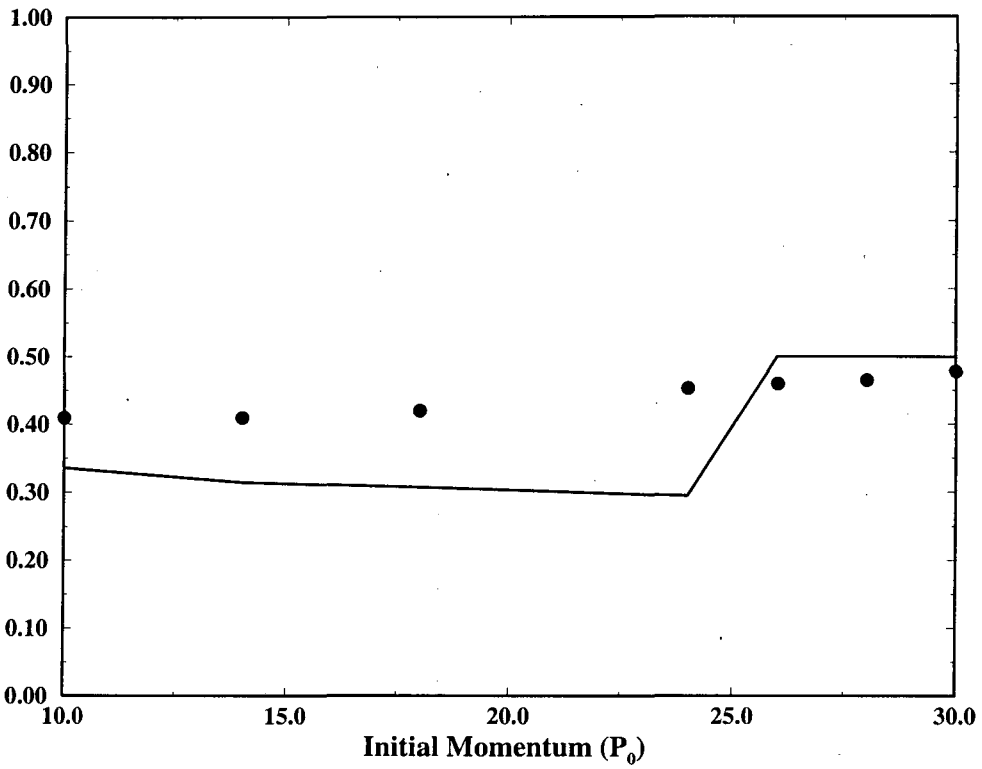

Figure 4.9: The transmission probability $P_{j\leftarrow 1}$ as a function of the initial momentum P_0 for the extended coupling case. The solid lines are the exact quantum results and the points are the LSC-IVR results. These results are for $j = 1$ and 2.

area are more important, and the classical dynamics in the LSC-IVR is less able to describe this behavior quantitatively.

Figure 4.8 shows the same plots as Figure 4.2 for the second version of the model, the case of two avoided crossing regions (cf. Figure 4.1b), where the possibility of Stuckelberg oscillations (i.e., interference effects between the two crossing regions) arises. The LSC-IVR is seen to describe this interference behavior quite well. The most significant error is again seen to be in the low energy threshold region.

Finally, Figure 4.9 shows the transmission probability for the third case, that with an extended coupling region (cf. Figure 4.1c). Since the diabatic states are very close in energy, the transmission probabilities are essentially identical for both final states. This was the case for which Tully's surface-hopping approach gave unphysical oscillations in the transmission probability. The LSC-IVR results do not exhibit this problem, but neither do they reproduce the sharp step-like structure in the quantum values for $P_0 \approx 25$ a.u. They

do, however, give the correct magnitude of the transmission probability over the whole energy range.

The linearized approximation to the SC-IVR, i.e., the LSC-IVR approximation of Eqs. (3.62) and (3.67), is thus seen to do a reasonably good job for these three model problems which have quite different dynamical features. The results are not quite as good as our previous ones using the full SC-IVR, but the present LSC-IVR calculation is much easier to carry out than the former.

4.4.2 The Spin-Boson Problem

The next test problem we consider is the so-called spin-boson problem,[156,157] which also consists of $N = 2$ electronic states but where the nuclear degrees of freedom are an infinite set of harmonic oscillators. This is about the only example of a system with many degrees of freedom for which accurate quantum mechanical results are available to serve as a benchmark for approximate treatments. It has often been used as a model for two interacting electronic states in a condensed phase medium, e.g., a radiationless transition or electron transfer process in a liquid, a solid, a cluster, or a protein.

The specific form of the 2×2 diabatic electronic matrix $H_{i,j}(\mathbf{Q})$ in this case is

$$\hat{H}_{\rm el}(\mathbf{Q}) = \begin{pmatrix} H_{11}(\mathbf{Q}) & H_{12}(\mathbf{Q}) \\ H_{21}(\mathbf{Q}) & H_{22}(\mathbf{Q}) \end{pmatrix} = \begin{pmatrix} V_0(\mathbf{Q}) + V_1(\mathbf{Q}) & \Delta \\ \Delta & V_0(\mathbf{Q}) - V_1(\mathbf{Q}) \end{pmatrix}, \tag{4.48}$$

where the off-diagonal electronic coupling Δ is independent of nuclear coordinates, and

$$V_0(\mathbf{Q}) = \sum_{k=1}^{F} \frac{1}{2} m_k \omega_k^2 Q_k^2, \tag{4.49a}$$

$$V_1(\mathbf{Q}) = \sum_{k=1}^{F} c_k Q_k. \tag{4.49b}$$

The total Hamiltonian of the spin-boson model,

$$\hat{H} = \hat{1} \sum_{k=1}^{F} \frac{P_k^2}{2m_k} + \hat{H}_{\rm el}(\mathbf{Q}), \tag{4.50a}$$

is typically expressed as

$$\hat{H} = H_0 \hat{1} + V_1(\mathbf{Q})\hat{\sigma}_z + \Delta \hat{\sigma}_x, \tag{4.50b}$$

where

$$H_0 = \sum_{k=1}^{F} \frac{P_k^2}{2m_k} + V_0(\mathbf{Q}), \tag{4.51}$$

and $\hat{\sigma}_z$ and $\hat{\sigma}_x$ are the Pauli spin matrices. The dynamics of the spin-boson model is fully specified by the combination of the coupling parameters $\{c_k\}$ and the distribution of frequencies that define the spectral density $J(\omega)$,

$$J(\omega) = \frac{\pi}{2}\sum_k \frac{c_k^2}{m_k\omega_k}\delta(\omega-\omega_k), \tag{4.52}$$

a common choice for which is the Ohmic case with exponential cutoff,

$$J(\omega) = \eta\omega e^{-\omega/\omega_c}. \tag{4.53}$$

This model is thus completely specified by the cutoff parameter ω_c and the coupling coefficient η (or more frequently the Kondo parameter $\alpha = 2\eta/\pi$).

We examine two relevant dynamical quantities of interest for the spin-boson model: the first is the time-dependent electronic population, defined as

$$D(t) = \frac{1}{Z_b}\mathrm{tr}\left[e^{-\beta(H_0+V_1)}|1\rangle\langle 1|e^{i\hat{H}t/\hbar}\hat{\sigma}_z e^{-i\hat{H}t/\hbar}\right] = \bar{P}_{1\leftarrow 1}(t) - \bar{P}_{2\leftarrow 1}(t), \tag{4.54}$$

where the initial electronic state is $|1\rangle$ with the nuclear degrees of freedom in Boltzmann equilibrium for the nuclear Hamiltonian of state 1, $H_0 + V_1$ ($Z_b = \mathrm{tr}[|1\rangle\langle 1|e^{-\beta(H_0+V_1)}]$); the second quantity is the spin correlation function, defined as

$$C(t) = \mathrm{Re}\,\frac{1}{Z}\mathrm{tr}\left[e^{-\beta\hat{H}}\hat{\sigma}_z e^{i\hat{H}t/\hbar}\hat{\sigma}_z e^{-i\hat{H}t/\hbar}\right], \tag{4.55}$$

where the bath and the two-level system are both in thermal equilibrium, and Z is the total partition function of the system and bath. The literature on these quantities for the spin boson model is vast: Mak and Chandler,[158] for example, performed a systematic study of the spin correlation function for a wide range of parameters to determine, among other things, the coherent-incoherent transition boundary. They also studied the temperature dependence of the decay rate of $C(t)$ for several sets of parameters. Makri *et al.*[159] performed calculations of the time-dependent electronic population also using path integral methods. These are the primary results to which we shall compare the LSC-IVR approximation.

For the spin-boson Hamiltonian in Eq. (4.50), the MM Hamiltonian of Eq. (4.15) is easily found to be

$$\begin{aligned} H(\mathbf{x},\mathbf{p},\mathbf{Q},\mathbf{P}) &= \sum_{k=1}^{F}\left[\frac{P_k^2}{2m_k} + \frac{1}{2}m_k\omega_k^2 Q_k^2\right] + \frac{1}{2}(x_1^2+p_1^2-x_2^2-p_2^2)\sum_{k=1}^{F}c_k Q_k \\ &+ \Delta(x_1x_2+p_1p_2). \end{aligned} \tag{4.56}$$

It is also immediately clear how to apply the LSC-IVR approximation of Eq. (3.67). For the time dependent electronic population of Eq. (4.54),the operators $\hat{A}$ and $\hat{B}$ of Eq. (3.67) are

$$\hat{A} = \frac{1}{Z_b} e^{-\beta(H_0+V_1)} |1\rangle\langle 1|, \tag{4.57}$$

$$\hat{B} = \hat{\sigma}_z = (|1\rangle\langle 1| - |2\rangle\langle 2|), \tag{4.58}$$

so that Eq. (3.67) give $D(t)$ as

$$D(t) = \frac{1}{(2\pi\hbar)^2} \int d\mathbf{x}_0 d\mathbf{p}_0 \int d\mathbf{Q}_0 d\mathbf{P}_0 W_\beta^+(\mathbf{Q}_0, \mathbf{P}_0) \rho_1^{\rm el}(\mathbf{x}_0, \mathbf{p}_0) \left[\rho_1^{\rm el}(\mathbf{x}_t, \mathbf{p}_t) - \rho_2^{\rm el}(\mathbf{x}_t, \mathbf{p}_t)\right], \tag{4.59}$$

where $W_\beta^\pm(\mathbf{Q}, \mathbf{P})$ is the Wigner transform of $e^{-\beta(H_0 \pm V_1)}/[Z_b(2\pi\hbar)^F]$,

$$\begin{aligned} W_\beta^\pm(\mathbf{Q}, \mathbf{P}) &= \prod_{k=1}^{F} \frac{\tanh(\beta\hbar\omega_k/2)}{\pi\hbar} \\ &\times \exp\left\{ \sum_{k=1}^{F} \frac{2\tanh(\beta\hbar\omega_k/2)}{\hbar\omega_k} \left[\frac{P_k^2}{2m_k} + \frac{1}{2} m_k \omega_k^2 \left(Q_k \pm \frac{c_k}{m_k\omega_k^2} \right)^2 \right] \right\}, \end{aligned} \tag{4.60}$$

and $\rho_n^{\rm el}(\mathbf{x}, \mathbf{p})$ is the Wigner transform of $|n\rangle\langle n|$ already given in Eq. (4.40) ($n = 1, 2$).

For the spin correlation function of Eq. (4.55), the situation is slightly more complicated. In this case the operators $\hat{A}$ and $\hat{B}$ of Eq. (3.67) are,

$$\hat{A} = \frac{1}{Z} e^{-\beta\hat{H}} \sigma_z, \tag{4.61}$$

$$\hat{B} = \hat{\sigma}_z, \tag{4.62}$$

one needs to find the Wigner transform of $\hat{A}$. It is not possible to obtain this quantity exactly without a fully quantum calculation, but a reasonable approximation can be obtained by using a split operator type approximation for $e^{-\beta\hat{H}}$,

$$\begin{aligned} \exp & \begin{pmatrix} -\beta(H_0+V_1) & -\beta\Delta \\ -\beta\Delta & -\beta(H_0-V_1) \end{pmatrix} \\ &\approx \begin{pmatrix} e^{-\beta(H_0+V_1)} & 0 \\ 0 & e^{-\beta(H_0-V_1)} \end{pmatrix} \exp \begin{pmatrix} 0 & -\beta\Delta \\ -\beta\Delta & 0 \end{pmatrix} \\ &= \begin{pmatrix} e^{-\beta(H_0+V_1)}\cosh(\beta\Delta) & -e^{-\beta(H_0+V_1)}\sinh(\beta\Delta) \\ -e^{-\beta(H_0-V_1)}\sinh(\beta\Delta) & e^{-\beta(H_0-V_1)}\cosh(\beta\Delta) \end{pmatrix}. \end{aligned} \tag{4.63}$$

The trace of $e^{-\beta\hat{H}}$, which is the partition function Z, is then,

$$Z = 2\cosh(\beta\Delta)\mathrm{tr}(e^{-\beta H_0})\exp\left[-\beta\sum_{k=1}^{F}\frac{c_k^2}{2m_k\omega_k^2}\right]. \tag{4.64}$$

Multiplying by $\hat{\sigma}_z$ and writing everything in the basis set representation, one obtains,

$$\begin{aligned} e^{-\beta\hat{H}}\hat{\sigma}_z &= \begin{pmatrix} e^{-\beta(H_0+V_1)}\cosh(\beta\Delta) & e^{-\beta(H_0+V_1)}\sinh(\beta\Delta) \\ -e^{-\beta(H_0-V_1)}\sinh(\beta\Delta) & -e^{-\beta(H_0-V_1)}\cosh(\beta\Delta) \end{pmatrix} \\ &= e^{-\beta(H_0+V_1)}\cosh(\beta\Delta)|1\rangle\langle 1| + e^{-\beta(H_0+V_1)}\sinh(\beta\Delta)|1\rangle\langle 2| \\ &\quad -e^{-\beta(H_0-V_1)}\sinh(\beta\Delta)|2\rangle\langle 1| - e^{-\beta(H_0-V_1)}\cosh(\beta\Delta)|2\rangle\langle 2|, \end{aligned} \tag{4.65}$$

so that the final result for the Wigner transform of $e^{-\beta\hat{H}}\hat{\sigma}_z/[Z(2\pi\hbar)^F]$ is,

$$\begin{aligned} \frac{1}{(2\pi\hbar)^F}A_w(\mathbf{x},\mathbf{p},\mathbf{Q},\mathbf{P}) &= W_\beta^+(\mathbf{Q},\mathbf{P})[\cosh(\beta\Delta)\rho_1^{\mathrm{el}}(\mathbf{x},\mathbf{p}) + \sinh(\beta\Delta)\rho_{12}^{\mathrm{el}}(\mathbf{x},\mathbf{p})] \\ &\quad - W_\beta^-(\mathbf{Q},\mathbf{P})[\sinh(\beta\Delta)\rho_{21}^{\mathrm{el}}(\mathbf{x},\mathbf{p}) + \cosh(\beta\Delta)\rho_2^{\mathrm{el}}(\mathbf{x},\mathbf{p})], \end{aligned} \tag{4.66}$$

where ρ_{12}^{el} and ρ_{21}^{el} are the Wigner transform of $|1\rangle\langle 2|$ and $|2\rangle\langle 1|$,

$$\rho_{12}^{\mathrm{el}}(\mathbf{x},\mathbf{p}) = 2^3(x_1 - ip_1)(x_2 + ip_2)\exp\left[-(x_1^2 + x_2^2 + p_1^2 + p_2^2)\right], \tag{4.67}$$

$$\rho_{21}^{\mathrm{el}}(\mathbf{x},\mathbf{p}) = 2^3(x_1 + ip_1)(x_2 - ip_2)\exp\left[-(x_1^2 + x_2^2 + p_1^2 + p_2^2)\right], \tag{4.68}$$

and $W_\beta^\pm(\mathbf{Q},\mathbf{P})$ is given in Eq. (4.60). The final result for the LSC-IVR approximation to $C(t)$ is therefore

$$\begin{aligned} C(t) &= \mathrm{Re}\,\frac{1}{(2\pi\hbar)^2}\int d\mathbf{x}_0\int d\mathbf{p}_0\int d\mathbf{Q}_0\int d\mathbf{P}_0 \\ &\quad \Big\{W_\beta^+(\mathbf{Q},\mathbf{P})[\cosh(\beta\Delta)\rho_1^{\mathrm{el}}(\mathbf{x},\mathbf{p}) + \sinh(\beta\Delta)\rho_{12}^{\mathrm{el}}(\mathbf{x},\mathbf{p})] \\ &\quad -W_\beta^-(\mathbf{Q},\mathbf{P})[\sinh(\beta\Delta)\rho_{21}^{\mathrm{el}}(\mathbf{x},\mathbf{p}) + \cosh(\beta\Delta)\rho_2^{\mathrm{el}}(\mathbf{x},\mathbf{p})]\Big\} \\ &\quad \left[\rho_1^{\mathrm{el}}(\mathbf{x}_t,\mathbf{p}_t) - \rho_2^{\mathrm{el}}(\mathbf{x}_t,\mathbf{p}_t)\right]. \end{aligned} \tag{4.69}$$

Eqs. (4.59) and (4.69) are the final LSC-IVR expressions for $D(t)$ and $C(t)$.

For comparison, Stock[101] recently carried out calculations for $D(t)$ using the mixed quantum-classical/SC-TDSCF approach, where the electronic transition between the two level system is treated quantum mechanically but the bath is treated classically. This approximation gives $D(t)$ in a form similar to Eq. (4.59),

$$D(t) = \frac{1}{2\pi}\int_0^{2\pi}d\theta\int d\mathbf{Q}_0 d\mathbf{P}_0 W_\beta^+(\mathbf{Q}_0,\mathbf{P}_0)\left[\rho_1^{\mathrm{TDSCF}}(\mathbf{x}_t,\mathbf{p}_t) - \rho_2^{\mathrm{TDSCF}}(\mathbf{x}_t,\mathbf{p}_t)\right], \tag{4.70}$$

where $\rho_{1,2}^{\mathrm{TDSCF}}$ is the probability of being in state 1 or 2. In our language, these probability functions are

$$\rho_1^{\mathrm{TDSCF}}(\mathbf{x}_t, \mathbf{p}_t) - \rho_2^{\mathrm{TDSCF}}(\mathbf{x}_t, \mathbf{p}_t) = (x_{1_t}^2 + p_{1_t}^2 - x_{2_t}^2 - p_{2_t}^2). \tag{4.71}$$

and the initial conditions of the electronic trajectories are

$$\begin{aligned} x_{1_0} &= \cos(\theta), \\ p_{1_0} &= \sin(\theta), \end{aligned} \tag{4.72}$$

$$x_{2_0} = p_{2_0} = 0, \tag{4.73}$$

where the θ ranges from 0 to 2π. It is clear that this is very different from our present approach.

Figure 4.10 shows the decay of the time-dependent electronic population, $D(t)$, for a "coherent" (i.e., oscillatory) case, Figure 4.10a, and also an "incoherent" (non-oscillatory) one, Figure 4.10b. The LSC-IVR results are seen to be in excellent agreement with Makri *et al*'s[159] accurate quantum results, showing that the LSC-IVR captures the essential features of the dynamics in both these cases. This also makes it clear that the oscillatory nature in the coherent case (Figure 4.10a) is of classical rather than quantum mechanical origin. For stronger couplings, i.e., larger α, the LSC-IVR results begin to deviate somewhat from the quantum results, as shown in Figure 4.11. However, the differences are still modest, and the LSC-IVR is in somewhat better agreement with the quantum results than the mixed quantum-classical/SC-TDSCF results obtained by Stock.

Mak and Chandler[158] studied the behavior of the spin correlation function, $C(t)$, for a variety of different parameters and determined the boundary between coherent and incoherent behavior. Figure 4.12 shows the results obtained from the LSC-IVR expression, Eq. (4.69), for three coupling values that span this boundary. One observes reasonably good agreement of the LSC-IVR results with the correct quantum values in all these case. [The approximations made to the Boltzmann operator, Eqs. (4.63)–(4.66), to obtain the Wigner function for the operator in Eq. (4.62) thus apparently cause no significant error.] The results of the LSC-IVR are actually somewhat better than the "non-interacting blip approximation"[156] for treating the spin-boson problem.

If coupling to the bath is sufficiently large, then $C(t)$ exhibits exponential decay for the short time regime, i.e.,

$$C(t) \approx Ae^{-t/\tau}, \tag{4.74}$$

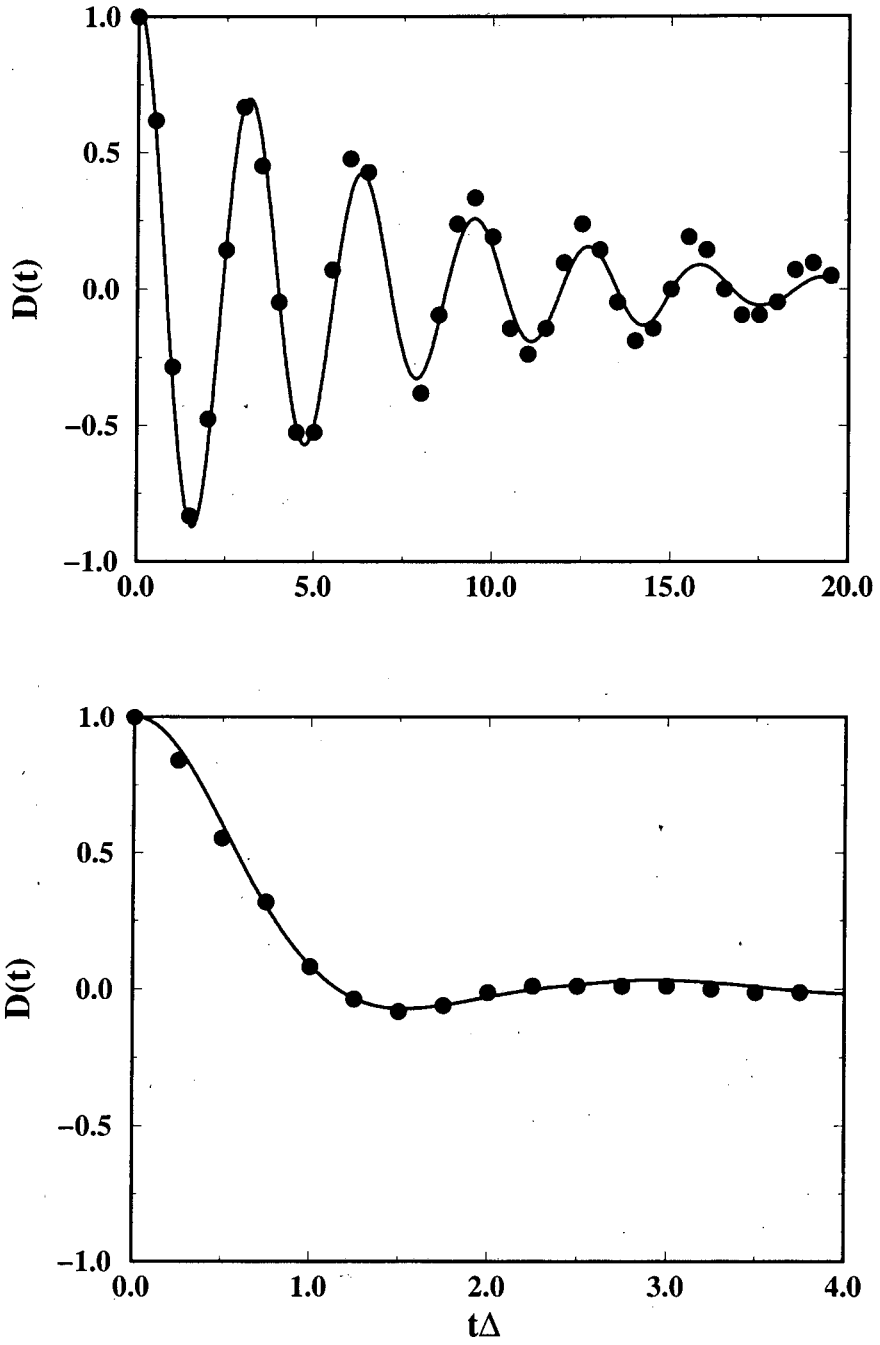

Figure 4.10: The time-dependent electronic population, $D(t)$, for two different parameter sets, showing (a) coherent oscillatory behavior and (b) incoherent relaxation behavior. The solid lines are the LSC-IVR results and the points are the exact path integral results. The cutoff frequency is $\omega_c = 2.5\Delta$. (a) $\alpha = 0.09$, $\beta\Delta = 5.0$. (b) $\alpha = 0.09$, $\beta\Delta = 0.1$.

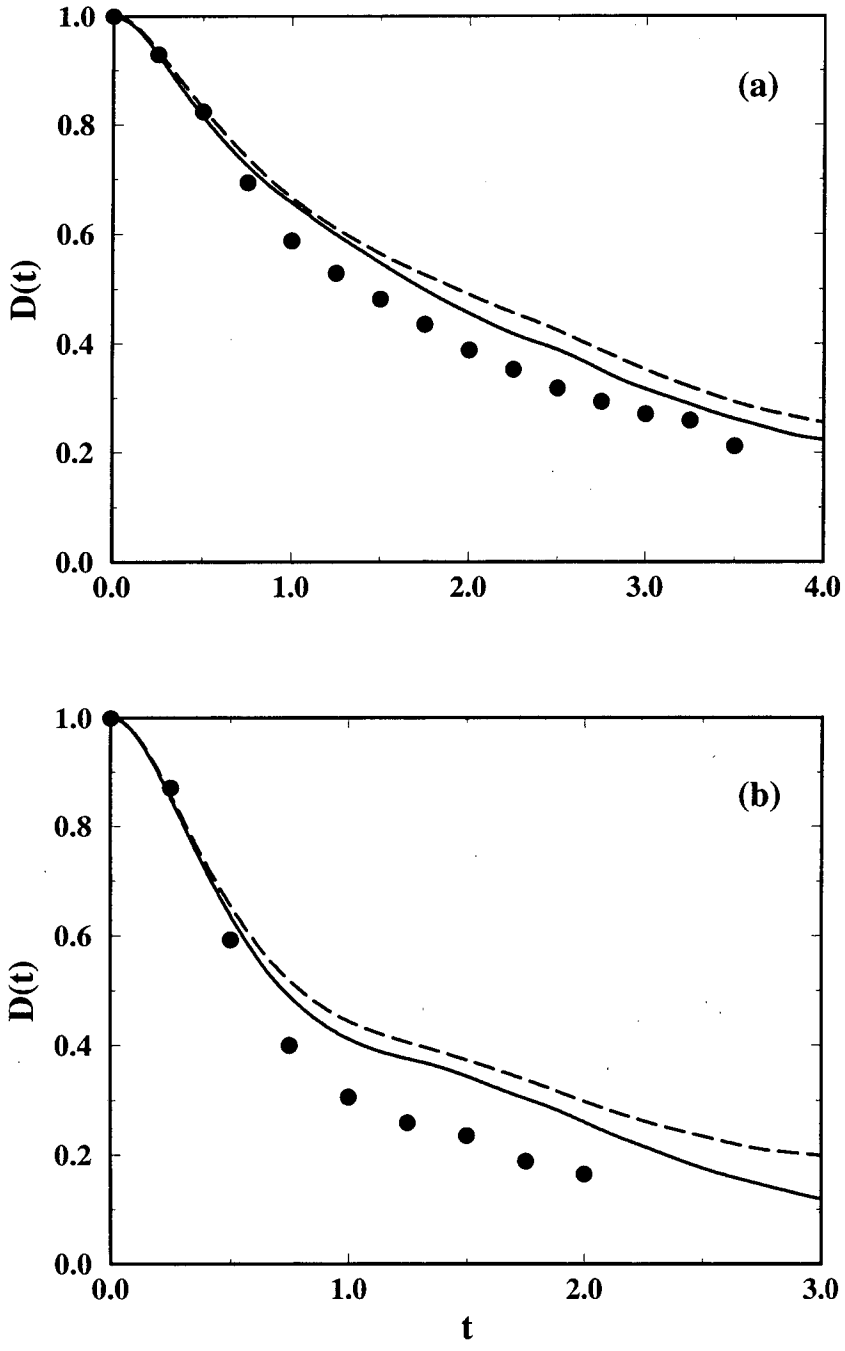

Figure 4.11: The time-dependent electronic population, $D(t)$, for higher coupling parameters, comparing the LSC-IVR results (solid line) and the mixed quantum-classical/SC-TDSCF results (dashed line) with the exact quantum results (points). $\alpha = 2.0$, $\omega_c = 1$ and $\beta = 0.25$. (a) $\Delta = 0.8$. (b) $\Delta = 1.2$.

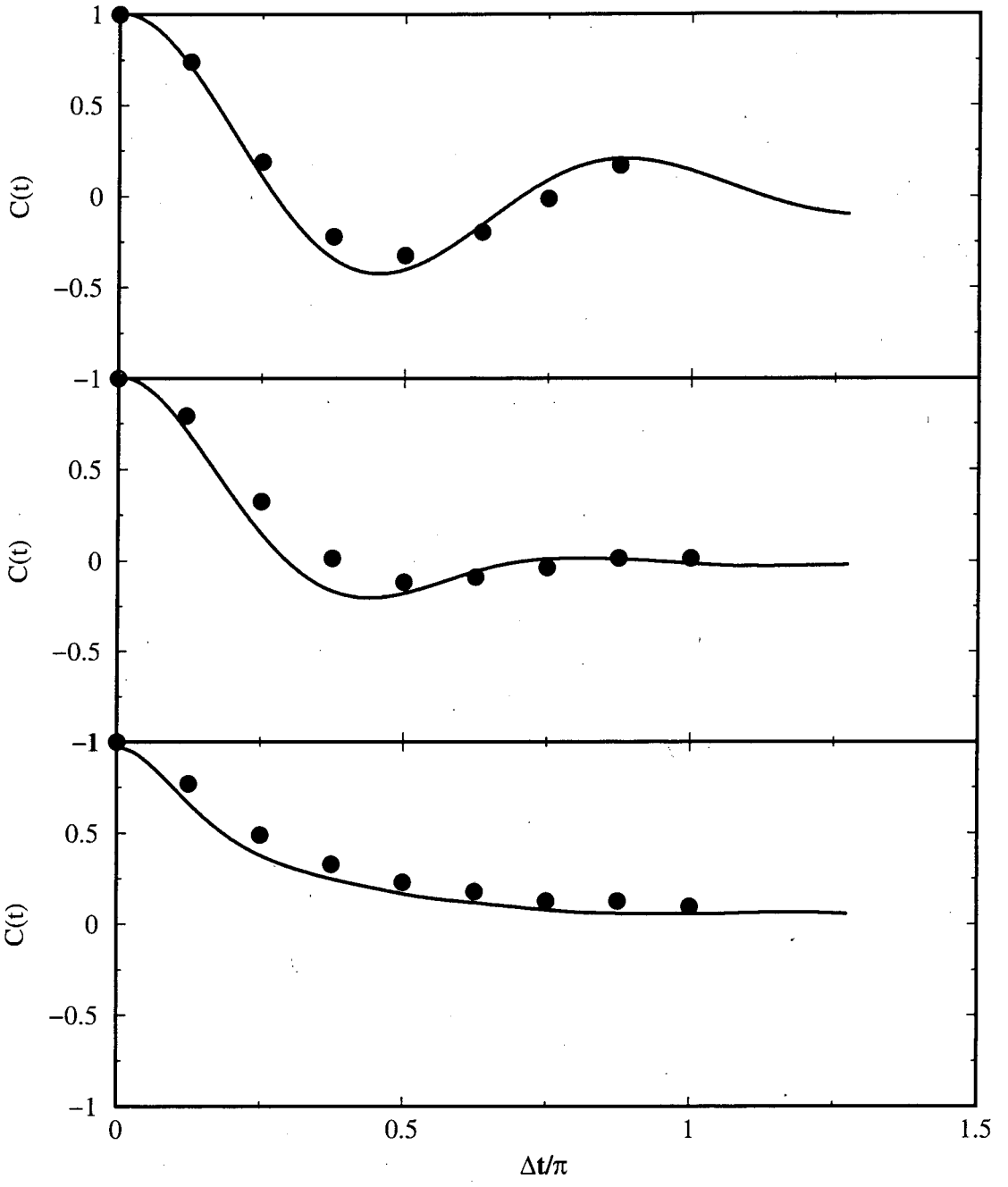

Figure 4.12: The spin correlation function, $C(t)$, for increasing values of the coupling, showing the transition from the coherent to incoherent relaxation. $\omega_c = 2.5\Delta$, $\beta = 2.5\Delta$. (a) In the coherent relaxation regime, $\alpha = 0.13$. (b) Near the coherent-incoherent boundary, $\alpha = 0.25$. (c) In the incoherent regime, $\alpha = 0.64$. The solid lines are the LSC-IVR results and the points are the exact path integral results.

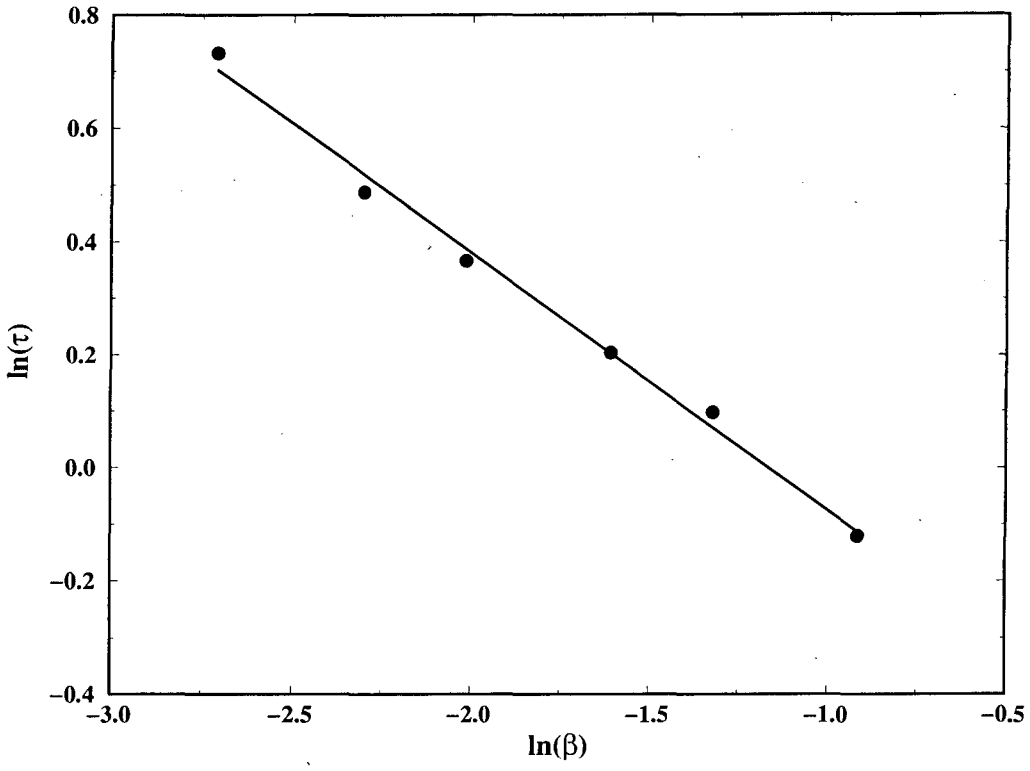

Figure 4.13: The temperature dependence of the short time relaxation constant (points) for the spin correlation function, $C(t)$, obtained with LSC-IVR. $\omega_c = 2.5\Delta$, $\alpha = 0.64$. The temperature dependence follows a inverse power-law, $\tau \approx T^{\delta}$, indicated by the fitted straight line. The LSC-IVR result for δ is 0.46.

so that one can define a rate constant τ^{-1} for transitions from one state of the two level system to the other. Figure 4.13 shows the results given by Eq. (4.69) for τ as a function of temperature for the parameters $\alpha = 0.64$, $\omega_c = 2.5\Delta$. The decay rate exhibits the correct inverse power-law dependence on temperature, $\tau \sim T^{\delta}$, and the LSC-IVR results are essentially in quantitative agreement with the exact results of Mak and Chandler. For higher coupling values, however, the procedure outlined in Eq. (4.63) to Eq. (4.66) for obtaining the Wigner transform involving the Boltzmann operator is not valid, so we will not consider this regime. One could, of course, carry out a more complete quantum calculation for the Boltzmann operator in order to obtain the Wigner function for the operator in Eq. (4.62), but this is not central to our present discussion of the LSC-IVR.

4.5 Concluding Remarks

We have presented a new analogue Hamiltonian for the dynamics of a N-level (electronic) system couple to other (nuclear) degrees of freedom. Electronic and nuclear degrees of freedom are thus treated on the same dynamical footing. Two limits of this model are discussed.

In the semiclassical limit, application of the approach to a variety of test problems shows it to provide a good description of non-adiabatic transitions in essentially all these cases. The only difficulties were seen at low energies, where the SC-IVR approach has had difficulties in the past for treating nuclear dynamics even on one potential surface. We believe that this model has a great deal of potential for providing a realistic and accurate description of electronically non-adiabatic dynamics in a variety of situations. Although the applicability of the SC-IVR to these problems will depend on the proper evaluation of the IVR integral.

In the classical limit, we have utilized the LSC-IVR theory of chapter 3 for nonadiabatic dynamics. The LSC-IVR is much easier to apply than the full SC-IVR: as seen from the resulting expressions [Eq. (3.62) and (3.67)], it involves the overlap of the Wigner distribution function for the initial state (or operator) with the classically time-evolved Wigner distribution for the final state (or operator). The actual dynamics in the LSC-IVR is thus completely classical, the Wigner distribution functions, however, effectively providing the quantum boundary conditions for the classical trajectories.

The LSC-IVR is seen to provide a reasonably good description of the three nonadiabatic scattering problems studied by Tully, including the effects of Stuckelberg oscillations (interference between nonadiabatic transitions at different times). It also provides a good description of time-dependent transition probabilities in the spin-boson problem (2 electronic states coupled to an infinite set of harmonic oscillators), including both coherent and incoherent decay and the transition between them. Altogether, this suggests that the LSC-IVR should be useful for simulating a wide range of nonadiabatic dynamic phenomenon in "real" molecular systems.

Chapter 5

Thermal Rate Constants

5.1 Introduction

The thermal rate constant, $k(T)$, has been a central topic of theoretical chemistry for almost a century.[131] The classic theory of the rate constant is the transition state theory (TST). Even though it based on classical mechanics and invented with equilibrium assumptions, it is still used by chemists in various forms for a wide variety of reactions. The rigorous quantum mechanical theory of reaction rates was proposed much later,[160,126] and only in recent years, has considerable progress been made in the development of quantum mechanical methods for the efficient calculation of rate constants for chemical reactions in small molecular systems.[161–172] Currently, essentially exact rate constants (for a given potential) can be obtained for a small group of reactions.

One of the original formulation[126] of these theories expresses the thermal rate constant as

$$k(T) = Q_r(T)^{-1} \lim_{t\to\infty} C_{fs}(t), \tag{5.1}$$

where $Q_r(T)$ is the reactant partition function (per unit volume for a bimolecular reaction) and $C_{fs}(t)$ is the "flux-side" correlation function,[173]

$$C_{fs}(t) = \mathrm{tr}\left[\hat{F}(\beta)\hat{h}(t)\right]; \tag{5.2a}$$

here $\hat{F}(\beta)$ is a combination of the flux operator $\hat{F}$ and the Boltzmann operator $\exp(-\beta\hat{H})$, often taken in the following symmetrized form[173]

$$\hat{F}(\beta) = e^{-\beta\hat{H}/2}\hat{F}e^{-\beta\hat{H}/2}, \tag{5.2b}$$

and $\hat{h}(t)$ is a time-evolved projection operator,

$$\hat{h}(t) = e^{i\hat{H}t/\hbar}\hat{h}e^{-i\hat{H}t/\hbar}, \tag{5.2c}$$

where $h(\mathbf{q})$ is a function of coordinates that is 1(0) on the product (reactant) side of the dividing surface separating the two. [$\hat{H}$ is the Hamiltonian operator of the molecular system and $\beta = (k_B T)^{-1}$.] Recently, applications have also focused on the flux-flux correlation function expression of the rate constant,

$$k(T) = Q_r(T)^{-1} \int_0^\infty dt C_{ff}(t), \tag{5.3a}$$

where

$$C_{ff}(t) = \mathrm{tr}[\hat{F}(\beta)\hat{F}(t)]. \tag{5.3b}$$

Eqs. (5.1) and (5.3a) are really identical because

$$\hat{F} = \frac{i}{\hbar}[\hat{H}, h(\hat{\mathbf{q}})]. \tag{5.3c}$$

The efficiency of the these approaches is primarily due to the fact that they focus directly on the rate constant and avoid dealing with the complete state-to-state reactive scattering problem. A variety of applications have been carried out for reactions of 3- and 4-atom molecular systems.[161–172]

The classical analog[174] of Eqs.(5.1)-(5.3a) has been widely used for treating reactions in condensed phases, and it is our goal to develop the quantum version of the theory to be able to describe quantum effects in such systems, e.g., reactions in solutions, clusters, biological environments, or on surfaces. Quantum effects tend to be averaged out in complex systems, but processes that involve the motion of hydrogen atoms — e.g., OH vibrations or bond-breaking, H_2O re-orientation, hydrogen bonding, and obviously electronically non-adiabatic processes (in photochemistry) — may often be poorly described by classical molecular dynamics. Furthermore, one can never know the extent to which quantum effects are significant without having a theoretical approach capable of describing them.

One strategy for doing this is to treat only a few degrees of freedom by quantum mechanics and the (many) others by classical mechanics, i.e., the popular mixed quantum-classical (Ehrenfest) model that has been widely used but which can have problems.[117] The alternative approach that we have been discussing in this thesis is the semiclassical (SC)

approximation to the rigorous quantum dynamics and the semiclassical initial value representation which is a potentially efficient way of implementing semiclassical approximations. Within the framework of the SC-IVR, we[134] have shown in chapter 3 how one can degenerate the description of *some* degrees of freedom to the classical level while still retaining the full semiclassical description of the rest — i.e., a mixed *semiclassical*-classical treatment (cf. chapter 3). Ovchinnikov and Apkarian[175–177] have independently used this idea very effectively in applications to vibrational relaxation processes in clusters and liquids.

The purpose of this chapter is to investigate the possibility of applying the semiclassical initial value representation and the much simpler linearized approximation to the flux-side correlation function of Eq. (5.1) and to see the extent to which they are able to describe quantum interference/coherence effects in thermal rate constants. First, we seek to determine the usefulness and limitations of the linearized approximation of the full SC-IVR, and the example we study is the application of LSC-IVR to an isomerization reaction model where a double well is coupled to an infinite bath of harmonic oscillators. This model allows us to compare the results to the exact quantum mechanical calculation of Topaler and Makri.[114] The LSC-IVR, however, is not able to describe quantum effects for longer times, therefore the full SC-IVR must be employed when we omit the harmonic bath and consider the 1-d double well potential by itself, a model of unimolecular isomerization of a isolated molecule. In this second example case, $C_{fs}(t)$ does not reach a limiting value as $t \to \infty$ [cf. Eq. (5.1)], i.e., $k(T)$ does not exist, for the particle oscillates back and forth in the double well forever. The dynamics of this coherent motion, as it manifests itself in the correlation function $C_{fs}(t)$, however, is precisely the phenomenon we are seeking to investigate, so it is an ideal test case for these purposes. Lastly, the forward-backward IVR of chapter 3 is also applied to the calculation of rate constants to see its accuracy in retaining the quantum mechanical interference and coherence effects in several model systems. The FB-IVR not only allows us to reduce the number of integrals we need to evaluate, oscillatory behavior that is difficult for the standard SC-IVR may also be ameliorate somewhat.

Of previous work, some of the discussion in this chapter is related to that of Voth, Chandler and Miller,[178] who used Eq. (5.1) with various approximations for the time-dependent factor $\hat{h}(t)$, applied to barrier crossing dynamics (but not the longer time coherence effects investigated here). Pollak *et al.*[119,120] independently used an approximate form of our linearized approximation for the rate constant and called it a quantum transition state theory.

5.2 Quantum Mechanical Thermal Rate Constant

For later theoretical development however, a more convenient starting point is the integrated form of the rate formula,

$$\begin{aligned} k(T) &= Q_r(T)^{-1} \lim_{t\to\infty} C_{fs}(t) \\ &= Q_r(T)^{-1} \lim_{t\to\infty} \mathrm{tr}[\hat{F}(\beta) e^{i\hat{H}t/\hbar} \hat{h} e^{-i\hat{H}t/\hbar}], \end{aligned} \tag{5.4}$$

where $\hat{F}(\beta)$ is formally $e^{-\beta\hat{H}}\hat{F}$, but since $e^{-\beta\hat{H}}$ commutes with $e^{i\hat{H}t/\hbar}\hat{h}e^{-i\hat{H}t/\hbar}$, we can write it as

$$\hat{F}(\beta) = e^{-(\beta-\lambda)\hat{H}} \hat{F} e^{-\lambda\hat{H}}, \tag{5.5}$$

where λ is a number between 0 and β. If $\lambda = \beta/2$, then we arrive at the symmetric form of the Boltzmannized flux operator [Eq.(5.2b)] which has been used extensively in the fully quantum mechanical evaluation of the rate constant. Here, since the rate constant does not depend on the value of λ, we can write it as,

$$\hat{F}(\beta) = \frac{1}{\beta} \int_0^\beta e^{-(\beta-\lambda)\hat{H}} \hat{F} e^{-\lambda\hat{H}} d\lambda, \tag{5.6}$$

and insert in the commutator form of the flux operator from Eq. (5.3c) to obtain

$$\begin{aligned} \hat{F}(\beta) &= \frac{i}{\beta\hbar} \int_0^\beta e^{-(\beta-\lambda)\hat{H}} \left[\hat{H}, \hat{h}\right] e^{-\lambda\hat{H}} d\lambda \\ &= \frac{i}{\beta\hbar} \int_0^\beta \frac{d}{d\lambda} \left(e^{-(\beta-\lambda)\hat{H}} \hat{h} e^{-\lambda\hat{H}} \right) d\lambda. \end{aligned} \tag{5.7}$$

The final result of all this is that the Boltzmannized flux operator can be written in the so called Kubo form,

$$\hat{F}(\beta) = \frac{i}{\beta\hbar} \left[\hat{h}e^{-\beta\hat{H}} - e^{-\beta\hat{H}}\hat{h}\right]. \tag{5.8}$$

Formally, these expressions all give the correct rate constants. For the semiclassical approximations in the next section, the Kubo version will be more convenient.

5.3 Linearization Approximation for Thermal Rate Constants

Before proceeding with a fully semiclassical theory of thermal rate constants, it is useful to first examine the more approximate LSC-IVR of chapter 3. The application of

the LSC-IVR expression of Eq. (3.67) to the flux-side correlation function of Eq. (5.1) thus gives

$$C_{fs}(t) = \frac{1}{(2\pi\hbar)^F} \int d\mathbf{q}_0 \int d\mathbf{p}_0 \; F_w^\beta(\mathbf{q}_0, \mathbf{p}_0) h(\mathbf{q}_t), \tag{5.9}$$

where $F_w^\beta(\mathbf{q}_0, \mathbf{p}_0)$ is the Wigner transform of the Boltzmannized flux operator,

$$F_w^\beta(\mathbf{q}, \mathbf{p}) = \int d\Delta\mathbf{q} \, e^{-i\mathbf{p}\cdot\Delta\mathbf{q}/\hbar} \langle \mathbf{q} + \Delta\mathbf{q}/2 | \hat{F}(\beta) | \mathbf{q} - \Delta\mathbf{q}/2 \rangle, \tag{5.10}$$

and $h(\mathbf{q}_t)$ is the only qunatity that depends on time. It should be immediately apparent how simple Eq. (5.9) is: it is essentially a classical trajectory calculation with the distribution of initial conditions given by the Wigner transform $F_w^\beta(\mathbf{q}_0, \mathbf{p}_0)$ rather than by its classical limit,

$$F_w^\beta(\mathbf{q}_0, \mathbf{p}_0) \overset{\text{CL}}{\to} e^{-\beta H(\mathbf{q}_0, \mathbf{p}_0)} \frac{\partial h(\mathbf{q}_0)}{\partial \mathbf{q}_0} \cdot \frac{\mathbf{p}_0}{m}. \tag{5.11}$$

As discussed in detail earlier in chapter 3, however, this linearization approximation produces only *classical* mechanics in the real time dynamics, with no quantum interference effects [cf. the classical time-dependent factor $h(\mathbf{q}_t)$ in Eq. (5.9)]. The only quantum effects in Eq. (5.9) are from the quantum treatment of the Boltzmannized flux operator and the Wigner transform of it. The consequences of this will be seen in the results discussed in section (5.4.2), where $C_{fs}(t)$ of Eq. (5.9) is observed to be accurate only for times up to $\approx \hbar\beta$. This is long enough, however, if the dynamics is simple barrier crossing, with no re-crossings involved, as in the assumption of transition state theory. Pollak *et al.*[119,120] have in fact used Eq. (5.9) (with an approximation to the classical time-dependent factor) to define a quantum transition state theory and seen it to work well for examples involving only direct barrier crossing dynamics.

5.3.1 Application to Isomerization Reaction in Condensed Phase

As we pointed out in chapter 3, the linearized approximation neglects all quantum mechanical interference effects and only retains a classical description of the problem. It was also argued that for complex systems with many degrees of freedom, the interference between the various trajectories may average out so that the only contribution comes from classical mechanics. This scenario is difficult to test since one would have to compare exact quantum mechanical results with the linearized approximation results. However, there is a case where this direct comparison can be made. For the problem of a small system linearly coupled to an infinite bath of *harmonic* oscillators, Feynman's influence functional

approach[179] allows one to "integrate out" the bath and perform essentially exact quantum mechanical calculation on the system-bath dynamics. One recent example of this application is for a double well potential coupled to an infinite bath of harmonic oscillators. This model frequently referred to as a model of unimolecular isomerization reaction in the condensed phase.

The system-bath Hamiltonian is for this model is

$$H = \frac{p_s^2}{2m_s} + V(s) + \sum_i \frac{P_i^2}{2m_i} + \frac{1}{2}m_i\omega_i^2\left(Q_i - \frac{c_i s}{m_j\omega_i^2}\right)^2, \tag{5.12a}$$

where (s, p_s) are the coordinate and momentum of the system and $(\mathbf{Q}, \mathbf{P})$ are the coordinates and momenta of the bath. The essential property of the harmonic bath is its spectral density

$$J(\omega) = \frac{\pi}{2}\sum_i \frac{c_i^2}{m_i\omega_i}\delta(\omega_i - \omega), \tag{5.12b}$$

which is chosen in the continuous Ohmic form with an exponential cutoff

$$J(\omega) = \eta\omega e^{-\omega/\omega_c}, \tag{5.12c}$$

where the cutoff frequence ω_c is chosen as 500 cm^{-1}. $V(s)$ is the 1-d double well potential

$$\begin{aligned} V(s) &= -a_1 s^2 + a_2 s^4 \\ &= -\frac{1}{2}m_s\omega_b^2 s^2 + \frac{m_s^2\omega_b^4}{16V_0^\dagger}, \end{aligned} \tag{5.12d}$$

where ω_b is the imaginary harmonic frequence at the top of the barrier, and $V_0^\dagger$ is the barrier height with respect to the bottom of the well. The specific parameters we have chosen correspond to the DW1 potential of Topaler and Makri[114] who performed the exact quantum calculations that will serve as a bench mark for our comparison below. The barrier height and the imaginary frequency for the DW1 potential are 2085 and 500 cm^{-1}, respectively, and the mass of the system is that of a proton. 300 bath modes are sufficient for an adequate description of the bath.

The evaluation of Eq. (5.9) thus reduces to starting classical trajectories with initial condition determined by the probability distribution $F_w^\beta(\mathbf{p}_0, \mathbf{q}_0)$. However, the exact evaluation of $F_w^\beta(\mathbf{p}_0, \mathbf{q}_0)$ is difficult. To circumvent this, we have used a normal mode approximation for the Hamiltonian around the barrier,

$$H \approx \frac{p^2}{2m_f} - \frac{1}{2}m_f\lambda^{\dagger 2}q_f^2 + V_0^\ddagger + \sum_i \frac{p_i^2}{2m_i} + \frac{1}{2}m_i\lambda_i^2 q_i^2 \tag{5.13}$$

where $\lambda^\dagger$ and λ_i are the imaginary and real frequencies at the saddle point and (q_f, p_f) and (q_i, p_i) are the corresponding coordinates and momenta, respectively. The flux operator involves only the reaction coordinate q_f and therefore the Wigner transformation of $\hat{F}_\beta$ is separable.

$$F_w^\beta(\mathbf{q},\mathbf{p}) = \bar{F}_w^\beta(q_f,p_f)\rho_w^\beta(\mathbf{q}_b,\mathbf{p}_b), \tag{5.14a}$$

where

$$\begin{aligned}\bar{F}_w^\beta(q_f,p_f) &= \left(\frac{\lambda^\dagger}{m_f\pi\hbar}\right)^{\frac{1}{2}} \frac{2p_f\tan(u^\dagger)}{\sin(2u^\dagger)} \exp\left[-\frac{m_f\lambda^\dagger}{\hbar}\cot(u^\dagger)q_f^2\right. \\ &\quad \left. - \frac{p_f^2}{m_f\lambda^\dagger\hbar}\tan(u^\dagger)\right] e^{-\beta V_0^\dagger},\end{aligned} \tag{5.14b}$$

and

$$\rho_w^\beta(\mathbf{q}_b,\mathbf{p}_b) = \prod_i \frac{\tanh(u_i)}{\sinh(u_i)} \exp\left[-\frac{2\tanh(u_i)}{\lambda_i\hbar}\left(\frac{p_i^2}{2m_i} + \frac{1}{2}m_i\lambda_i^2 q_i^2\right)\right], \tag{5.14c}$$

and $u^\dagger = \hbar\beta\lambda^\dagger/2$ and $u_i = \hbar\beta\lambda_i/2$. Eq. (5.14) thus provides a simple analytic result for the Wigner function of the Boltzmannized flux operator within the normal mode approximation. Note that although the quadratic approximation is used for $F_w^\beta(\mathbf{q},\mathbf{p})$, the trajectory themselves are computed with the exact Hamiltonian.

Due to the properties of the parabolic barrier approximation, Eq. (5.14b) is only valid when $u^\dagger < \pi/2$ or $T > T_c = \hbar\lambda^\dagger/\pi k_B$. Furthermore, for temperatures slightly above T_c, the coordinate distribution in Eq. (5.14b) is so broad that the quadratic approximation to the potential may fail. Higher order expansions around the saddle point are then needed to account for the anharmonic effects. Wigner transformations, for most cases, can only be done numerically for 1-d system and therefore including these anharmonic effects is more difficult. Nevertheless, applications of the system-bath separation ideas where the system coordinate is treated more exact and the bath is treated more approximately for calculating the Wigner function perhaps has more practical utility. In the next section, another approximate way of obtaining rate constants below T_c will also be discussed.

The "transition state" limit of Eq. (5.9), i.e., taking $h(\mathbf{q}_t)$ to be $h(\mathbf{q}_0)$ is what Pollak et al.[119,120] has called a quantum transition state theory. In the case of 1-d parabolic barrier, the rate constant

$$k(T) = Q_r^{-1}(T) = \int dp_0 \int dq_0 h(q_0)\bar{F}_w^\beta(p_0,q_0), \tag{5.15}$$

can be calculated analytically to give

$$k(T)Q_r^{-1}(T) = \kappa \frac{1}{\hbar\beta} e^{-\beta V_0^\dagger}, \tag{5.16}$$

where

$$\kappa = \frac{\hbar\beta\lambda^\dagger}{2\sin(\hbar\beta\lambda^\dagger/2)}, \tag{5.17}$$

which is recognized to be this exact result for the parabolic barrier.

Application of Eqs. (5.9) and (5.14) to the system-bath model of Eq. (5.12) is straightforward. Calculations are performed as a function of the coupling parameter η at two temperatures, 200K and 300K. At $T = 300K$, the temperature is sufficiently above T_c for all η's of interest that the harmonic approximation of Eq. (5.14) gives accurate results for the Wigner distribution function. 3000 trajectories are needed to obtain converged results. For 200K, however, the temperature is below or near T_c in the small η regime and Eq. (5.14) is no longer valid. Therefore, diagonal anharmonicity, i.e., numerical evaluation of the Wigner distribution function along the reaction coordinate, is employed for this case.

The results are plotted in Figure 5.1 as the transmission coefficient, κ, defined by

$$\kappa = k(T)/k_{\mathrm{TST,CL}}(T) \tag{5.18}$$

where

$$k_{\mathrm{TST,CL}}(T) = \frac{\omega_0}{2\pi} e^{-\beta V_0^\dagger}, \tag{5.19}$$

with ω_0 being the frequency of the reactant well in Eq. (5.12d). Figure 5.1a shows the results for $T = 300K$ for which there is quantitative agreement with the accurate quantum results of Topaler and Makri.[114] The $T = 200K$ results are shown in Figure 5.1b and though it is not completely quantitative, the results are still excellent for this quite practical approach. To gain some insight into the nature of the dynamics, Figure 5.2 shows the time dependence of $\kappa(t)$ which is related to the correlation function by

$$\kappa(t) = (Q_r k_{\mathrm{TST,CL}})^{-1} C_{fs}(t), \tag{5.20}$$

at $T = 300K$ for a case of strong coupling (Figure 5.2a) and also one of weak coupling (Figure 5.2b). The long time limit of $\kappa(t)$ would be the quantum transmission coefficient defined in Eq. (5.18). Figure 5.2a is a classic example of "direct" barrier crossing dynamics for which quantum transition state theory is a good approximation. As seen in many of the previous applications, it takes time of $\sim \hbar\beta$ (27fs at $300K$) for $\kappa(t)$ to reach its transition

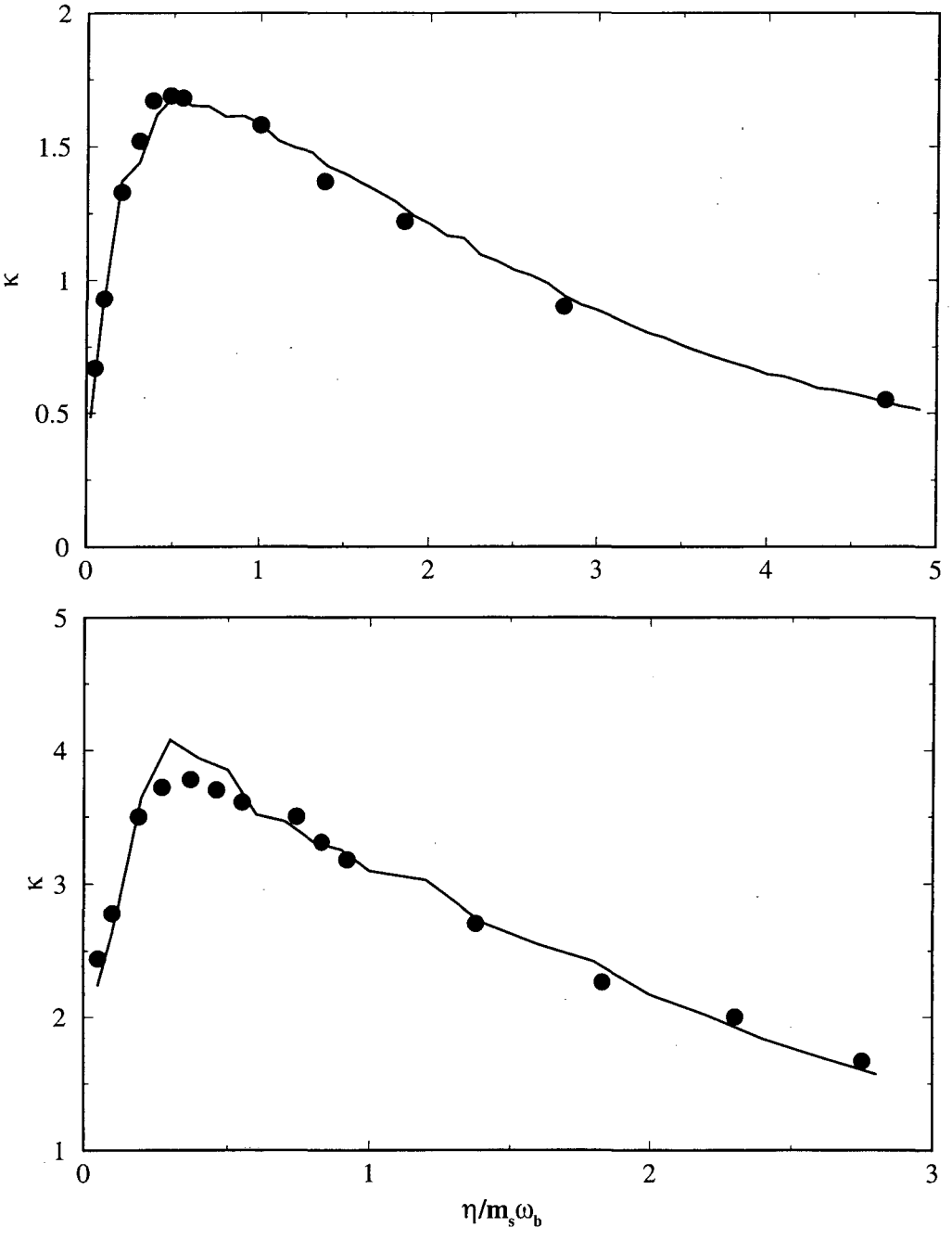

Figure 5.1: The transmission coefficient $\kappa = k/k_{\mathrm{TST,CL}}$ as a function of coupling parameter $\eta/m_s\omega_b$. The solid lines are the results of the linearized approximation of Eq. (2.57) and the points are from the quantum path integral calculation of Topaler and Makri.[114] (upper panel) T=300K; (lower panel) T=200K.

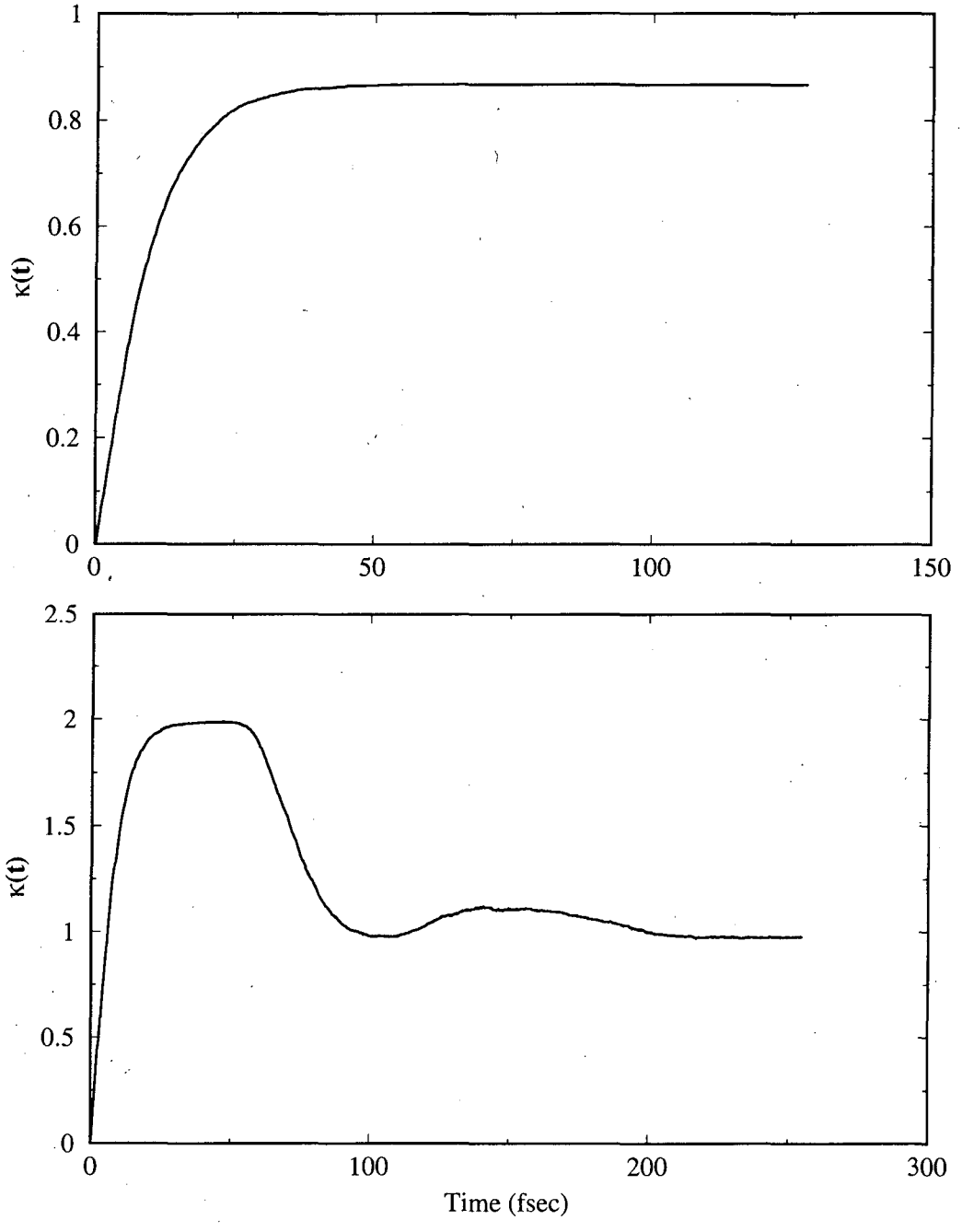

Figure 5.2: The time dependence of $\kappa(t)$ for two cases at T=300K. (upper panel) strong coupling; (lower panel) weak coupling.

state theory (TST) "plateau" value and there is no hint of recrossing dynamics in this case. Figure 5.2b, on the other hand, shows strong characteristic of recrossing: by $\hbar\beta$ =27 fs $\kappa(t)$ has reached its TST plateau value, but here the coupling to the bath is not strong enough to prevent trajectories from recrossing the dividing surface before the $t \rightarrow \infty$ limit of the correlation function is reached. It is impressive that the approximate theory of Eq. (5.9) is able to describe both of these situations accurately.

The good agreement here between the linearized approximation of Eq. (5.9) and the exact quantum mechanical results for this system-bath example confirms our earlier conjecture that for complex systems, the quantum mechanical interference effects, essentially all the oscillatory terms in Eq. (3.84d) have averaged out. Therefore the linearized approximation, which does give the correct quantum results for short times, should be able to capture most of the dynamics in these systems of many degrees of freedom. Coupled with its calculational ease of use, it should be a very practical theory for many problems.

5.3.2 Analytically Continued Rate Constants with the Linearized Approximation

The harmonic approximation for the Wigner function of the Boltzmannized flux operator is very convenient for any practical calculations of the rate constant. But, as was mentioned, for temperatures below $T_c = \hbar\lambda^\dagger/\pi k_B$, this approximation is not valid and one has to resort to a fully quantum mechanical calculation of the Wigner function. A possible way of circumventing this is to proceed with an analytic continuation approach where the flux side correlation function in Eq. (5.2a) is rewritten as

$$\begin{aligned} C_{fs}(t) &= \mathrm{tr}[e^{-\beta\hat{H}/2}\hat{F}e^{-\beta\hat{H}/2}e^{i\hat{H}t/\hbar}\hat{h}e^{-i\hat{H}t/\hbar}] \\ &= \mathrm{tr}[e^{-\beta_0\hat{H}/2}\hat{F}e^{-\beta_0\hat{H}/2}e^{i\hat{H}t/\hbar-\beta_1\hat{H}/2}\hat{h}e^{-i\hat{H}t/\hbar-\beta_1\hat{H}/2}]; \end{aligned} \tag{5.21}$$

here $\beta_0 + \beta_1 = \beta$. The expressions in Eq. (5.21) are identical, but one sees that $C_{fs}(t)$ can now be written as

$$C_{fs}(t) = C_{fs}(\beta_0, \beta_1; t) = C_{fs}(\beta_0, t_1 = i\hbar\beta_1/2; t) \tag{5.22}$$

where

$$C_{fs}(\beta_0, t_1; t) = \mathrm{tr}[e^{-\beta_0\hat{H}/2}\hat{F}e^{-\beta_0\hat{H}/2}e^{i\hat{H}(t+t_1)/\hbar}\hat{h}e^{-i\hat{H}(t-t_1)/\hbar}]. \tag{5.23}$$

Thus, C_{fs} is the analytic continuation of $C_{fs}(\beta_0, t_1; t)$ into the complex plane, the assumption being $C_{fs}(\beta_0, t_1; t)$ does not have any singularities.

Now, a linearized approximation can be made to the correlation function in Eq. (5.23). We proceed in the standard way, after inserting the SC-IVR expression of Eq. (2.9), this correlation function becomes,

$$\begin{aligned} C_{fs}(\beta_0,t,t') &= (2\pi\hbar)^{-F}\int d\mathbf{p}_0 d\mathbf{q}_0 \int d\mathbf{p}_0' d\mathbf{q}_0' \langle \mathbf{q}_0|\hat{F}(\beta_0)|\mathbf{q}_0'\rangle \left[\det(\mathbf{M_{qp}}\cdot\mathbf{M'_{qp}})\right]^{\frac{1}{2}} \\ &\quad \exp\left[\frac{i}{\hbar}S_t(\mathbf{p}_0,\mathbf{q}_0) - S_{t'}(\mathbf{p}_0',\mathbf{q}_0')\right]\delta(\mathbf{q}_t-\mathbf{q}_{t'})h(\mathbf{q}_t), \end{aligned} \tag{5.24}$$

where $t = t - t_1$, $t' = t + t_1$, $\mathbf{M_{qp}} = \partial\mathbf{q}_t/\partial\mathbf{p}_0$, $\mathbf{M'_{qp}} = \partial\mathbf{q}_{t'}/\partial\mathbf{p}_0'$, $\mathbf{q}_t = \mathbf{q}_t(\mathbf{p}_0,\mathbf{q}_0)$ and $\mathbf{q}_t' = \mathbf{q}_t(\mathbf{p}_0',\mathbf{q}_0')$. Again making the sum and difference transformation as in Eq. (3.56c), and assuming that

$$\mathbf{M_{qp}} = \frac{\partial\mathbf{q}_t}{\partial\mathbf{p}_0} \approx \frac{\partial\bar{\mathbf{q}}_t}{\partial\bar{\mathbf{p}}_0}, \tag{5.25a}$$

$$\mathbf{M'_{qp}} = \frac{\partial\mathbf{q}_{t'}}{\partial\mathbf{p}_0'} \approx \frac{\partial\bar{\mathbf{q}}_{t'}}{\partial\bar{\mathbf{p}}_0}, \tag{5.25b}$$

we can now expand the phase difference in the exponential as

$$\begin{aligned} S_t(\mathbf{p}_0,\mathbf{q}_0) - S_{t'}(\mathbf{p}_0',\mathbf{q}_0') &= S_t(\bar{\mathbf{p}}_0,\bar{\mathbf{q}}_0) - S_{t'}(\bar{\mathbf{p}}_0,\bar{\mathbf{q}}_0) - \bar{\mathbf{p}}_0\Delta\mathbf{q} \\ &+ \frac{1}{2}\left[\bar{\mathbf{p}}_t^T\cdot\mathbf{M_{qq}} + \bar{\mathbf{p}}_{t'}^T\cdot\mathbf{M'_{qq}}\right]\cdot\Delta\mathbf{q} \\ &+ \frac{1}{2}\left[\bar{\mathbf{p}}_t^T\cdot\mathbf{M_{qp}} + \bar{\mathbf{p}}_{t'}^T\cdot\mathbf{M'_{qp}}\right]\cdot\Delta\mathbf{p}, \end{aligned} \tag{5.25c}$$

and the delta function becomes

$$\delta(\mathbf{q}_t-\mathbf{q}_{t'}) = \delta\left[\bar{\mathbf{q}}_t - \bar{\mathbf{q}}_{t'} + \frac{1}{2}(\mathbf{M_{qq}}+\mathbf{M'_{qq}})\cdot\Delta\mathbf{q} + \frac{1}{2}(\mathbf{M_{qp}}+\mathbf{M'_{qp}})\cdot\Delta\mathbf{p}\right]. \tag{5.25d}$$

The integrals over $\Delta\mathbf{q}$ and $\Delta\mathbf{p}$ can now be performed, the steps are analogous to the manipulations in section 3.2.1 for the mixed semiclassical-classical theory. The end result is that Eq. (5.24) becomes

$$\begin{aligned} C_{fs}(\bar{\beta},t,t') &= (2\pi\hbar)^{-F}\int d\mathbf{p}_0 d\mathbf{q}_0 \frac{\left[\det(\mathbf{M_{qp}}\cdot\mathbf{M'_{qp}})\right]^{\frac{1}{2}}}{\frac{1}{2}\det(\mathbf{M_{qp}}+\mathbf{M'_{qp}})} e^{i[S_t(\mathbf{p}_0,\mathbf{q}_0)-S_{t'}(\mathbf{p}_0,\mathbf{q}_0)]/\hbar} F_w^{\beta_0}(\tilde{\mathbf{p}}_0,\mathbf{q}_0) \\ &\quad \exp\frac{i}{\hbar}\left[(\mathbf{p}_t\cdot\mathbf{M_{qp}}+\mathbf{p}_{t'}\cdot\mathbf{M'_{qp}})\cdot(\mathbf{M_{qp}}+\mathbf{M'_{qp}})^{-1}\cdot(\mathbf{q}_{t'}-\mathbf{q}_t)\right]h(\mathbf{q}_t), \end{aligned} \tag{5.26a}$$

where the bars over $(\mathbf{p}_0,\mathbf{q}_0)$ have been dropped and

$$\begin{aligned} \tilde{\mathbf{p}}_0 &= \mathbf{p}_0 + \frac{1}{2}\left[(\mathbf{p}_t\cdot\mathbf{M_{qp}}+\mathbf{p}_{t'}\cdot\mathbf{M'_{qp}})\cdot(\mathbf{M_{qp}}+\mathbf{M'_{qp}})^{-1}\cdot(\mathbf{M_{qq}}+\mathbf{M'_{qq}})\right] \\ &\quad -\frac{1}{2}\left[\mathbf{p}_t\cdot\mathbf{M_{qq}}+\mathbf{p}_{t'}\cdot\mathbf{M'_{qq}}\right]. \end{aligned} \tag{5.26b}$$

Again, by making the approximation that $\tilde{\mathbf{p}} \approx \mathbf{p}_0$ and

$$\frac{\left[\det(\mathbf{M_{qp}} \cdot \mathbf{M'_{qp}})\right]^{\frac{1}{2}}}{\frac{1}{2}\det(\mathbf{M_{qp}} + \mathbf{M'_{qp}})} \approx 1 \tag{5.26c}$$

we arrive at the following expression for the two time correlation function, $C_{fs}(\beta_0, t, t')$,

$$\begin{aligned} C_{fs}(\beta_0, t, t') &= (2\pi\hbar)^{-F} \int d\mathbf{p}_0 d\mathbf{q}_0 \; e^{i[S_t(\mathbf{p}_0,\mathbf{q}_0) - S_{t'}(\mathbf{p}_0,\mathbf{q}_0)]/\hbar} F_w^{\beta_0}(\mathbf{p}_0, \mathbf{q}_0) h(\mathbf{q}_t) \\ &\quad \exp\frac{i}{\hbar}\left[(\mathbf{p}_t \cdot \mathbf{M_{qp}} + \mathbf{p}_{t'} \cdot \mathbf{M'_{qp}}) \cdot (\mathbf{M_{qp}} + \mathbf{M'_{qp}})^{-1} \cdot (\mathbf{q}_{t'} - \mathbf{q}_t)\right]. \end{aligned} \tag{5.27}$$

The advantage of working with the two time correlation function instead of the correlation function in Eq. (5.2a) is that β_0 can be much smaller than β. If the temperature is below T_c, one can choose a β_0 that is above T_c with a the harmonic approximation for $F_w^{\beta_0}(\mathbf{p}_0, \mathbf{q}_0)$ in Eq. (5.27) and analytically continue $C_{fs}(\beta_0, t, t')$ to the actual temperature.

This very procedure is performed for the simple barrier crossing example of an Eckhart barrier. The Hamiltonian is

$$H = \frac{p^2}{2m} + V_0 \mathrm{sech}^2(aq) \tag{5.28}$$

with parameters that correspond approximately to the $H + H_2$ reaction: $V_0 = 0.425$ eV, $a = 1.36$ a.u. and $m = 1224$ a.u. For this example, β_0 is chosen to be $1/1200K$, well above the T_c of $700K$. However, from Figure 5.3 one see that we are able to obtain the rate constant below T_c very well, only after reaching $\sim 200K$ does one begin to see significant deviations. Keep in mind that only one correlation function is needed for all temperatures shown.

It is also interesting to see the that further approximations to Eq. (5.27) lead to other meaningful expressions. First, we set $\mathbf{M_{qp}} \approx \mathbf{M'_{qp}}$, this maybe convenient numerically since $(\mathbf{M_{qp}} + \mathbf{M'_{qp}})$ can be zero and cause the phase factor to diverge. This then leads to the following formula for the extra phase in the exponent in Eq. (5.27)

$$\frac{i}{\hbar}\left[(\mathbf{p}_t \cdot \mathbf{M_{qp}} + \mathbf{p}_{t'} \cdot \mathbf{M'_{qp}}) \cdot (\mathbf{M_{qp}} + \mathbf{M'_{qp}})^{-1} \cdot (\mathbf{q}_{t'} - \mathbf{q}_t)\right] \approx \frac{i}{2\hbar}\left[(\mathbf{p}_t + \mathbf{p}_{t'}) \cdot (\mathbf{q}_{t'} - \mathbf{q}_t)\right]. \tag{5.29}$$

Now one can notice that this extra phase factor can be written as

$$\frac{i}{2\hbar}\left[(\mathbf{p}_t + \mathbf{p}_{t'}) \cdot (\mathbf{q}_{t'} - \mathbf{q}_t)\right] \approx \int_{\mathbf{q}_t}^{\mathbf{q}_{t'}} \mathbf{p} d\mathbf{q} = \int_t^{t'} \mathbf{p} \cdot \dot{\mathbf{q}} d\tau, \tag{5.30}$$

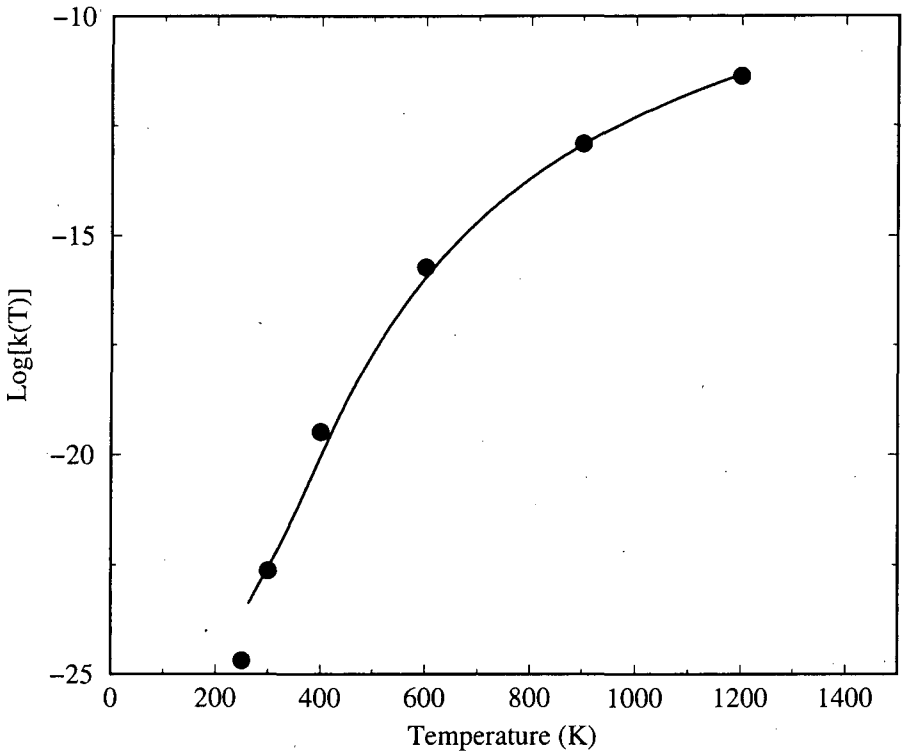

Figure 5.3: The Log of the rate constant $k(T)$ as function of the temperature for the 1-d eckhart barrier. The solid line is the analytic continuation result from the two time correlation function of Eq. (5.27) with $1/\beta_0 = 1200K$. The solid points are the exact quantum mechanical results.

i.e., it is the trapezoid approximation for the above integral. Combining with the difference of the actions in the exponent of Eq. (5.27), one has

$$\frac{i}{2\hbar}\left[(\mathbf{p}_t + \mathbf{p}_{t'})\cdot(\mathbf{q}_{t'} - \mathbf{q}_t)\right] + \frac{i}{\hbar}\left[S_t - S_{t'}\right] \approx \frac{i}{\hbar}\int_t^{t'} H(\mathbf{p},\mathbf{q})d\tau, \tag{5.31}$$

and if the Hamiltonian is time independent, the two time correlation function of Eq. (5.27) now becomes,

$$C_{fs}(\beta_0, t, t') = (2\pi\hbar)^{-F}\int d\mathbf{p}_0 d\mathbf{q}_0 F_w^{\beta_0}(\mathbf{p}_0,\mathbf{q}_0)h(\mathbf{q}_t)\exp\left[\frac{i}{\hbar}H(\mathbf{p}_0,\mathbf{q}_0)(t'-t)\right], \tag{5.32}$$

for which the analytic continuation is trivial. One finally obtains that the flux-side correlation function of Eq. (5.2a) may be approximated by

$$C_{fs}(\beta, t) = (2\pi\hbar)^{-F}\int d\mathbf{p}_0 d\mathbf{q}_0\ F_w^{\beta_0}(\mathbf{p}_0,\mathbf{q}_0)h(\mathbf{q}_t)\exp\left[-\beta_1 H(\mathbf{p}_0,\mathbf{q}_0)\right]. \tag{5.33}$$

Eq. (5.33) is an extremely simple expression that allows one to utilize the Harmonic approximation for the Wigner function of the Boltzmannized flux operator to obtain rate constants far below T_c. It is also very easy to calculate this expression as there are no oscillatory parts in the integrand. Tests for its accuracy and practical utility is still on going work.

5.4 SC-IVR for Thermal Rate Constants

Even with the great success of the linearized approximation to the SC-IVR, one recognize that it is not possible for the LSC-IVR to include quantum mechanical interference effects in the flux-side correlation function when they are important. In order to have a description of them, it is necessary to examine the application of the full SC-IVR methodology to the rate constant calculations.

In a coordinate representation, the flux-side correlation function of Eq. (5.2a) becomes

$$C_{fs}(t) = \int d\mathbf{q} \int d\mathbf{q}' \int d\mathbf{q}'' \; \langle \mathbf{q}|\hat{F}(\beta)|\mathbf{q}'\rangle \langle \mathbf{q}'|e^{i\hat{H}t/\hbar}|\mathbf{q}''\rangle \; h(\mathbf{q}'') \; \langle \mathbf{q}''|e^{-i\hat{H}t/\hbar}|\mathbf{q}\rangle. \tag{5.34}$$

There are, however, several ways of implementing the semiclassical approximation, Eq. (2.9), in Eq. (5.34). Perhaps the simplest is to choose $\mathbf{q}''$ in Eq. (5.34) as the initial value $\mathbf{q}_0$ for both propagators, and using the symmetry relations of the propagator matrix elements

$$\begin{aligned} \langle \mathbf{q}'|e^{-i\hat{H}t/\hbar}|\mathbf{q}\rangle &= \langle \mathbf{q}|e^{-i\hat{H}t/\hbar}|\mathbf{q}'\rangle \\ &= \langle \mathbf{q}'|e^{i\hat{H}t/\hbar}|\mathbf{q}\rangle^*, \end{aligned} \tag{5.35}$$

one readily obtains the following SC-IVR expression for the correlation function

$$\begin{aligned} C_{fs}(t) = \; & \frac{1}{(2\pi\hbar)^F} \int d\mathbf{q}_0 \int d\mathbf{p}_0 \int d\mathbf{p}_0' \; \langle \mathbf{q}_t|\hat{F}(\beta)|\mathbf{q}_t'\rangle \; h(\mathbf{q}_0) \\ & \left[\det\left(\frac{\partial \mathbf{q}_t}{\partial \mathbf{p}_0}\right) \det\left(\frac{\partial \mathbf{q}_t'}{\partial \mathbf{p}_0'}\right)\right]^{\frac{1}{2}} \exp\left[\frac{i}{\hbar}(S_t(\mathbf{q}_0,\mathbf{p}_0) - S_t(\mathbf{q}_0,\mathbf{p}_0'))\right], \end{aligned} \tag{5.36}$$

where $\mathbf{q}_t' = \mathbf{q}_t(\mathbf{q}_0,\mathbf{p}_0')$. One thus runs two classical trajectories, both beginning at the same position $\mathbf{q}_0$ in the product region, with different initial momenta. The only awkward feature of this expression is that the trajectories begin in the product region and must terminate in the transition state region (where $\langle \mathbf{q}|\hat{F}(\beta)|\mathbf{q}'\rangle$ localizes $\mathbf{q}$ and $\mathbf{q}'$), and the sampling of initial conditions for this purpose may not be efficient.

A second way of implementing the SC-IVR, in order to have the initial positions $\mathbf{q}_0$ sampled from the Boltzmannized flux factor, is to choose $\mathbf{q}$ in Eq. (5.34) to be $\mathbf{q}_0$; then $\mathbf{q}'' = \mathbf{q}_t(\mathbf{q}_0, \mathbf{p}_0)$, and $\mathbf{q}' = \mathbf{q}'_t \equiv \mathbf{q}(\mathbf{q}_t, \mathbf{p}'_0; t)$. The expression for the correlation function is

$$C_{fs}(t) = \frac{1}{(2\pi\hbar)^F} \int d\mathbf{q}_0 \int d\mathbf{p}_0 \int d\mathbf{p}'_0 \, \langle \mathbf{q}'_t | \hat{F}(\beta) | \mathbf{q}_0 \rangle \, h(\mathbf{q}_t) \left[\det \left(\frac{\partial \mathbf{q}_t}{\partial \mathbf{p}_0} \right) \det \left(\frac{\partial \mathbf{q}'_t}{\partial \mathbf{p}'_0} \right) \right]^{\frac{1}{2}} \exp \left[\frac{i}{\hbar} (S_t(\mathbf{q}_0, \mathbf{p}_0) - S_t(\mathbf{q}_t, \mathbf{p}'_0)) \right]; \quad (5.37)$$

i.e., here one begins a trajectory at $(\mathbf{q}_0, \mathbf{p}_0)$ in the transition state region, runs it for time t into the product region, then restarts it with a new momentum $\mathbf{p}'_0$, runs it for time t, at which time it must be back in the transition state region. Figure 5.4 indicates these two possible strategies.

Finally, a third way of implementing the SC approach is to begin both trajectories in the transition state region (cf. Figure 5.4c), i.e., to choose $\mathbf{q} = \mathbf{q}_0$ and $\mathbf{q}' = \mathbf{q}'_0$ in Eq. (5.34), whereby one obtains the following expression for the correlation function,

$$C_{fs}(t) = \frac{1}{(2\pi\hbar)^F} \int d\mathbf{q}_0 \int d\mathbf{q}'_0 \int d\mathbf{p}_0 \int d\mathbf{p}'_0 \, \langle \mathbf{q}_0 | \hat{F}(\beta) | \mathbf{q}'_0 \rangle \, \delta_F(\mathbf{q}_t - \mathbf{q}'_t) h(\mathbf{q}_t) \left[\det \left(\frac{\partial \mathbf{q}_t}{\partial \mathbf{p}_0} \right) \det \left(\frac{\partial \mathbf{q}'_t}{\partial \mathbf{p}'_0} \right) \right]^{\frac{1}{2}} \exp \left[\frac{i}{\hbar} (S_t(\mathbf{q}_0, \mathbf{p}_0) - S_t(\mathbf{q}'_0, \mathbf{p}'_0)) \right]. \quad (5.38)$$

where $\mathbf{q}'_t = \mathbf{q}(\mathbf{q}'_0, \mathbf{p}'_0; t)$. The disadvantages of this approach are clear: one has four (multidimensional) integration variables to integrate over, rather than three as in Eqs. (5.36) and (5.37), and the integral contains a delta function which requires the two trajectories to end at the same point in the product region. This later problem (the delta function) can be ameliorated by switching to a modified version of the generalized Herman-Kluk (coherent state) IVR in Eq. (2.14). The modification that we use here, the $\gamma_0 \to \infty$ limit (which converts the initial coherent state into a coordinate state), gives the following SC-IVR for the propagator

$$\langle \mathbf{q} | e^{-i\hat{H}t/\hbar} | \mathbf{q}_0 \rangle = \frac{1}{(2\pi i\hbar)^{F/2}} \int d\mathbf{p}_0 D_t(\mathbf{q}_0, \mathbf{p}_0) \left(\frac{\gamma_t}{4\pi} \right)^{F/4} \langle \mathbf{q} | \mathbf{p}_t, \mathbf{q}_t; \gamma_t \rangle e^{iS_t(\mathbf{q}_0, \mathbf{p}_0)/\hbar}, \quad (5.39a)$$

where

$$D_t(\mathbf{q}_0, \mathbf{p}_0) = \det \left[\frac{\partial \mathbf{q}_t}{\partial \mathbf{p}_0} + \frac{i}{\hbar \gamma_t} \frac{\partial \mathbf{p}_t}{\partial \mathbf{p}_0} \right]^{\frac{1}{2}}. \quad (5.39b)$$

[The $\gamma_t \to \infty$ limit of Eq. (5.39) would convert it into the previously used coordinate space SC-IVR, Eq. (2.9).] Using Eq. (5.39) for the propagator, the following expression is

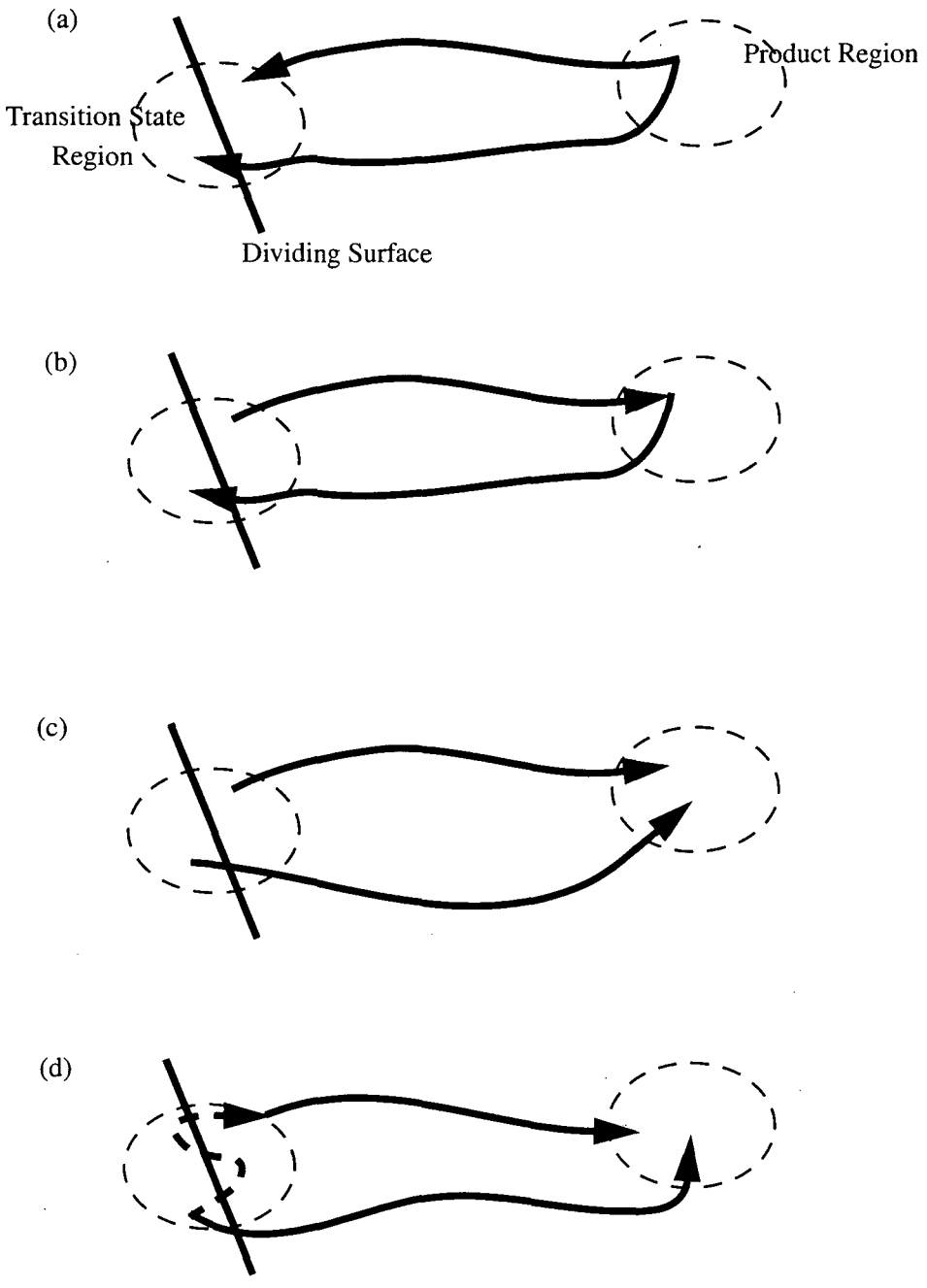

Figure 5.4: Sketch of trajectory configurations in coordinate space that have non-zero contributions to the integrand in Eq. (3.54) (a), Eq. (5.37) (b) Eq.(5.40) (c) and Eq. (5.44) (d). The dashed trajectory in (d) is the imaginary time trajectory on the upside down potential.

obtained for the correlation function

$$C_{fs}(t) = \frac{1}{(2\pi\hbar)^F}\int d\mathbf{q}_0 \int d\mathbf{q}_0' \int d\mathbf{p}_0 \int d\mathbf{p}_0' \, \langle \mathbf{q}_0|\hat{F}(\beta)|\mathbf{q}_0'\rangle \, \langle \mathbf{p}_t'\mathbf{q}_t'|\hat{h}|\mathbf{p}_t\mathbf{q}_t\rangle \left(\frac{\gamma_t}{4\pi}\right)^{F/2} D_t(\mathbf{q}_0,\mathbf{p}_0) D_t(\mathbf{q}_0',\mathbf{p}_0')^* \exp\left[\frac{i}{\hbar}(S_t(\mathbf{q}_0,\mathbf{p}_0) - S_t(\mathbf{q}_0',\mathbf{p}_0'))\right] \quad (5.40a)$$

Finally, because the coherent states are localized in position, the following approximation should be reasonable,

$$\langle \mathbf{p}_t'\mathbf{q}_t'|\hat{h}|\mathbf{p}_t\mathbf{q}_t\rangle = h(\mathbf{q}_t)\; h(\mathbf{q}_t')\langle \mathbf{p}_t'\mathbf{q}_t'|\mathbf{p}_t\mathbf{q}_t\rangle, \quad (5.40b)$$

where the coherent state overlap is

$$\langle \mathbf{p}_t'\mathbf{q}_t'|\mathbf{p}_t\mathbf{q}_t\rangle = \exp\left[-\frac{\gamma_t}{4}(\mathbf{q}_t - \mathbf{q}_t')^2 - \frac{(\mathbf{p}_t - \mathbf{p}_t')^2}{4\gamma_t\hbar^2} + \frac{i}{2\hbar}(\mathbf{p}_t + \mathbf{p}_t')\cdot(\mathbf{q}_t - \mathbf{q}_t')\right]. \quad (5.40c)$$

Comparing Eq. (5.38) to Eq. (5.40), one sees that in the latter the two trajectories are not required to land at the same point but rather that the two final points in phase space, $(\mathbf{q}_t, \mathbf{p}_t)$ and $(\mathbf{q}_t', \mathbf{p}_t')$, are required to be in roughly the same phase space cell.

All three strategies of implementing the SC-IVR — Eqs. (5.36), (5.37), or (5.40) — are essentially equivalent; the choice between them is purely one of convenience, and it is not immediately obvious which will turn out to be most useful in applications to complex systems. For the present 1-d application all are possible.

5.4.1 Semiclassical Approximation for the Boltzmann Operator

In section 5.4 it was assumed that the Boltzmannized flux operator $\hat{F}(\beta)$ is obtained by fully quantum mechanical methods, and this may indeed be feasible even for complex systems. As an alternative and perhaps more efficient possibility, however, we note that it can also be obtained by a semiclassical approximation. Referring to Eq. (5.8), one this needs to construct matrix elements of the Boltzmann operator $e^{-\beta\hat{H}}$, which is the same as the time evolution operator $e^{-i\hat{H}t/\hbar}$ for the imaginary time $t = -i\hbar\beta$. It was noted by one of us[36] some years ago, though, that motion in imaginary time is equivalent to motion in real time on the upside-down potential energy surface; e.g., Newton's equations

$$m\frac{d^2}{dt^2}\mathbf{q}(t) = -\frac{\partial V}{\partial \mathbf{q}} \quad (5.41)$$

becomes

$$m\frac{d^2}{d\tau^2}\mathbf{q}(\tau) = +\frac{\partial V}{\partial \mathbf{q}}, \quad (5.42)$$

where $\tau = it$ is a real time-like variable, which varies from 0 to $\hbar\beta$ to obtain $e^{-\beta\hat{H}}$. The SC-IVR expression for the Boltzmann operator, which is the analog of Eq. (2.9), is therefore

$$\langle \mathbf{q}|e^{-\beta\hat{H}}|\mathbf{q}_0\rangle \equiv \int d\bar{\mathbf{p}}_0\, \delta(\mathbf{q}-\mathbf{q}_\beta) \left[\det\left(\frac{\partial \mathbf{q}_\beta}{\partial \bar{\mathbf{p}}_0}\right)/(2\pi\hbar)^F\right]^{\frac{1}{2}} e^{-S_\beta(\mathbf{q}_0,\bar{\mathbf{p}}_0)/\hbar}, \tag{5.43a}$$

where $\bar{\mathbf{p}}(\tau) = m\mathbf{q}'(\tau)$ is the real momentum-like variable, $\mathbf{q}_\beta = \mathbf{q}(\mathbf{q}_0, \bar{\mathbf{p}}_0; \hbar\beta)$ is the coordinate that evolves along the classical trajectory on the upside-down potential energy surface with initial conditions $(\mathbf{q}_0, \bar{\mathbf{p}}_0)$, and S_β is the classical action,

$$S_\beta(\mathbf{q}_0, \bar{\mathbf{p}}_0) = \int_0^{\hbar\beta} d\tau\, \frac{\bar{\mathbf{p}}(\tau)^2}{2m} + V(\mathbf{q}(\tau)). \tag{5.43b}$$

This semiclassical approximation for the Boltzmann operator is most conveniently implemented via Eq. (5.40) for the flux-side correlation function. Together with Eqs. (5.43a) and (5.8), it gives the correlation function as

$$\begin{aligned} C_{fs}(t) \;=\; & \frac{1}{(2\pi\hbar)^F}\int d\mathbf{q}_0 \int d\bar{\mathbf{p}}_0 \int d\mathbf{p}_0 \int d\mathbf{p}_0'\, \frac{[h(\mathbf{q}_\beta)-h(\mathbf{q}_0)]}{i\hbar\beta} \left[\det\left(\frac{\partial \mathbf{q}_\beta}{\partial \bar{\mathbf{p}}_0}\right)/(2\pi\hbar)^F\right]^{\frac{1}{2}} \\ & e^{-S_\beta(\mathbf{q}_0,\bar{\mathbf{p}}_0)/\hbar} \langle \mathbf{p}_t'\mathbf{q}_t'|\hat{h}|\mathbf{p}_t\mathbf{q}_t\rangle \left(\frac{\gamma_t}{4\pi}\right)^{F/2} D_t(\mathbf{q}_0,\mathbf{p}_0) D_t^*(\mathbf{q}_\beta,\mathbf{p}_0') \\ & \exp\left[\frac{i}{\hbar}(S_t(\mathbf{q}_0,\mathbf{p}_0) - S_t(\mathbf{q}_\beta,\mathbf{p}_0'))\right], \end{aligned} \tag{5.44}$$

One thus begins a purely imaginary time trajectory (i.e., real trajectory on the up-side down potential) with initial conditions $(\mathbf{q}_0, \bar{\mathbf{p}}_0)$ and integrates it for (imaginary) time $\hbar\beta$ to position $\mathbf{q}_\beta$; $\mathbf{q}_0$ and $\mathbf{q}_\beta$ must be on the opposite sides of the dividing surface. From $\mathbf{q}_0$ and $\mathbf{q}_\beta$ one initiates trajectories with momenta $\mathbf{p}_0$ and $\mathbf{p}_0'$ and integrates for time t; the final coordinate $\mathbf{q}_t = \mathbf{q}(\mathbf{q}_0, \mathbf{p}_0; t)$ and $\mathbf{q}_t' = \mathbf{q}(\mathbf{q}_\beta, \mathbf{p}_0'; t)$ must land within the same phase space cell in order to contribute. Fig. 1d shows this schematically.

The semiclassical Boltzmann operator can also be employed with the linearization approximation for the real time dynamics, i.e., in Eq. (5.9). The necessary steps, indicated below, are straightforward:

$$\begin{aligned} C_{fs}(t) \;&=\; \frac{1}{(2\pi\hbar)^F}\int d\mathbf{q}_0 \int d\mathbf{p}_0 \int d\Delta\mathbf{q}\, e^{-i\mathbf{p}_0\cdot\Delta\mathbf{q}/\hbar}\, \langle \mathbf{q}_0 + \Delta\mathbf{q}/2|\hat{F}(\beta)|\mathbf{q}_0 - \Delta\mathbf{q}/2\rangle\, h(\mathbf{q}_t) \\ &=\; \frac{1}{(2\pi\hbar)^F}\int d\mathbf{q}_0 \int d\mathbf{q}_0' \int d\mathbf{p}_0\, e^{-i\mathbf{p}_0\cdot(\mathbf{q}_0'-\mathbf{q}_0)/\hbar}\, \langle \mathbf{q}_0'|\hat{F}(\beta)|\mathbf{q}_0\rangle\, h\left[\mathbf{q}_t\left(\mathbf{p}_0, \frac{\mathbf{q}_0+\mathbf{q}_0'}{2}\right)\right] \\ &=\; \frac{1}{(2\pi\hbar)^F}\int d\mathbf{q}_0 \int d\mathbf{p}_0 \int d\bar{\mathbf{p}}_0\, \frac{[h(\mathbf{q}_0)-h(\mathbf{q}_\beta)]}{i\hbar\beta}\, e^{-i\mathbf{p}_0\cdot(\mathbf{q}_\beta-\mathbf{q}_0)/\hbar} \\ &\qquad \times \left[\det\left(\frac{\partial \mathbf{q}_\beta}{\partial \bar{\mathbf{p}}_0}\right)/(2\pi\hbar)^F\right]^{\frac{1}{2}} e^{-S_\beta(\mathbf{q}_0,\bar{\mathbf{p}}_0)/\hbar}\, h\left[\mathbf{q}_t\left(\mathbf{p}_0, \frac{\mathbf{q}_0+\mathbf{q}_\beta}{2}\right)\right]. \end{aligned} \tag{5.45}$$

Again, the end points of the imaginary time trajectory with initial conditions $(\mathbf{q}_0, \bar{\mathbf{p}}_0)$ must straddle the dividing surface; however, only one real time trajectory is run, its initial position being the average of the end points of the imaginary time trajectory, $(\mathbf{q}_0 + \mathbf{q}_\beta)/2$, with initial momentum $\mathbf{p}_0$.

5.4.2 Results and Discussion of Test Calculations

We wish to test the extent to which the SC-IVR of Section 5.4, and the linearized approximation to it in Section 5.3, can describe coherence and other quantum effects in the thermal rate constants. To this end we look at the flux-side correlation function $C_{fs}(t)$ for a 1-d double well potential, for which the Hamiltonian is

$$H = \frac{p^2}{2m} - \frac{1}{2} m\omega^{\ddagger 2} x^2 + \frac{m^2 \omega^{\ddagger 4}}{16 V_0} x^4. \tag{5.46}$$

This is the same system we considered earlier via the linearized approximation to the SC-IVR, but with a harmonic bath coupled to it. As noted in the Introduction, without the bath degrees of freedom $C_{fs}(t)$ does not reach a constant value as $t \to \infty$ — i.e., $k(T)$ does not exist — but the re-crossing dynamics manifested in $C_{fs}(t)$ should accentuate coherence/interference effects, and this thus provides an even more stringent test of the SC theories. The mass of the particle is that of an H atom, the barrier height, $V_0 = 2085$ cm^{-1} (≈ 6 kcal/mol), is typical of H atom transfer reactions, and the imaginary barrier frequency is $\omega^\ddagger = 500$ cm^{-1}. The calculations were carried out for T =300°K and 900°K.

Figure 5.5 first shows the results of the linearized approximation (solid points) to the SC-IVR for $C_{fs}(t)$ given by Eq. (5.9), compared to the exact quantum (solid line) and the completely classical (open points) results [given by Eq. (5.9) with Eq. (5.11)]. Several observations are apparent. First note that for short times — up to $\sim$ 50 fsec at 300°K (Figure 5.5a) and $\sim$ 25 fsec at 900°K (Figure 5.5) — $C_{fs}(t)$ takes on an approximately constant or plateau value; this is the transition state theory (TST) or barrier crossing rate constant [when divided by the reactant partition function in Eq. (5.1)] that would be the $t \to \infty$ limit if there were no re-crossing dynamics. The *classical* correlation function begins at its TST value at $t = 0$, but the quantum and semiclassical correlation functions take a time of $\sim \hbar\beta$ (27 fsec for 300°K, 9 fsec for 900°K) to reach their plateau values. At 900°K (Figure 5.5b) one sees that all three curves have approximately the same plateau value, but at 300°K (Figure 5.5a) the classical plateau value is $\sim$ 25% lower than the QM

and SC value; this is due to tunneling effects in the TST rate constant, and one sees that the linearized SC theory describes this quite well. (This is consistent with earlier work[50] in our group showing that the SC-IVR is able to describe moderate levels of tunneling — e.g., tunneling probabilities down to $\sim 10^{-5}$ for H atom motion — though not the 'deep' tunneling region that requires explicit use of complex trajectories[47,48,51,52].)

The time dependence beyond the plateau region in Figure 5.5 is the result of re-crossing dynamics, and one sees that in this region the linearized SC approximation is essentially the same as the classical result. Furthermore, at 900°K (Figure 5.5b) the classical and SC correlation functions follow the QM result fairly well up to $t \approx 150$ fsec and then deviate considerably; at 300°K they follow it not well at all past the plateau region. Thus the linearized SC approximation is able to describe quantum effects well in the short time regime of TST-like dynamics, but is not able to describe quantum effects in the longer time re-crossing dynamics.

Figure 5.6 now shows the full SC-IVR results (solid points) for the correlation function [calculated via Eq. (5.44)] compared to the exact quantum (solid line) and linearized SC (open points) values, and one sees that the full SC-IVR indeed does describe the correct quantum behavior for times well into the re-crossing regime (up to 200 fsec, as long as the SC-IVR calculations were carried out). The comparison is particularly revealing for 300°K (Figure 5.6a), where the linearized SC results (open points) deviate drastically from the quantum correlation function for times past the short-time TST plateau region. The effort required for the full SC-IVR calculation, however, is quite large; the integration over the initial conditions were carried out presently by an unweighted Monte Carlo procedure (with finite cut-offs) and required $\sim 10^6$ trajectories. A more sophisticated Monte Carlo procedure would perhaps make this more efficient.

The SC-IVR results in Figure 5.6 used the semiclassical approximation for the Boltzmann operator, Eq. (5.44). To show that this introduces little error, Figure 5.7 displays a comparison of the results obtainable with the linearized SC approximation for the real time propagation with the quantum and SC versions of the Boltzmann operator [Eq. (5.45)]. One sees that the results obtained with the SC approximation to the Boltzmann operator are in good agreement with the QM one; little error is introduced by the SC approximation, so that one has a semiclassical description for both the imaginary and real time evolution.

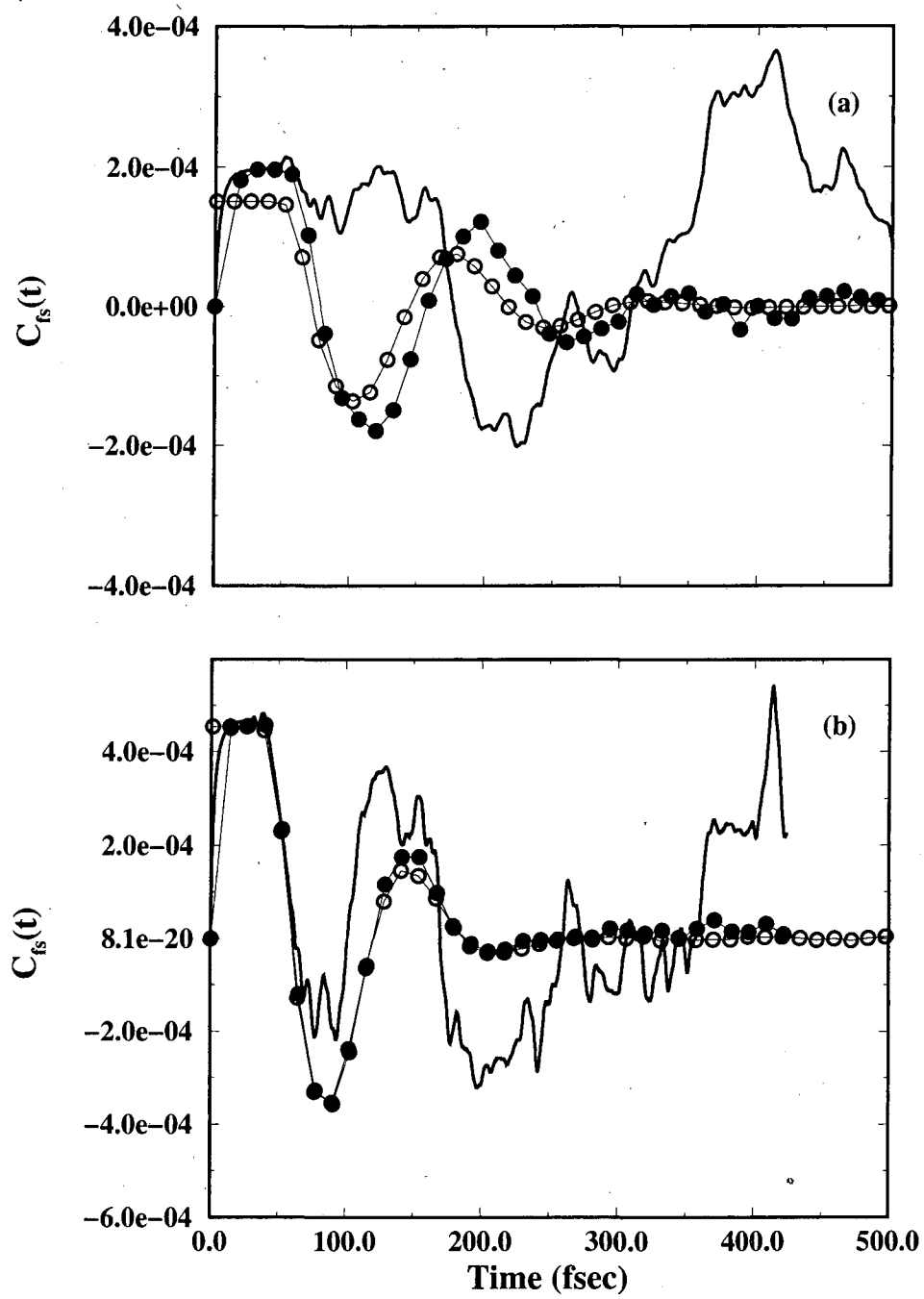

Figure 5.5: The correlation function $C_{fs}(t)$ as given by the exact quantum calculation (solid line), the linearized approximation of Eq. (5.9) (solid points) and the fully classical method of Eq. (5.11) (open points). (a) $300K$, (b) $900K$.

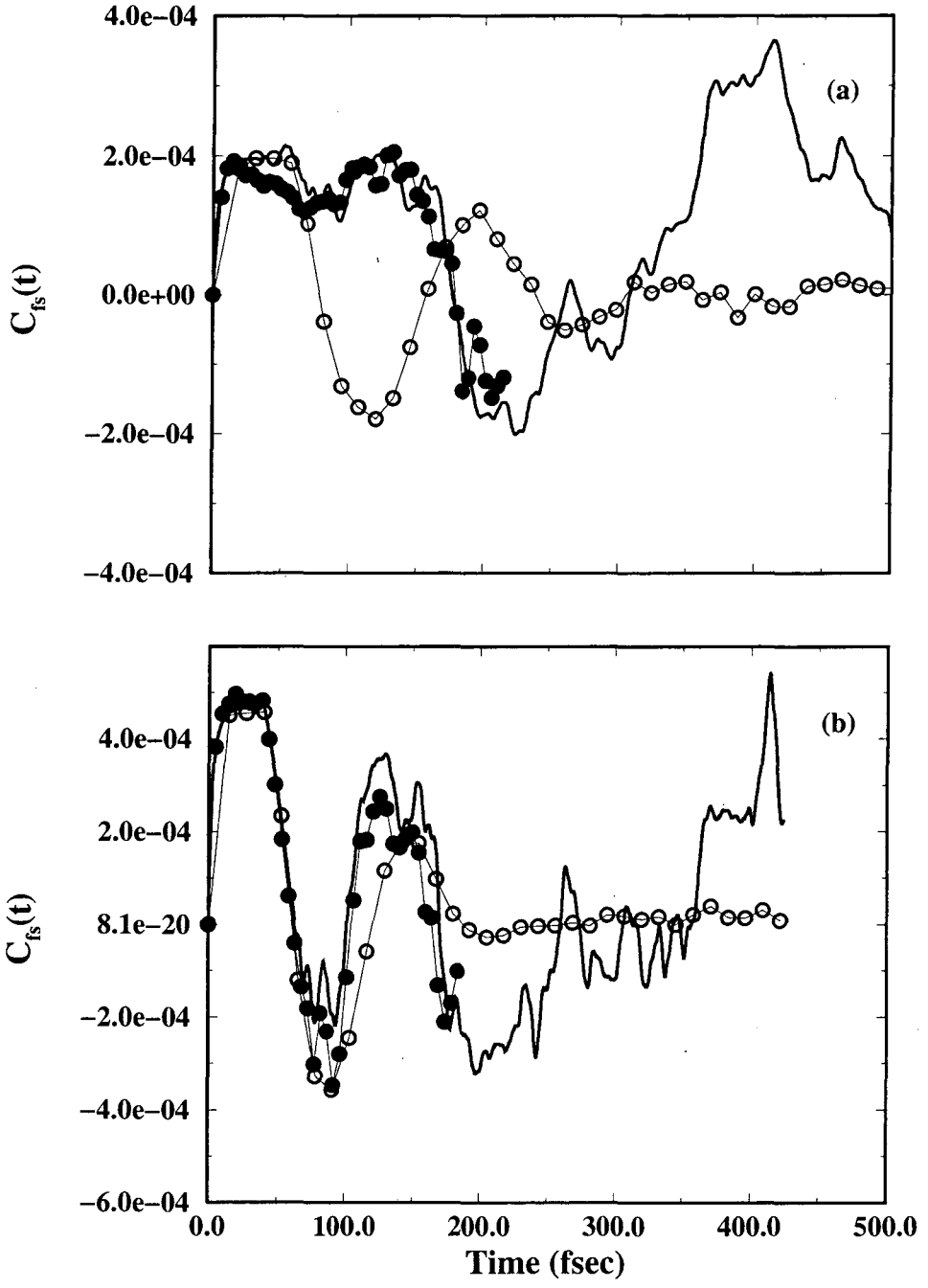

Figure 5.6: The correlation function $C_{fs}(t)$ given by the exact quantum calculation (solid line), the full SC-IVR model of Eq. (5.44) (solid points), and the linearization approximation of Eq. (5.9) (open points). (a) $300K$, (b) $900K$.

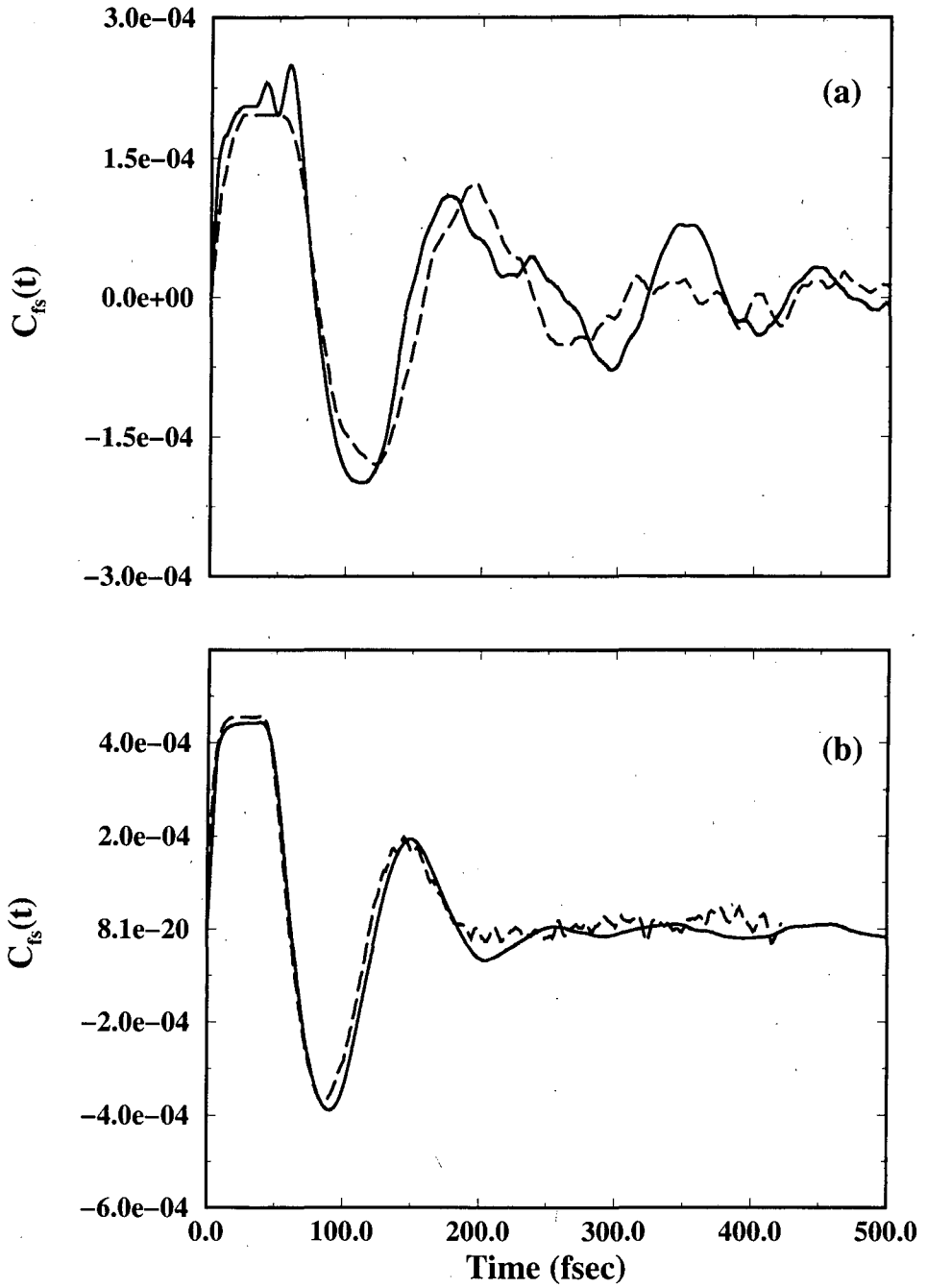

Figure 5.7: The correlation function $C_{fs}(t)$ obtained with the linearization approximation of Eq. (5.9), where the matrix elements of the Boltzmannized flux operator are obtained quantum mechanically (dashed line) and semiclassically via Eq. (5.45) (solid line). (a) $300K$, (b) $900K$.

5.5 Forward-Backward IVR for Thermal Rate Constants

Since the flux-side correlation function involves the evaluation of a trace, it is natural for the implementation of the forward-backward IVR of chapter 3. Thus, $C_{fs}(t)$ corresponds to operator $\hat{A}$ in Eq. (3.94) being the Boltzmannized flux operator

$$\hat{A} = e^{-\beta\hat{H}/2}\hat{F}e^{-\beta\hat{H}/2}, \tag{5.47a}$$

and $\hat{B}$ being the heaviside function that is 0(1) on the reactant (product) side of a dividing surface which separates reactants and products,

$$\hat{B} = \hat{h}[s(\mathbf{q})], \tag{5.47b}$$

where $s(\mathbf{q}) = 0$ defines the dividing surface; $\hat{F}$ is the flux operator associated with this dividing surface

$$\hat{F} = \frac{i}{\hbar}\left[\hat{H}, \hat{h}(s(\mathbf{q}))\right]. \tag{5.47c}$$

Operator $\hat{B}$ in Eq. (5.47b) is thus not of the simple form in Eq. (3.97), but by Fourier transforming the Heaviside function, one can express it as a one dimensional integral over operators of this form,

$$h[s(\hat{\mathbf{q}})] = \int_{-\infty}^{\infty} dp_s [2\pi i(p_s - i\epsilon)]^{-1} e^{ip_s s(\hat{\mathbf{q}})/\hbar} \tag{5.47d}$$

where ϵ is a small positive constant. One thus applies the FB-IVR to the operator $\hat{B} = e^{ip_s s(\hat{\mathbf{q}})/\hbar}$ and then integrates the result over the Fourier transform parameter p_s. The FB-IVR for the flux-side correlation function is therefore given by

$$\begin{aligned} C_{fs}(t) \;=\; & \int_{-\infty}^{\infty} dp_s (2\pi i p_s)^{-1} (2\pi\hbar)^{-F} \int d\mathbf{p}_0 \int d\mathbf{q}_0 C_0(\mathbf{p}_0, \mathbf{q}_0; p_s) \\ & e^{iS_0(\mathbf{p}_0,\mathbf{q}_0;p_s)/\hbar} \langle \mathbf{p}_0\mathbf{q}_0|\hat{F}(\beta)|\mathbf{p}_0'\mathbf{q}_0'\rangle \end{aligned} \tag{5.48a}$$

where the "momentum jump" at time t of the FB-IVR [cf. Eq. (3.101)] is

$$\mathbf{p}_t \to \mathbf{p}_t + p_s \left[\frac{\partial s(\mathbf{q})}{\partial \mathbf{q}}\right]_{\mathbf{q}=\mathbf{q}_t}, \tag{5.48b}$$

and the FB action is

$$S_0(\mathbf{p}_0, \mathbf{q}_0; p_s) = \int_0^t dt'[\mathbf{p}\cdot\dot{\mathbf{q}} - H(\mathbf{p},\mathbf{q})] + p_s s(\mathbf{q}_t) + \int_t^0 dt'[\mathbf{p}\cdot\dot{\mathbf{q}} - H(\mathbf{p},\mathbf{q})]. \tag{5.48c}$$

Here $\mathbf{p}_0' = \mathbf{p}_0'(\mathbf{p}_0, \mathbf{q}_0; p_s)$, $\mathbf{q}_0' = \mathbf{q}_0'(\mathbf{p}_0, \mathbf{q}_0; p_s)$, and the "$i\epsilon$" in Eq. (5.47d) has been dropped since other factors in the integrand are zero if $p_s = 0$. [Note that the "momentum jump" defined by Eq. (5.48b) is in the direction normal to the dividing surface.] The FB-IVR result for $C_{fs}(t)$ thus involves only a *one dimensional* integral in addition to the single phase space average over initial conditions, only slightly more involved than the linearized SC-IVR expression [Eq. (3.67)].

Before proceeding, it is useful to note some general properties of $C_{fs}(t)$ that simplify its evaluation. With the use of Eq. (5.47d), the rigorous expression for the flux-side correlation function is

$$C_{fs}(t) = \int_{-\infty}^{\infty} dp_s \frac{1}{2\pi i p_s} \mathrm{tr}[\hat{F}(\beta)\hat{U}(p_s)], \tag{5.49}$$

where

$$\hat{U}(p_s) = e^{i\hat{H}t/\hbar} e^{ip_s s(\hat{\mathbf{q}})/\hbar} e^{-i\hat{H}t/\hbar}. \tag{5.50}$$

Since $\hat{F}(\beta)$ is hermitian, one has the following relations

$$\mathrm{tr}[\hat{F}(\beta)\hat{U}(p_s)]^* = \mathrm{tr}[\hat{F}(\beta)\hat{U}(p_s)^\dagger] = \mathrm{tr}[\hat{F}(\beta)\hat{U}(-p_s)], \tag{5.51}$$

so that the imaginary part of $\mathrm{tr}[\hat{F}(\beta)\hat{U}(p_s)]$ is an odd function of p_s. Therefore the integrand in Eq. (5.49) is an even function of p_s, and one only needs to integrate over positive values of p_s,

$$C_{fs}(t) = \mathrm{Re} \int_0^{\infty} dp_s \frac{1}{i\pi p_s} \mathrm{tr}[\hat{F}(\beta)\hat{U}(p_s)], \tag{5.52}$$

thus simplifying the calculation.

5.5.1 1-d Eckhart Barrier

The first example we consider is again the simple barrier transmission where the Hamiltonian is identical to that in Eq. (5.28). To evaluate the matrix element $\langle p_0 q_0|\hat{F}(\beta)|p_0' q_0'\rangle$ in Eq. (5.48a), we express the Boltzmannized fluxed operator by its eigenfunction expansion, i.e.,

$$\hat{F}(\beta) = \sum_n f_n |u_n\rangle\langle u_n|, \tag{5.53}$$

where

$$\hat{F}(\beta)|u_n\rangle = f_n|u_n\rangle. \tag{5.54}$$

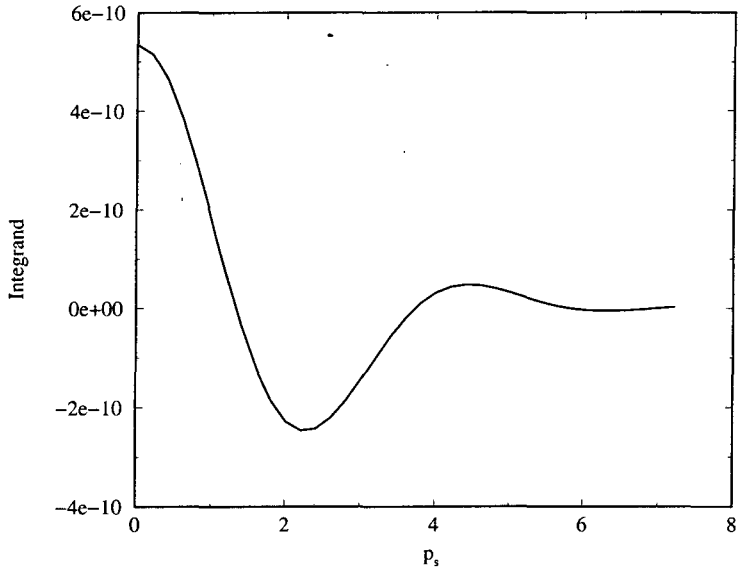

Figure 5.8: The integrand of Eq. (5.52) as a function of the momentum jump, p_s, for the 1-d Eckhart barrier at $t = 10$ fsec and $T = 300K$.

The matrix element thus becomes

$$\langle p_0 q_0 | \hat{F}(\beta) | p_0' q_0' \rangle = \sum_n f_n \langle p_0 q_0 | u_n \rangle \langle u_n | p_0' q_0' \rangle, \tag{5.55}$$

and the evaluation of Eq. (5.48a) is then accomplished by Monte Carlo sampling of the initial distribution $|\langle p_0 q_0 | u_n \rangle|$.

Figure 5.8 shows the dependence of the integrand of Eq. (5.52) on the momentum jump variable p_s, for $T = 300K$ and $t \approx 10$ fsec, just as it reaches the "plateau" region. It has some oscillatory character but not of a severe nature. Figure 5.9 then shows $C_{fs}(t)$ at several different times, and they are in good agreement with the correct quantum value over the whole time span. For this example $C_{fs}(t)$ shows the typical behavior of a "direct" reaction, rising to its plateau value in a time of $\sim \hbar\beta$. For this temperature the tunneling correction function $\kappa \equiv k_{\rm QM}/k_{\rm CL}$ is about 2.

5.5.2 1-d Double Well

A more complicated example is the 1-d double well potential where the Hamiltonian is again the double well of Eq. (5.46). Unlike the barrier example, the flux-side correlation function for this system does not have a well-defined long time limit, and in the previous section where we carried out both LSC-IVR and SC-IVR calculations, one observed

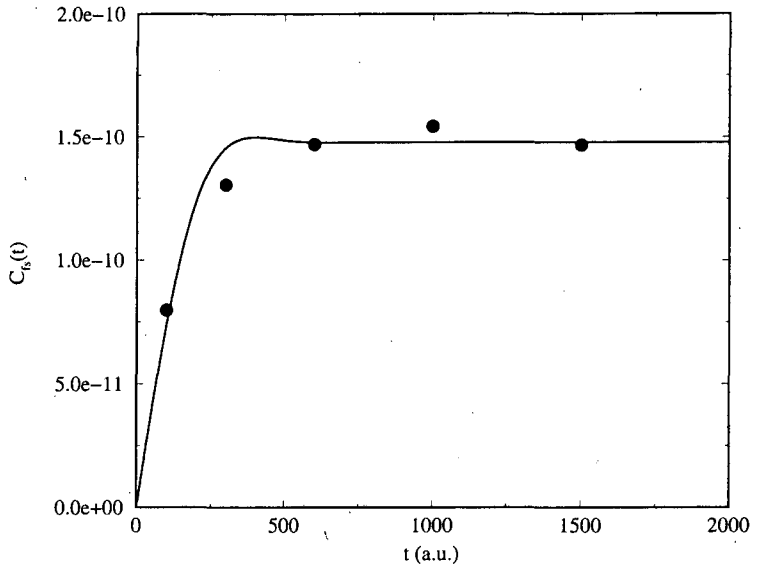

Figure 5.9: The flux-side correlation function for the 1-d Eckhart barrier at $T = 300K$. The solid line is the quantum mechanical result and the solid points the FB-IVR results.

quantum mechanical interference structure that persists to all times. This example thus tests the accuracy of the FB-IVR approach for describing quantum mechanical interference effects. Figure 5.10 again shows the dependence of the integrand of Eq. (5.52) as a function of p_s, for $t = 242$ fsec and $T = 300K$. One sees that the integrand is well localized and free of rapid oscillations. This allows us to Monte Carlo sample all of the integration variables, (p_0, q_0, p_s), together. Figure 5.11 shows the comparison of the FB-IVR flux-side correlation function for this system at $300K$ with the exact quantum mechanical correlation function over a wide time interval. The result here is very good not only because the overall agreement is satisfactory, but also because the longest time we are able to propagate is $\sim$ 500 fs, about twice as long as we were able to obtain via the standard SC-IVR. Furthermore, unlike the SC-IVR which becomes increasingly difficult as the time increases, the numerical effort of the FB-IVR for the longest time is almost the same as that for the shortest time.

5.5.3 A System Coupled to Ten Bath Modes

The final example is the double well potential of the previous section with the addition of ten harmonic ("bath") degrees of freedom coupled to it. This is a ten mode

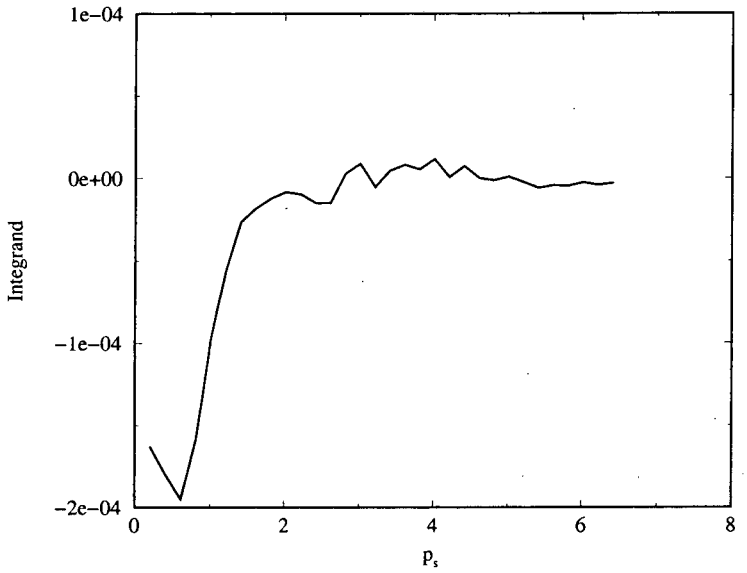

Figure 5.10: The integrand of Eq. (5.52) as a function of the momentum jump, p_s, for the 1-d double well potential for $t = 242$ fsec. and $T = 300K$.

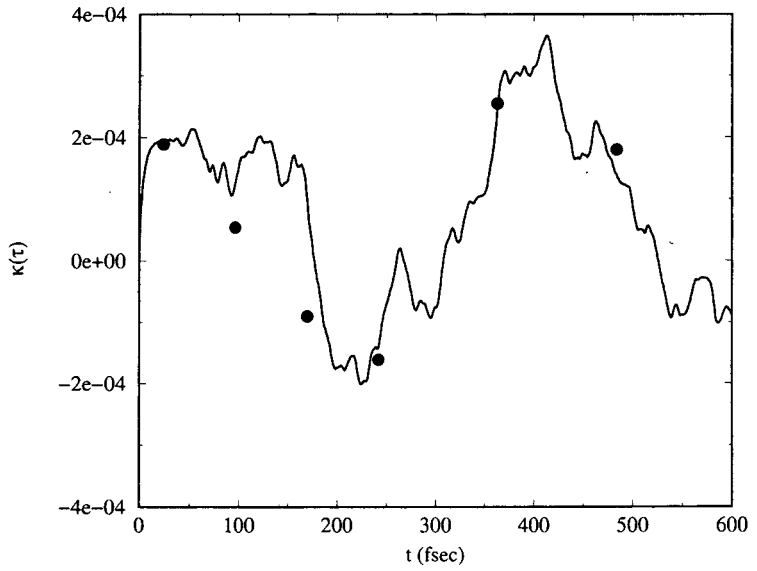

Figure 5.11: The flux-side correlation function for the double well potential at $T = 300K$. The solid line is the quantum mechanical result and the solid points the FB-IVR results.

ω_i	$c_i/\sqrt{m_i}$
221.7	0.21
443.3	0.34
665.0	0.41
886.7	0.44
1108.3	0.44
1330.0	0.43
1551.7	0.40
1773.3	0.36
1995.0	0.33
2216.7	0.29

Table 5.1: Frequencies and coupling constants (in cm^{-1}) for the harmonic bath in section 5.5.3.

version of the popular system-bath problem, for which the Hamiltonian is

$$H = H_0(p_s, s) + \sum_{i=1}^{10} \frac{p_i^2}{2m_i} + \frac{1}{2} m_i \omega_i^2 (q_i - \frac{c_i}{m_i \omega_i^2} s)^2, \tag{5.56}$$

where $H_0(p_s, s)$ is given by Eq. (5.46). The frequencies $\{\omega_i\}$ and coupling constants $\{c_i\}$ are chosen from the usual Ohmic (with exponential cutoff) spectral density

$$J(\omega) = \frac{\pi}{2} \sum_{i=1}^{10} \frac{c_i^2}{m_i \omega_i} \delta(\omega - \omega_i) = \eta \omega e^{-\omega/\omega_c}, \tag{5.57}$$

and their specific values are listed in Table 5.1.

The version of this problem with an infinite bath of harmonic modes has been well studied both quantum mechanically and classically.[180] Our study of it using the linearized approximation to the SC-IVR — the LSC-IVR discussed in the section (5.3.1) [Eq. (5.9)] — gave results in excellent agreement with accurate quantum results for the problem. Therefore, since we do not have accurate quantum results for the present ten mode version of the model, here we compare the results of our FB-IVR calculation to those of the LSC-IVR. As before, matrix elements of the Boltzmannized flux operator are obtained by a normal mode approximation at the transition state.

The coupling constants in Table 5.1 are chosen to correspond to a value of η that is near the maximum in the "Kramer's turnover" of the rate constant versus coupling strength. The flux correlation function is thus expected to exhibit features of re-crossing dynamics,

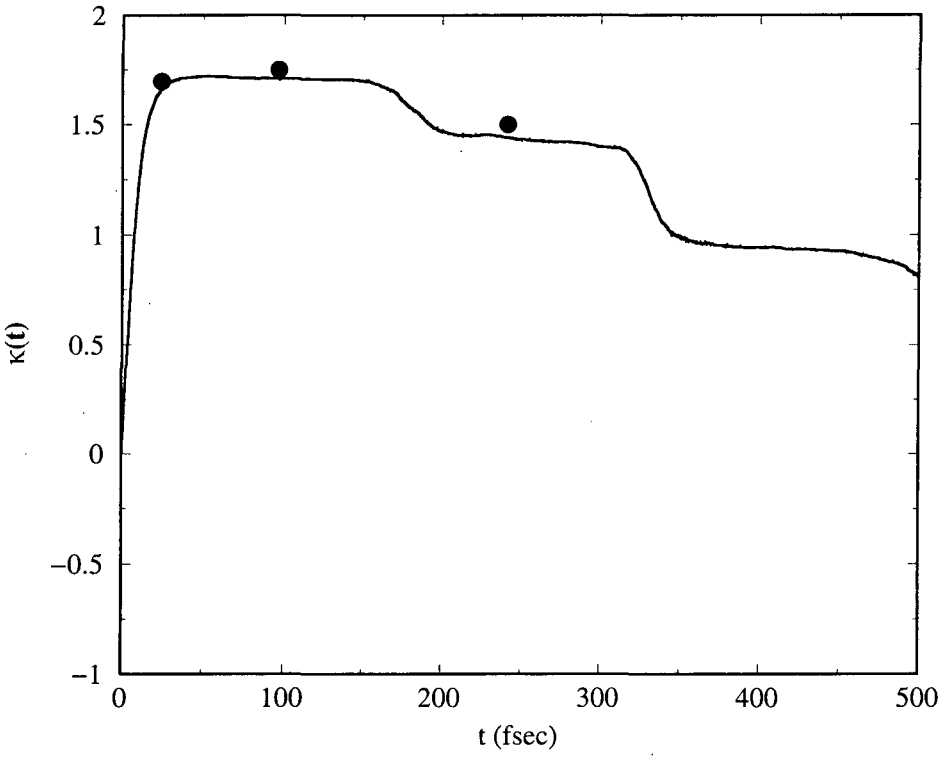

Figure 5.12: The flux-side correlation function for the double well potential coupled to ten harmonic modes, the example of section 5.5.3, at $T = 300K$. The solid line is the linearized SC-IVR (LSC-IVR) result and the solid points the FB-IVR results.

and this is indeed seen in Figure 5.12, which shows the flux-side correlation function scaled by the classical rate constant defined in Eq. (5.18). The correlation function is seen to rise in typical fashion to its transition state value in a time of $\sim \hbar\beta$ and then to show structure due to flux that re-crosses the dividing surface. The results of the FB-IVR calculation agree well with those of the LSC-IVR, suggesting that perhaps ten bath modes are sufficient to quench some of the quantum effects in the recrossing region.

5.6 Concluding remarks

The goal of this work has been to investigate the extent to which the semiclassical initial value representation, and the linearized approximation to it, are able to describe quantum effects in thermal rate constants. The conclusions are that the linearized approximation to the SC theory is able to describe quantum effects in the short time ($t \leq \hbar\beta$)

dynamics that corresponds to direct barrier crossing, i.e., transition state theory-like dynamics, but the description of the longer time re-crossing dynamics is essentially that given by classical mechanics. The complete SC-IVR treatment, however, is able to describe the quantum effects in the longer time re-crossing dynamics, though these calculations become progressively more difficult the longer the time. Also, the SC approximation for the Boltzmann operator introduces essentially no error; one is thus able to have a complete semiclassical theory, i.e., for the imaginary time (Boltzmann operator) as well as real time propagation.

The linearized approximation, though was not able to describe quantum effects for the 1-d double well not coupled to a harmonic bath, did extraordinarily well in obtaining the rates when the bath is coupled to the system. For practical considerations, the linearized approximation to the SC theory is much easier to implement than the full SC-IVR: the real time part of it is a classical molecular dynamics calculation, with the imaginary time part (i.e., the Boltzmann operator) treated either quantum mechanically or semiclassically. The fact that it describes the short time TST-like dynamics correctly, and provides a classical description of the longer time re-crossing dynamics, should make it very useful for many applications, particularly for complex molecular systems where quantum effects are often quenched by the many coupled degrees of freedom.

Lastly, several applications of the FB-IVR to flux-side correlation functions were presented in section 5.5, with very encouraging results. Together with other approaches for simplifying the SC-IVR calculations — e.g., stationary phase Monte Carlo filtering — the FB-IVR is a significant step toward making these methods useful for describing quantum effects in complex molecular systems.

Chapter 6

Future Outlook

With the increasing interest in quantum dynamics of large systems, it is clear that the semiclassical approximations studied in this thesis will be very useful for these purposes. We have explored some applications of the semiclassical initial value representation to a range of problems in chemical physics, including the calculation of wavefunctions, spectrum, nonadiabatic dynamics, thermal rate constants and correlation functions for system-bath problems. From these examples, it appears that the SC-IVR should be a very important tool both as a fundamental theory as well as for practical applications.

On the practical side, SC-IVR offers the only viable way of including quantum effects with classical trajectory calculations, and ways of more effective implementation should be further explored. We have presented several strategies on this front — e.g. stationary phase Monte Carlo and forward-backward IVR — and with them, applications to systems of 10-20 degrees of freedom should become routine within the foreseeable future. These problems are already quite beyond the scope of exact quantum mechanical methods and should be a significant advancement in bring quantum mechanics to "complex" systems. For even large systems where hundreds of degrees of freedom are involved, the application of the full SC-IVR is not as straightforward, therefore several cases must be considered. One: when quantum effects are quenched by the many degrees of freedom in the problem, linearized SC-IVR offers a very appealing approach for studying these systems. The LSC-IVR does have quantum effects for equilibrium properties such as partition functions, and provides exact quantum boundary conditions for classical trajectories. Therefore it has quantum effects for a short times, but long time dynamics is completely classical. The difficult aspect of this route is that one can never know if quantum effects are indeed

negligible. Two: quantum effects are important in a smaller subsystem only. For this case, some of the mixed quantum-classical methods reviewed here as well as the mixed semiclassical-classical approach presented in chapter 3 should be applicable. The caution for these mixed methods is that results depend heavily on ones choice of "system" and "bath" and careful understanding of the physics for each problem is required. Three: quantum effects are important and no obvious partition of the system and bath is possible. Here, one indeed will have to resort to the full SC-IVR, probably at a great expense. Even with the judicious use of FB-IVR and Filinov smoothing methods and etc., one cannot escape from the necessity of dealing with interference (and therefore oscillatory integrands) if one wants to include quantum effects. Consequently, the effort of these calculation will always be much greater than just classical mechanics. Ultimately, the understanding of when these three cases occur is perhaps just as important as the technical proficiency in using these different methods.

On the fundamental side, it is clear that the conceptual picture of classical limit of quantum mechanics is not fully complete and more investigations on this question is still an interesting topic of research. We have seen from very simple arguments that the semiclassical limit is still far from classical mechanics. Classical mechanics only emerged when the interference terms are negligible. Therefore, a very compelling topic for investigation would be towards a more precise location of this quantum to classical "transition boundary." Answers to this question will also go a long way in helping us for the practical application of semiclassical and classical methods as well.

References

[1] G. Wentzel, Z. Phys. **38**, 518 (1926).

[2] H. A. Kramers, Z. Phys. **39**, 828 (1926).

[3] L. Brillouin, C. R. Acad. Sci. Paris **183**, 24 (1926).

[4] M. V. Berry and K. E. Mount, Rep. Prog. Phys. **35**, 315 (1972).

[5] M. Born, *The Mechanics of the Atom* (Frederick Ungar Pub. Co., New York, 1960).

[6] M. V. Berry and N. L. Balazs, J. Phys. A **12**, 625 (1979).

[7] I. C. Percival, Adv. Chem. Phys. **36**, 1 (1977).

[8] J. H. Van Vleck, Proc. Natl. Acad. Sci. U.S.A. **14**, 178 (1928).

[9] M. C. Gutzwiller, J. Math. Phys. **8**, 1979 (1967).

[10] C. Morette, Phys. Rev. **81**, 848 (1951).

[11] P. Choquard, Helv. Phys. Acta **28**, 89 (1955).

[12] I. M. Gelfand and A. M. Yaglom, J. Math. Phys. **1**, 48 (1960).

[13] V. P. Maslov and M. V. Fedoriuk, *Semiclassical Approximations in Quantum Mechanics* (Reidel, Boston, 1981).

[14] J. B. Delos, Adv. Chem. Phys. **65**, 161 (1986).

[15] R. G. Littlejohn, J. Stat. Phys. **68**, 7 (1992).

[16] M. C. Gutzwiller, J. Math. Phys. **11**, 1791 (1970).

[17] M. C. Gutzwiller, J. Math. Phys. **12**, 343 (1971).

[18] M. C. Gutzwiller, J. Math. Phys. **14**, 139 (1973).

[19] M. C. Gutzwiller, J. Math. Phys. **18**, 806 (1977).

[20] M. C. Gutzwiller, Phys. Rev. Lett. **45**, 150 (1980).

[21] M. C. Gutzwiller, Physica **5D**, 183 (1982).

[22] M. C. Gutzwiller, Physica Scripta **T9**, 184 (1985).

[23] M. C. Gutzwiller, *Chaos in Classical and Quantum Mechanics* (Springer-Verlag, Berlin, 1990).

[24] M. V. Berry and M. Tabor, Proc. R. Soc. Lond. A **349**, 101 (1976).

[25] G. S. Ezra, K. Richter, G. Tanner, and D. Wintgen, J. Phys. B **24**, L413 (1991).

[26] M. Sieber and F. Steiner, Phys. Rev. Lett. **67**, 1941 (1991).

[27] G. Tanner *et al.*, Phys. Rev. Lett. **67**, 2410 (1991).

[28] P. Gaspard and D. Alonso, Phys. Rev. A **47**, 3468 (1993).

[29] M. V. Berry, Proc. R. Soc. Lond. A **400**, 229 (1985).

[30] M. V. Berry, Proc. R. Soc. Lond. A **423**, 219 (1989).

[31] E. J. Heller, in *Quantum Chaos and Statistical Nuclear Physics (Lecture Notes in Physics 263)*, edited by T. H. Seligman and H. Nishioka (Springer-Verlag, Berlin, 1986).

[32] J. Wilkie and P. Brumer, Phys. Rev. A **55**, 27 (1997).

[33] J. Wilkie and P. Brumer, Phys. Rev. A **55**, 43 (1997).

[34] J. R. Taylor, *Scattering Theory* (John Wiley & Sons, Inc., New York, 1972).

[35] W. H. Miller, Adv. Chem. Phys. **25**, 69 (1974).

[36] W. H. Miller, J. Chem. Phys. **62**, 1899 (1975).

[37] E. J. Heller, J. Chem. Phys. **62**, 1544 (1975).

[38] E. J. Heller, J. Chem. Phys. **65**, 1289 (1976).

[39] E. J. Heller, J. Chem. Phys. **66**, 5777 (1977).

[40] E. J. Heller, J. Chem. Phys. **67**, 3339 (1977).

[41] E. J. Heller, Phys. Rev. Lett. **53**, 1515 (1985).

[42] M. J. Davis and E. J. Heller, J. Chem. Phys. **71**, 3383 (1979).

[43] M. J. Davis and E. J. Heller, J. Chem. Phys. **75**, 3916 (1981).

[44] R. Heather and H. Metiu, Chem. Phys. Lett. **118**, 558 (1985).

[45] S. Sawada, R. Heather, B. Jackson, and H. Metiu, J. Chem. Phys. **83**, 3009 (1985).

[46] S. Sawada and H. Metiu, J. Chem. Phys. **84**, 227 (1986).

[47] T. F. George and W. H. Miller, J. Chem. Phys. **56**, 5637 (1972).

[48] T. F. George and W. H. Miller, J. Chem. Phys. **56**, 5722 (1972).

[49] T. F. George and W. H. Miller, J. Chem. Phys. **57**, 2458 (1972).

[50] S. Keshavamurthy and W. H. Miller, Chem. Phys. Lett. **218**, 189 (1994).

[51] K. G. Kay, J. Chem. Phys. **107**, 2313 (1997).

[52] N. T. Maitra and E. J. Heller, Phys. Rev. Lett. **78**, 3035 (1997).

[53] H. Goldstein, *Classical Mechanics* (Addison-Wesley, Reading, MA, 1980).

[54] W. H. Miller, J. Chem. Phys. **53**, 3578 (1970).

[55] K. G. Kay, J. Chem. Phys. **100**, 4377 (1994).

[56] K. G. Kay, J. Chem. Phys. **100**, 4432 (1994).

[57] K. G. Kay, J. Chem. Phys. **101**, 95 (1994).

[58] E. J. Heller, J. Chem. Phys. **94**, 2723 (1991).

[59] G. Campolieti and P. Brumer, J. Chem. Phys. **96**, 5969 (1992).

[60] G. Campolieti and P. Brumer, Phys. Rev. A **50**, 997 (1994).

[61] D. Provost and P. Brumer, Phys. Rev. Lett. **74**, 250 (1995).

[62] M. F. Herman and E. Kluk, Chem. Phys. **91**, 27 (1984).

[63] E. Kluk, M. F. Herman, and H. L. Davis, J. Chem. Phys. **84**, 326 (1986).

[64] A. R. Walton and D. E. Manolopoulos, Mol. Phys. **87**, 961 (1996).

[65] M. L. Brewer, J. S. Hume, and D. E. Manolopoulos, J. Chem. Phys. **106**, 4832 (1997).

[66] A. R. Walton and D. E. Manolopoulos, Chem. Phys. Lett. **244**, 448 (1995).

[67] S. Garaschchuk and D. J. Tannor, Chem. Phys. Lett. **262**, 477 (1996).

[68] F. Grossmann, Chem. Phys. Lett. **262**, 470 (1996).

[69] V. A. Mandelshtam and M. Ovchinnikov, J. Chem. Phys. **108**, 9206 (1998).

[70] Y. Weissman, J. Chem. Phys. **76**, 4067 (1982).

[71] R. G. Littlejohn, Phys. Rep. **138**, 193 (1986).

[72] J. R. Klauder, Ann. Phys. **180**, 108 (1987).

[73] F. Grossmann, Phys. Rev. A **57**, 3256 (1998).

[74] J. D. Doll, D. L. Freeman, and T. L. Beck, Adv. Chem. Phys. **78**, 61 (1994).

[75] N. Makri and W. H. Miller, Chem. Phys. Lett. **139**, 10 (1987).

[76] V. S. Filinov, Nucl. Phys. B **271**, 717 (1986).

[77] M. F. Herman, Chem. Phys. Lett. **275**, 445 (1997).

[78] B. W. Spath and W. H. Miller, J. Chem. Phys. **104**, 95 (1996).

[79] G. Campolieti and P. Brumer, J. Chem. Phys. **109**, 2999 (1998).

[80] M. J. Elrod and R. J. Saykally, J. Chem. Phys. **103**, 933 (1995).

[81] M. J. Elrod and R. J. Saykally, J. Chem. Phys. **103**, 921 (1995).

[82] J. H. Van Vleck, Rev. Mod. Phys. **23**, 213 (1951).

[83] R. N. Porter, L. M. Raff, and W. H. Miller, J. Chem. Phys. **63**, 2214 (1975).

[84] D. W. Noid, B. Broocks, S. K. Gray, and S. L. Marple, J. Phys. Chem. **92**, 3386 (1988).

[85] V. A. Mandelshtam and H. S. Taylor, J. Chem. Phys. **107**, 6577 (1997).

[86] P. Morse and H. Feshbach, *Methods of Theoretical Physics* (McGraw-Hill, New York, 1953), Vol. I.

[87] N. P. Blake and H. Metiu, J. Chem. Phys. **101**, 223 (1994).

[88] M. Ben-Nun and R. D. Levine, Chem. Phys. **201**, 163 (1995).

[89] Z. Li and R. B. Gerber, J. Chem. Phys. **102**, 4056 (1995).

[90] J. Cao, C. Minichino, and G. A. Voth, J. Chem. Phys. **103**, 1391 (1995).

[91] L. Liu and H. Guo, J. Chem. Phys. **103**, 7851 (1995).

[92] C. Scheuer and P. Saalfrank, J. Chem. Phys. **104**, 2869 (1995).

[93] J. Fang and C. C. Martens, J. Chem. Phys. **104**, 3684 (1996).

[94] S. Consta and R. Kapral, J. Chem. Phys. **104**, 4581 (1996).

[95] P. Bala, P. Grochowski, B. Lesyng, and J. A. McCammon, J. Phys. Chem. **100**, 2535 (1996).

[96] A. B. McCoy, J. Chem. Phys. **97**, 986 (1995).

[97] G. D. Billing, Chem. Phys. Lett. **30**, 391 (1975).

[98] G. D. Billing, J. Chem. Phys. **99**, 5849 (1993).

[99] R. B. Gerber, V. Buch, and M. A. Ratner, J. Chem. Phys. **77**, 3022 (1982).

[100] V. Buch, R. B. Gerber, and M. A. Ratner, Chem. Phys. Lett. **101**, 44 (1983).

[101] G. Stock, J. Chem. Phys. **103**, 1561 (1995).

[102] G. Stock, J. Chem. Phys. **103**, 2888 (1995).

[103] N. Makri and W. H. Miller, J. Chem. Phys. **87**, 5781 (1987).

[104] H. D. Meyer, U. Mathe, and L. S. Cederbaum, Chem. Phys. Lett. **165**, 73 (1990).

[105] H. D. Meyer, U. Mathe, and L. S. Cederbaum, J. Chem. Phys. **97**, 3199 (1992).

[106] J. C. Tully and R. K. Preston, J. Chem. Phys. **55**, 562 (1971).

[107] J. C. Tully, J. Chem. Phys. **93**, 1061 (1990).

[108] P. J. Kuntz, J. Chem. Phys. **95**, 141 (1991).

[109] B. J. Schwartz, E. R. Bittner, O. V. Prezhdo, and P. J. Rossky, J. Chem. Phys. **104**, 5942 (1996).

[110] A. I. Krylov *et al.*, J. Chem. Phys. **104**, 3651 (1996).

[111] A. G. Redfield, Adv. Magn. Reson. **1**, 1 (1965).

[112] A. M. Walsh and R. D. Coalson, Chem. Phys. Lett. **198**, 293 (1992).

[113] C. Scheurer and P. Saalfrank, Chem. Phys. Lett. **245**, 201 (1995).

[114] N. Topaler and N. Makri, J. Chem. Phys. **101**, 7500 (1994).

[115] R. Egger and C. H. Mak, Phys. Rev. B **50**, 15210 (1994).

[116] W. H. Miller, Adv. Chem. Phys. **30**, 77 (1975).

[117] H. Wang, X. Sun, and W. H. Miller, J. Chem. Phys. **108**, 9726 (1998).

[118] M. Hillary, R. F. O'Connell, M. O. Scully, and E. P. Wigner, Phys. Rep. **106**, 121 (1984).

[119] E. Pollak and J. L. Liao, J. Chem. Phys. **108**, 2733 (1998).

[120] J. Shao, J. L. Liao, and E. Pollak, J. Chem. Phys. **108**, 9711 (1998).

[121] J. S. Cao and G. A. Voth, J. Chem. Phys. **104**, 273 (1996).

[122] R. E. Kline Jr. and P. G. Wolynes, J. Chem. Phys. **88**, 4334 (1988).

[123] V. Khidekel, V. Chernyak, and S. Mukamel, in *Femtochemistry: Ultrafast Chemical and Physical Processes in Molecular Systems*, edited by M. Chergui (World Scientific, Singapore, 1996), p. 507.

[124] R. C. Brown and E. J. Heller, J. Chem. Phys. **75**, 186 (1981).

[125] H. W. Lee and M. O. Scully, J. Chem. Phys. **73**, 2238 (1980).

[126] W. H. Miller, J. Chem. Phys. **61**, 1823 (1974).

[127] V. S. Filinov, Y. V. Medvedev, and V. L. Kamskyri, Mol. Phys. **85**, 711 (1995).

[128] V. S. Filinov, Mol. Phys. **88**, 1517 (1996).

[129] W. H. Zurek and J. P. Paz, Phys. Rev. Lett. **72**, 2508 (1994).

[130] N. Makri and K. Thompson, Chem. Phys. Lett. **291**, 101 (1998).

[131] W. H. Miller, Faraday Disc. Chem. Soc. **110**, 1 (1998).

[132] H. Weyl, Z. Phys. **46**, 1 (1927).

[133] N. H. McCoy, Proc. Nat. Acad. Sci. **18**, 674 (1932).

[134] X. Sun and W. H. Miller, J. Chem. Phys. **106**, 916 (1997).

[135] L. D. Landau, Physik. Z. Sowjetunion U.S.S.R. **2**, 46 (1932).

[136] C. Zener, Proc. Roy. Soc. (London) A **137**, 696 (1932).

[137] E. C. G. Stuckelberg, Helv. Phys. Acta. **5**, 369 (1932).

[138] H. Nakamura and C. Zhu, Comments At. Mol. Phys. **32**, 249 (1996).

[139] D. C. Clary, J. Phys. Chem. **98**, 10678 (1994).

[140] F. N. Dzegilenko and J. M. Bowman, J. Chem. Phys. **105**, 2280 (1996).

[141] L. M. Raff and D. L. Thompson, in *Theory of Chemical Reaction Dynamics*, edited by M. Baer (CRC, Boca Raton, Fl, 1984), Vol. III.

[142] Edited by W. L. Hase, *Advances in Classical Trajectory Methods* (JAI, Greenwich, CT., 1993).

[143] P. Pechukas, Phys. Rev. **181**, 181 (1969).

[144] F. Webster, E. T. Wang, P. J. Rossky, and R. A. Friesner, J. Chem. Phys. **100**, 4835 (1994).

[145] W. H. Miller and C. W. McCurdy, J. Chem. Phys. **69**, 5163 (1978).

[146] C. W. McCurdy, H. D. Meyer, and W. H. Miller, J. Chem. Phys. **70**, 3177 (1979).

[147] H. D. Meyer and W. H. Miller, J. Chem. Phys. **70**, 3214 (1979).

[148] H. D. Meyer and W. H. Miller, J. Chem. Phys. **71**, 2156 (1979).

[149] E. Neria and A. Nitzan, J. Chem. Phys. **99**, 1109 (1993).

[150] R. D. Coalson, D. G. Evans, and A. Nitzan, J. Chem. Phys. **101**, 436 (1994).

[151] F. Strocchi, Rev. Mod. Phys. **38**, 36 (1966).

[152] G. Stock and M. Thoss, Phys. Rev. Lett. **78**, 578 (1997).

[153] J. J. Sakurai, *Modern Quantum Mechanics* (Addison-Wesley, Reading, MA, 1994).

[154] R. F. Currier and M. F. Herman, J. Chem. Phys. **82**, 4509 (1985).

[155] E. E. Nikitin, *Theory of Elementary Atomic and Molecular Processes in Gases* (Clarendon, Oxford, 1974).

[156] A. J. Leggett *et al.*, Rev. Mod. Phys. **59**, 1 (1987).

[157] D. Chandler, in *Liquids, Freezing and the Glass Transition, Les Houches 51, part 1*, edited by D. Levesque, J. P. Hansen, and J. Zinn-Justin (Elsevier Science, North Holland, 1991).

[158] C. H. Mak and D. Chandler, Phys. Rev. A **44**, 2352 (1991).

[159] D. E. Markov and N. Makri, Chem. Phys. Lett. **221**, 482 (1994).

[160] T. Yamamoto, J. Chem. Phys. **33**, 281 (1960).

[161] W. H. Miller, in *Dynamics of Molecules and Chemical Reactions*, edited by Z. J. Zhang and R. Wyatt (Marcel Dekker, New York, 1996).

[162] T. J. Park and J. C. Light, J. Chem. Phys. **88**, 4897 (1988).

[163] D. Brown and J. C. Light, J. Chem. Phys. **97**, 5465 (1992).

[164] D. H. Zhang and J. C. Light, J. Chem. Phys. **104**, 6184 (1995).

[165] W. H. Thompson and W. H. Miller, J. Chem. Phys. **106**, 142 (1997).

[166] T. C. Germann and W. H. Miller, J. Phys. Chem. **101**, 6358 (1997).

[167] H. Wang, W. H. Thompson, and W. H. Miller, J. Chem. Phys. **107**, 7194 (1997).

[168] D. H. Zhang and J. C. Light, J. Chem. Phys. **106**, 551 (1997).

[169] U. Manthe, J. Chem. Phys. **102**, 9205 (1995).

[170] U. Manthe, J. Chem. Phys. **105**, 6989 (1995).

[171] F. Matzkies and U. Manthe, J. Chem. Phys. **106**, 2646 (1997).

[172] F. Matzkies and U. Manthe, J. Chem. Phys. **108**, 4828 (1998).

[173] W. H. Miller, S. D. Schwartz, and J. W. Tromp, J. Chem. Phys. **79**, 4889 (1983).

[174] D. Chandler, J. Chem. Phys. **68**, 1823 (1978).

[175] M. Ovchinnikov and V. A. Apkarian, J. Chem. Phys. **105**, 10312 (1996).

[176] M. Ovchinnikov and V. A. Apkarian, J. Chem. Phys. **106**, 5775 (1997).

[177] M. Ovchinnikov and V. A. Apkarian, J. Chem. Phys. **108**, 2277 (1998).

[178] G. A. Voth, D. Chandler, and W. H. Miller, J. Phys. Chem. **93**, 7009 (1989).

[179] R. P. Feynman, *Statistical Mechanics* (Addison-Wesley, Reading, MA, 1972).

[180] P. Hanggi, P. Talkner, and M. Borkovec, Rev. Mod. Phys. **62**, 251 (1990).

Ernest Orlando Lawrence Berkeley National Laboratory
One Cyclotron Road | Berkeley, California 94720

Prepared for the U.S. Department of Energy under Contract No. DE-AC03-76SF00098